IL
NUOVO CIMENTO
ORGANO DELLA SOCIETÀ ITALIANA DI FISICA
SOTTO GLI AUSPICI DEL CONSIGLIO NAZIONALE DELLE RICERCHE

VOL. XV, N. 4 *Serie decima* 16 Febbraio 1960

Field Metrics.

P. SEN
National Physical Laboratory - New Delhi

(ricevuto il 24 Settembre 1959)

Summary. — A correlation between the metric along which a field propagates and its commutation relations or Feynman propagation function is postulated and the metrics for the fields whose wave equations are known or the wave equations for the fields whose metrics are known are deduced. The metrics of known fields are seen to have simple quadratic forms which define the interaction terms uniquely and from such metrics the interaction terms for nucleon meson, β decay and μ decay interactions are derived.

1. – Introduction.

One of the several bases of classical mechanics is the concept of the metric and the corresponding geodesic [1] from which the principle of conservation of energy, momentum and mass is derivable and the most outstanding proof of this basis is Einstein's theory of gravitation. In quantum mechanics the field equations are generally based on the principle of conservation of energy, momentum and mass and the metric or the geodesic are not explicitly utilized although the correlation between the commutation relations, Feynman propagation function and the metric may be foreseen and is actually well known for the electromagnetic field.

(1) L. LANDAU and E. LIFSHITZ: *The Classical Fields* (Cambridge, Mass. 1951).

Here we have assumed that this correlation is generally true and have then derived those metrics which are correlated to the boson and fermion field wave equations. For free boson and fermion fields we find that these metrics are quadratic forms in space, time and proper time ([2]) co-ordinates and that the wave function in the proper time co-ordinate is a Hankel transformation of the wave function in the mass co-ordinate which is the conjugate co-ordinate of the proper time co-ordinate and satisfies a Bessel equation in these co-ordinates. This makes possible mass quantization for the boson and fermion fields by means of suitable boundary conditions but this is not further investigated here.

Then the metrics for free fields are generalized and their simple quadratic form is maintained such that the Dirac Maxwell equations for interacting electron and electromagnetic fields are obtained from our postulated correlation. Field metrics of this form are seen to define the interaction term uniquely and this is illustrated by determining the nucleon meson, β decay and μ decay interactions. Finally, conversely, from the Einsteins metric for the gravitational field the wave equation for a particle field in interaction with the gravitational field is deduced.

2. – Free fields.

We note that the metric, which defines the surface along which a field propagates, the commutation relations and the Feynman propagation function of the electromagnetic field are correlated ([3]),

$$(1) \qquad (12)^2 A_\mu(1),\, A_\nu(2) = 0 \sim \begin{cases} [A_\mu(1),\, A_\nu(2)] = \delta_{\mu\nu}\varepsilon(12)_0\delta(12)^2\,, \\ L_{\mu\nu}(12) = \delta_{\mu\nu}/((12)^2 + i\varepsilon), \qquad \varepsilon \to +0, \end{cases}$$

and that the Maxwell equations can be derived from the commutation relations or the Feynman propagation function in (1).

The introduction of the proper time co-ordinate τ as an independent fifth co-ordinate ([2]), so that $\bar{x}(\bar{1})$ indicates the co-ordinates of space, time and proper time of the point $(\bar{1})$, permits the postulate that for a field $\pi(\bar{1})$ which propagates along the surface $(\bar{1}\bar{2})^2 \equiv (12)^2 - \tau(\bar{1}\bar{2})^2 = 0$, $\tau(\bar{1}\bar{2}) = \tau(\bar{1}) - \tau(\bar{2})$, there exists a similar correlation also,

$$(2) \qquad (\bar{1}\bar{2})^2\,\pi(\bar{1}),\, \pi(\bar{2}) = 0 \sim \begin{cases} [\pi(\bar{1}),\, \pi(\bar{2})] = \varepsilon(12_0)\,\delta(\bar{1}\bar{2})^2\,, \\ L(\bar{1}\bar{2}) = 1/((\bar{1}\bar{2})^2 + i\varepsilon)\,. \end{cases}$$

([2]) J. SCHWINGER: *Phys. Rev.*, **82**, 664 (1951).

([3]) The notation of P. SEN: *Nuovo Cimento*, **3**, 390 (1956) is used here. A'_μ (1) here is equal to $A'_\mu(1)/\sqrt{\hbar c}$ there so that λ here is equal to $e/\sqrt{\hbar c}$.

Then by means of the Hankel transformations [4]

$$(3)\qquad \begin{cases} F(\tau) = \int_0^\infty \tau J_1(\varkappa\tau) F^H(\varkappa)\,\mathrm{d}\varkappa\,, & F^H(\varkappa) = \int_0^\infty \varkappa J_1(\varkappa\tau) F(\tau)\,\mathrm{d}\tau\,, \qquad \tau > 0\,, \\ F(\tau) = \int_0^\infty \tau J_1(\varkappa\tau) F^H(\varkappa)\,\mathrm{d}\varkappa\,, & F^H(\varkappa) = \int_{-\infty}^0 \varkappa J_1(\varkappa\tau) F(\tau)\,\mathrm{d}\tau\,, \qquad \tau < 0\,, \end{cases}$$

$$(4)\qquad \int_0^\infty J_1(\varkappa\tau)\varkappa J_1(\varkappa u)\,\mathrm{d}\varkappa = \delta(u-\tau)/u\,,$$

we obtain

$$(5)\qquad \varepsilon(12)_0\,\delta(\bar{1}\bar{2})^2 = -\frac{i}{(2\pi)^3}\int\!\!\int_0^\infty \exp\left[ip\cdot(12)\right]\tau(\bar{1}\bar{2})\,J_1\big(\varkappa\tau(\bar{1}\bar{2})\big)\,\varepsilon(p_0)\,\delta(p^2+\varkappa^2)\,\mathrm{d}^4p\,\mathrm{d}\varkappa,$$

$$(6)\qquad 1/\big((\bar{1}\bar{2})^2+i\varepsilon\big) = \frac{1}{(2\pi)^4}\int\!\!\int_0^\infty \exp\left[ip\cdot(12)\right]\tau(\bar{1}\bar{2})\,J_1\big(\varkappa\tau(\bar{1}\bar{2})\big)\,1/(p^2+\varkappa^2-i\varepsilon)\,\mathrm{d}^4p\,\mathrm{d}\varkappa,$$

and the commutation relations in (2) give the boson commutation relations as well as the boson field equations,

$$(7)\qquad \big(\Box(1)+\varphi_B(\tau)\big)\,\pi(\bar{1}) = 0\,, \qquad \pi(\bar{1}) = \int \tau J_1(\varkappa\tau)\,\pi_\varkappa(1)\,\mathrm{d}\varkappa\,,$$

$$(8)\qquad \varphi_B(\tau)\,T_B(\varkappa\tau) = \varkappa^2 T_B(\varkappa\tau)\,, \qquad T_B\big(\varkappa\tau(\bar{1})\big)\,T_B\big(\varkappa\tau(\bar{2})\big) = \tau(\bar{1}\bar{2})\,J_1\big(\varkappa\tau(\bar{1}\bar{2})\big)\,.$$

We note that the introduction of the fifth co-ordinate τ is a formal device, that only its conjugate transform $\varkappa$ is physically significant and that it is eliminated from the final wave equation so that although the metric introduced here is abstract it presents even additional information about the physical magnitudes with which it is connected.

According to Dirac's procedure the equations (2) allow the reduction

$$(9)\qquad (\bar{1}\bar{2})^2 = \big(\gamma\cdot(12)+\tau(\bar{1}\bar{2})\big)\big(\gamma\cdot(12)-\tau(\bar{1}\bar{2})\big)\,,$$

$$(10)\qquad \big(\gamma\cdot(12)+\tau(\bar{1}\bar{2})\big)\,\psi(\bar{1}),\ \psi(\bar{2}),\ \psi^c(\bar{1}),\ \psi^c(\bar{2}) = 0$$

$$\sim \begin{cases} \{\overline{\psi}(\bar{1}),\ \psi(\bar{2})\} = \{\overline{\psi}^c(\bar{1}),\ \psi^c(\bar{2})\} = \varepsilon(12)_0\,\delta\big(\gamma\cdot(12)+\tau(\bar{1}\bar{2})\big), \\ K_F(\bar{1}\bar{2}) = K_F^c(\bar{1}\bar{2}) = 1/\big(\gamma\cdot(12)+\tau(\bar{1}\bar{2})+i\varepsilon\big) \end{cases}$$

---

[4] G. Watson: *Theory of Bessel Functions* (Cambridge, 1952).

and we note the relations

$$\int_0^\infty J_2(\varkappa\tau)\varkappa^2 J_1(\varkappa u)\,\mathrm{d}\varkappa = u^{-2}\frac{\partial}{\partial u}\left(u\,\delta(u-\tau)\right), \tag{11}$$

$$z\varepsilon(x_0)(\gamma\cdot x+\tau)\,\delta(\bar{x}^2) = \begin{cases} \varepsilon(x_0)\displaystyle\int_0^\infty J_1(\varkappa\tau)\left(\frac{\tau^3}{2}\,\gamma\cdot\frac{\partial}{\partial x}+\tau^2\right)\frac{\varkappa}{\sqrt{x^2}}\,J_1(\varkappa\sqrt{x^2})\,\mathrm{d}\varkappa \\ \quad \text{or} \\ \varepsilon(x_0)\displaystyle\int_0^\infty J_2(\varkappa\tau)\left(\frac{\tau^2}{\varkappa}\,\gamma\cdot\frac{\partial}{\partial x}+\frac{\tau^3\varkappa}{2}\right)\frac{\varkappa}{\sqrt{x^2}}\,J_1(\varkappa\sqrt{x^2})\,\mathrm{d}\varkappa\,, \end{cases} \tag{12}$$

so that if an operator $\varphi_F(\tau)$ is defined such that

$$\varphi_F(\tau)\psi'(\bar{1}) = \varkappa\psi'(\bar{1})\,, \tag{13}$$

the commutation relations in (10) give the Dirac equations which define a fermion field and its charge conjugate field.

3. – Interacting fields.

Let the surfaces along which two interacting fields $A(\bar{1}, \tilde{B}(\bar{1}))$, and $B(\bar{1}, \tilde{A}(\bar{1}))$ propagate be defined by

$$((\bar{1}\bar{2})^2+\eta_A\tilde{\bar{B}}(\bar{1})\tilde{B}(\bar{2}))\,A(\bar{1}, \tilde{B}(\bar{1}))=0\,, \quad ((\bar{1}\bar{2})^2+\eta_B\tilde{\bar{A}}(\bar{1})\tilde{A}(\bar{2}))\,B(\bar{1}, \tilde{A}(\bar{1}))=0\,, \tag{14}$$

respectively where η_A, η_B are constants and $\tilde{A}$, $\tilde{B}$ are the conjugate field transforms of A, B just as τ is the conjugate transform of $\varkappa$ and like τ they serve as a formal device.

The usefulness of the metrics (14) may be illustrated by the following examples:

1) Electron and electromagnetic fields. Let

$$\eta_A\tilde{\bar{\psi}}'(\bar{1})\tilde{\psi}'(\bar{2}) = \lambda\gamma_\mu\tilde{\bar{\psi}}'(\bar{1})\gamma_\nu\tilde{\psi}'(\bar{2})\,, \qquad \eta_B\tilde{A}'_\mu(1)\tilde{A}'_\nu(2) = \lambda^2\gamma_\mu\tilde{A}'_\mu(1)\gamma_\nu\tilde{A}'_\nu(2)\,. \tag{15}$$

Then by a reduction of the form (9) and (10) for the electron field $\psi'(\bar{1}, \tilde{A}'_\mu(1))$ the equations (14) give the correlations

$$(12)^2A'_\mu(1)+\lambda\tilde{j}'_\mu(\bar{1}, \bar{2})\gamma_\nu A'_\nu(1) = 0 \tag{16}$$

$$\sim \begin{cases} [A'_\mu(1), A'_\nu(2)] = \delta_{\mu\nu}\varepsilon(12)_0\delta\left((12)^2+\lambda\tilde{j}'_\mu(\bar{1}, \bar{2})\gamma_\nu\right), \\ L'_{\mu\nu}(1, 2) = \delta_{\mu\nu}/\left((12)^2+\lambda j'_\mu(\bar{1}, \bar{2})\gamma_\nu+i\varepsilon\right), \end{cases}$$

$$(17)\qquad (\gamma\cdot(12)+\tau(\bar{1}\bar{2})-i\lambda\gamma\cdot\tilde{A}'(1))\,\psi'(\bar{1},\tilde{A}'_\mu(1)) =$$

$$\sim\begin{cases}\{\bar{\psi}'(\bar{1},\tilde{A}'_\mu(1)),\ \psi'(\bar{2},\tilde{A}'_\mu(\bar{2}))\} = \varepsilon(12)_0\,\delta(\gamma\cdot(12)+\tau(\bar{1}\bar{2})-i\lambda\gamma\cdot\tilde{A}'(1))\,,\\ K'_F(\bar{1},\bar{2}) = 1/(\gamma\cdot(12)+\tau(\bar{1}\bar{2})-i\lambda\gamma\cdot\tilde{A}'(1)+i\varepsilon)\,,\end{cases}$$

$$(18)\qquad (\gamma\cdot(12)+\tau(\bar{1}\bar{2})+i\lambda\gamma\cdot\tilde{A}'(1))\,\psi^{\sigma'}(\bar{1},\tilde{A}'_\mu(1)) = 0$$

$$\sim\begin{cases}\{\bar{\psi}^{\sigma'}(\bar{1},\tilde{A}'_\mu(1)),\ \psi^{\sigma'}(\bar{2},\tilde{A}'_\mu(2))\} = \varepsilon(12)_0\,\delta(\gamma\cdot(12)+\tau(\bar{1}\bar{2})+i\lambda\gamma\cdot\tilde{A}'(1))\,,\\ K^{\sigma'}_F(\bar{1},\bar{2}) = 1/(\gamma\cdot(12)+\tau(\bar{1}\bar{2})+i\lambda\gamma\cdot\tilde{A}'(1)+i\varepsilon)\,,\end{cases}$$

where $\tilde{j}'_\mu(\bar{1},\bar{2}) = \tilde{\bar{\psi}}'(\bar{1})\gamma_\mu\tilde{\psi}'(\bar{2})$ and the Dirac Maxwell equations follow from the commutation relations in (16), (17), (18) by means of suitable transformations of the form (2) and (8), that is for example,

$$(19)\qquad \varepsilon(12)_0\,\delta((12)^2+\lambda\gamma\cdot\tilde{j}'(\bar{1},\bar{1})) =$$

$$= -\frac{i}{(2\pi)^3}\iint\exp\,[ip\cdot(12)]\,T(\tilde{\psi}',\psi')\,\varepsilon(p_0)\,\delta(p^2+\lambda\gamma\cdot j'(\bar{1}))\,\mathrm{d}^4p\,\mathrm{d}\psi'\,,$$

$$(20)\qquad A'_\mu(1,\tilde{\psi}'(\bar{1})) =$$

$$=\int T(\tilde{\psi}',\psi')\,A'_\mu(1,\psi'(\bar{1}))\,\mathrm{d}\psi'\,,\quad \varphi_A(\tilde{\psi}')\,T=(\tilde{\psi}',\psi')\gamma\cdot j'(\bar{1})\,T(\tilde{\psi}',\psi')\,,$$

where $j'_\mu(\bar{1}) = \bar{\psi}'(\bar{1})\,\gamma_\mu\psi'(\bar{1})$.

2) Nucleon meson fields. Since η is taken to be a constant the equations (14) allow only scalar or pseudoscalar interactions between nucleons and mesons of spin 0.

3) β interaction. We note that the nature of β decay excludes interactions between similar or conjugate particles and that either charge conserving or nucleon mass conserving quadratic forms (14) can be constructed. Then eight wave equations are obtained for each type of the equations (14) and the interaction term is found to be antisymmetric with respect to the interchange of charged, uncharged, heavy and light particles so that the β interaction is the Critchfield Wigner mixture of scalar and pseudoscalar terms [5]. For μ-meson decay $\mu = \mathrm{e}+\nu+\nu^c$ where there are two conjugate interacting particles the interaction term is antisymmetric with respect to the interchange of neutral particles only and therefore the μ decay interaction is a given mixture [5] of all the five types of interaction terms.

---

[5] R. H. Good: *Rev. Mod. Phys.*, **27**, 187 (1955).

4) Einstein metric. For gravitational field metric $\tau^2 = g_{\mu\nu}(12)(12)^\mu(12)^\nu$ using the abbreviation $x^\mu = (12)^\mu$ we note that

$$(21) \qquad (x_\mu x^\mu - \tau^2)\pi_g(\bar{1}) = 0 \sim \begin{cases} [\pi_g(\bar{1}), \pi_g(\bar{2})] = \varepsilon(x^0)\,\delta(x_\mu x^\mu - \tau^2)\,, \\ L_g(\bar{1}, \bar{2}) = 1/(x_\mu x^\mu - \tau^2 + i\varepsilon)\,, \end{cases}$$

$$(22) \qquad \varepsilon(x^0)\,\delta(x_\mu x^\mu - \tau^2) =$$

$$= -\frac{i}{(2\pi)^3}\int_0^\infty\!\!\int \exp\,[iP_{(\alpha)}X^{(\alpha)}]\tau J_1(\varkappa\tau)\varepsilon(P^{(0)})\,\delta(P_{(\alpha)}P^{(\alpha)} + \varkappa^2)\,\mathrm{d}^4P^{(\alpha)}\mathrm{d}\varkappa\,,$$

$$(23) \qquad g_{\mu\nu} = \lambda_{(\alpha)\mu}\lambda^{(\alpha)}{}_\nu\,, \qquad X_{(\alpha)} = \lambda_{(\alpha)\mu}x^\mu\,, \qquad X^{(\alpha)} = \lambda^{(\alpha)}{}_\mu x^\mu\,, \qquad x_\mu x^\mu = X_{(\alpha)}X^{(\alpha)}\,,$$

provided the tetrad $\lambda^{(\alpha)}{}_\mu$ is so chosen that $\varepsilon(x^0) = \varepsilon(X^{(0)})$ and obtain the wave equation for the particle field $\pi_{g,\varkappa}(1)$ interacting with the gravitational field,

$$(24) \qquad \left(\frac{\partial}{\partial X_{(\alpha)}}\cdot\frac{\partial}{\partial X^{(\alpha)}} - \varkappa^2\right)\pi_{g,\varkappa}(1) = 0\,,$$

which corresponds to the geodesic equation (6),

$$(25) \qquad \frac{\mathrm{d}}{\mathrm{d}\tau}v^{(\alpha)} - \gamma^{(\alpha)}_{(\beta)(\gamma)}v^{(\beta)}v^{(\gamma)} = 0\,.$$

* * *

This work was done at the Istituto di Fisica dell'Università di Torino and the author is very grateful to Professor G. Wataghin for kind hospitality and for helpful discussions.

(6) E. A. E. Pirani: *Act. Phys. Pol.*, **15**, 389 (1956).

RIASSUNTO (*)

Si postula una correlazione tra la metrica lungo la quale un campo si propaga e le sue relazioni di commutazione, ossia la funzione di propagazione di Feynmann, e si deducono le metriche dei campi di cui si conoscono le equazioni d'onda, o le equazioni d'onda dei campi di cui si conoscono le metriche. Si vede che le metriche dei campi conosciuti hanno semplici formule quadratiche che definiscono univocamente i termini di interazione e da queste metriche si derivano i termini di interazione per le interazioni nucleone-mesone, del decadimento β e del decadimento μ.

(*) *Traduzione a cura della Redazione.*

IL NUOVO CIMENTO Vol. XV, N. 4 16 Febbraio 1960

A Survey of Relativistic Transformations (*).

M. F. Kaplon and T. Yamanouchi
University of Rochester - Rochester, N. Y.

(ricevuto l'8 Ottobre 1959)

Summary. — The usefulness of invariance properties in calculating various kinematical quantities relevant to particle physics is outlined and examples given. General formulae relating to the transformation of distributions from one Lorentz system to another are given and their uses demonstrated. Particular application is made to the γ-ray distribution arising from π^0-decay.

1. – Introduction.

In the process of considering certain problems in γ-ray astronomy the authors had occasion to work out a number of relationships concerning the transformation of γ-ray distribution (the γ-rays arising from π^0-decay) from one Lorentz system to another. It was thought that these might be useful to other workers, particularly with the expected rise in activity in particle physics requiring exact relativistic relations. At the same time we considered it useful to expand the scope somewhat and present somewhat more general results of use. No pretense is presented as to originality or completeness and no effort has been expended on our part to search the literature.

2. – Use of invariance.

It is usually the practice in obtaining such quantities as thresholds, formulas for Q-values of decaying particles, etc., to go to the center of mass system (c.m.) or rest system (R.S.) as the case may be and then transform back to the laboratory system (L.S.). This labor may be conveniently circum-

(*) This research was supported in part by the Office of Scientific Research, USAF and the AEC.

vented by appropriate use of invariance properties. It is convenient to use 4 vectors of energy-momentum which we denote by $\tilde{P}$ with components $(E; \boldsymbol{P})$. We take for the 4 scalar product of two vectors $\tilde{P}_1$ and $\tilde{P}_2$, $\tilde{P}_1 \cdot \tilde{P}_2 = E_1 E_2 - \boldsymbol{P}_1 \cdot \boldsymbol{P}_2$; thus $(\tilde{P}_1)^2 = M_1^2$.

Consider thus the problem of determining the threshold for the reaction

$$(\mathrm{A}) + (\mathrm{B}) \to \sum_{i=1}^{n} (i)\,,$$

where by (A) and (B) we mean the initial particles (*e.g.* (A) could be a π^+-meson and (B) a proton) and by $\sum_i^n (i)$ we mean the final state desired (for the example above a possible final state is $(1) = \pi^+$, $(2) = \mathrm{p}$ and the remaining particles could be any combination satisfying charge, baryon and strangeness conservation). Now the threshold is defined with respect to the c.m. system as that state in which all the particles (i) are at rest. If we denote the 4-vectors of the particles by $\tilde{P}$ with an appropriate subscript, energy-momentum conservation is represented by $\tilde{P}_\mathrm{A} + \tilde{P}_\mathrm{B} = \sum_{i=1}^{n} \tilde{P}_i$: If we take the scalar product of this equation with itself we have $(\tilde{P}_\mathrm{A} + \tilde{P}_\mathrm{B}) \cdot (\tilde{P}_\mathrm{A} + \tilde{P}_\mathrm{B}) = \left(\sum_i^n \tilde{P}_i\right) \cdot \left(\sum_{i=1}^{n} \tilde{P}_i\right)$. This is an invariant equation and either side can be evaluated in any Lorentz system. If we want the threshold we evaluate the right hand side in the c.m. in which case the vector $\sum_i^n \tilde{P}_i$ has components $\left(E = \sum_{i=1}^{n} M_i;\ \boldsymbol{P} = 0\right)$. The left hand side corresponds to the physical situation. For the case that particle B is at rest we have

$$(E_\mathrm{A} + M_\mathrm{B})^2 - (\boldsymbol{P}_\mathrm{A})^2 = \left(\sum_{i=1}^{n} M_i\right)^2,$$

or

$$T_\mathrm{A} = E_\mathrm{A} - M_\mathrm{A} = \frac{\left(\sum_{i=1}^{n} M_i\right)^2 - (M_\mathrm{A} + M_\mathrm{B})^2}{2M_\mathrm{B}} = \text{Threshold Kinetic Energy.}$$

For the case that particle B is not at rest we have after some manipulation

$$E_\mathrm{A} = \Big\{E_\mathrm{B}\Big[\Big(\sum_{i=1}^{n} M_i\Big)^2 - (M_\mathrm{A}^2 + M_\mathrm{B}^2)\Big] + P_\mathrm{B} \cos\theta \Big\{\Big[\Big(\sum_{i=1}^{n} M_i\Big)^2 - (M_\mathrm{A} + M_\mathrm{B})^2\Big] \cdot \Big[\Big(\sum_{i=1}^{n} M_i\Big)^2 - (M_\mathrm{A} - M_\mathrm{B})^2\Big] - 4M_\mathrm{A}^2 P_\mathrm{B}^2 \sin^2\theta\Big\}^{\frac{1}{2}}\Big\} \Big/ [2(M_\mathrm{B}^2 + P_\mathrm{B}^2 \sin^2\theta)]\,,$$

where $\boldsymbol{P}_\mathrm{A} \cdot \boldsymbol{P}_\mathrm{B} = P_\mathrm{A} P_\mathrm{B} \cos\theta$.

Another application is to the Q-value of decaying particles. Let the scheme be

$$\Lambda \to \sum_{i=1}^{n} (i) .$$

The conservation laws read

$$\tilde{P}_\Lambda = \sum_{i=1}^{n} \tilde{P}_i$$

and on squaring

$$M_\Lambda^2 = \Big(\sum_{i=1}^{n} E_i\Big)^2 - \Big(\sum_{i=1}^{n} \boldsymbol{P}_i\Big)^2 .$$

By definition $M_\Lambda = Q + \sum_{i=1}^{n} M_i$, so that

$$Q = \Big\{\Big(\sum_{i=1}^{n} E_i\Big)^2 - \Big(\sum_{i=1}^{n} \boldsymbol{P}_i\Big)^2\Big\}^{\frac{1}{2}} - \sum_{i=1}^{n} M_i$$

is a relation valid in any Lorentz frame.

Other useful applications occur by treating a given state partly in one system and partly in another. For example, suppose one observed the decay in flight of a neutral particle into a π^+ and a π^--meson and wished to test this for consistency with the decay $\tau^0 \to \pi^+ + \pi^- + \pi^0$.

This reads

$$\tilde{P}_{\tau^0} = \tilde{P}_{\pi^+} + \tilde{P}_{\pi^-} + \tilde{P}_{\pi^0} \qquad \text{or} \qquad \tilde{P}_{\tau^0} - \tilde{P}_{\pi_0} = \tilde{P}_{\pi^+} + \tilde{P}_{\pi^-} .$$

Square and evaluate the l.h.s. in the τ_0 R.S. and the r. h. s. in the system of observation. Since in the R.S., $\tilde{P}_{\tau^0}$ is $(M_{\tau^0}; 0)$ we have

$$M_{\tau^0}^2 + M_{\pi^0}^2 - 2 M_{\tau^0} E'_{\pi^0} = M_{\pi^+}^2 + M_{\pi^-}^2 + 2(E_{\pi^+} E_{\pi^-} - \boldsymbol{P}_{\pi^+} \cdot \boldsymbol{P}_{\pi^-}) ,$$

where E'_{π^0} is the π^0 energy in the rest system of the τ_0 and has a finite maximum value. The r.h.s. can be evaluated from the observations and the corresponding calculated value of E'_{π^0} checked for consistency.

Next consider the problem of determining the relative velocity of the c.m. and L.S. In a given Lorentz frame (the L.S.) a group of particles of four momenta $\tilde{P}_i$ can be regarded as a mass $M^* = \big[(\sum_i P_i)^2\big]^{\frac{1}{2}}$ travelling with the velocity $\boldsymbol{\beta} = \sum_i \boldsymbol{P}_i / \sum_i E_i$. In the c.m. system for which $\sum_i \boldsymbol{P}'_i = 0$, the mass M^* has $\boldsymbol{\beta}' = 0$; therefore the center of mass system moves with respect to the Laboratory with the velocity $\boldsymbol{\beta} = \sum_i \boldsymbol{P}_i / \sum E_i$.

Perhaps the most useful application of invariance properties is that of determining the Jacobian for the transformation from one Lorentz frame to another. This starts with a well known property that $\mathrm{d}^3\boldsymbol{P}/E$ is an invariant [1]. Using primes to denote another Lorentz system we have

$$\frac{\mathrm{d}^3\boldsymbol{P}}{E} = \frac{P^2 \mathrm{d}P \mathrm{d}\Omega}{E} = p \mathrm{d}E \mathrm{d}\Omega,$$

and thus

$$\mathrm{d}E' \mathrm{d}\Omega' = \frac{P}{p'} \mathrm{d}E \mathrm{d}\Omega = \frac{\sin\theta'}{\sin\theta} \mathrm{d}E \mathrm{d}\Omega , \tag{1a}$$

the latter using the invariance of transverse momentum. Alternately we may write this as

$$\mathrm{d}E' \mathrm{d}\Omega' = \frac{p}{[\gamma^2(E - \boldsymbol{\beta}\cdot\boldsymbol{p})^2 - M^2]^{\frac{1}{2}}} \mathrm{d}E \mathrm{d}\Omega , \tag{1b}$$

where $\gamma = 1/\sqrt{1-\beta^2}$ is the usual Lorentz factor and $\boldsymbol{\beta}$ the velocity of the primed system with respect to the unprimed. In the next section we shall start with the above relation as the basic one.

3. – We shall consider here the transformation from one Lorentz system to another of a given distribution in energy and angle. For sake of definiteness (but with no loss of generality) it will be convenient to think of this as going from the c.m. to the L. system. We denote by γ and $\boldsymbol{\beta}$ the Lorentz factor and velocity of the c.m. with respect to the Lab. The transformation will be along the direction $\boldsymbol{\beta}$ which also serves as defining the Z direction of the spherical polar co-ordinates in each system. Particle quantities referred to the c.m. will be denoted by bars with a subscript 0 and with respect to the L. system they are unbarred; thus

$$\bar{E}_0 = \gamma(E_0 - \beta p_0 \cos\theta) ; \tag{2a}$$

$$\bar{P}_0 \cos\bar{\theta} = \gamma(P_0 \cos\theta - \beta E_0) . \tag{2b}$$

It will be convenient to express particle energies and momenta in units of the rest mass so that $E_0 \to \gamma_0$ and $P_0 \to \sqrt{\gamma_0^2 - 1}$, etc. We take as given the distribution in the c.m. system: $F(\bar{\gamma}_0, \bar{\theta})\mathrm{d}\bar{\gamma}_0 \mathrm{d}\bar{\Omega}$ as the number of particles with energy between $\bar{\gamma}_0$ and $\bar{\gamma}_0 + \mathrm{d}\bar{\gamma}_0$ lying in the element of solid angle $\mathrm{d}\bar{\Omega}$.

---

[1] L. LANDON and E. LIFSCHITZ: *The Classical Theory of Fields* (Reading, Mass., 1951), p. 31.

From Section **2**, (1) we have

$$F(\gamma_0, \theta) = \frac{\sqrt{\gamma_0^2 - 1}}{[\gamma^2\gamma_0^2(1 - \beta\beta_0 \cos\theta)^2 - 1]^{\frac{1}{2}}} F[\bar{\gamma}_0(\gamma_0, \theta), \bar{\theta}(\gamma_0, \theta)] , \tag{3}$$

where $\bar{\gamma}(\gamma_0, \theta)$ and $\bar{\theta}(\gamma_0, \theta)$ are given by (2*a*) and (2*b*). Equation (3) needs limits defining its domain. We distinguish three cases: i) $\bar{\gamma}_0^M < \gamma$, ii) $\bar{\gamma}_0^M = \gamma$ and iii) $\bar{\gamma}_0^M > \gamma$, where $\bar{\gamma}_0^M$ is the maximum energy of emission in the c. m. system. By solving (2*a*) for γ_0 (with $\bar{\gamma}_0 \to \bar{\gamma}_0^M$) we find

$$\gamma_0^{\pm} = \frac{(\bar{\gamma}_0^M/\gamma) \pm \beta \cos\theta \left[(\bar{\gamma}_0^M/\gamma)^2 - (1 - \beta^2 \cos^2\theta)\right]^{\frac{1}{2}}}{1 - \beta^2 \cos^2\theta} . \tag{4}$$

Using (2*a*) we have

$$\text{(i)} \quad \frac{\bar{\gamma}_0^M}{\gamma} < 1, \qquad \cos\theta \geqslant \left[\frac{\gamma^2 - (\bar{\gamma}_0^M)^2}{\gamma^2 - 1}\right]^{\frac{1}{2}}, \tag{5a}$$

$$\text{(ii)} \quad \frac{\bar{\gamma}_0^M}{\gamma} = 1, \qquad \theta \leqslant \pi/2 , \tag{5b}$$

$$\text{(iii)} \quad \frac{\bar{\gamma}_0^M}{\gamma} > 1, \qquad \text{all } \theta \text{ allowed} . \tag{5c}$$

Thus the domain of (3) is defined for the 3 cases as

$$\begin{cases} \text{(i)} \quad \gamma_0^- \leqslant \gamma_0 \leqslant \gamma_0^+ ; & \cos\theta \geqslant \left[\dfrac{\gamma^2 - (\bar{\gamma}_0^M)^2}{\gamma^2 - 1}\right]^{\frac{1}{2}} ; \quad \dfrac{\bar{\gamma}_0^M}{\gamma_0} < 1 , \\ \text{(ii)} \quad 1 \leqslant \gamma_0 \leqslant \dfrac{1 + \beta^2 \cos^2\theta}{1 - \beta^2 \cos^2\theta} ; & 0 \leqslant \cos\theta \leqslant 1 ; \quad \dfrac{\bar{\gamma}_0^M}{\gamma} = 1 , \\ \text{(iii)} \quad 1 \leqslant \gamma_0 \leqslant \gamma_0^+ ; & -1 \leqslant \cos\theta \leqslant 1 ; \quad \dfrac{\bar{\gamma}_0^M}{\gamma} > 1 . \end{cases} \tag{6}$$

Of interest also are the distributions $F_1(\gamma)$ and $F_2(\theta)$, respectively the energy (irrespective of angle) and angular (irrespective of energy) distributions in the L. system. These are obtained by integrating over the appropriate variable. Previously [2] one of us (M.F.K.) has given formulae for obtaining $F_2(\theta)$, in that case doing the integrations on the particle energy in the c.m. system. The procedure here is to integrate over the complete differential expression

[2] H. L. Bradt, M. F. Kaplon and B. Peters: *Helv. Phys. Acta*, **23**, 24 (1950).

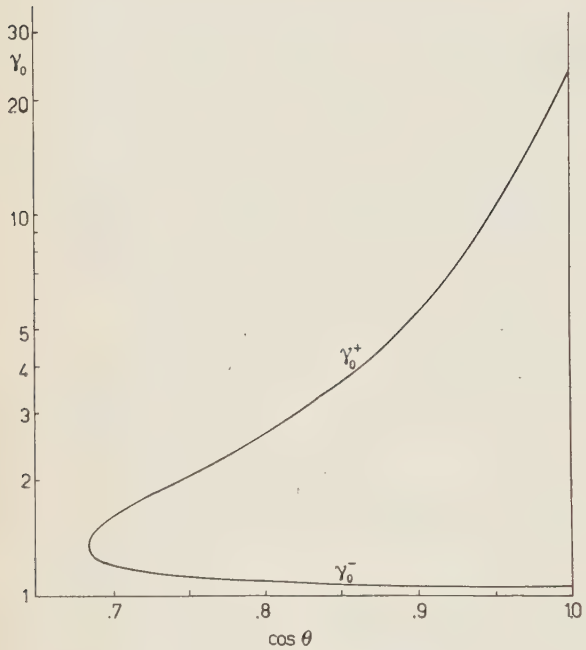

Fig. 1. – Allowed region in the γ_0-cos θ plane for the case $\bar{\gamma}_0^M < \gamma$.

in the L. system. For each case i), ii) or iii), the limits of integration are most readily visualized by drawing the allowed region in (γ_0, cos θ) space. This is illustrated schematically for i) in Fig. 1. It is seen that for θ fixed γ_0 satisfies $\gamma_0^- \leqslant \gamma_0 \leqslant \gamma_0^+$ thus we have

$$(6a)\qquad \begin{cases} F_2(\theta) = \int_{\gamma_0^+}^{\gamma_0^-} F(\gamma_0, \theta)\, \mathrm{d}\gamma_0; \\ \sqrt{\dfrac{\gamma^2 - (\bar{\gamma}_0^M)^2}{\gamma^2 - 1}} \leqslant \cos\theta \leqslant 1, \\ \dfrac{\bar{\gamma}_0^M}{\gamma} < 1, \end{cases}$$

and for γ_0 fixed, the limits on θ are found as the solutions to $\gamma_0^-(\theta) = \gamma_0$ and $\gamma_0^+(\theta) = \gamma_0$, yielding

$$(6b)\qquad \begin{cases} F_1(\gamma_0) = \int_{\theta_-}^{\theta_+}\!\!\int F(\gamma_0, \theta)\, \mathrm{d}\Omega; \\ \cos\theta_+ = \dfrac{\gamma_0 - (\bar{\gamma}_0^M/\gamma)}{\beta\sqrt{\gamma_0^2 - 1}} \leqslant \cos\theta \leqslant 1 = \cos\theta_-; \end{cases} \qquad \gamma\bar{\gamma}_0^M(1-\beta\bar{\beta}_0^M) \leqslant \gamma_0 \leqslant \gamma\bar{\gamma}_0^M(1+\beta\bar{\beta}_0^M).$$

Case iii), $\bar{\gamma}_0^M > \gamma$ yields on analysis

$$(7a)\qquad F_2(\theta) = \int_1^{\gamma_0^+} F(\gamma_0, \theta)\, \mathrm{d}\gamma_0; \qquad -1 \leqslant \cos\theta \leqslant 1, \qquad \frac{\bar{\gamma}_0^M}{\gamma} > 1,$$

and

$$(7b)\qquad F_1(\gamma_0) = \int\!\!\int F(\gamma_0, \theta)\, \mathrm{d}\Omega; \qquad -1 \leqslant \cos\theta \leqslant 1, \qquad 1 \leqslant \gamma_0 \leqslant \bar{\gamma}_0^M\gamma(1 - \beta\bar{\beta}_0^M)$$

$$= \int_{\theta_-}^{\theta_+}\!\!\int F(\gamma_0, \theta)\, \mathrm{d}\Omega;$$

θ_+, θ_- same as i) $\qquad \gamma\bar{\gamma}_0^M(1 - \beta\bar{\beta}_0^M) \leqslant \gamma_0 \leqslant \gamma\bar{\gamma}_0^M(1 + \beta\bar{\beta}_0^M)$.

Case ii) $\bar{\gamma}_0^M = \gamma$ is obtained as a limiting case of either i) or iii) and yields

$$F_2(\theta) = \int_{\mathrm{i}}^{\substack{(1+\beta^2\cos^2\theta)\\(1-\beta^2\cos^2\theta)}} F(\gamma_0, \theta)\,\mathrm{d}\gamma_0\,, \qquad 0 \leqslant \cos\theta \leqslant 1, \tag{8a}$$

$$F_1(\gamma_0) = \int_0^{\cos^{-1}\left[\frac{1}{\beta}\sqrt{\frac{\gamma_0-1}{\gamma_0+1}}\right]} \int F(\gamma_0, \theta)\,\mathrm{d}\Omega; \qquad 1 \leqslant \gamma_0 \leqslant \frac{1+\beta^2}{1-\beta^2}\,. \tag{8b}$$

For the case that $F(\bar{\gamma}_0, \bar{\theta}) = F(\bar{\theta})\delta(\bar{\gamma}_0 - \bar{\gamma}_0')$ the above relations for $F_2(\theta)$ yield the usual formula for transforming a differential cross-section for a two body final state from one Lorentz system to another; in this case $\bar{\gamma}_0' = \bar{\gamma}_0^M$. In general for a δ-function energy spectrum in the c.m. they yield the laboratory energy and angular distribution.

Another quantity of interest in recent years is the transverse momentum distribution ([3]). This is most readily obtained in the c.m. system since it is invariant to Lorentz transformation. Here it is convenient to write

$$F(\bar{E}_0, \bar{\theta})\,\mathrm{d}\bar{E}_0\,\mathrm{d}\bar{\Omega} = F(\bar{E}_0, \bar{\theta})\,\mathrm{d}\bar{\Omega}\,\frac{\bar{p}\,\mathrm{d}\bar{p}}{\bar{E}_0}$$

The change of variables is from $\bar{\theta}$, $\bar{p}$ to $\bar{\theta}$ and $p_T = \bar{p}\sin\bar{\theta}$. The Jacobian,

$$J\left(\frac{\bar{\theta}, \bar{p}}{\bar{\theta}, p_T}\right) = \frac{1}{\sin\bar{\theta}}\,,$$

so that

$$F(p_T) = 2\pi P_T \int_0^{\pi} \frac{\mathrm{d}\bar{\theta}\,F[\bar{E}(P_T, \bar{\theta}), \bar{\theta}]}{[P_T^2 + M^2\sin^2\bar{\theta}]^{\frac{1}{2}}}\,, \tag{9}$$

where

$$\bar{E}(P_T, \bar{\theta}) = \frac{[P_T^2 + M^2\sin^2\bar{\theta}]^{\frac{1}{2}}}{\sin\bar{\theta}}\,,$$

and M is the rest mass of the particle whose transverse momentum distribution is being obtained. In the above we have tacitly assumed that the c.m. distribution is such that there is no correlation between energy and angle.

([3]) O. Minakawa, Y. Nishimura, M. Tsuzuki, H. Yamanouchi, H. Aizu, H. Hasegawa, Y. Ishii, S. Tokunaga, Y. Fujimoto, S. Hasegawa, J. Nishimura, K. Niu, K. Nishikawa, K. Imaeda and M. Kazuno: *Suppl. Nuovo Cimento*, **11**, 112 (1959).

If such should not be the case, the limits of integration on $\bar{\theta}$ have to be determined in accord with the constraint. This latter would be the case if the transverse momentum distribution were obtained from $F(E_0, \theta)$ in which case it is clear that in general such constraints occur. Unless this is borne in mind, the experimental determination of $F(P_T)$ from observations on laboratory distributions will vary depending on the domain of the distribution sampled. It is clear for example by reference to Fig. 1, that for the case $\bar{\gamma}_0^M < \gamma$, that the range of P_T depends on the angle of observation and that observations restricted to some arbitrary angular range in the L. system may yield a biased sampling.

Again let us measure P_T in units of the particle rest mass; then $\gamma_0 = \sqrt{(P_T^2/\sin^2\theta) + 1}$ and an inequality of the form $\gamma_0^- \leqslant \gamma_\pi \leqslant \gamma_0^+$ goes over into

$$\sin\theta \sqrt{(\gamma_0^-)^2 - 1} \leqslant P_T \leqslant \sin\theta \sqrt{(\gamma_0^+)^2 - 1}\,.$$

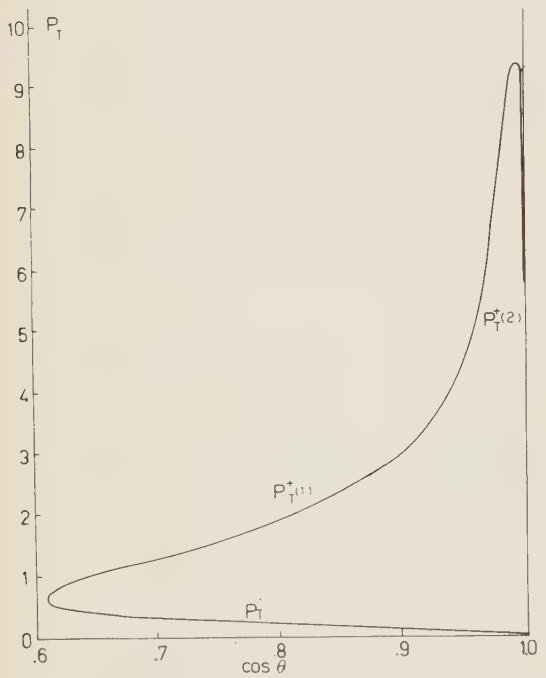

Fig. 2. – Allowed region in the P_T-cos θ (specifically here for $\gamma > \bar{\gamma}_0^M$, $\gamma = 10$, $\bar{\gamma}_0^M = 8$).

The allowed region in the P_T-cos θ plane lies inside the curves defined by

$$P_T^{\pm} = \sin\theta \sqrt{(\gamma_0^{\pm})^2 - 1}\,.$$

The shape of such curves is shown in Fig. 2 for the case $\gamma = 10$; $\bar{\gamma}_0^M = 8$. It is clear from this that if one restricts observations to arbitrary domains of θ, that biases are introduced. It is seen that along the branches labelled $P_T^+(i)$, cos θ is double valued while along P_T^-, it is single valued. For

$$0 \leqslant P_T \leqslant \bar{\beta}_0^M \beta \left[1 - \left(\frac{\bar{\gamma}_0^M}{\gamma}\right)^2\right]^{\frac{1}{2}},$$

cos θ varies between the limits defined by

$$P_T^- = \sin\theta \sqrt{(\gamma_0^-)^2 - 1} \quad \text{and} \quad P_T^+(2) = \sin\theta \sqrt{(\gamma_0^+)^2 - 1};$$

for

$$\beta_0^M \beta \left[1 - \left(\frac{\bar{\gamma}_0^M}{\gamma}\right)^2\right]^{\frac{1}{2}} \leqslant P_T \leqslant \sqrt{(\gamma_2^{\max})^2 - 1}\,,$$

$\cos\theta$ varies between the limits defined by

$$P_T^{+}(i) = \sin\theta\sqrt{(\gamma_0^{+})^2 - 1}\,, \qquad i = 1 \text{ and } 2.$$

These limits are rather complicated algebraic expressions for cases i) and iii) and we give them only for case ii), $\bar{\gamma}_0^{M} = \gamma$ for which they are

$$(10) \qquad \left\{\frac{(P_T^2 + 2) - (2/\gamma\beta)\sqrt{(\gamma\beta)^2 - P_T^2}}{4 + \beta^2 P_T^2}\right\}^{\frac{1}{2}} \leqslant \cos\theta \leqslant \left\{\frac{(P_T^2+2) + (2/\gamma\beta)\sqrt{(\gamma\beta)^2 - P_T^2}}{4 + \beta^2 P_T^2}\right\}^{\frac{1}{2}}.$$

In this case (now in the L. system)

$$(11) \qquad F(P_T) = 2\pi P_T \int_{\theta_-}^{\theta_+} \mathrm{d}\theta \, \frac{F[\gamma_0(P_T, \theta), \theta]}{[P_T^2 + M^2 \sin^2\theta]^{\frac{1}{2}}} \qquad 0 \leqslant P_T \leqslant \gamma\beta, \ \bar{\gamma}_0^{M} = \gamma,$$

where $\theta_{\pm}$ are defined by (10) and $\gamma_0(P_T, \theta)$ is previously given.

It seems appropriate at this point to discuss a little further the biases that may occur in obtaining the P_T distribution experimentally. In high energy interaction studies in which such measurements are made, of necessity one is forced to observations of P_T in a restricted angular range in the L. system. The Japanese group [3] has used the narrow forward cone while other laboratories [4] have in addition used parts of the wide cone. If the c.m. distribution does indeed have symmetry about $\theta = \pi/2$ and the Laboratory sampling corresponds to either $0 \leqslant \theta \leqslant \pi/2$ or $\pi/2 \leqslant \bar{\theta} \leqslant \pi$, then no biases are introduced; if it is otherwise then the observations are subject to bias. It is of course quite difficult to discuss the magnitude of an error introduced without some model for guidance. To obtain some feeling for this we shall consider the average transverse momentum

$$(12) \qquad \langle P_T \rangle = \iint F(\bar{\gamma}_0, \bar{\theta}) \sqrt{\bar{\gamma}_0^2 - 1} \sin\bar{\theta} \, \mathrm{d}\bar{\gamma}_0 \, \mathrm{d}\bar{\Omega} \,.$$

For this average to correspond to an experimental determination $F(\bar{\gamma}_0, \bar{\theta})$ must be normalized to unity in the c.m. system corresponding to the range of observation in the L. system. Suppose $F(\bar{\gamma}_0, \bar{\theta}) = N/\bar{\gamma}_0^2$, a Heisenberg [5]

---

[4] B. Edwards, J. Losty, D. H. Perkins, K. Pinkau and J. Reynolds: *Phil. Mag.*, **3**, no. 27, 237 (1958); M. Schein: Pvt. Comm. from the Chicago Group.

[5] W. Heisenberg: *Zeits. Phys.*, **133**, 65 (1952).

type of spectrum; here N is the normalization constant. A complete sampling yields

$$\langle P_T\rangle_0 = \frac{\pi}{4}\int_1^{\bar\gamma_0^M} \mathrm{d}\bar\gamma_0 \frac{\sqrt{\bar\gamma_0^2-1}}{\bar\gamma_0^2} \Big/ \int_1^{\bar\gamma_0^M} \frac{\mathrm{d}\bar\gamma_0}{\bar\gamma_0^2} = \frac{\pi}{4}\left(\frac{\log\left[\bar\gamma_0^M(1+\bar\beta_0^M)\right]-\bar\beta_0^M}{\bar\gamma_0^M-1}\right)\bar\gamma_0^M . \tag{13}$$

On the other hand a laboratory sampling over some defined range of angles and energies (such that a momentum measurement is possible) will correspond to a definition of a certain angular and energy range in the c.m. system.

We consider the case $\bar\gamma_0^M > \gamma$ and laboratory observations corresponding to $\theta > \pi/2$. The only that part of the c.m. energy spectra $\bar\gamma_0 > \gamma$ is being sampled corresponding to an angular range in the c.m. system, $-1 \leqslant \cos\bar\theta \leqslant -\beta/\bar\beta_0$. Thus for this case the normalization factor N is given by

$$\frac{1}{N} = 2\pi\int_\gamma^{\bar\gamma_0^M} \frac{\mathrm{d}\bar\gamma_0}{\bar\gamma_0^2}\left(1-\frac{\beta}{\beta_0}\right),$$

and

$$\langle P_T\rangle_{\mathrm{Exp.}} = 2\pi N\int_\gamma^{\bar\gamma_0^M} \frac{\mathrm{d}\bar\gamma_0}{\bar\gamma_0^2}\sqrt{\bar\gamma_0^2-1}\int_{\cos^{-1}(-\beta/\bar\beta_0)}^{\pi}\sin^2\bar\theta\,\mathrm{d}\bar\theta , \tag{14}$$

for the case that both $\gamma \gg 1$ and $\bar\gamma_0^M \gg 1$ we have approximately

$$\langle P_T\rangle_{\mathrm{Exp.}} = \frac{\gamma\bar\gamma_0^M}{\sqrt{2}\,(\bar\gamma_0^M-\gamma)\,(1-\beta)}\left[(1-\beta)^{\frac{3}{2}}\log\left(\frac{\sqrt{\bar\beta_0^M-\beta}+\sqrt{1-\beta}}{1-\bar\beta_0^M}-\right.\right.$$
$$\left.\left.-\,(\bar\beta_0^M-\beta)^{\frac{1}{2}}\left(\frac{\bar\beta_0^M\beta}{3}-(1-\beta)\right)\right)\right].$$

For example for $\bar\gamma_0^M = 100$ and $\gamma = 50$ we find $\langle P_T\rangle_0 = 3.42$ and $\langle P_T\rangle_{\mathrm{exp}} = 5.18$. Though this is not a tremendous difference it is intended to illustrate the point in question and to underline the fact that measurements of P_T using different sampling can yield misleading results. For the Heisenberg model we have approximately at very high energies $\gamma_0^M = \exp\left[2(M/\mu)(\eta/c)\gamma^{\frac{1}{2}}\right]$, where M/μ is the nucleon to particle mass ratio, η is the inelasticity of the collision and c is a constant in the relation giving the variation of average multiplicity with laboratory energy of the incident proton $N = C(E_p/M)^{\frac{1}{4}}$. For π-mesons $C \sim 3$ and $\eta \sim 0.2$ and one has that $\bar\gamma_0^M > \gamma$ for $\gamma \geqslant 15$ (corresponding to a laboratory energy of about 450 GeV for the incident proton).

4. – The distribution of γ-rays arising from π^0-decay.

We begin by considering the differential (in energy and angle) γ-ray spectrum arising from the decay of a single π^0-meson moving with energy $\bar{E}_\pi = \bar{\gamma}_\pi \mu$ and velocity (in units of c) $\bar{\boldsymbol{\beta}}_\pi$. In the rest system of the π^0 the differential γ-ray spectrum (normalized to unity) is

$$\Gamma_R(\bar{E}'_\nu, \bar{\theta}'_\nu) = \frac{1}{4\pi}\,\delta(\bar{E}'_\nu - 1)\,, \tag{15}$$

where we measure the γ-ray energy in units of $\mu/2$ ($\frac{1}{2}$ the π^0-rest mass). The distribution in the system with respect to which the π^0 has velocity $\bar{\boldsymbol{\beta}}_\pi$ is using (1*b*) with $M = 0$

$$\Gamma_{\bar{\pi}}(\bar{E}_\nu, \bar{\theta}_\nu) = \frac{\delta[\bar{\gamma}_\pi \bar{E}_\nu(1 - \bar{\boldsymbol{\beta}}_\pi \cdot \boldsymbol{t}) - 1]}{4\pi\bar{\gamma}_\pi(1 - \bar{\boldsymbol{\beta}}_\pi \cdot \boldsymbol{t})}\,, \tag{16}$$

$$\bar{\gamma}_\pi(1 - \bar{\beta}_\pi) \leqslant \bar{E}_\nu \leqslant \bar{\gamma}_\pi(1 + \bar{\beta}_\pi)\,,$$

where $\boldsymbol{t}$ is a unit vector in the direction of the γ-ray. This is the well known result that the energy distribution of γ-rays from a single π^0-decay of fixed velocity is a square pulse whose limits are given above.

In general one is interested in obtaining the γ-ray distribution arising from some given energy and angular distribution of the π^0. If this distribution, which we may think of as being given in the c.m. can be written as $F(\bar{E}_\pi, \bar{\theta}_\pi) = f_1(\bar{E}_\pi) f_2(\bar{\theta}_\pi)$, it then suffices to consider only the angular distribution a fixed π^0 energy since

$$f_1(\bar{E}_\pi) = \int \mathrm{d}\bar{E}'_\pi \delta(\bar{E}'_\pi - \bar{E}_\pi) f_1(\bar{E}'_\pi)\,.$$

This is the case we shall consider since it seems the only one susceptible to a general treatment (6). This being the case, we may write

$$f_2(\bar{\theta}_\pi) = \sum_l A_l P_l(\cos\bar{\theta}_\pi)\,, \tag{17}$$

which we assume normalized to unity. We then seek the γ-ray distribution arising from the angular distribution of π^0 in the reference system (c.m.)

(6) The possibility of obtaining the result in this form was pointed out by Prof. J. B. French.

of (17). The co-ordinate system and notation is defined in Fig. 3. We have then

$$\Gamma_{\text{c.m.}}(\bar{E}_\nu, \bar{\theta}_\nu) = \frac{1}{4\pi\bar{\gamma}_\pi}\int_0^\pi \sin\bar{\theta}_\pi \,\mathrm{d}\bar{\theta}_\pi \int_0^{2\pi} \mathrm{d}\bar{\varphi}_\pi \frac{\delta[\bar{\gamma}_\pi \bar{E}_\nu(1-\boldsymbol{\beta}_\pi\cdot\boldsymbol{t})-1]}{1-\boldsymbol{\beta}_\pi\cdot\boldsymbol{t}} \sum_l A_l P_l(\cos\bar{\theta}_\pi).$$

Using the spherical harmonic addition theorem we have

$$P_l(\boldsymbol{\epsilon}_0\cdot\boldsymbol{\eta}) = P_l(\boldsymbol{\epsilon}_0\cdot\boldsymbol{t})\, P_l(\boldsymbol{\eta}\cdot\boldsymbol{t}) + 2\sum_{m=1}^{l}\frac{(l-m)!}{(l+m)!}\cos m(\bar{\varphi}_\pi - \bar{\varphi}_\nu) P_l^m(\boldsymbol{\epsilon}_0\cdot\boldsymbol{t}) P_l^m(\boldsymbol{\eta}\cdot\boldsymbol{t}).$$

We use $\boldsymbol{t}$ as an axis for integration over $\mathrm{d}\bar{\Omega}_\pi$ and note that the term involving $\sum_m$ vanishes on the $\bar{\varphi}_\pi$ integration. Performing the integration $\sin\bar{\theta}_\pi \mathrm{d}\bar{\theta}_\pi = -\mathrm{d}(-\boldsymbol{t}\cdot\boldsymbol{\eta})$ using the properties of the δ-function we have

$$\Gamma_{\text{c.m.}}(\bar{E}_\nu, \bar{\theta}_\nu) = \frac{1}{2\bar{\gamma}_\pi\bar{\beta}_\pi}\sum_l A_l P_l(\cos\bar{\theta}_\nu) P_l\left[\frac{1}{\bar{\beta}_\pi}\left(1-\frac{1}{\bar{\gamma}_\pi\bar{E}_\nu}\right)\right] \tag{18}$$

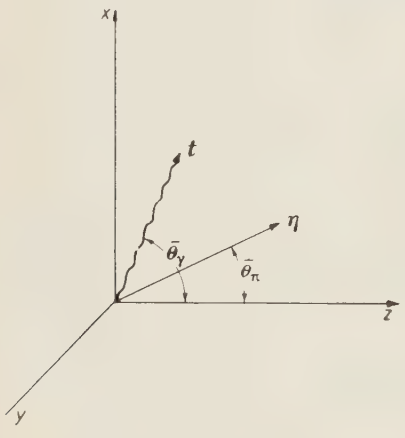

$\boldsymbol{\epsilon}$ is a unit vector in Z direction
$\boldsymbol{\eta}$ is a unit vector in π^0 direction
$\boldsymbol{t}$ is a unit vector in γ-ray direction

Fig. 3. – Coordinate system and particle directions in c.m. system used for integrations.

for $\bar{\gamma}_\pi(1-\bar{\beta}_\pi) \leqslant \bar{E}_\nu \leqslant \bar{\gamma}(1+\bar{\beta}_\pi)$; $=0$ otherwise.

We are next interested in obtaining the γ-ray distribution in the laboratory system of reference. As before let γ and β be the Lorentz factor and velocity of the c.m. with respect to the L. system. We have $\bar{E}_\nu = \gamma E_\nu(1-\beta\cos\theta_\nu)$ and

$$\cos\bar{\theta}_\nu = \frac{\cos\theta_\nu - \beta}{1-\beta\cos\theta_\nu},$$

where, as previously, the unbarred quantities refer to the L. system (clearly we are going to transform using as before the direction defined by $\boldsymbol{\beta}$ as the polar axis in each system). Applying (1*b*) again appropriately and with the relation above we have

$$\Gamma_L(E_\nu, \theta_\nu) = \frac{1}{2\bar{\gamma}_\pi\bar{\beta}_\pi\gamma(1-\beta\cos\theta_\nu)}\sum_l A_l P_l \cdot \left(\frac{\cos\theta_\nu-\beta}{1-\beta\cos\theta_\nu}\right) P_l\left[\frac{1}{\bar{\beta}_\pi}\left(1-\frac{1}{\bar{\gamma}_\pi\gamma E_\nu(1-\beta\cos\theta_\nu)}\right)\right],$$

$$\text{for } \frac{\bar{\gamma}_\pi(1-\beta_\pi)}{\gamma(1-\beta\cos\theta_\nu)} \leqslant E_\nu \leqslant \frac{\bar{\gamma}_\pi(1+\beta_\pi)}{\gamma(1-\beta\cos\theta_\nu)}; \quad = 0 \text{ otherwise}.$$

A special case of the above has been quoted by COCCONI and SILVERMAN [7] (*i.e.* $f_2(\bar{\theta}_\pi) = A + B\cos^2\bar{\theta}_\pi = (A + (B/3))P_0 + 2/3BP_2$).

From (19) one may obtain $\Gamma_L(\theta_\nu)$ and $\Gamma_L(E_\nu)$, respectively the angular distribution (irrespective of energy) and the energy distribution (irrespective of angle) by integrating, with appropriate limits, over E_ν or θ_ν as the case may be. Here again, the limits depend on the relative magnitude of γ and $\bar{\gamma}_\pi$ and we have again the three cases to consider; i) $\bar{\gamma}_\pi < \gamma$; ii) $\bar{\gamma}_\pi = \gamma$ and iii) $\bar{\gamma}_\pi > \gamma$. As before ii) is obtained as a limiting case of either i) or iii).

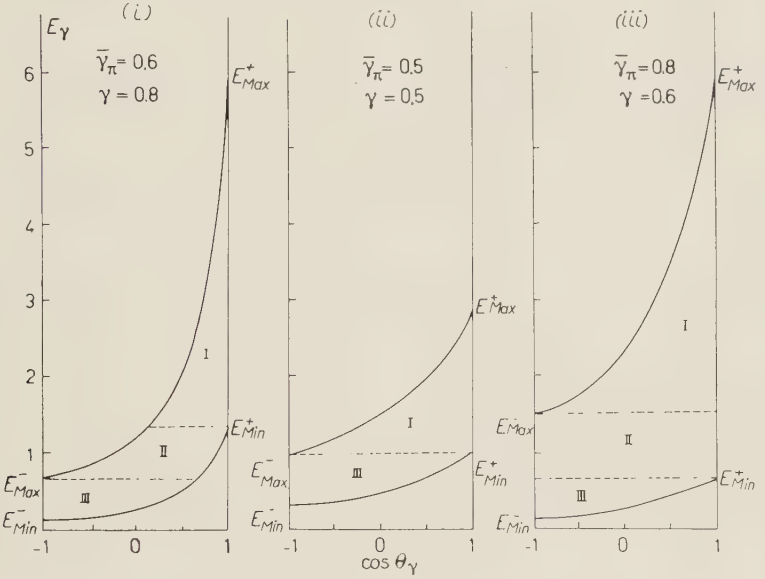

Fig. 4. – Allowed region in the E_ν-$\cos\theta$ plane for cases (i), (ii) and (iii).

As illustration we consider i) in some detail. The allowed region in the E_ν-$\cos\theta_\nu$ plane is illustrated in Fig. 4 and lies between the two curves labelled E_{min} and E_{max}. The labelled ordinates are:

$$E^{\pm}_{max} = \frac{\bar{\gamma}_\pi(1 + \bar{\beta}_\pi)}{\gamma(1 \mp \beta)}; \qquad E^{\pm}_{min} = \frac{\gamma_\pi(1 - \beta_\pi)}{\gamma(1 \mp \beta)}.$$

It is seen from the figure that the following inequalities define the limits of

---

[7] F. COCCONI and A. SILVERMAN: *Phys. Rev.*, **88**, 1230 (1952).

integration on θ_ν for the three regions in case i) $\bar{\gamma}_\pi < \gamma$,

$$(20a)\ \text{(i)}\quad \begin{cases} \text{I}_{(i)} & \dfrac{1}{\beta}\left[1-\dfrac{\bar{\gamma}_\pi(1+\bar{\beta}_\pi)}{\gamma E_\nu}\right] \leqslant \cos\theta_\nu \leqslant 1; & E^+_{\min} \leqslant E_\nu \leqslant E^+_{\max}; \\ \text{II}_{(i)} & \dfrac{1}{\beta}\left[1-\dfrac{\gamma_\pi(1+\beta_\pi)}{\gamma E_\nu}\right] \leqslant \cos\theta_\nu \leqslant \dfrac{1}{\beta}\left[1-\dfrac{\gamma_\pi(1-\beta_\pi)}{\gamma E_\nu}\right]; & E^-_{\max} \leqslant E_\nu \leqslant E^+_{\min}; \\ \text{III}_{(i)} & -1 \leqslant \cos\theta_\nu \leqslant \dfrac{1}{\beta}\left[1-\dfrac{\bar{\gamma}_\pi(1-\bar{\beta}_\pi)}{\gamma E_\nu}\right]; & E^-_{\min} \leqslant E_\nu \leqslant E^-_{\max}; \end{cases}$$

a similar consideration yields for ii) and iii) the following: for ii) $\bar{\gamma}_\pi = \gamma$ the middle region vanishes and we have with $\bar{\beta}_\pi = \beta$

$$(20b)\ \text{(ii)}\quad \begin{cases} \text{I}_{(ii)} & \dfrac{1}{\beta}\left[1-\dfrac{(1+\beta)}{E_\nu}\right] \leqslant \cos\theta_\nu \leqslant 1; & 1 \leqslant E_\nu \leqslant \dfrac{1+\beta}{1-\beta}; \\ \text{III}_{(ii)} & -1 \leqslant \cos\theta_\nu \leqslant \dfrac{1}{\beta}\left[1-\dfrac{(1-\beta)}{E_\nu}\right]; & \dfrac{1-\beta}{1+\beta} \leqslant E_\nu \leqslant 1; \end{cases}$$

and for case iii), $\bar{\gamma}_\pi > \gamma$ we have

$$(20c)\ \text{(iii)}\quad \begin{cases} \text{I}_{(iii)} & \dfrac{1}{\beta}\left[1-\dfrac{\bar{\gamma}_\pi(1+\bar{\beta}_\pi)}{\gamma E_\nu}\right] \leqslant \cos\theta_\nu \leqslant 1; & E^-_{\max} \leqslant E_\nu \leqslant E^+_{\max}; \\ \text{II}_{(iii)} & -1 \leqslant \cos\theta_\nu \leqslant 1; & E^+_{\min} \leqslant E_\nu \leqslant E^-_{\max}; \\ \text{III}_{(iii)} & -1 \leqslant \cos\theta_\nu \leqslant \dfrac{1}{\beta}\left[1-\dfrac{\bar{\gamma}_\pi(1-\bar{\beta}_\pi)}{\gamma E_\nu}\right]; & E^-_{\min} \leqslant E_\nu \leqslant E^+_{\min}. \end{cases}$$

Thus one has

$$(21)\qquad \Gamma_L(E_\nu) = 2\pi \int_{\theta_{\min}}^{\theta_{\max}} \sin\theta_\nu \, \mathrm{d}\theta_\nu \Gamma_L(E_\nu, \theta_\nu)\,,$$

where $\theta_{\min}$, $\theta_{\max}$ are defined by (20a), (20b) or (20c) and Γ_L by (19). We note that for a given pair of values of β and $\bar{\beta}_\pi$, the range of energies defined for E_ν for the regions I, II, III is the same for cases i) and iii).

To obtain the angular distribution $\Gamma_L(\theta_\nu)$ the situation is quite a bit simpler since for fixed $\cos\theta_\nu$, E_ν satisfies for all three cases

$$(20d)\qquad \frac{\bar{\gamma}_\pi(1-\bar{\beta}_\pi)}{\gamma(1-\beta\cos\theta_\nu)} \leqslant E_\nu \leqslant \frac{\bar{\gamma}_\pi(1+\bar{\beta}_\pi)}{\gamma(1-\beta\cos\theta_\nu)}\,,$$

by making a change of variable from E_ν to X where

$$X = \frac{1}{\bar{\beta}_\pi}\left(1 - \frac{1}{\bar{\gamma}_\pi \gamma E_\nu (1 - \beta \cos\theta_\nu)}\right),$$

the angular distribution is given for all three cases by

$$(22) \qquad \Gamma_L(\theta_\nu) = \frac{1}{2\bar{\gamma}_\pi^2 \gamma^2 (1 - \beta\cos\theta_\nu)^2} \cdot$$

$$\cdot \sum_l A_l P_l\left(\frac{\cos\theta_\nu - \beta}{1 - \beta\cos\theta_\nu}\right) \int_{-1}^{1} \frac{\mathrm{d}X}{(1 - \bar{\beta}_\pi X)^2} P_l(X).$$

If the π^0 energy spectrum is not a δ function then the limits require again more consideration. With our previous assumption we have the spectrum $f_1(\bar{E}_\pi)$ (or $f_1(\bar{\gamma}_\pi)$) which is assumed normalized to unity, and we desire $\Gamma_L(E_\nu, \theta_\nu)$ integrated over the π^0 energy spectrum. The situation is represented schematically in Fig. 5; here the allowed region for fixed θ_ν is represented in the E_ν-$\bar{\gamma}_\pi$ plane. A fixed value of E_ν is obtained for region A or B by a variation of $\bar{\gamma}_\pi$ from the value defined by E_ν^+ or E_ν^- respectively to $\bar{\gamma}_\pi^M$, where $\bar{\gamma}_\pi^M$ is the maximum π^0 energy in the c.m. system. The two regions yield the same limits and we have

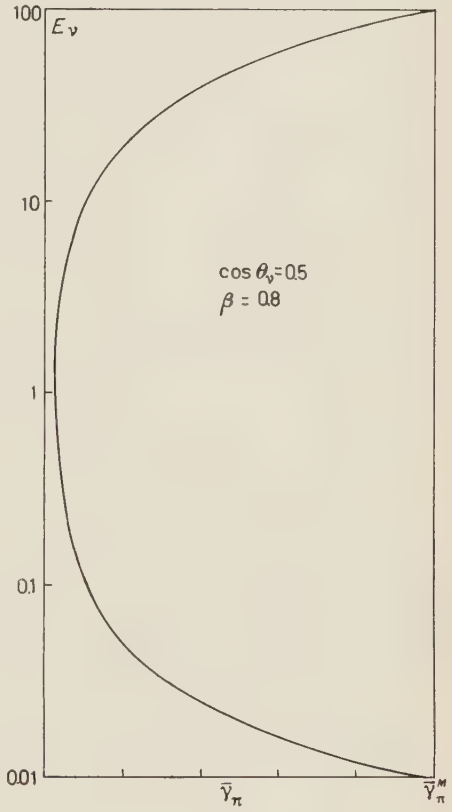

Fig. 5. – Allowed region in the E_ν-$\bar{\gamma}_\pi$ plane.

$$(23a) \qquad \bar{\gamma}_\pi^{\min} = \frac{\gamma^2 E_\nu^2 (1 - \beta\cos\theta_\nu)^2 + 1}{2\gamma E_\nu (1 - \beta\cos\theta_\nu)} \leqslant \bar{\gamma}_\pi \leqslant \bar{\gamma}_\pi^M = \bar{\gamma}_\pi^{\max},$$

$$(23b) \qquad E_\nu^-(\theta_\nu) = \frac{\bar{\gamma}_\pi^M (1 - \bar{\beta}_\pi^M)}{\gamma(1 - \beta\cos\theta_\nu)} \leqslant E_\nu \leqslant \frac{\bar{\gamma}_\pi^M (1 + \bar{\beta}_\pi^M)}{\gamma(1 - \beta\cos\theta_\nu)} = E_\nu^+(\theta_\nu),$$

so that

$$(24) \qquad \Gamma_L(E_\nu, \theta_\nu) = \frac{1}{2\gamma(1 - \beta\cos\theta_\nu)} \sum_l A_l P_l\left(\frac{\cos\theta_\nu - \beta}{1 - \beta\cos\theta_\nu}\right) \int_{\bar{\gamma}_\pi^{\min}}^{\bar{\gamma}_\pi^M} \frac{\mathrm{d}\bar{\gamma}_\pi f_1(\bar{\gamma}_\pi)}{\bar{\gamma}_\pi \bar{\beta}_\pi} \cdot$$

$$\cdot P_l\left|\frac{1}{\bar{\beta}_\pi}\left(1 - \frac{1}{\gamma E_\nu \bar{\gamma}_\pi (1 - \beta\cos\theta_\nu)}\right)\right| \quad \text{for } E_\nu^-(\theta_\nu) \leqslant E_\nu \leqslant E_\nu^+(\theta_\nu); \quad = 0 \text{ otherwise}.$$

To obtain either $\bar{I}_L(E_\nu)$ or $\bar{I}_L(\theta_\nu)$ from $\bar{I}_L(E_\nu, \theta_\nu)$ the previous limits, (20*a*), (20*b*), (20*c*) and (20*d*) hold with $\bar{\gamma}_\pi$ and $\bar{\beta}_\pi$ therein replaced by $\bar{\gamma}_\pi^M$ and $\bar{\beta}_\pi^M$.

As an elementary application we consider the case of monoenergetic π^0 produced isotropically in the c.m. system $\left(\sum_l A_l P_l(\cos\bar{\theta}_\pi) = 1/4\pi\right)$. The angular distribution is

$$I_L^0(\theta_\nu) = \frac{1}{4\pi\gamma^2(1-\beta\cos\theta_\nu)^2},$$

and the energy distribution is for case i) $\bar{\gamma}_\pi < \gamma$

$$I_L^0(E_\nu) = \frac{1}{4\gamma\beta\bar{\gamma}_\pi\bar{\beta}_\pi} \begin{cases} \log\dfrac{E_{\max}^+}{E_\nu}, & \text{region I}, \\ \log\dfrac{1+\bar{\beta}_\pi}{1-\bar{\beta}_\pi} & \text{region II}, \\ \log\dfrac{E_\nu}{E_{\min}^-} & \text{region III}. \end{cases}$$

Case iii), $\bar{\gamma}_\pi > \gamma$ is obtained from the above by the replacement $\bar{\beta}_\pi \to \beta$, $\beta \to \bar{\beta}_\pi$ and case ii) can be obtained directly from the above letting $\bar{\beta}_\pi = \beta$ in which case region II disappears. The typical appearance of such a distribution is presented in Fig. 6 (for $\bar{\beta}_\pi = 0.95$, $\beta = 0.99$); it would be the same for $\bar{\beta}_\pi = 0.99$, $\beta = 0.95$, while for $\beta = \bar{\beta}_\pi$ the flat topped region disappears. While these particular distributions are characterized by $I_L^0(E_\nu)$ having a

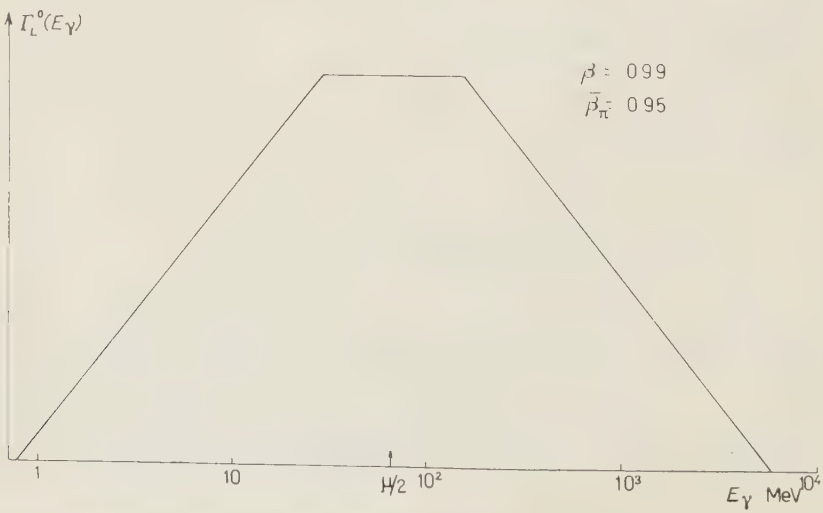

Fig. 6. Laboratory γ-ray energy distribution arising from isotropic c.m. monoenergetic π^0; ($\beta_{\text{c.m.}} = \beta = 0.99$, $\bar{\beta}_\pi = 0.95$).

maximum (or relative maximum) of $E_\nu = 1$ (*i.e.* at $M/2$), the average γ-ray energy is $\langle E_\nu \rangle_0 = \bar{\gamma}_\pi \gamma$.

An important application of these results occurs when the c.m. coincides with the L. system, (*i.e.* $\beta = 0$) and the π^0 distribution is isotropic; *e.g.* π^0 produced in proton-antiproton annihilation at rest or the π^0 production occuring from proton-proton collisions of cosmic rays in a postulated source such as the Crab Nebula ([8]) (here we ignore the small recession velocity). For these assumptions we have $F(\bar{\gamma}_\pi, \bar{\theta}_\pi) = (1/4\pi) f_1(\bar{\gamma}_\pi)$ so that $\sum_l A_l P_l = 1/4\pi$. Then from (24) with $\beta = 0$ we find

$$(25) \qquad \bar{I}_L^0(E_\nu, \theta_\nu) = \frac{1}{8\pi} \int_{\frac{E_\nu^2+1}{2E_\nu}}^{\bar{\gamma}_\pi^M} \mathrm{d}\bar{\gamma}_\pi \frac{f_1(\bar{\gamma}_\pi)}{\sqrt{\bar{\gamma}_\pi^2 - 1}}; \quad \sqrt{\frac{1-\beta_\pi^M}{1+\beta_\pi^M}} \leqslant E_\nu \leqslant \sqrt{\frac{1+\beta_\pi^M}{1-\beta_\pi^M}};$$

$= 0$ otherwise.

By differentiating $\bar{I}_L^0(E_\nu, \theta_\nu)$ with respect to E_ν we find that maximum occurs at $E_\nu = 1$ regardless of the form of $f_1(\bar{\gamma}_\pi)$. Further, one can easily show that

$$f_1\left(\frac{E_\nu^2+1}{2E_\nu}\right) = -\frac{E_\nu}{E_\nu+1} \frac{\partial \bar{I}_L^0(E_\nu, \theta_\nu)}{\partial E_\nu} \qquad \text{for } E_\nu > 1,$$

$$= \frac{E_\nu}{E_\nu+1} \frac{\partial \bar{I}_L^0(E_\nu, \theta_\nu)}{\partial E_\nu}. \qquad \text{for } E_\nu < 1.$$

Thus from observations on the γ-ray energy distribution (which is isotropic) one may construct the form of the π^0 energy spectrum in the system of observation. For the astronomical application alluded to, this is the laboratory π^0 energy distribution integrated over the proton energy spectrum.

Finally we consider the transverse momentum distribution of the γ-rays. Again it is simpler to work from the c.m. system. We have (adapting (9)) for a general distribution

$$F_\nu(P_T) = 2\pi \int_{\bar{\theta}_{\min}}^{\bar{\theta}_{\max}} \mathrm{d}\bar{\theta}_\nu \bar{I}_{\text{c.m.}}[\bar{\theta}_\nu, \bar{E}_\nu(P_T, \bar{\theta}_\nu)]; \qquad \bar{E}_\nu = \frac{P_T}{\sin \bar{\theta}_\nu},$$

and for our particular case

$$(28) \qquad F_\nu(P_T) = \pi \sum_l A_l \int_{\theta_{\min}}^{\bar{\theta}_{\max}} \mathrm{d}\theta_\nu P_l(\cos \theta_\nu) \int_{\frac{P_T + \sin^2 \bar{\theta}_\nu}{2P_T \sin \bar{\theta}_\nu}}^{\bar{\gamma}_\pi^M} \mathrm{d}\gamma_\pi f_1(\bar{\gamma}_\pi) \frac{P_l[1/\beta_\pi(1 - \sin \bar{\theta}_\nu/\gamma_\pi)]}{\sqrt{\gamma_\pi^2 - 1}},$$

([8]) G. R. Burbidge: *Astrophys. Journ.*, **127**, 48 (1958).

where

$$1-P_T^2\frac{(1+\bar{\beta}_\pi^M)}{(1-\bar{\beta}_\pi^M)}\leqslant\cos^2\bar{\theta}\leqslant 1-P_T^2\frac{(1-\bar{\beta}_\pi^M)}{(1+\bar{\beta}_\pi^M)};\qquad 0\leqslant P_T\leqslant\sqrt{\frac{1-\bar{\beta}_\pi^M}{1+\bar{\beta}_\pi^M}}.$$

and

$$0\leqslant\cos^2\bar{\theta}_\nu\leqslant 1-P_T^2\frac{(1-\bar{\beta}_\pi^M)}{(1+\bar{\beta}_\pi^M)};\qquad \sqrt{\frac{1-\bar{\beta}_\pi^M}{1+\bar{\beta}_\pi^M}}\leqslant P_T\leqslant\sqrt{\frac{1+\bar{\beta}_\pi^M}{1-\bar{\beta}_\pi^M}}=P_T^{\max},$$

and $F_\nu(P_T)=0$ otherwise.

In the above limits for $\bar{\theta}_\nu$, the positive $\sqrt{\cos^2\bar{\theta}_\nu}$ is taken for $0\leqslant\bar{\theta}_\nu\leqslant\pi/2$ and the negative root for $\pi/2\leqslant\bar{\theta}_\nu\leqslant\pi$. If the angular distribution is an even function of $\cos\bar{\theta}_\nu$, then one need take only the limits for $0\leqslant\bar{\theta}_\nu\leqslant\pi/2$ and multiply the result by two. It is clear here that the same admonition discussed previously with respect to experimental determination of transverse momentum distribution applies here also.

RIASSUNTO (*)

Si sottolinea, e se ne dà un esempio, l'utilità delle proprietà invarianti nel calcolare varie grandezze cinematiche importanti nella fisica delle particelle. Si danno formule generali riferentisi alla trasformazione della distribuzione da un sistema di Lorentz ad un altro e se ne mostrano gli usi. Se ne fa un'applicazione particolare alla distribuzione di raggi γ derivanti dal decadimento del π^0.

(*) *Traduzione a cura della Redazione.*

IL NUOVO CIMENTO Vol. XV, N. 4 16 Febbraio 1960

A Soluble Model in Field Theory.

II. – Unstable particle and bound state description.

E. Kazes

Physics Department, The Pennsylvania State University - University Park, Pa.

(ricevuto il 19 Ottobre 1959)

Summary. — Examining a model presented earlier we performed a calculation of unstable particle production and decay without separating these two processes. The usual separation of production and decay is seen to be valid for a time t, such that

$$\frac{\hbar}{\mu_3 c^2} \ll t \ll 2\tau \ln 2\pi\tau t^2 Q^3 , \qquad Q \gg \frac{1}{\tau} ,$$

where Q is the energy above threshold for unstable particle production and τ is the lifetime. When the above conditions are valid the unstable states possess a simple enough time development to be characterized with a particle label. Our model also predicts bound state production for suitable cut-off functions. The Nishijima-Zimmermann formalism for handling bound states in conjunction with dispersion relations reproduces direct calculations.

Introduction.

In a previous paper to be referred to as (I) a generalization of the Lee model was presented and its solution given with the restriction that the free and complete Hamiltonians possess the same stable one particle states. In order to examine closely a somewhat realistic description of unstable particle production, which are created by strong interactions and decay by a different

(*) Supported in part by the Atomic Energy Commission under Contract no. AT(30-1)-2399.

(I) E. Kazes: *Nuovo Cimento*, **14**, 815 (1959).

mode, our previous model has been modified such that $m_3 > m_4 + \mu_4$. Of course in this case there is not a stable ψ_3 particle and the meaning attached to the particle label must be closely examined. In previous treatments of unstable particles it is assumed that such a system is suitably prepared at some arbitrary time to correspond to a bare unstable particle and then its time development is determined by the Schrödinger equation ([1-5]). This description is of course arbitrary and does not take into account the production mechanism which should affect the space-time development of all end products. It will be shown that this customary separation of the production and decay of an unstable particle is an approximation that is very good in most experiments for life-times larger than 10^{-17} s.

In our model we have examined the scattering state of the ψ_2, φ_2 particles and identified unstable particle production with that part of the end products that decrease faster than $1/r$ at large distances. Examination of the $\psi_2 + \varphi_2 \to \psi_4 + \varphi_4 + \varphi_3$ production amplitude reveals that there is a resonance at an energy $\omega_3 \simeq m_2 + \omega_2 - m_3$ instead of a pole that is present when ψ_3 is stable. By a suitable choice of the cut-off the model also predicts a bound state of ψ_4, φ_4 particles of mass $M < m_4 + \mu_4$. In this case the production amplitude has a pole for $m_2 + \omega_2 = M$.

The unstable particle production amplitude reveals that exponential decay is not valid for very large times or for a very broad resonance, a fact which was first pointed out by KHALFIN ([6]), and in the region where it is valid the renormalized unstable particle mass has an observable meaning and is the quantity required to conserve energy. Furthermore, the deviation from exponential decay occurs earlier as the production energy approaches threshold. For a broad resonance the space-time development of the unstable products is not a pure exponential but a superposition of them, in this case more than a few parameters are required to specify the time development of the system and the particle label with its underlying simplicity assumption is not valid. For example the (3.3) resonance in pion-nucleon scattering should not be thought as the decay of an unstable particle.

To examine the NISHIJIMA ([7]) and ZIMMERMANN ([8]) formalism of bound

([1]) V. GLASSER and G. KÄLLEN: *Nucl. Phys.*, **2**, 706 (1956).

([2]) R. OKABAYASHI and S. SATO: *Prog. Theor. Phys.*, **17**, 30 (1957).

([3]) H. ARAKI, Y. MUNAKATA, M. KARVAGUCHI and T. GOTÔ: *Prog. Theor. Phys.*, **17**, 419 (1957).

([4]) G. HÖHLER: *Zeits. f. Phys.*, **152**, 546 (1958).

([5]) M. LÉVY: *Nuovo Cimento*, **13**, 115 (1959).

([6]) L. A. KHALFIN: *Dokl. Akad. Nauk, S.S.S.R.* **111**, 345 (1956); **115**, 227 (1957) also *Journ. Exp. Theor. Phys.*, **6**, 1053 (1958).

([7]) K. NISHIJIMA: *Prog. Theor. Phys.*, **17**, 765 (1957).

([8]) W. ZIMMERMANN: *Nuovo Cimento*, **10**, 597 (1958).

states, direct and dispersion theoretical calculations of stable particle production and scattering are compared, and the results are shown to be identical. It may be surmized that dispersion relations are valid even when the spectra of the complete and bare Hamiltonians are different in more realistic models.

1. – Unstable particles.

In the stable particle description of reference (I) the bare masses were related to the renormalized quantities through the eigenvalue problem

$$\left| \begin{array}{l} H|\psi_1\rangle = m_1|\psi_1\rangle\,, \\ H|\psi_3\rangle = m_3|\psi_3\rangle\,. \end{array} \right. \tag{1.1}$$

Since for an unstable ψ_3 particle the second of the above equations is not valid we shall merely define m_3 in terms of the bare mass m_3^0 such that

$$\left| \begin{array}{l} m_3 = m_3^0 + \delta m_3\,, \\ \delta m_3 = g_4^{0^2} \sum\limits_{k} \dfrac{R(\omega_4)^2}{2\omega_4 V} \dfrac{P}{m_3 - m_4 - \omega_4}\,, \end{array} \right. \tag{1.2}$$

and later relate it to the mass of the unstable particle under a suitable measurement.

We shall use a strong enough cut-off to produce convergence throughout and will later define renormalized coupling constants in a way that is convenient for dispersion relations, that is as the residue at the pole.

The observed mass M_λ of any stable state having the same quantum numbers as the ψ_3 field is determined from the equation

$$D^0(M_\lambda) = 0\,, \tag{1.3}$$

where

$$D^0(x) = x - m_3^0 - g_4^{0^2} \sum_{k} \frac{R(\omega_4)^2}{2\omega_4 V} \frac{P}{x - m_4 - \omega_4}\,, \tag{1.4}$$

thus although an unstable particle of mass m_3 obeys equation (1.3) the wave function of this state is given by

$$|\Psi(M_\lambda)\rangle = Z_2^{\frac{1}{2}}(M_\lambda) \left| |0,\,0,\,1,\,0;\,0,\,0,\,0\rangle + \right. \\ \left. - g_4^0 \sum_{k} \frac{R(\omega_4)}{(2\omega_4 V)^{\frac{1}{2}}} \frac{P}{M_\lambda - m_4 - \omega_4} |0,\,0,\,0,\,1;\,0,\,0,\,k\rangle \right|, \tag{1.5}$$

and for $M_\lambda = m_3$, $Z_2(m_3) = 0$. This formally shows that $|\psi_3\rangle$ is not a meaningful eigenstate of H. There will be additional roots to equ. (1.3) for $M_\lambda < m_4 + \mu_4$ if

$$m_4 + \mu_4 - m_3^0 > g_4^{0^2} \sum_k \frac{R(\omega_4)^2}{2\omega_4 V} \frac{1}{\mu_4 - \omega_4}, \tag{1.6}$$

since $x - m_3^0$ goes to $-\infty$ as $x \to -\infty$ whereas the sum in equ. (1.4) goes to zero.

Of course such a root corresponds to a bound state of the ψ_4, φ_4 particles. It is seen that bound state production is compatible with the production of unstable states, since for

$$m_3 > m_4 + \mu_4$$

from equ. (1.2) and (1.6)

$$\delta m_3 = g_4^{0^2} \sum_k \frac{R(\omega_4)^2}{2\omega_4 V} \frac{P}{m_3 - m_4 - \omega_4} > g_4^{0^2} \sum_k \frac{R(\omega_4)^2}{2\omega_4 V} \frac{1}{\mu_4 - \omega_4},$$

and this condition will be satisfied if R is peaked near μ_4.

Since it will be useful to discuss renormalization anew we shall give the amplitudes β, φ, Φ_3, Φ_4 of (I) in terms of unrenormalized quantities,

$$\begin{cases} \beta = \Big[m_2 + \omega_2 + i\varepsilon - (m_1 - \delta m_1) - g_2^{0^2} \sum_{k'} \dfrac{u(\omega_2')^2}{2\omega_2' V} \dfrac{1}{\omega_2 + i\varepsilon - \omega_2'} - \\ \qquad - g_3^{0^2} \sum_k \dfrac{U(\omega_3)^2}{2\omega_3 V} \dfrac{1}{D(m_2 + \omega_2 + i\varepsilon - \omega_3)} \Big]^{-1} g_2^0 \dfrac{u(\omega_2)}{(2\omega_2 V)^{\frac{1}{2}}}, \\ \varphi(k') = \dfrac{g_2^0}{\omega_2 + i\varepsilon - \omega_2'} \dfrac{u(\omega_2')}{(2\omega_2' V)^{\frac{1}{2}}} \beta, \\ \Phi_3(k') = \dfrac{g_3^0}{D(m_2 + \omega_2 + i\varepsilon - \omega_3')} \dfrac{U(\omega_3')}{(2\omega_3' V)^{\frac{1}{2}}} \beta, \\ \Phi_4(k', k'') = \dfrac{g_4^0}{m_2 + \omega_2 + i\varepsilon - (m_4 + \omega_3' + \omega_4'')} \dfrac{R(\omega_4'')}{(2\omega_4'' V)^{\frac{1}{2}}} \Phi_3(k'), \end{cases} \tag{1.7}$$

where

$$D(z) \equiv z - m_3^0 - g_4^{0^2} \sum_k \frac{R(\omega_4)^2}{2\omega_4 V} \frac{1}{z - m_4 - \omega_4}. \tag{1.8}$$

It is seen that

$$(m_2 + \omega_2 - m_3 - \omega_3') \Phi_3(k')$$

which represents the ψ_3, φ_3 production amplitude for stable particles when evaluated on the energy shell, is zero in our case [9].

The cross-section for ψ_4, φ_4, ψ_3 production is seen to have a resonance behavior at $\omega_3 \simeq m_2 + \omega_2 - m_3$ since $\mathrm{Re}\,(m_3 + i\varepsilon) = 0$ by comparison with (1.2) and if

$$\mathrm{Im}\, D(m_3 + i\varepsilon) \ll \mu_3 \tag{1.9}$$

the resonance becomes very narrow.

2. – Co-ordinate representation for unstable states.

It is clear that φ and Φ_4 have a stationary outgoing wave form at large distances. Since $\Phi_3(k)$ is independent of direction and an even function of k

$$\Phi_3(r) = \frac{1}{(2\pi)^{\frac{3}{2}}}\int \exp\,[i\boldsymbol{k}\cdot\boldsymbol{r}]\,\Phi_3(k)\,\mathrm{d}^3k = -\frac{i}{(2\pi)^{\frac{1}{2}}r}\int_{-\infty}^{+\infty}\exp\,[ikrk\,\Phi_3(k)\,\mathrm{d}k\,. \tag{2.1}$$

Letting

$$\mathrm{d}(z) = \frac{z - M}{D(z)}\,,$$

where M is the mass of the only bound ψ_4, φ_4 state, it is clear that $\mathrm{d}(z)$ has a cut along the real axis for

$$\mathrm{Re}\, z > m_4 + \mu_4$$

and

$$\mathrm{d}(z = M) = \frac{1}{D'(M)}\,.$$

It is easily seen that $\mathrm{d}(z)$ has no singularities off the real axis, thus

$$\mathrm{d}(z) = \frac{1}{D'(M)} + \frac{z - M}{\pi}\int_{m_4+\mu_4}^{\infty}\frac{\mathrm{Im}\,\mathrm{d}(x' + i\varepsilon)}{(x' - z)(x' - M)}\,\mathrm{d}x'\,,$$

and

$$\frac{1}{D(x + i\varepsilon)} = \frac{1}{(x + i\varepsilon - M)D'(M)} + \frac{1}{\pi}\int_{m_4+\mu_4}^{\infty}\frac{\mathrm{Im}\, D^{-1}(x' + i\varepsilon)\,\mathrm{d}x'}{x' - x - i\varepsilon}\,. \tag{2.2}$$

---

[9] M. L. Goldberger and S. B. Treiman: *Phys. Rev.*, **113**, 1663 (1959).

For the remainder of this Section we shall assume that there are no bound states and ignore the pole at M. In the co-ordinate representation such a pole corresponds to an asymptotically stationary state.

Using equ. (2.2) in (1.17) and (2.1)

$$\Phi_3(r) = -\frac{i}{2\pi^2 r} g_3^0 \beta \int_{m_4+\mu_4}^{\infty} \mathrm{d}x \,\mathrm{Im}\, D^{-1}(x+i\varepsilon) \int_{\infty}^{\infty} k \frac{U(\omega_3)}{\omega_3^{\frac{1}{2}}} \frac{\exp[ikr]\,\mathrm{d}k}{x+\omega_3-m_2-\omega_2-i\varepsilon}, \tag{2.3}$$

where we have interchanged the k and x integrations. The integrand of the second integral is an analytic function of k in the upper-half complex k-plane outside a cut from $k=i\mu_3$ to $k=i\infty$ and the zeros of the denominator if $U(\omega_3)$ is analytic function of ω_3 in this region. We shall make this assumption throughout.

Defining

$$G(x) = \int_{-\infty}^{\infty} k\,\mathrm{d}k \frac{U(\omega_3)}{\omega_3^{\frac{1}{2}}} \frac{\exp[ikr]}{x+\omega_3-m_2-\omega_2-i\varepsilon} = \tag{2.4}$$

$$= \int_{-\infty}^{+\infty} k\,\mathrm{d}k \frac{U(\omega_3)}{\omega_3^{\frac{1}{2}}} \frac{x-m_2-\omega_2-\omega_3-i\varepsilon}{(x-m_2-\omega_2-i\varepsilon)^2-k^2-\mu_3^2} \exp[ikr],$$

it will be evaluated from the residue at the pole of the integrand and terms of order $\exp[-\mu_3 r]$ coming from the cut, which will be ignored since we are interested in distances large compared to the μ_3 Compton wavelength. The discussion will be limited to energies above the threshold for unstable particle production. When

$$m_4+\mu_4 < x < m_2+\omega_2-\mu_3,$$

or

$$x > m_2+\omega_2+\mu_3,$$

the zeros of the denominator in the integrand of equ. (2.4) are near the real axis in the complex k-plane. Whereas for

$$m_2+\omega_2-\mu_3 < x < m_2+\omega_2+\mu_3$$

the zeros are between the origin and $i\mu_3$. Since at the poles either

$$x-m_2-\omega_2-\omega_3 = 0$$

or

$$x-m_2-\omega_2+\omega_3 = 0$$

for $x > m_2 + \omega_2$, the residue at the pole is zero, and substituting (2.4) in (2.3) we obtain

$$(2.5) \qquad \Phi_3(r) = -\frac{1}{\pi^{\frac{1}{2}} r} g_3^0 \beta \cdot$$

$$\cdot \Bigg[\int_{m_4+\mu_4}^{m_2+\omega_2-\mu_3} \mathrm{d}x (m_2+\omega_2-x)^{\frac{1}{2}} U(m_2+\omega_2-x) \operatorname{Im} D^{-1}(x+i\varepsilon) \exp\left[ir\sqrt{(m_2+\omega_2-x)^2 - \mu_3^2}\right] +$$

$$+ \int_{m_2+\omega_2-\mu_3}^{m_2+\omega_2} \mathrm{d}x (m_2+\omega_2-x)^{\frac{1}{2}} U(m_2+\omega_2-x) \operatorname{Im} D^{-1}(x+i\varepsilon) \exp\left[-r\sqrt{\mu_3^2 - (m_2+\omega_2-x)^2}\right] +$$

$$+ O(\exp[-\mu_3 r]) \Bigg] .$$

In the absence of bounded states it was noted that $D(z)$ has no zeros off the real axis. The zeros on the real axis arising from bound states occur for $\operatorname{Re} z < m_4 + \mu_4$. As has been pointed out by Lévy for the Lee model $R^2(x)$ should have an analytic continuation if the ψ_1, φ_1 forward scattering amplitude satisfies a dispersion relation. For our purpose it will suffice to assume that $R^2(z)$ has no poles above the real axis and for $\operatorname{Re} z > \mu_4$. With these assumptions, the continuation of

$$\operatorname{Im} D^{-1}(x+i\varepsilon) = -\frac{g_4^{0^2}}{4\pi} \frac{R^2(x-m_4)}{|D(x+i\varepsilon)|^2} \sqrt{(x-m_4)^2 - \mu_4^2}\, \theta(x-m_4-\mu_4) ,$$

off the real axis becomes

$$-\frac{g_4^{0^2}}{4\pi} \frac{R^2(z-m_4)}{D(z) D_1(z)} \sqrt{(z-m_4)^2 - \mu_4^2} ,$$

where $D_1(z)$ is the analytic continuation of $D(\omega+i\varepsilon)^*$ off the real axis. And although $D(z)$ has no zeros off the real axis, $D_1(z)$ may have a zero.

It is clear that $D(z)$ and $D_1(z)$ are the continuation of $D(x+i\varepsilon)$ into the first and second Riemann sheets respectively. Thus the zeros of $|D(x+i\varepsilon)|^2$ are those of $D(x+i\varepsilon)$ in the second Riemann sheet, and this zero will be seen to reproduce the decay of an unstable system [1,2].

Letting the zero of $D_1(z)$ below the real axis be $z_0 = x_0 + iy_0$ with $y_0 < 0$, the first integral of equ. (2.5) can be reduced to integrals along C_1 and C_2 (see Fig. 1) and

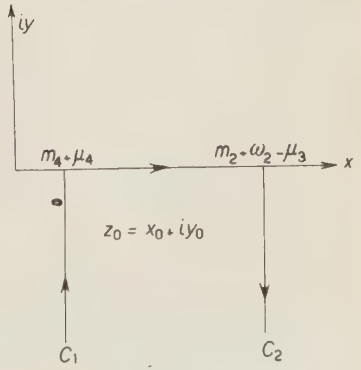

Fig. 1.

a residue;

$$(2.6)\qquad \int_{m_4+\mu_4}^{m_2+\omega_2-\mu_3} \mathrm{d}x\,(m_2+\omega_2-x)^{\frac{1}{2}}\,U(m_2+\omega_2-x)\cdot$$

$$\cdot \operatorname{Im} D^{-1}(x+i\varepsilon)\exp\left[ir\sqrt{(m_2+\omega_2-x)^2-\mu_3^2}\right] = -\frac{g_4^{0^2}\,i}{2}\,(m_2+\omega_2-z_0)^{\frac{1}{2}}\left((z_0-m_4)^2-\mu_4^2\right)^{\frac{1}{2}}\cdot$$

$$\cdot U(m_2+\omega_2-z_0)\,\frac{R^2(z_0-m_4)}{D(z_0)\,D_1'(z_0)}\exp\left[i\sqrt{(m_2+\omega_2-z_0)^2-\mu_3^2}\right] -$$

$$-\left(\int_{C_1}+\int_{C_2}\right)(m_2+\omega_2-z)^{\frac{1}{2}}\,U(m_2+\omega_2-z)\operatorname{Im} D^{-1}(z)\exp\left[ir\sqrt{(m_2+\omega_2-z)^2-\mu_3^2}\right],$$

where

$$D_1'(z) - \frac{\mathrm{d}}{\mathrm{d}z}\,D_1(z)\ \ [10]\,.$$

Should $\Phi_3(r)$ correspond to the wave function of an unstable ψ_3 particle of lifetime $\tau \sim 1/\gamma$, and a stable φ_3 particle at a distance r from one another then one might expect that

$$\Phi_3(r) \sim \frac{1}{r}\exp\left[-\frac{r}{v}\frac{\gamma}{2}\right],$$

where v is the velocity of the stable particle. Of course, for $r\mu_3 \sim 1$ this result will not hold due to the interaction of these two particles. Combining equ. (2.5) and (2.6) it seems that if the resonance of the function D is not very narrow, $\Phi_3(r)$ represents a superposition of decaying amplitudes. In this case the description of ψ_3 as a particle is not desirable since it does not possess the simplicity associated with the notion of a particle. For very large r equ. (2.5) yields

$$(2.7)\qquad \Phi_3(r) = -\frac{2}{\sqrt{\pi}r^3}\,g_3^0\beta\operatorname{Im} D^{-1}(m_2+\omega_2-\mu_3+i\varepsilon)\,\frac{U(\mu_3)}{\sqrt{\mu_3}}\,;$$

this result is in agreement with Khalfin's in that the decay is slower than exponential for large times. We shall later determine the limits in which exponential decay is valid. For a narrow resonance and a distance that is not too

---

[10] It should be noted that the same result would be obtained if in the integrand of the first integral of equ. (2.5) all quantities outside the exponential are approximated by a resonance denominator $(x-m_3)^2+(\gamma/2)^2$ and if all slowly varying quantities are evaluated at $x = m_3$.

large using equ. (2.5) and (2.6)

$$\Phi_3(r) = \frac{g_3^0 i}{2\sqrt{\pi}} \beta g_4^{02} \frac{R^2(z_0 - m_4)}{D(z_0)\, D_1'(z_0)} U(m_2 + \omega_2 - z_0) \cdot \cdot (m_2 + \omega_2 - z_0)^{\frac{1}{2}} ((z_0 - m_4)^2 - \mu_4^2)^{\frac{1}{2}} \frac{\exp\left[ir\sqrt{(m_2 + \omega_2 - z_0)^2 - \mu_3^2}\right]}{r}. \tag{2.8}$$

We now calculate z_0 subject to the condition of a narrow resonance, noting that for z_0 below the real axis

$$\begin{cases} D(z_0) = D^{\nu}(z_0) + \dfrac{g_4^{02}}{4\pi} i R^2(z_0 - m_4)\sqrt{(z_0 - m_4)^2 - \mu_4^2}\,, \\ D_1(z_0) = D^{\nu}(z_0) - \dfrac{g_4^{02}}{4\pi} i R^2(z_0 - m_4)\sqrt{(z_0 - m_4)^2 - \mu_4^2}\,. \end{cases} \tag{2.9}$$

Letting

$$z_0 = m_3 - i\frac{\gamma}{2}, \qquad \gamma > 0, \tag{2.10}$$

and ignoring terms of order $g_4^{02} \cdot \gamma$ it follows from equs. (1.2), (1.4), (2.9) that

$$\begin{cases} \gamma = \dfrac{g_4^{02}}{2\pi} R^2(m_3 - m_4)\sqrt{(m_3 - m_4)^2 - \mu_4^2}\,, \\ D\left(m_3 - i\dfrac{\gamma}{2}\right) = -i\gamma\,. \end{cases} \tag{2.11}$$

Substituting (2.11) in equ. (2.8)

$$\Phi_3(r) = -g_3^0 \beta\sqrt{\pi} \frac{(m_2 + \omega_2 - m_3)^{\frac{1}{2}} U(m_2 + \omega_2 - m_3)}{D_1'(m_3 - i\gamma/2)} \cdot \cdot \frac{\exp[irq_3]}{r} \exp\left[-\frac{r}{v}\frac{\gamma}{2}\right], \tag{2.12}$$

where

$$q_3 = \sqrt{(m_2 + \omega_2 - m_3)^2 - \mu_3^2}\,, \tag{2.13}$$

$$v = \frac{q_3}{m_2 + \omega_2 - m_3}. \tag{2.14}$$

This result has an obvious interpretation as being the wave function of a stable φ_3 particle of momentum q_3 and that of an unstable ψ_3 particle which has decayed by an amount $\exp[-(r/v)(\gamma/2)]$ by the time φ_3 reaches r. From equ. (2.13) it follows that in this process the energy taken by the stable par-

ticle is determined by the renormalized mass m_3. Thus for a narrow resonance and distances that are not too large the decaying part of the scattering state has an interpretation characterized by a few parameters, which is natural to associate with the creation of an unstable ψ_3 particle.

In order to get a transparent estimate of the distance at which non-exponential decay becomes noticeable we take

$$\operatorname{Im} D^{-1}(m_2+\omega_2+i\varepsilon-\mu_3) \simeq -\frac{g_4^{02}}{4\pi}\frac{R^2(m_2+\omega_2-m_4-\mu_3)}{(m_2+\omega_2-\mu_3-m_3)^2}\cdot$$

$$\cdot\sqrt{(m_2+\omega_2-m_4-\mu_3)^2-\mu_4^2}\,\theta(m_2+\omega_2-m_4-\mu_4-\mu_3)\,,$$

$$D_1'\left((m_3-i\frac{\gamma'}{2}\right) \simeq 1\,,$$

in equ. (2.7) and (2.12) respectively, and let

$$n-\frac{r}{v}\gamma'\,.$$

Near the threshold for the production of ψ_3, φ_3 the non-exponential behavior (2.7) exceed the exponential expression (2.12) if

$$\exp[-n/2] < \frac{1}{2\pi}\frac{\gamma^3}{(m_2+\omega_2-m_3-\mu_3)_3}\frac{1}{n^2}\,, \tag{2.15}$$

where n is time measured in units of $1/\gamma$. This shows that deviations from exponential decay appear earlier the closer to threshold the unstable particle is produced. Since equ. (2.7) is sensitive to the energy above threshold it follows that whenever (2.15) is satisfied the decay not only fails to be exponential but is also more sensitive to the details of production. Should production be close enough to threshold for equ. (2.15) to be satisfied in the first few lifetimes, the description of the unstable system as a decaying particle fails and also the separation of production and decay ceases to be valid. Since a particle with a lifetime of 10^{-17} s has $\gamma \simeq 100$ eV, in most experiments dealing with this or larger lifetimes it becomes impossible to satisfy (2.15) for a few lifetimes and the usual separation of production and decay of unstable particles is a very good approximation. Taking $\mu_3 c^2 = 140$ MeV, a kinetic energy for φ_3 of 100 kV above threshold and $\gamma = 100$ eV, equ. (2.15) is valid for $n > 60$. If $\gamma = 10^5$ eV, $n > 5$, but in this case one would not expect exponential decay even for smaller times since the resonance energy falls near the upper bound of the second integral of equ. (2.5) and there is no reason to neglect the contribution of the second integral or the contributions from C_1 and C_2 in equ. (2.6).

3. – Dispersion theory approach.

In this section we shall briefly compare the direct and dispersion theoretical calculation of the ψ_2, φ_2 scattering amplitude in order to determine the limitation imposed if any, by the difference of the spectra of H and H_0. We shall now include the bound ψ_4, φ_4 state $|\psi_3\rangle$ into the spectrum of H, but omit the ψ_3 spectum that is present when $m_3 < m_4 + \mu_4$.

Defining as in (I)

$$f(\omega_2) = g_2 Z_2(1)^{\frac{1}{2}} \frac{u(\omega_2)}{\beta(2\omega_2 V)^{\frac{1}{2}}},$$

and using equ. (1.7) we can extend it analytically as

$$f(z) = Z_2(1)\left[m_2 + z - m_1 + \delta m_1 - g_2^{02} \sum_k \frac{u(\omega_2')^2}{2\omega_2' V} \frac{1}{z - \omega_2'} - \right. \tag{3.1}$$
$$\left. - g_3^{02} \sum_k \frac{U(\omega_3)^2}{2\omega_3 V} \frac{1}{D(m_2 + z - \omega_3)}\right].$$

Substituting equ. (1.2) in (1.8)

$$D(z) = (z - m_3)\left[1 + g_4^{02} \sum_k \frac{R(\omega_4)^2}{2\omega_4 V} \frac{P}{(m_3 - m_4 - \omega_4)(z - m_4 - \omega_4)}\right],$$

we let

$$D(z) = (z - m_3) L_p(z), \tag{3.2}$$

where

$$L_p(z) = 1 + g_4^{02} \sum_k \frac{R(\omega_4)^2}{2\omega_4 V} \frac{P}{(m_3 - m_4 - \omega_4)(z - m_4 - \omega_4)}.$$

Setting $f(m_1 - m_2) = 0$ and using equ. (3.2) it follows that

$$\delta m_1 = g_1^{02} \sum_k \frac{u(\omega_2)^2}{2\omega_2 V} \frac{1}{m_1 - m_2 - \omega_2} + g_3^{02} \sum_k \frac{U(\omega_3)^2}{2\omega_3 V} \frac{1}{(m_1 - m_3 - \omega_3) L_p(m_1 - \omega_3)},$$

which is the same result that follows from equ. (1.1). From differentiating equ. (3.1) it follows that

$$f'(m_1 - m_2) = Z_2(1)\left[1 + g_2^{02} \sum \frac{u(\omega_2)^2}{2\omega_2 V} \frac{1}{(m_1 - m_2 - \omega_2)^2} - \right.$$
$$\left. + g_3^{02} \sum_k \frac{U(\omega_3)^2}{2\omega_3 V} \frac{D'(m_1 - \omega_3)}{D(m_1 - \omega_3)^2}\right] = 1,$$

where we defined

$$\langle 0 | \psi_1 | \psi_1 \rangle = Z_2^{\frac{1}{2}}(1) .$$

Aside from kinematical factors this shows that the residue at the pole of the ψ_2, φ_2 scattering amplitude is g_2^2 where $g_2 = g_2^0 Z_2^{\frac{1}{2}}(1)$ is the renormalized coupling constant.

Comparing equ. (1.4) and (1.5) it follows that

$$\langle \psi_3 | \psi_3 | 0 \rangle = Z_2^{\frac{1}{2}}(M) = \frac{1}{D'(M)^{\frac{1}{2}}} , \tag{3.3}$$

where $|\psi_3\rangle$ is the bound ψ_4, φ_4 system.

From equ. (3.1) and (3.3)

$$\begin{aligned} f(\omega + i\varepsilon) - f(\omega - i\varepsilon) = \frac{i}{2\pi} Z_2(1) \Big[& g_2^{02} u(\omega)^2 \sqrt{\omega^2 - \mu_3^2}\, \theta(\omega - \mu_2) + \\ & + g_3^{02} Z_2(M)\ U(m_2 + \omega - M)^2 \sqrt{(m_2 + \omega - M)^2 - \mu_2^2}\, \theta(m_2 + \omega_2 - M - \mu_3) + \\ & + g_3^{02} g_4^{02} \sum_k \frac{U(\omega_3)^2}{2\omega_3 V} \sqrt{(m_2 + \omega - \omega_3 - m_4)^2 - \mu_4^2}\, \frac{R(m_2 + \omega - \omega_3 - m_4)^2}{|D(m_2 + \omega - \omega_3)|^2} \cdot \\ & \cdot \theta(m_2 + \omega - m_4 - \mu_4 - \omega_3) \Big] . \end{aligned} \tag{3.4}$$

To obtain the ψ_2, φ_2 scattering amplitude by dispersion relations we calculate $\operatorname{Im} N(\omega)$ of (1): accounting for the particle spectrum of the total Hamiltonian

$$\begin{aligned} \operatorname{Im} N(\omega) = \pi \{ & |\langle \psi_1 | j_2^+(0) | \psi_2 \rangle|^2 \delta(m_1 - m_2 - \omega) + \\ & + \sum_k |\langle \psi_2 \varphi_2' | j_2(0)^+ | \psi_2 \rangle|^2 \delta(\omega_2' - \omega_2) + \sum_{k'} |\langle \psi_3 \varphi_3' | j_2(0)^+ | \psi_2 \rangle|^2 \delta(M + \omega_3' - m_2 - \omega) + \\ & + \sum_{k', k''} |\langle \psi_4 \varphi_3' \varphi_4'' | j_2(0)^+ | \psi_2 \rangle|^2 \delta(m_4 + \omega_3' + \omega_4'' - m_2 - \omega) \} , \end{aligned} \tag{3.5}$$

where again the summation is over out states only. Applying the Lehmann, Symanzik-Zimmermann formalism to $\langle \psi_3 \varphi_3 | j_2(0)^+ | \psi_2 \rangle$ by including the bound state $|\psi_3\rangle$ into the particle spectrum at $t = -\infty$ we obtain

$$\langle \psi_3 \varphi_{3\,\mathrm{out}} | j_2(0)^+ | \psi_2 \rangle = \frac{U(\omega_3)}{(2\omega_3 V)^{\frac{1}{2}}} \frac{(2\omega_2 V)^{\frac{1}{2}}}{u(\omega_2)} \langle \psi_3 | j_0(0) | \psi_2 \varphi_{2\,\mathrm{in}} \rangle , \tag{3.6}$$

where

$$M + \omega_3 = m_2 + \omega_2 ,$$

and using equ. (2.1) and (2.2) of (1) and (3.3) in (3.6) it follows that

$$\Psi_3 \varphi_{3\,\mathrm{out}} | j_2(0)^+ | \psi_2 \rangle = \frac{U(\omega_3)}{(2\omega_3 V)^{\frac{1}{2}}} \frac{g_3^0}{g_2^0} Z_2^{\frac{1}{2}}(M) N(\omega_2) .$$

Likewise

$$\langle \psi_4 \varphi_4 \varphi_{3\,\mathrm{out}} | j_2(0)^+ | \psi_2 \rangle = \frac{U(\omega_3)}{(2\omega_3 V)^{\frac{1}{2}}} \frac{g_3^0}{g_2^0} \langle \psi_4 \varphi_{4\,\mathrm{out}} | \psi_3^+ | 0 \rangle N(\omega_2) ,$$

where again

$$m_4 + \omega_4 + \omega_3 = m_2 + \omega_2 .$$

Following the procedure of (1) it is again seen that the dispersion relation solution is in agreement with the direct solution, $|\Psi_3\rangle$ now plays the role $|\psi_3\rangle$ played when it was stable. The case where there is no bound state is equivalent to taking $Z_2(M) = 0$.

4. – Conclusions.

The customary separation of creation and decay of unstable particles is seen to be an approximation that is not valid for small times of the order of $\hbar/\mu_3 c^2$ and for very large times. Furthermore, unstable states have a simple characteristic describable by a mass m_3 and a lifetime τ when the resonance width of their stable decay products is very small compared to all relevant masses in the system, and when they are produced above the threshold with energies that are large compared to $1/\tau$. Thus Matthew's and Salam's description of unstable particles with first moment of the density matrix should be an approximation that is valid only for lifetimes of the order of 10^{-17} seconds or longer.

Dispersion relations are also seen to be valid for bound state production and in the case where the free and complete Hamiltonians have different stable states.

(11) P. T. Matthews and A. Salam: *Phys. Rev.*, **112**, 283 (1959).

* * *

I would like to thank Dr. R. WINTER for valuable discussions during the course of this work.

RIASSUNTO (*)

Esaminando un modello presentato precedentemente si è effettuato un calcolo della produzione e del decadimento di particelle instabili senza separare questi due processi. Si vede che l'usuale separazione della produzione dal decadimento è valida per un tempo t tale che

$$\frac{\hbar}{\mu_3 c^2} \ll t \ll 2\tau \ln \pi\tau t^2 Q^3 , \qquad Q \gg \frac{1}{\tau} ,$$

in cui Q è l'energia sopra la soglia per la produzione di particelle instabili e τ è la vita media. Quando le suddette condizioni sono verificate, gli stati instabili ammettono uno sviluppo rispetto al tempo abbastanza semplice per essere caratterizzato con l'indice di una particella. Il nostro modello predice anche la produzione di stati legati per opportune funzioni di taglio. Il formalismo di Nishijima-Zimmermann per trattare gli stati legati in riferimento a relazioni di dispersione riproduce i calcoli diretti.

(*) *Traduzione a cura della Redazione.*

IL NUOVO CIMENTO Vol. XV, N. 4 16 Febbraio 1960

Elastic scattering $\pi^- + p$ at 915 MeV.

S. Bergia, L. Bertocchi, V. Borelli, G. Brautti, L. Chersovani, L. Lavatelli (*), A. Minguzzi-Ranzi, R. Tosi, P. Waloschek and V. Zoboli

Istituto di Fisica dell'Università - Bologna
Istituto di Fisica dell'Università - Trieste
Istituto Nazionale di Fisica Nucleare - Sezioni di Bologna e Trieste

(ricevuto il 23 Ottobre 1959)

Summary. — The differential cross-section for elastic scattering $\pi^- + p$ has been determined on the basis of 1421 events observed in a propane bubble chamber. The angular distribution presents a backward bump ($\theta > 90°$) of $(31.5 \pm 1.3)\%$. The amplitude at 0° obtained extrapolating the angular distribution by means of a least squares fit is compared with the value obtained from the dispersion relations and the optical theorem. New values of the pion proton cross-sections were taken into account for the dispersion relation integrals. Using the same best fit of the angular distribution a value for the interaction radius is obtained from considerations based on the diffraction scattering part.

1. – Introduction.

The events analysed in the present work were obtained in the 12 in. propane bubble chamber of the Columbia University, exposed to a pion beam of the Brookhaven Cosmotron. The same film was previously used for the

(*) John Simon Guggenheim Fellow, at present at the University of Illinois, Urbana, Ill.

analysis of strange particle events (1). Details of the exposures (2) and the measurement method used (3) have already been published.

In the present paper we describe some experimental details concerning the measurement of the $\pi^- + p$ elastic scattering angular distribution and the corrections included. The angular distribution is fitted with a polynomial which allows an extrapolation up to 0°. The value obtained at 0° is compared with the predictions made with the help of dispersion relations. Further on we deduce the interaction radius (optical radius) by fitting the forward amplitude with a diffraction scattering formula and we discuss briefly the backward scattering.

2. – Experimental part.

2·1. Elastic scattering events $(\pi + p)$ can be separated with reasonable efficiency from the background of two prong stars of the propane chamber. As is well known (4-6), this can done by means of angular measurements in which the coplanarity and the correlation between scattering and recoil angle are determined. For the application of this method it is very useful to know *a priori* the energy of the incident pions. To this purpose we

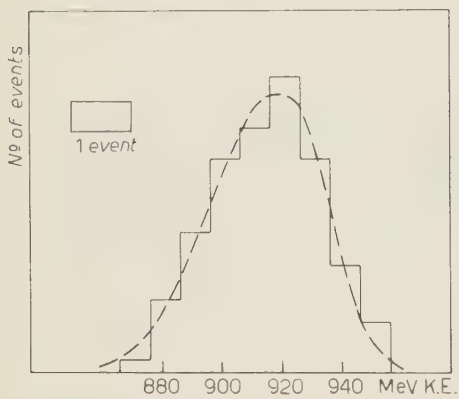

Fig. 1. – Energy spectrum of the incident pion, obtained from the reactions $\pi^- + p \to \Lambda^0 + \theta^0$ observed in the same film.

(1) F. Eisler, R. Plano, A. Prodell, N. Samios, M. Schwartz, J. Steinberger, P. Bassi, V. Borelli, G. Puppi, H. Tanaka, P. Waloschek, V. Zoboli, M. Conversi, P. Franzini, I. Mannelli, R. Santangelo, V. Silvestrini, G. L. Brown, D. A. Glaser and C. Graves: *Nuovo Cimento*, **7**, 222 (1958); **10**, 150 (1598); *Phys. Rev.*, **108**, 1353 (1957).

(2) F. Eisler, R. Plano, A. Prodell, N. Samios, M. Schwartz, J. Steinberger, P. Bassi, V. Borelli, G. Puppi, H. Tanaka, P. Waloschek, V. Zoboli, M. Conversi, P. Franzini, I. Mannelli, R. Santangelo and V. Silvestrini: *Nuovo Cimento*, **10**, 468 (1958).

(3) V. Borelli, P. Franzini, I. Mannelli, A. Minguzzi-Ranzi, R. Santangelo, F. Saporetti, V. Silvestrini, P. Waloschek and V. Zoboli: *Nuovo Cimento*, **10**, 525 (1958).

(4) M. Chrétien, J. Leitner, N. P. Samios, M. Schwartz and J. Steinberger: *Phys. Rev.*, **108**, 383 (1957).

(5) A. R. Erwin and J. K. Kopp: *Phys. Rev.*, **109**, 1364 (1958).

(6) L. Baggett: *Rad. Lab. UCRR* 8302 (1958).

have used data from a previous work done with the same photographs ([2]); the events of the type $\pi^- + p \to \Lambda^0 + \theta^0$ have allowed a fairly good determination of the energy of the beam. In Fig. 1 the events observed are plotted as a function of the incident pion energy. The spectrum has its maximum at 920 MeV. The mean energy is 915 MeV and we used this value in the present experiment.

As it will be shown later the elastic scattering events have confirmed that value of the mean energy. The energy spread of the beam is limited to $\pm 1\%$ by means of several collimators and a stearing magnet. The spread shown in Fig. 1 is mostly due to the measurement error in the $\Lambda^0 + \theta^0$ events.

2·2. *Selection of the events.* – We used the following criteria for the selection of the elastic scattering events:

a) The measured angles must be compatible with those which are expected for an « hydrogen » event. This means that the « non correlation » and the « non-coplanarity » as defined later, are zero within the error of measurement.

b) If the proton stops inside the chamber, its range must be compatible with the measured angles.

c) The vertex of the event must be contained in a well defined « fiducial region ». This region is at least 5 cm away from any chamber wall or window.

d) The curvature and ionization of the tracks (checked visually) must be compatible with those expected for an elastic event; in doubtful cases curvatures were measured (*).

e) If the pion scatters froward, its projected scattering angle (as seen in a fixed view) must be larger than 7°. This cut-off is introduced in order to avoid scanning losses and allows an easier correction of the angular distribution in the forward region.

As « non-coplanarity » in criterion *a*) we used the angle between the incident track and the plane of the two emerging ones. Fig. 2 is a plot of the « correlation » between the recoil proton angle

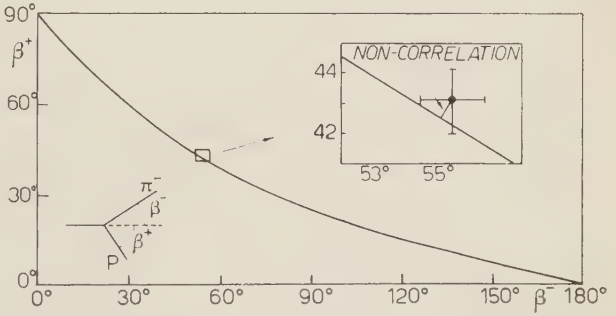

Fig. 2. – Recoil proton angle as a function of the pion scattering angle as it was used for the identification of the elastic scattering events.

(*) A magnetic field of 13.400 G was applied to the chamber.

and the pion scattering angle in the laboratory system. A typical event, with its measurement errors is shown on the right side in enlarged scale. As « non-correlation » parameter we used the minimum distance from the points defined by the event to the 915 MeV curve. In the case of elastic events this parameter means a measurement error; we expressed it in degree units in the same scale as the angles represented in Fig. 2. It may be noticed that the measurement errors are different for each event, with a certain dependence on the scattering angle. For this reason the criterion *a*) must be applied taking into account the uncertainties in all measured angles.

Fig. 3. – Correlation plot with the sign corresponding to « above » or « below » the curve of Fig. 2.

If the value of the beam energy has been correctly assigned, we expect the « non-correlation » parameter to be nearly symmetric around zero if we take the sign corresponding to «above» or «below» the 915 MeV curve of Fig. 2. This is shown in Fig. 3 and confirms the energy determination with the Λ^0+0^0 events.

During the scanning about 3000 two-prong events were selected and analysed as possible « elastic H_2 ». From these, 1421 were found to be in agreement with the five selection criteria.

2·3. *Carbon contamination.* – It is possible to estimate the number of two-prong stars produced in carbon (or hydrogen events with an additional neutral pion) for which the angular measurements have simulated an elastic event. This can be done comparing the coplanarity and correlation plots of all our events. In Fig. 4 is shown the coplanarity of all events for which the « non-correlation » was less than 2°. The shaded region represents those events classified as « carbon », some of them because the angular measurements were incompatible with coplanarity and some others because the range of the proton, which yields a more precise check of the « elasticity », has been taken into account. Fig. 5 represents the « non-correlation » for events which are coplanar within 2°. Both plots give the same result: we expect to have 26 carbon events included in our H_2 sample. This means a contamination of $(2\pm1)\%$ which has been neglected in the analysis of the angular distribution.

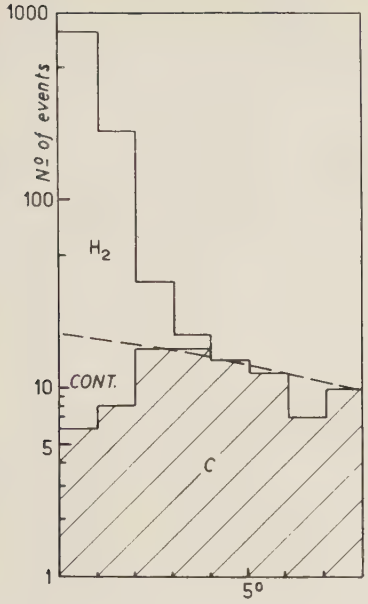

Fig. 4. – « Coplanarity » (in degrees) for correlated two-prong events.

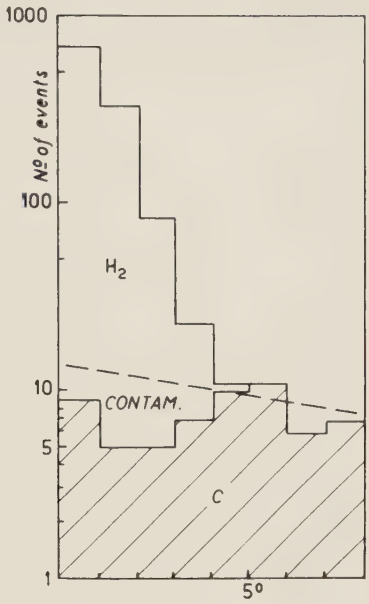

Fig. 5. – « Correlation » for coplanar two-prong events.

2·4. *Scanning bias.* – Very steep events are easily overlooked during the scanning. All pictures have been scanned by two physicists and at least two views were carefully inspected. Nevertheless the azimuth angles distribution (azimuth around the beam direction) shows that a certain number of events contained in nearly vertical planes have been missed. Since the bias is different for every scattering angle, it was determined separately for different regions of the CMS angular distribution. The maximum loss was found to be 12%, corresponding to those cases in which the pion is emitted at nearly 90° in the laboratory.

For forward scattering angles the steep events were eliminated *a priori* with the selection criterion *e*); a geometrical correction was applied to each interval of cos θ_{CM}.

No important bias can be seen for

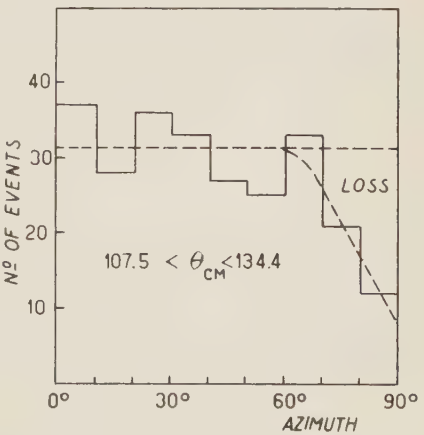

Fig. 6. – Distribution of the azimuth angles of the plane of the events around the line of flight of the incident track, shown for one interval of θ_{CM}.

completely backward events. These events are easy to find due to the magnetic field that « opens » the backscattering pion from the incident one, and because their tracks are relatively flat.

2·5. *Corrected angular distribution.* – Applying to each interval of $\cos\theta_{CM}$ the correction for selection criterion or for scanning bias we obtain the distribution shown in Fig. 7. Table I gives also the corresponding numbers. The

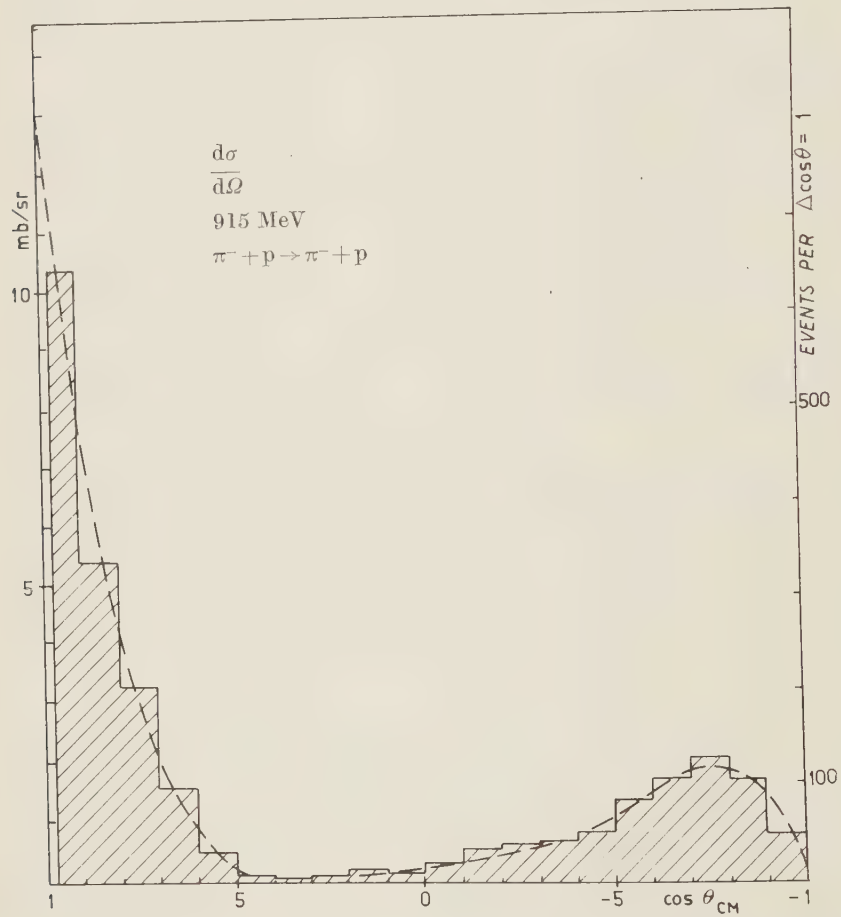

Fig. 7. – Corrected angular distribution with the sixth degree least square fit curve.

curve corresponds to a best fitting 6-th degree polynomial, as is explained in the next section. The scale in mbarn/sr was obtained by normalizing the angular distribution to an elastic cross-section of 19.8 mbarn.

TABLE I. – *Elastic scattering events*, π^-+p, 915 MeV.

Cos. scatt. angle	Real No. of events	Corrected No. of events	Cos. scatt. angle	Real No. of events	Corrected No. of events
+.9625	62	332.0	— .025	5	5.3
+.925	198	322.5	— .075	12	12.7
+.875	129	178.0	— .125	13	13.8
+.825	126	162.5	— .175	16	17.0
+.775	92	114.0	— .225	22	23.5
+.725	76	92.2	— .275	15	16.2
+.675	54	63.2	— .325	16	17.4
+.625	32	36.8	— .375	21	23.1
+.575	18	20.5	— .425	15	16.7
+.525	9	10.2	— .475	30	33.6
+.475	3	3.4	— .525	29	32.5
+.425	3	3.3	— .575	44	48.9
+.375	2	2.2	— .625	53	58.3
+.325	1	1.1	— .675	44	49.0
+.275	0	0	— .725	49	53.0
+.225	3	3.2	— .775	69	73.9
+.175	4	4.3	— .825	45	47.7
+.125	7	7.5	— .875	53	56.2
+.075	4	4.2	— .925	38	29.7
+.025	3	3.2	— .975	16	16.9

3. – Statistical analysis of the angular distribution.

For further work on the measured angular distribution it is useful to describe the result in form of a best fitting polynomial of adequate degree. This analysis was done on the Computer « Illiac » of the University of Illinois. Best fit curves were calculated for polynomials of the form

$$\mathrm{d}\sigma/\mathrm{d}\Omega = \sum_{0}^{I} a_i \cdot \cos^i \theta_{\mathrm{CM}} ,$$

using the least squares method. In Table II are given the coefficients for polynomials from third to eight degree together with their standard errors.

Furthermore we have analysed the « goodness » of the fits from a stastistical point of view [7]. In the last column of Table II and also in Fig. 8, the function

$$\sqrt{S/N-(I+1)} \; ; \qquad S = \sum_{j=1}^{N} (Y(x_j) - Y_j)^2 / G(x_i)$$

[7] J. OREAR: *UCRL-Report* 8417.

TABLE II.

Degree	a_i (mbarn/sr)	Standard error	$\sqrt{S/40-(I+1)}$ (*)
3	.090	.095	.001 406
	— 2.536	.336	
	4.416	.383	
	6.917	.666	
4	.331	.076	.000 981
	— 2.243	.241	
	.203	.726	
	7.219	.466	
	5.722	.916	
5	.211	.038	.000 470
	— .712	.181	
	.399	.349	
	— 3.074	.970	
	6.103	.441	
	10.348	.951	
6	.228	.044	.000 471
	— .674	.187	
	— .187	.691	
	— 3.048	.973	
	8.417	2.390	
	10.238	.957	
	— 1.916	1.943	
7	.225	.044	.000 477
	— .621	.269	
	— .180	.697	
	— 3.671	2.463	
	8.526	2.457	
	11.894	6.099	
	— 2.053	2.032	
	1.148	4·169	
8	.217	.048	.000 483
	— .661	.282	
	.330	1.186	
	— 3.540	2.504	
	4.862	7.260	
	12.063	6.182	
	5.448	14.107	
	— 1.460	4.248	
	— 4.486	8.401	

(*) In arbitrary units.

is shown for the different polynomials. $Y(x_j)$ are the ordinates of the angular distribution, Y_j the measured values, $G(x_j)$ the weight assigned to each point; I is the degree and N is the number of measured points. The optimum fit is that of 5-th degree while a higher degree is unwarranted. It is interesting to notice that for all higher degrees the coefficient of the 5-th degree term is the more important, it is always of the order of 10 mbarn/sr and it is defined outside the standard errors. The polynomials with lower than 5-th degree are very poor fits.

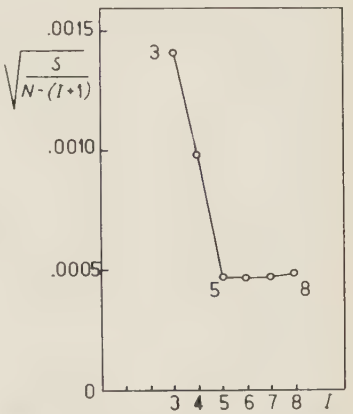

Fig. 8. – Test of the « goodness » of the different least squares polynomials fitted to the angular distribution.

A fifth degree curve means that at least F-waves must be taken into account if a description in partial waves should be attempted. However, such analysis is only possible if restrictive conditions are imposed in order to reduce the number of partecipating waves, *i.e.* to reduce the number of parameters that will describe the experiment. With 4 values of l, two possible states of total angular momentum and two of isotopic spin, a total of 14 complex amplitudes are available; each coefficient of the angular distribution relates them in form of one equation.

The standard error to be assigned to the value of $d\sigma/d\Omega$ when it is obtained from the polynomial has been computed for several points of the sixth degree curve. These errors are given in Table III. Of special interest for later application is the error in the forward amplitude; the differential cross-section is $(d\sigma/d\Omega)_{0^\circ} = (13.06 \pm 0.42)$ mbarn/sr. This value will be discussed in the next section in connection with the results obtained from dispersion relations.

TABLE III. – *Standard errors in the ordinates obtained with the 6-th degree fit.*

$a_i \cos^i \theta_{CM}$	$d\sigma/d\Omega$ (mbarn/sr)	$a_i \cos^i \theta_{CM}$	$d\sigma/d\Omega$ (mbarn/sr)
1.00	13.06 ± 0.42	-0.20	0.39 ± 0.06
0.80	4.30 ± 0.16	-0.40	0.77 ± 0.08
0.60	0.90 ± 0.08	-0.60	1.43 ± 0.10
0.70	0.05 ± 0.03	-0.80	1.80 ± 0.15
0.20	0.08 ± 0.03	-1.00	0.03 ± 0.24
0.00	0.23 ± 0.04		

4. – Dispersion relations for the forward amplitude.

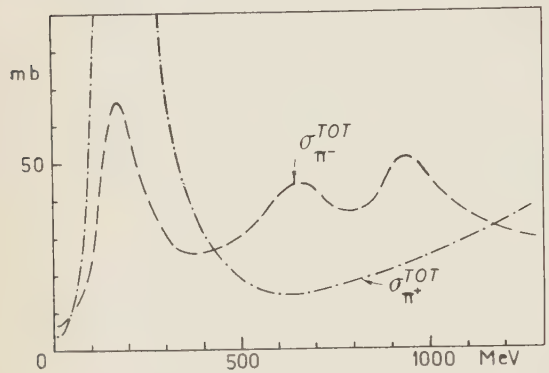

Fig. 9. – Pion-proton cross-sections used for the dispersion relation calculations, as a function of the K.E. (LAB) of the incident pion.

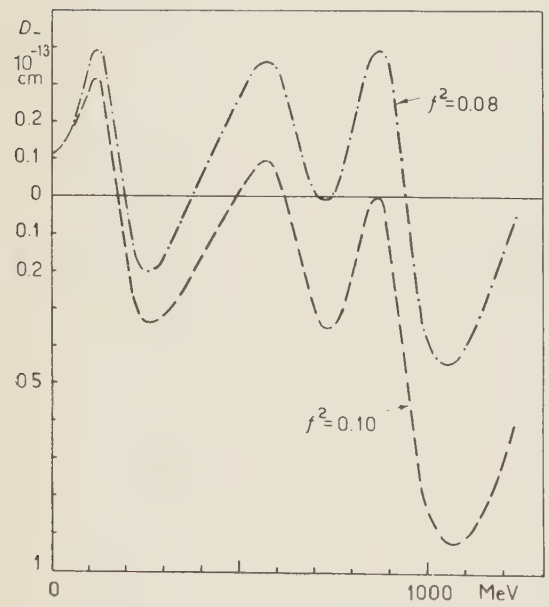

Fig. 10. – Real part of the forward scattering amplitude, as a function of the K.E. (LAB) of the incident pion.

The real part of the forward scattering amplitude (D_-) can be predicted by means of dispersion relations ([8]). Calculations for this purpose were performed by STERNHEIMER ([9]) using the formula given by GOLDBERGER, MIYAZAWA and OEHME ([8]). The essential part in determining the general behaviour of D_- turns out to be an integral over the total π-p cross-section of the form

$$P\int_{\mu}^{\infty}\frac{\sigma_{\pi^-}^{\mathrm{TOT}}(\omega')\,\mathrm{d}\omega'}{p'(\omega'-\omega)}$$

(ω is the pion energy). The contribution of the pole at ω is proportional to the slope of the $\sigma_{\pi}^{\mathrm{TOT}}$ curve ($\mathrm{d}\sigma/\mathrm{d}\omega'$). Another important term contains the π-p interaction coupling constant f^2.

Recently the total π-p cross-sections were remeasured in the 500 to 1000 MeV region ([10,11])

([8]) M. L. GOLDBERGER, H. MIYATZAWA and R. OEHME: *Phys. Rev.*, **99**, 986 (1955).
([9]) R. M. STERNHEIMER: *Phys. Rev.*, **101**, 384 (1956).
([10]) R. R. CRITTENDEN, J. H. SCANDRETT, W. D. SHEPHARD, W. D. WALKER, and J. BALLAM: *Phys. Rev. Letters*, **2**, 121 (1959).
([11]) H. C. BURROWER, D. O. CALDWELL, D. H. FRISCH, D. A. HILL, D. M. RITSON, R. A. SCHLUTER and M. A. WAHLING: *Phys. Rev. Letters*, **2**, 119 (1959).

and it was possible to resolve two peaks, as is shown in Fig. 9. The situation for the dispersion relation formula is now quite different and we repeated Sternheimer's calculations obtaining a curve shown in Fig. 10 for D_- (*). In order to compare this result with the experiment we must get the imaginary part of the forward scattering amplitude by means of the optical theorem: $\mathrm{Im}\, f_{(0^\circ)} = \sigma_T/4\pi\lambda$. From both, real and imaginary part, we get the expected forward scattering amplitude as is plotted in Fig. 11. One may compare these curves with those obtained from the older cross-sections given by Cool, Piccioni and Clark [12].

The small effect of D_- on the forward cross-sections makes it rather hopeless to get in the near future some conclusion on the π-p interaction constant, as can be seen from the experimental points plotted in Fig. 11.

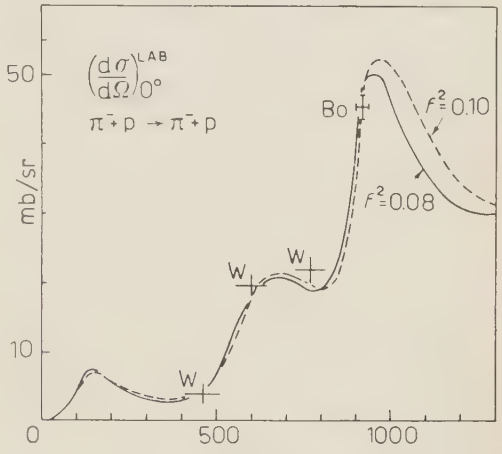

Fig. 11. – Forward scattering amplitude for two values of the pion-proton coupling constant f^2, as a function of the K.E. (LAB) of the incident pion. The points « W » were obtained extrapolating the data of Crittenden *et al.* [10].

5. – Diffraction scattering.

On the basis of several assumptions a further analysis of the angular distribution can be done. It seems reasonable, for instance, to investigate the forward peak in terms of diffraction scattering, at least for very small angles where spin effect should be not important. This can be done based on the extrapolated values of the angular distribution since an interpretation as diffraction scattering for measurable angles is no longer possible, as we shall show.

Following the method developed by Ito, Minami and Tanaka [13] we describe the diffraction peak at small angles with the approximate but very

(*) These computations were performed (numerically) at the IBM 650 of the Centro Calcoli of the University of Bologna.

(12) R. Cool, O. Piccioni and D. Clark: *Phys. Rev.*, **103**, 1082 (1956).

(13) D. Ito, S. Minami and H. Tanaka: *Nuovo Cimento*, **9**, 208 (1958).

convenient formula:

$$\frac{\mathrm{d}\sigma}{\mathrm{d}\Omega} = \left(\frac{b/2}{a - \cos\theta}\right)^2$$

in which the constant a is related to the optical radius R:

$$a = 1 + (2/K \cdot R)^2 .$$

As long as $(\mathrm{d}\sigma/\mathrm{d}\Omega)^{\frac{1}{2}}$ is a linear function of $(1 - \cos\theta)$ we can apply these formulae. In Fig. 12 we have plotted $(\mathrm{d}\sigma/\mathrm{d}\Omega)^{-\frac{1}{2}}$ and we conclude that only for $(1 - \cos\theta) < 0.1$ the approximation to our experimental curve is good enough. From this first portion we get:

$$a = 1.275 ; \quad b = 2.22\sqrt{mb} ; \quad R_{\mathrm{opt}} = 1.23 \cdot 10^{-13} \text{ cm} .$$

In Fig. 13 the diffraction scattering obtained with these constants is compared with the experimental angular distribution.

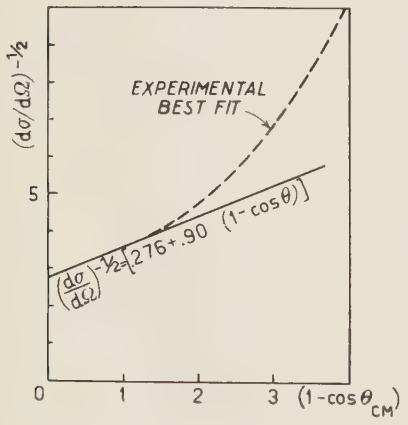

Fig. 12. – Plot of $(\mathrm{d}\sigma/\mathrm{d}\Omega)^{-\frac{1}{2}}$ as a function of $(1 - \cos\theta)$ for the diffraction scattering analysis.

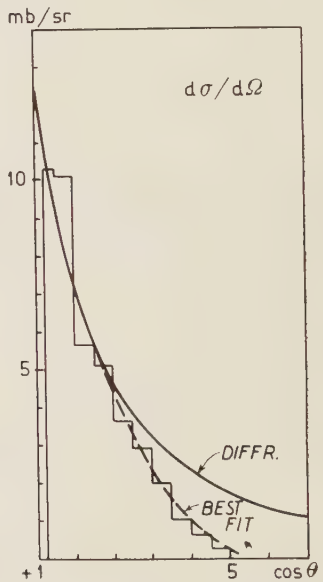

Fig. 13. – Diffraction scattering obtained with the parameters valid at very small angles, compared with the experimental angular distribution.

Going on in the analysis of Ito *et al.* we get the « effective angular momentum » (weighted mean of the angular momenta involved):

$$\langle l \rangle = 2.3 .$$

This should mean that D-waves are important in the diffraction peak but that also waves of higher l are present.

6. – Backward scattering.

An analysis of this part of the spectrum was attempted by different authors. It seems suggestive to justify this part with only spin-flip terms. The form of the bump is easily fitted with different mixtures of D and F waves or D and P waves or all three ([5]) (also here D waves are essential). The crucial point for this type of assumption is the zero of the angular distribution at 180° necessary for all spin-flip terms. For this reason we have specially checked for all type of biases in that region. The value for the backward amplitude obtained from our best fit curve is:

$$(\mathrm{d}\sigma/\mathrm{d}\Omega)_{180^\circ} = (0.03 \pm 0.24) \text{ mbarn/sr} .$$

CHRÉTIEN ([14]) has attempted to explain the backward bump with an optical model which takes into account the structure of the nucleon (hard core without spin). By this proceeding the total amount ot backward scattering is reasonably obtained but it becomes difficult to justify the small value of $\mathrm{d}\sigma/\mathrm{d}\Omega$ at 180°.

Another interesting characteristic of the backward « bump » is its disappearance at lower and higher energies, as can be seen comparing our results with the data obtained by CRITTENDEN *et al.* ([10]) (at 450, 600 and 750 MeV) and those of CHRÉTIEN *et al.* ([4]) at 1300 MeV.

* * *

We are very grateful to the bubble chamber group of the Columbia University, in particular to Prof. J. STEINBERGER for allowing us to perform the measurements here presented on their films and for much advice and help.

The continuous encouragement and interest of Prof. G. PUPPI are gratefully acknowledged. For many helpful discussions we thank Profs. C. FRANZINETTI, A. MINGUZZI, H. TANAKA, G. MINAMI, M. CHRÉTIEN and E. PEREZ FERREIRA. We are indebted to Prof. J. SNYDER and to Mr. D. HUTCHINSON

([14]) M. CHRÉTIEN: *Nuovo Cimento*, **15**, 565 (1960).

for facilities and help in the computations with the Illiac. One of us (L.L.) wishes to thank Prof. G. PUPPI and the staff of the « Istituto di Fisica A. Righi » in Bologna for the warm hospitality extended to him during the 1957-58 academic year.

RIASSUNTO

È stata determinata, in base a 1421 eventi osservati in una camera a bolle a propano, la sezione d'urto differenziale nello scattering elastico $\pi^- + p$. La distribuzione angolare presenta un notevole contributo all'indietro ($\theta > 90°$) del $(31.5 \pm 1.3)\%$ L'ampiezza a 0° è stata ottenuta estrapolando la distribuzione angolare mediante minimi quadrati ed è stata confrontata con il valore ottenuto per mezzo delle relazioni di dispersione e del teorema ottico. Nel calcolo degli integrali delle relazioni di dispersione sono stati tenuti in conto i nuovi valori della sezione d'urto pione protone. Da considerazioni basate sulla parte di diffrazione dello scattering è stato ottenuto, usando lo stesso migliore adattamento della distribuzione angolare, un valore per il raggio d'interazione.

Phenomenological Potential for π-p Scattering in the 1 GeV Region (*).

M. Chrétien

Brandeis University - Waltham, Mass.

(ricevuto il 23 Ottobre 1959)

Summary. — It is shown that a nuclear potential with a repulsive core can quantitatively describe the large backward scattering observed in π^--p scattering for pion energies around 1 GeV. With an infinite repulsive core ($V=\infty$ from 0 to r), surrounded by a complex well ($V=V_r+iV_i$ from r to R) a phase shift calculation gives best agreement with experiment for $R=1.1\cdot10^{-13}$ cm, $r/R=0.2$, $V_r=-60$ MeV, $V_i=-40$ MeV.

The scattering of negative pions of energies of about 1 GeV and more has been investigated by several groups [1-8]. Around 1 GeV the characteristic features are a considerable backward scattering ($\sim 20\,\%$) for the elastic events

(*) Research partly supported by the National Science Foundation.

(1) W. D. Walker, F. Hushfar and W. D. Shephard: *Phys. Rev.*, **104**, 526 (1956).

(2) A. R. Erwin and J. K. Kopp: *Phys. Rev.*, **109**, 1364 (1958).

(3) M. Chrétien, J. Leitner, N. P. Samios, M. Schwartz and J. Steinberger: *Phys. Rev.*, **108**, 383 (1957).

(4) L. M. Eisberg, W. B. Fowler, R. M. Lea, W. D. Shephard, R. P. Shutt, A. M. Thorndike and W. L. Whittemore: *Phys. Rev.*, **97**, 797 (1955).

(5) W. D. Walker: *Phys. Rev.*, **108**, 872 (1957).

(6) G. Maenchen, W. B. Fowler, W. M. Powell and R. W. Wright: *Phys. Rev.*, **108**, 850 (1957).

(7) S. Bergia, B. Bertocchi, V. Borelli, G. Brautti, L. Chersovani, L. Lavatelli, A. Minguzzi-Ranzi, R. Tosi, P. Waloschek and V. Zoboli: *Nuovo Cimento*, **15**, 551 (1960).

(8) V. Borelli, A. Minguzzi-Ranzi, P. Waloschek and V. Zoboli: private communication.

and a large inelastic cross-section (see Table I and Fig. 1). It was pointed out by several authors that a complex square well, with $V = \text{const}$ inside the well, is not able to produce the observed angular distribution. Such a poten-

TABLE I.

Kinetic energy (Lab. Syst.) of in coming pion (GeV)	0.915	0.9	0.96	0.96	0.95	1.3	1.4	4.5	5.0
Elastic cross-section (mb)	19.8	20±3	—	18.6±3	19.1±1.6	10.1±0.8	10.0±0.8	6.5	6.0 (a)
Total cross-section (mb)	45±3	—	—	—	45 ±3	30 ±3	34.6±2.7	28.7	22.5±2.4
R (10^{-13} cm) (b)	—	1.1	—	1.1	—	1.08±0.06	1.18±0.10	1.0	0.9±0.15
Transparency (c)	—	—	—	—	—	0.6	0.61±0.10	—	0.6
Events with 60°	—	75	—	—	—	—	20%	—	—
Events with >90°	31.5± ±1.3%	—	26%	—	27%	19%	—	—	2(?) events
Number of events	1421	75	99	150	420	850	110	18	27
Method (d)	PBC	EMU	HBC	HDC	HBC	PBC	HDC	EMU	HDC
Reference	(7)	(1)	(8)	(1)	(2)	(3)	(4)	(5)	(6)

(a) As corrected in (5).
(b) From fit to diffraction peak.
(c) Defined as $\sigma_{abs}/\pi R_0^2$.
(d) HBC: hydrogen bubble chamber - HDC: hydrogen diffusion chamber - PBC: propane bubble chamber - EMU: emulsion.

tial with a radius $R \sim 1 \cdot 10^{-13}$ cm would result in the observed forward (« diffraction ») peak, but would give only a few ($\leqslant 8$) per cent of backward scattering. The latter could be explained by a core inside the well, of much smaller radius, which would produce a spread out angular distribution. The real part of the core and the well potential would have to have opposite signs in order to produce the observed, very conspicuous minimum between the forward peak and the backward bump. Such hard core potentials were actually derived from meson theory in certain approximations. On the whole, however, field theory cannot make detailed quantitative predictions in this energy region. Apart from purely mathematical difficulties the question of the consistency of the whole theory is still open. Under these circumstances it seemed worthwhile investigating, whether such a simple potential with reasonable values for the parameters could give quantitative agreement. It is not obvious, of

course, whether the notion of a potential makes much sense at these energies, but at least it would provide an economical way of describing the observed data.

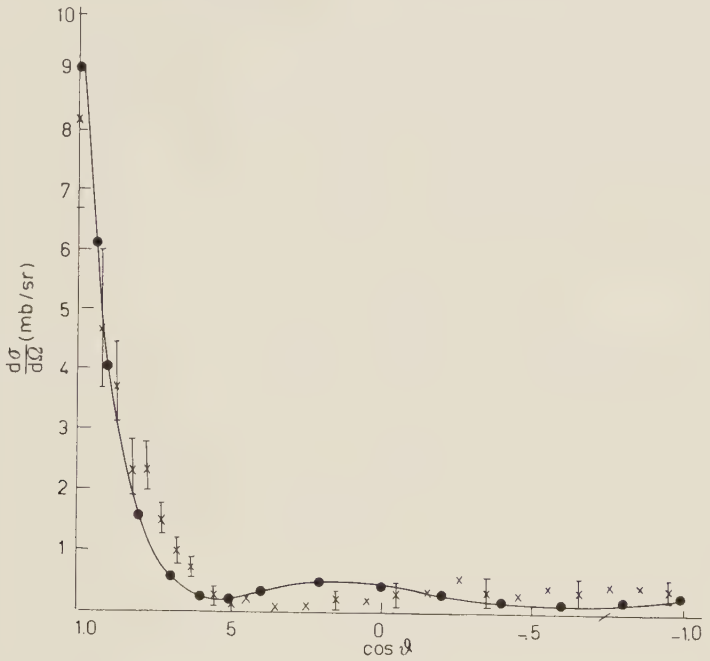

Fig. 1.

The scattering of the pion by the proton is described by the Klein-Gordon equation

$$(\nabla^2 + (E - V)^2 - m^2)\psi = 0 .$$

It turns out that the simplest choice for V, a central potential with a repulsive core of infinite height and radius r, surrounded by a complex attractive square well, is sufficient to give good agreement with the experimental data at 1.3 GeV ([3]), The agreement could be improved by taking a core with tapered instead of vertical sides.

There is certainly reason to assume that the potential has spin and velocity dependent terms as well, but the data at 1.3 GeV do not allow a meaningful estimate of its magnitude. It seems certain, however, that a spin dependent term alone, *i.e.*, without a hard core, would not explain the observed backward scattering at 1.3 GeV (the cross-section would then be $\sim \sin^2 \vartheta$ in the neighborhood of 180°). At lower energies the situation seems to be different. According to the latest measurements at 915 and 960 MeV ([7,8]), the cross-section

has a well-defined second maximum in the backward direction and goes to zero at 180°. As K_0R is of the order of 1 ($K_0R = 3.6$ for 1 GeV and $R = 10^{-13}$ cm), it is possible that the contributions of the spin-dependent and the spin-independent term to the cross-section vary considerably over this energy region. So far no calculations have been done at these lower energies.

For the potential with the infinite step at r the boundary condition for ψ is simply $\psi(r) = 0$. Together with the boundary conditions at R one finds (see *e.g.* L. L. SCHIFF: *Quantum mechanics*) for the phase shifts δ_l:

$$\operatorname{tg}\delta_l = -\gamma_l \frac{z-\alpha_l}{z-\beta_l},$$

$$\alpha_l = -k_0 R j_l'(k_0R)/j_l(k_0R),$$

$$\beta_l = -k_0 R n_l'(k_0R)/n_l(k_0R),$$

$$\gamma_l = -j_l(k_0R)/n_l(k_0R),$$

$$z = -kR\,\frac{n_l(kR)j_l'(kr) - j_l(kR)n_l'(kr)}{n_l(kR)j_l(kr) - j_l(kR)n_l(kr)},$$

$$k_0 = \sqrt{E^2 - m^2},$$

$$k = \sqrt{(E-V)^2 - m^2},$$

E = center of mass energy of incoming pion.

From the phase shifts one then calculates

$$\sigma_{el} = \frac{\pi}{k_0^2}\sum (2l+1)\,|\exp[2i\delta_l] - 1|^2,$$

$$\sigma_{abs} = \frac{\pi}{k_0^2}\sum (2l+1)\,(1 - |\exp[2i\delta_l]|)^2,$$

$$d\sigma_{el} = \frac{1}{4k_0^2}\,|\sum (2l+1)P_l(\cos\vartheta)(\exp[2i\delta_l] - 1)|^2,$$

$$B = \int_0^{180^\circ} d\sigma_{el}/\sigma_{el} = \text{backward scattering ratio.}$$

The calculations were done for several sets of values for r, R, V_r, and V_i, some of which are shown in Table II. The values of the parameters for which

TABLE II.

	R (10^{-13} cm)	r/R	$-V_r$ (MeV)	$-V_i$ (MeV)	σ_{el} (mb)	σ_{total} (mb)	$d\sigma_{el}/d\Omega$ (0°) (mb/sr)	B (%)
Potential Q	1.1	0.2	60	40	9.2	27.9	9.0	15
P	1.1	0.2	50	40	7.7	26.4	7.3	16
N	1.1	0.2	75	40	12.0	31.8	12.7	13
M	1.1	0.25	75	40	11.9	31.1	11.4	15
K	1.15	0.25	75	40	12.9	34.4	12.5	15
C	1.05	0.25	50	50	6.5	23.8	4	8
Observed [3]	—	—	—	—	10.1 ± 0.8	30 ± 3	8.2 ± 1.6	19

satisfactory agreement with experiment could be obtained (for certain combinations) lie within the following ranges:

$$R: \quad (1.05 \div 1.15) \cdot 10^{-13} \text{ cm},$$

$$r/R: \quad 0.2 \div 0.3,$$

$$V_r: \quad ((-25) \div (-75)) \text{ MeV},$$

$$V_i: \quad ((-20) \div (-40)) \text{ MeV}.$$

For no core, $r/R = 0$, the largest backward scattering ratio was $B = 8\%$. For $r/R = 0.4$ the angular distribution produced by the core becomes so strong that the minimum after the diffraction peak completely disappears. Obviously, a core of finite height would allow a wider range of acceptable values for r/R.

For the best fitting potential, Q, the angular distribution is shown together with the experimental result [3]. For small and large angles the agremeent is very satisfactory. The slight discrepancy at intermediate angles is to be expected from the very unrealistic shape of the potential. The cross-section in the neighborhood of the minimum depends strongly on the potential around r. With a repulsive core with tapered sides one could get less core scattering in the neighborhood of the minimum for the same amount of backward scattering, which is just what one needs. Unfortunately such a potential makes the calculation prohibitively complicated.

It is tempting to apply a similar phenomenological potential to the low energy pion-proton scattering. It is immediately clear that the repulsive and the attractive part will produce phase shifts of opposite sign. The s-phase shift will therefore be small. The p-wave is not influenced appreciably by the core; its phase shift will increase as $(p/mc)^3$ and go through a resonance. At

higher energies there should be a d-resonance. A quantitative calculation makes, of course, little sense without including the isotopic spin. For a radius $R = 1.18 \cdot 10^{-13}$ cm one needs a core of $0.7 \cdot 10^{-13}$ cm and a potential of $V = -400$ MeV to get a small s-phase, $\delta_s = 0.4\, p/mc$, and a p-phase of the right magnitude, $\delta_p = 0.09\, (p/mc)^3$. With these values the p-phase has a sharp maximum at a pion energy of ~ 300 MeV.

RIASSUNTO (*)

Si dimostra che un potenziale nucleare con un centro repulsivo può descrivere quantitativamente il forte scattering all'indietro osservato nello scattering π^--p per energie del pione attorno ad 1 GeV. Con un centro repulsivo infinito ($V = \infty$ da 0 ad r), circondato da una buca complessa ($V = V_r + iV_i$ da r ad R) un calcolo dello spostamento di fase dà il migliore accordo con l'esperimento per $R = 1.1 \cdot 10^{-13}$ cm, $r/R = 0.2$, $V_r = -60$ MeV, $V_i = -40$ MeV.

(*) *Traduzione a cura della Redazione.*

IL NUOVO CIMENTO Vol. XV, N. 4 16 Febbraio 1960

Bremsstrahlung Linear Polarization.

J. W. Motz and R. C. Placious

National Bureau of Standards - Washington, D. C.

(ricevuto il 26 Ottobre 1959)

Summary. — This work presents a general quantitative description of the bremsstrahlung linear polarization on the basis of original experimental data and available theoretical calculations. The results give the dependence of the polarization on *a*) the initial electron kinetic energy, T_0, in a range from 10^{-2} to 10^3 MeV, *b*) the photon energy in a range from 0.1 T_0 to T_0, *c*) the photon emission angle in a range from 0 to 180 degrees, and *d*) the atomic number of the target in a range from 4 to 79. The experimental data were obtained for a range of electron energies from 0.05 to 1.0 MeV with beryllium, aluminum, and gold targets. Theoretical estimates of the polarization were calculated from the Sommerfeld-Kirkpatrick-Wiedmann results for the non-relativistic energy region, the Olsen-Maximon results for the extreme relativistic energy region, and the Gluckstern-Hull (Born approximation) results for the intermediate energy region. Final results are expressed in terms of the peak polarization and the corresponding peak angle as a function of the electron and photon energies, and best estimates of the polarization are given on the basis of the combined experimental and theoretical data.

1. – Introduction.

1·1. *Definition and description.* – Photons emitted in the bremsstrahlung process exhibit linear [1] and circular [2] polarization properties. These properties depend on the conditions of production and of observation. This paper deals only with the *linear polarization* of the bremsstrahlung produced by a

[1] C. G. Barkla: *Trans. Roy. Soc.*, **204**, 467 (1905).

[2] M. Goldhaber, L. Grodzins and A. W. Sunyar: *Phys. Rev.*, **106**, 826 (1957).

beam of electrons incident on a thin target and observed at a given emission angle regardless of the electron spin orientation or recoil direction. This linear polarization, P, is defined as

$$P = \frac{d\sigma_\perp(E_0, k, \theta_0, Z) - d\sigma_\parallel(E_0, k, \theta_0, Z)}{d\sigma_\perp + d\sigma_\parallel} . \tag{1}$$

where $d\sigma$ is the bremsstrahlung differential cross-section for the emission of photons received by an ideal detector that only accepts radiation polarized perpendicular ($d\sigma_\perp$) or parallel ($d\sigma_\parallel$) to the emission plane (given by the directions of the photon and the incident electron). This cross-section is integrated over the direction of the recoil electron and is summed over the final and averaged over the initial electron spin states. Furthermore, this cross-section is a function of the total energy, E_0, of the incident electron, the photon energy, k, the photon emission angle, θ_0, with respect to the incident electron direction, and the atomic number, Z, of the target. Positive (or negative) values of the polarization indicate that the radiation is polarized prevalently perpendicular (or parallel) to the emission plane.

It is important to emphasize that the bremsstrahlung linear polarization considered in this paper and defined in eq. (1) places no restrictions on the spin state or direction of the recoil electron. Consequently, this polarization is produced by a combination of different effects related to the motion of the Dirac electron ([3]), and the polarization behavior provides only a very limited amount of information about the elementary bremsstrahlung process. Although the linear polarization is defined for unpolarized electron beams, calculations ([4,5]) have shown that this polarization is independent of the initial electron spin state. Therefore under the conditions specified by the Born approximation ([4]) and in any case for small scattering angles ([5]), the present results apply to electron beams that are either polarized or unpolarized.

At *non-relativistic* electron energies, the bremsstrahlung linear polarization is closely associated with the orbital motion of the electron. Low energy bremsstrahlung consists overwhelmingly of electric dipole radiation with the electric vector in the direction of the electron acceleration. This simple classical result can be used to describe the general features of the bremsstrahlung linear polarization. A diagram of the initial and final electron momenta, $\boldsymbol{p}_0$ and $\boldsymbol{p}$ respectively, is shown in Fig. 1 for the emission of *a*) a high frequency photon,

([3]) These effects have been pointed out and analyzed by U. FANO, K. W. MCVOY, and J. ALBERS: *Phys. Rev.*, **116**, 1147 (1959).

([4]) C. FRONSDAL and H. ÜBERALL: *Nuovo Cimento*, **8**, 163 (1958); *Phys. Rev.*, **111**, 580 (1958). These calculations show that the linear polarization is independent of the initial electron spin state only in the Born approximation.

([5]) H. OLSEN and L. C. MAXIMON: *Phys. Rev.*, **114**, 887 (1959).

$p \ll p_0$, and *b*) a low frequency photon, $p \sim p_0$. In case *a*), the electron momentum difference, $\boldsymbol{p}_0 - \boldsymbol{p}$, has a large component *parallel* to $\boldsymbol{p}_0$ at any electron recoil angle, and the radiation source resembles an oscillating electric dipole *parallel* to $\boldsymbol{p}_0$. In case *b*), the bremsstrahlung process approaches the conditions in Rutherford scattering where most of the electrons have small recoil angles; therefore the electron momentum difference, $\boldsymbol{p}_0 - \boldsymbol{p}$, has a large component perpendicular to $\boldsymbol{p}_0$, and the radiation source resembles an oscillating electric dipole *perpendicular* to $\boldsymbol{p}_0$. Accordingly, if the radiation is observed in a direction perpendicular to $\boldsymbol{p}_0$ and to the plane of the diagram in Fig. 1, the polarization has a reversal feature: the high frequency photons tend to be polarized parallel to the emission plane, and the low frequency photons tend to be polarized perpendicular to the emission plane. If the radiation is observed in the forward or backward direction, the polarization at all frequencies is zero because of the symmetry conditions.

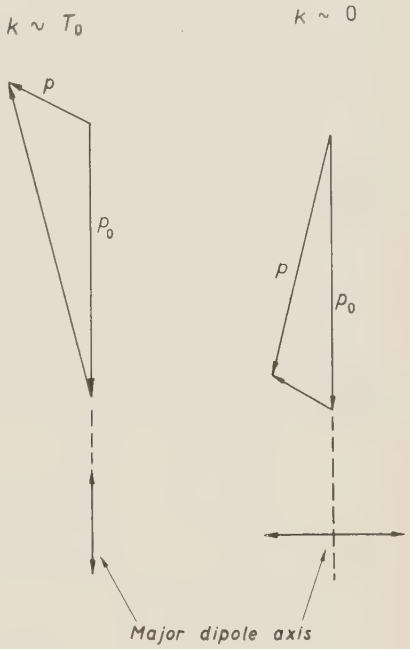

Fig. 1. – Vector diagrams of the initial, $\boldsymbol{p}_0$, and the final, $\boldsymbol{p}$, electron momenta for (*a*) high frequency photons where the photon energy, k, is approximately equal to the initial electron kinetic energy, T_0 (or $p \ll p_0$), and (*b*) low frequency photons where $k \sim 0$ (or $p \sim p_0$). For non-relativistic electrons, the major dipole axis is given by the direction of the large component of the momentum difference, $\boldsymbol{p}_0 - \boldsymbol{p}$.

At relativistic electron energies, the dependence of the bremsstrahlung linear polarization on the orbital motion of the electron is complicated by the intimate relationship between the spin and momentum of the Dirac electron ([3]). Spin effects become important in the production of the *high frequency radiation* with the result that the parallel linear polarization decreases; in fact, because of the interference effects between orbital and spin currents ([3]), there is a polarization reversal in this frequency region in which the radiation at small and large emission angles is polarized parallel and perpendicular respectively to the emission plane. In contrast, the perpendicular polarization of the *low frequency radiation* becomes larger as the electron energy increases because spin effects are relatively unimportant in this frequency region and because there is a greater probability for the occurrence of transverse acceleration effects (see Fig. 1 where $k \sim 0$).

This general description of the polarization behavior indicates that there are basically two different types of polarization reversals. The first type of reversal can be explained from classical considerations in terms of the orbital motion of the electron; it occurs as the photon energy changes from the low to the higy frequency region for a given emission angle and electron energy. The second type of reversal can be explained from relativistic considerations in terms of spin-orbit interference effects; it occurs as the photon emission angle changes from small to large values for high frequency photons and relativistic electron energies. These reversals are most prominent at electron energies of the order of the electron rest mass, and each type has been confirmed by experimental observations ([6,7]).

1'2. *Previous work.* – The bremsstrahlung linear polarization defined in eq. (1) has been estimated by three types of calculations involving different approximations. A brief description of these calculations is given in the following:

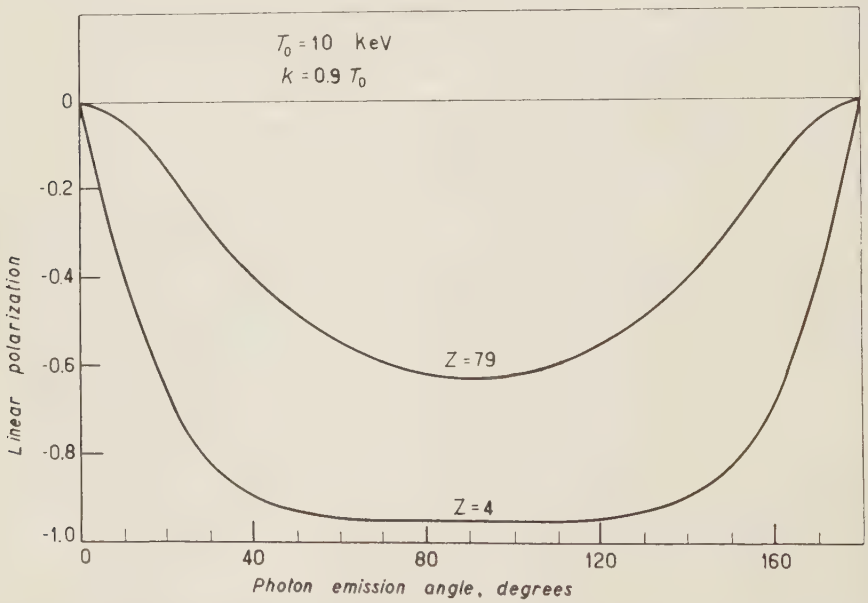

Fig. 2. Angular depencence of the high frequency linear polarization predicted by the Sommerfeld-Kirkpatrick-Wiedmann calculations ([9]) for a photon energy, k, equal to 9 keV with an initial electron kinetic energy, T_0, of 10 keV, and with a beryllium ($Z=4$) and a gold ($Z=79$) target.

([6]) J. W. MOTZ: *Phys. Rev.*, **104**, 557 (1956).
([7]) J. W. MOTZ and R. C. PLACIOUS: *Phys. Rev.*, **112**, 1039 (1958).

1) SOMMERFELD ([8]) has derived the non-relativistic dipole matrix element for the bremsstrahlung process with Coulomb wave functions and with no screening corrections. The Sommerfeld matrix element has been evaluated by KIRKPATRICK and WIEDMANN ([9]) for selected values of the electron energy, the photon energy, and the target material. In the present paper, the pola-

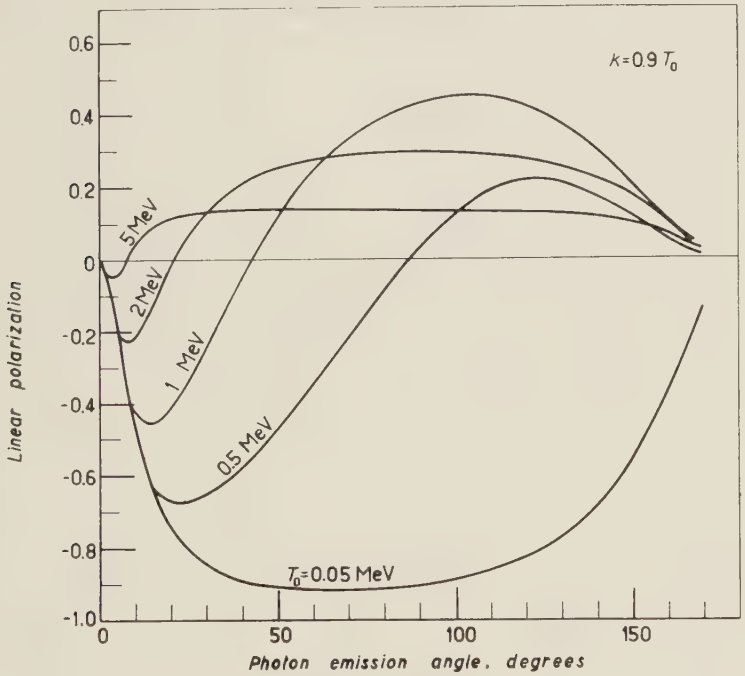

Fig. 3. – Angular dependence of the high frequency linear polarization predicted by the Gluckstern-Hull calculations ([10]) (without the screening correction) for photon energies, k, equal to 0.9 T_0, where the initial electron kinetic energy, T_0, is equal to 0.05, 0.5, 1, 2 and 5 MeV.

rization values predicted by the Sommerfeld theory have been taken from the Kirkpatrick-Wiedmann calculations which are summarized in Figs. 2-5 in reference ([9]). The Sommerfeld theory is valid only for electron energies with $\beta_0 \ll 1$, where β_0 is the ratio of the electron velocity to the velocity of light. In addition because screening effects are neglected, the accuracy of the Sommerfeld predictions is uncertain for very low electron energies (< 1 keV) and for high Z targets.

([8]) A. SOMMERFELD: *Ann. Phys.*, **11**, 257 (1931).
([9]) P. KIRKPATRICK and L. WIEDMANN: *Phys. Rev.*, **67**, 321 (1945).

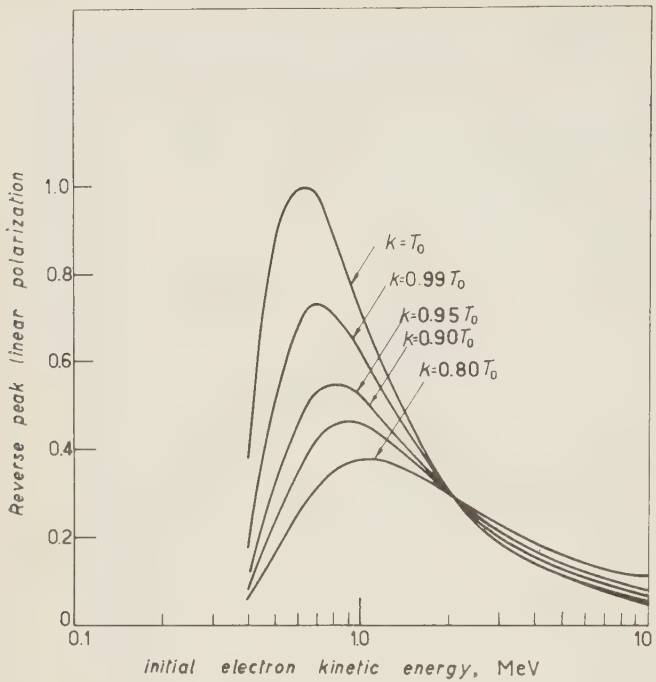

Fig. 4. – Dependence of the large angle peak perpendicular polarization (which is reverse to the small angle parallel polarization) on the initial electron kinetic energy, T_0, for photon energies, k, equal to $0.80T_0$, $0.90T_0$, $0.95T_0$, $0.99T_0$ and $1.0T_0$. These curves are predicted by the Gluckstern-Hull calculations [10] (without the screening correction).

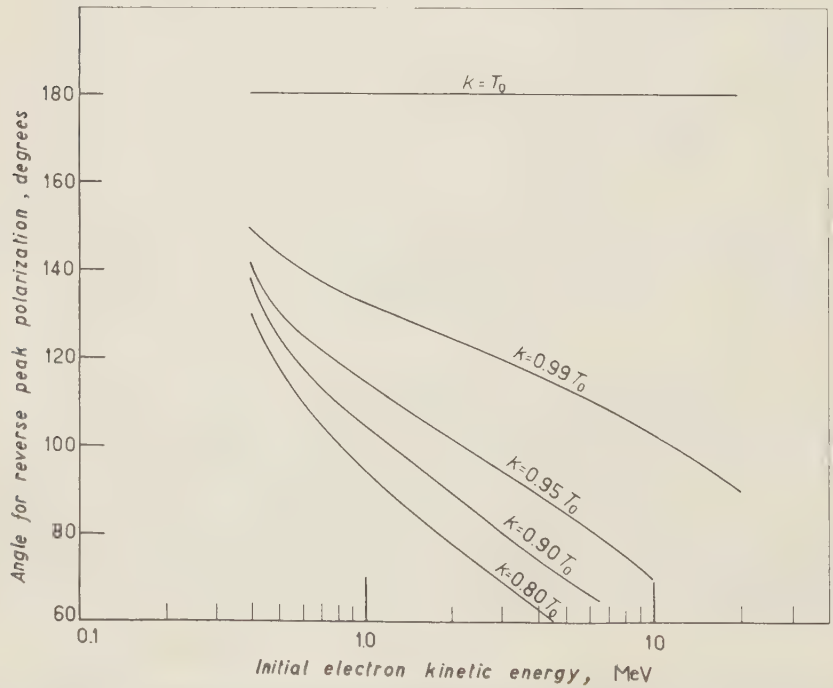

Fig. 5. - Photon emission angles corresponding to the reverse peak polarization plotted in Fig. 4, as a function of the initial electron kinetic energy, T_0, for photon energies, k, equal to $0.80T_0$, $0.90T_0$, $0.95T_0$, $0.99T_0$, and $1.0T_0$.

2) GLUCKSTERN and HULL ([10]) have derived relativistic cross-section formulas for the bremsstrahlung linear polarization by the Born-approximation procedure. These calculations are given with and without screening corrections and are valid only for the condition that $(2\pi Z/137\beta_0)$, $(2\pi Z/137\beta) \ll 1$, where β_0 and β are the ratios of the initial and final electron velocities in a collision to the velocity of light. The results of the Gluckstern-Hull predictions that are presented in this paper have been calculated from formulas (4.1), (4.2), (4.3), (13.1), and (13.2) in reference ([10]). Their approximate screening corrections break down for high frequency photons and are used only for comparisons involving low frequency photons. This same type of calculation has also been made by FRONSDAL and ÜBERALL ([4]) with a more accurate screening correction. However, the results of these two calculations do not differ appreciably in the intermediate electron energy region.

3) OLSEN and MAXIMON ([5]) have derived an extreme relativistic formula for the linear polarization in a relatively simple form with relativistic Coulomb wave functions (Sommerfeld-Maue). This formula includes screening corrections and is valid for arbitrary Z with an accuracy of the order of

$$\left(\frac{Z}{137}\right)^2 \frac{\ln (E/m_0c^2)}{E/m_0c^2} ,$$

where E is the total energy of the recoil electron. These calculations break down for electron energies below about 20 MeV, and require that E_0, E, and $k \gg m_0c^2$ and $p_0\theta_0 \sim 1$, where p_0 is the momentum of the initial electron in m_0c units. The results of the Olsen-Maximon calculations that are presented in this paper have been obtained from formulae (7.3) and (6.29) in reference ([5]). Previous calculations in this energy region were made in the Born approximation by MAY and WICK ([11]).

Very little experimental data are available on the quantitative behavior of the bremsstrahlung linear polarization. The main experimental results are summarized in the following:

1) For non-relativistic electron energies (30 to 40 keV), KULENKAMPFF ([12]), PISTON ([12]), and KULENKAMPFF, LEISEGANG, and SCHEER ([13]), measured the dependence of the linear polarization on the photon energy for thin aluminum targets at a 90 degree emission angle. The most recent results at 34 keV ([13])

([10]) R. L. GLUCKSTERN and M. H. HULL jr.: *Phys. Rev.*, **90**, 1030 (1953).

([11]) M. MAY and G. C. WICK: *Phys. Rev.*, **81**, 628 (1951); M. MAY: *Phys. Rev.*, **84**, 265 (1951).

([12]) H. KULENKAMPFF: *Phys. Zeits.*, **30**, 514 (1929); D. S. PISTON: *Phys. Rev.*, **49**, 275 (1936).

([13]) H. KULENKAMPFF, S. LEISEGANG and M. SCHEER: *Zeits. Phys.*, **137**, 435 (1954).

show reasonable agreement with the Sommerfeld theory for the upper half of the frequency region.

2) For electron energies of the order of the electron rest mass, MOTZ [6] measured the dependence of the linear polarization on the photon energy at a 20-degree emission angle with 1 MeV electrons incident on thin aluminum and gold targets, and MOTZ and PLACIOUS [7] measured the angular dependence of the polarization near the high frequency limit with 0.5 MeV electrons incident on thin beryllium and gold targets. The experimental results showed qualitative agreement with the Gluckstern-Hull predictions, although there were quantitative difference for the small angles and the high-Z targets.

3) For relativistic electron energies that are large compared to the electron rest mass, DUDLEY, INMAN, and KENNEY [14] measured the angular dependence of the polarization of 6 MeV photons for 24 MeV electrons incident on an aluminum target, and their results were not precise enough to test the theory. However, good agreement between experimental results and the Olsen-Maximon predictions was obtained by JAMNIK and AXEL [15], who measured the angular dependence of the polarization of 15.1 MeV photons for 25 MeV electrons incident on aluminum and platinum targets.

1·3. *Present work.* – The purpose of this work is 1) to give new experimental results for the angular dependence of the bremsstrahlung linear polarization in the electron energy range from 0.05 to 1.0 MeV where only Born-approximation calculations are available, and 2) to summarize the polarization behavior in the electron energy range from approximately 10^{-2} to 10^{3} MeV, on the basis of all available experimental and theoretical results.

The dependence of the linear polarization on the photon emission angle (in the range from 0 to 130 degrees) was measured for photon energies, k, approximately equal to $0.9\,T_0$ with T_0 (initial electron kinetic energy) equal to 0.05, 0.10, 0.25, 0.50, and 1.0 MeV, and to $0.1\,T_0$ with T_0 equal to 0.5 and 1.0 MeV. Data were obtained with thin targets of beryllium, aluminum, and gold. The experimental method used in these measurements has been described previously [6]. The polarimeter depends on the polarization sensitivity of the Compton process. For the selection of particular energy intervals in the bremsstrahlung spectrum in which the photon energies are larger than 100 keV, the polarimeter was operated as a double-crystal Compton spectrometer in the same manner as in the previous measurements [6,7]. However, for photon energies less than or equal to 100 keV ($k = 0.9\,T_0$ for $T_0 = 0.05$ and 0.10 MeV, and $k = 0.1\,T_0$ for $T_0 = 0.5$ and 1.0 MeV) where the recoil electron

[14] J. M. DUDLEY, F. W. INMAN and R. W. KENNEY: *Phys. Rev.*, **102**, 925 (1956).
[15] D. JAMNIK and P. AXEL: *Phys. Rev.* (To be published).

energies become less than 10 keV, the above method was modified so that only the energies of the Compton-scattered photons detected by the NaI crystal (see Fig. 3 in reference [6]) were selected with a pulse height analyzer. In these latter measurements, background pulses and Compton-escape pulses generated by higher energy photons were corrected for by measuring the counting rate differences that were obtained with and without the following filters inserted in front of the NaI crystal: 0.01 in. tin for $k = 0.1\,T_0$ with $T_0 = 500$ keV, 0.03 in. lead for $k = 0.1\,T_0$ with $T_0 = 1000$ keV, 0.06 in. tin for $k = 0.9\,T_0$ with $T_0 = 100$ keV, and 0.03 in. lead for $k = 0.9\,T_0$ with $T_0 = 50$ keV.

Estimates of the bremsstrahlung polarization were calculated from the results of the Sommerfeld-Kirkpatrick-Wiedmann theory [8,9], the Gluckstern-Hull theory [10], and the Olsen-Maximon theory [5]. These estimates give the dependence of the polarization on the photon energy and emission angle for electron energies in a range from 10^{-2} to 10^3 MeV and for Z values of 4 (beryllium), 13 (aluminum), and 79 (gold). The important details of these theoretical results are presented in this paper. The more accurate polarization estimates are given by the Sommerfeld theory in the non-relativistic region and by the Olsen-Maximon theory in the extreme-relativistic region. In the intermediate energy region, the estimates obtained from the Gluckstern-Hull (Born-approximation) theory are compared with the present experimental values. From these results the most accurate estimates for the peak values of the bremsstrahlung polarization at various photon energies are deduced as a function of the initial electron kinetic energy.

The polarization behaviour as a function of the initial electron energy shows important differences between the high and low frequency regions of the bremsstrahlung spectrum. There is a significant distinction between the two regions with regard to the relative importance of various factors such as spin, orbit, screening, and Coulomb [16] effects. Therefore, for the sake of a more logical and simplified presentation, the high frequency and low frequency polarization results are separated. For each region, results are given for the polarization dependence on the initial electron kinetic energy, the photon emission angle, and the target atomic number.

2. – The high frequency region.

The high frequency region of the bremsstrahlung spectrum is defined approximately as the region in which the final electron momentum is small compared to the initial momentum. In this region Coulomb and spin effects are

[16] According to common usage (see *e.g.* ref. [20]), the « Coulomb effect » or the « Coulomb correction » indicates the difference between the exact and the Born-approximation bremsstrahlung cross section.

important, and except for very low and very high electron energies, screening effects can be neglected.

The high frequency linear polarization tends to be *parallel* to the emission plane except for certain conditions discussed in Section 2·2, and the parallel polarization increases as the photon energy approaches the high frequency limit. The quantitative features of the high frequency polarization depend on the initial electron energy, the photon emission angle, and the atomic number of the target.

2·1. *Non-relativistic electron energies.* – For small electron energies where $\beta_0 \sim 0$, the Sommerfeld theory ([8]) predicts that the parallel polarization has a peak value at 90 degrees. This peak value is less than unity because not all of the electron recoil angles associated with the observed photons are in the emission plane and because the Coulomb field of the target atom tends to change the initial electron direction before the photon is emitted. An example of the influence of this Coulomb effect ([16]) on the polarization is shown in Fig. 2 which gives the angular dependence of the polarization predicted by the Sommerfeld-Kirkpatrick-Wiedmann results ([9]) for 9 keV photons produced by 10 keV electrons incident on a gold and a beryllium target. Because the Coulomb effect increases with Z, the results in Fig. 2 show that the peak polarization is smaller with gold than with beryllium. Also, as the neutral electron energy decreases in this non-relativistic region, the polarization will decrease because the Coulomb effect becomes larger. For example, according to the Sommerfel-Kirkpatrick-Wiedmann results ([9]), the peak polarization at the high frequency limit with a beryllium target decreases from approximately -0.89 to -0.68 as the initial electron energy decreases from 1 keV to 0.1 keV. As the initial electron energy decreases to zero, SCHERZER ([17]) has estimated that the peak polarization has a limiting value of 0.6 independent of the photon energy or the atomic number of the target.

For very small electron energies, screening corrections are important for high Z elements throughout the spectrum and must be applied to the Sommerfeld calculations. Although such corrections are not available, it is interesting to note that the qualitative effect of screening in the high frequency region of the bremsstrahlung spectrum is to *increase the parallel polarization* by giving an effectively smaller atomic number for the target nucleus. This increase is contrary to the effect produced in the low frequency region where the screening correction *decreases the perpendicular polarization* (see Sections 3·1, 3·2 and 3·3).

([17]) O. SCHERZER: *Ann. d. Phys.*, **13**, 137 (1932).

2·2. *Relativistic electron energies.* – As the electron energy increases, the peak parallel polarization of the high frequency photons increases in the non-relativistic region (owing to the decreasing Coulomb effect ([16])) up to a maximum value, and then decreases as relativistic effects become more important. Simultaneously, the peak polarization angle becomes progressively smaller.

The relativistic effects that are responsible for the decrease in the parallel polarization consist of: *a*) an increasing transverse acceleration in which the impact parameters become larger as the initial electron energy increases ([18]), with a corresponding increase in the component of the charge acceleration perpendicular to the initial electron direction, and *b*) electron spin-flip effects. Effect *a*) increases the component of the bremsstrahlung electric vector which is perpendicular to the emission plane (see Section **1**·1). Effect *b*) interferes with the orbital current sources of the bremsstrahlung ([3]) to the extent that under certain conditions of interference between spin-orbit currents, the dominant component of the electric vector is perpendicular to the emission plane ([7]).

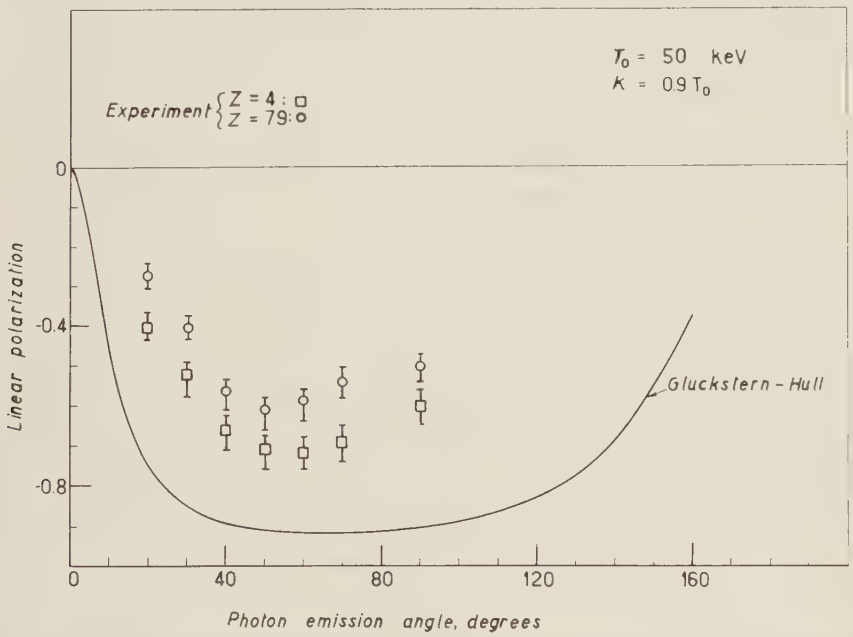

Fig. 6. – Angular dependence of the bremsstrahlung linear polarization for an initial electron kinetic energy, T_0, equal to 50 keV. The solid line is predicted by the Gluckstern-Hull calculations ([10]) (without the screening correction) for a photon energy, k, equal to 45 keV. The experimental points with a 0.3 mg/cm² beryllium target (squares) and a 0.13 mg/cm² gold target (circles) were obtained for a photon energy interval between approximately 42 and 50 keV.

([18]) W. HEITLER: *The Quantum Theory of Radiation*, 3rd ed. (London, 1954), p. 249.

The general behavior of the high frequency linear polarization described above is predicted by the Gluckstern-Hull theory [10]. Fig. 3 gives the angular dependence of the polarization predicted by the Gluckstern-Hull calculations [10] (with no screening) for various electron kinetic energies, T_0, and for high frequency photons with energies equal to $0.9T_0$. The parallel polarization has a broad peak at the lowest electron energy, and as the electron energy increases, the peak polarization becomes smaller and shifts to smaller angles. For electron energies of the order of the electron rest mass, there is a reversal in which the

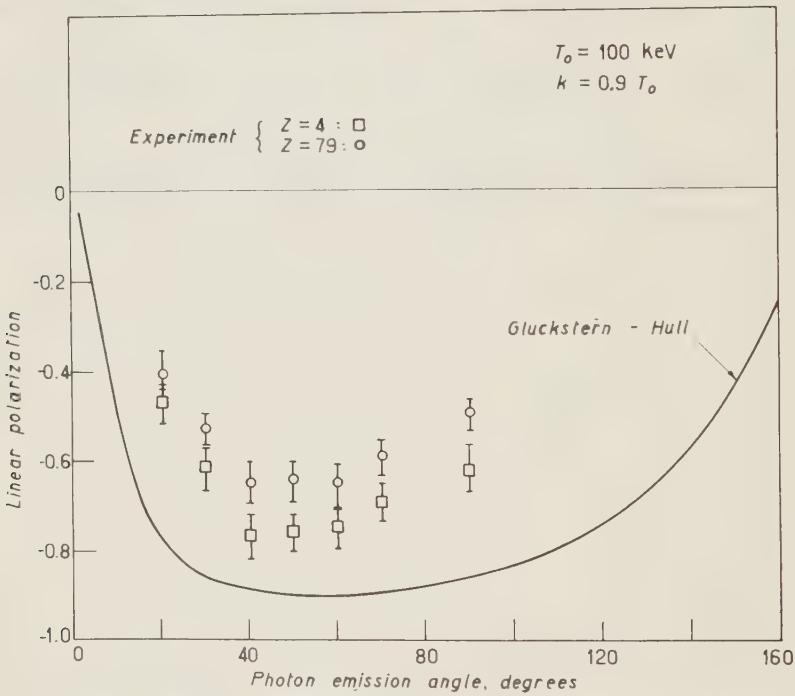

Fig. 7. Angular dependence of the bremsstrahlung linear polarization for an initial electron kinetic energy, T_0, equal to 100 keV. The solid line is predicted by the Gluckstern-Hull calculations [10], (without the screening correction) for a photon energy, k, equal to 90 keV. The experimental points with a 0.3 mg/cm² beryllium target (squares) and a 0.30 mg/cm² gold target (circles) were obtained for a photon energy interval between approximately 85 and 100 keV.

photons emitted at large angles tend to be polarized perpendicular to the emission plane. The perpendicular polarization that occurs in Fig. 3 for high frequency photons at large angles depends on the electron energy. The dependence of the reverse *peak* values on the electron kinetic energy, T_0, which is predicted by the Gluckstern-Hull formulas [10], is shown in Fig. 4 for high frequency photons with energies equal to T_0, $0.99T_0$, $0.95T_0$, $0.90T_0$, and $0.80T_0$. The peak values approach unity toward the high frequency limit and

the maximum peak value occurs at electron kinetic energies close to the electron rest energy. As the electron energy increases above 1 MeV, the peak perpendicular polarization decreases to small values because of the increasing importance of a spin-flip process which yields no linear polarization ([3]). The angles corresponding to the peak values for the perpendicular polarization in Fig. 4 were estimated from the Gluckstern-Hull formulas, and are plotted in Fig. 5 for the same range of electron and photon energies. The breakdown of the Born-approximation is especially severe at the high frequency limit where the peak angle (shown in Fig. 5) becomes 180 degrees. Because of this breakdown, the results given in Figs. 3 to 5 cannot be expected to provide more than a qualitative description of the polarization.

In the extreme-relativistic region of electron energies, no accurate predictions or measurements of the polarization are available for the high frequency limit. The Olsen-Maximon calculations ([5]) break down near this limit and are only valid for cases where the energy of the recoil electron is greater than at least 5 MeV.

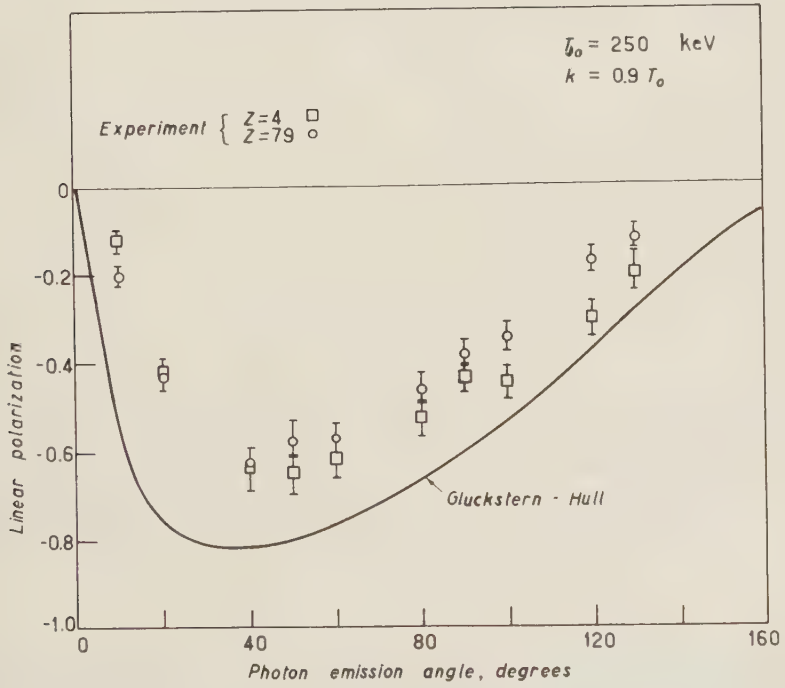

Fig. 8. – Angular dependence of the bremsstrahlung linear polarization for an initial electron kinetic energy, T_0, equal to 250 keV. The solid line is predicted by the Gluckstern-Hull calculations ([10]) (without the screening correction) for a photon energy, k, equal to 225 keV. The experimental points with a 4.3 mg/cm² beryllium target (squares) and a 0.21 mg/cm² gold target (circles) were obtained for a photon energy interval between approximately 210 and 250 keV.

2·3. *Experimental results for high frequency photons.* – The high frequency polarization measurements were made for photon energies equal to approximately $0.9\,T_0$, where T_0 is the initial electron kinetic energy. The range of electron energies extended from 50 to 1000 keV. For each electron energy, the bremsstrahlung polarization was measured as a function of the photon emission angle (from 10 to 130 degrees) for both beryllium and gold targets.

The experimental results are shown in Figs. 6 through 10. For this range of electron energies, the measurements are compared with the predictions of the Gluckstern-Hull calculations ([10]) (without the screening correction).

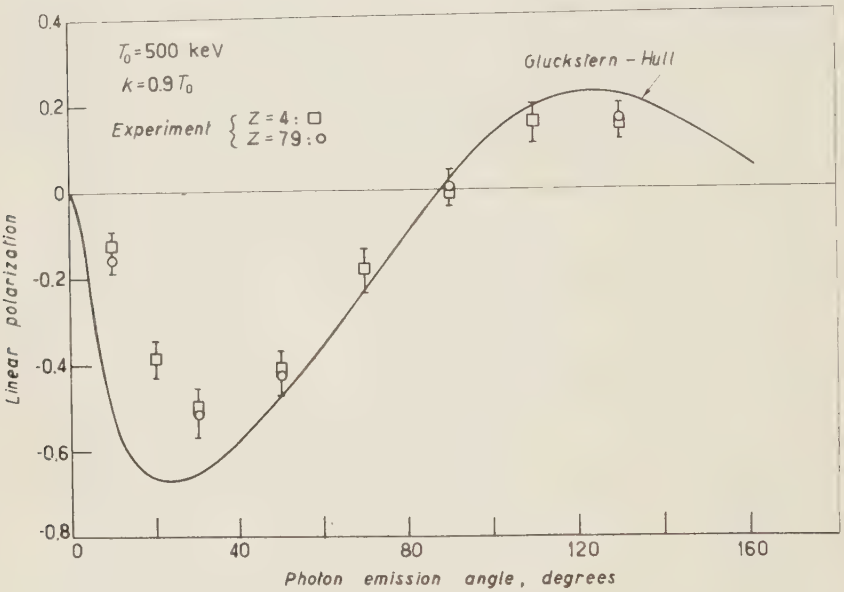

Fig. 9. – Angular dependence of the bremsstrahlung linear polarization for an initial electron kinetic energy, T_0, equal to 500 keV. The solid line is predicted by the Gluckstern-Hall calculations ([10]) (without the screening correction) for a photon energy, k, equal to 450 keV. The experimental points with a 4.3 mg/cm² beryllium target (squares) and a 0.21 mg/cm² gold target (circles) were obtained for a photon energy interval between approximately 420 and 500 keV.

The results show that the Gluckstern-Hull calculations overestimate the experimental values for the polarization at 50 keV, 100 keV, and 250 keV, and the differences decrease at 500 keV and 1000 keV. The largest differences occur at the small angles. The experimental results show that the polarization has a Z-dependence which is determined by the initial electron kinetic energy and which is consistent with the Sommerfeld predictions in the non-relativistic

region (see Section 4·1). The Z-dependence of the polarization changes with the electron energy in that the polarization is smaller for high Z than for low Z targets for electron energies below 500 keV (except for small angles at 250 keV) and the reverse is true at 1 000 keV; at 500 keV, the polarization is independent of Z. This pattern of the Z-dependent behavior can be seen more clearly in Section 4·1 where the peak polarization values are considered.

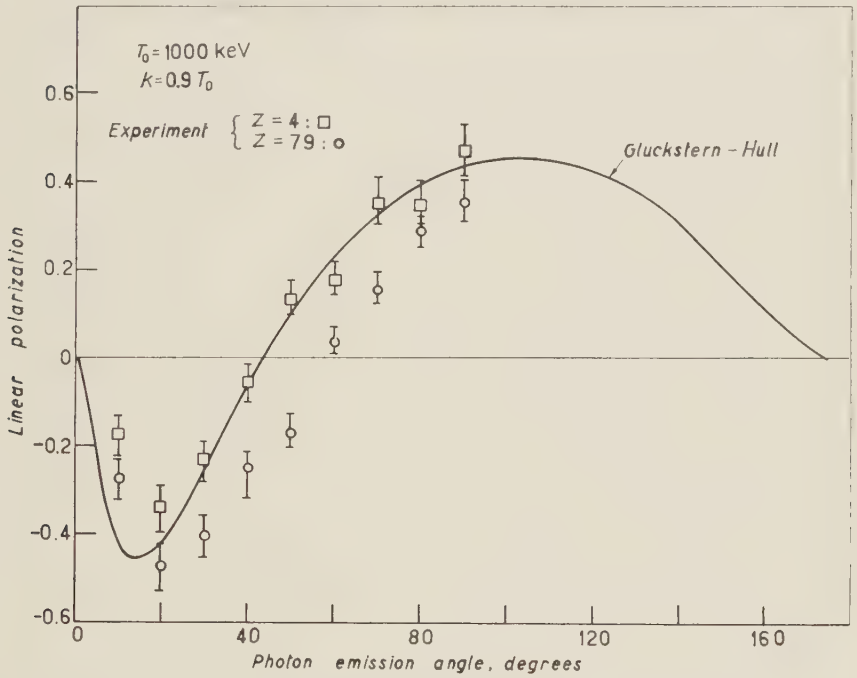

Fig. 10. – Angular dependence of the bremsstrahlung linear polarization for an initial electron kinetic energy, T_0, equal to 1 000 keV. The solid line is predicted by the Gluckstern-Hull calculations [10] (without the screening correction) for a photon energy, k, equal to 900 keV. The experimental points with a 4.3 mg/cm² beryllium target (squares) and a 0.43 mg/cm² gold target (circles) were obtained for a photon energy interval between approximately 850 and 1 000 keV.

The experimental results clearly verify the polarization reversals predicted at both 500 keV and 1 000 keV at the large emission angles. The variation of the Z-dependence of the perpendicular polarization with electron energy is uncertain, although it appears that the polarization is less (except for the Z-independence at 500 keV) for large Z than for small Z. As shown in Fig. 4, the reversal effect gives appreciable perpendicular polarization only in a small range of electron energies from roughly 0.4 to 3.0 MeV.

3. – The low frequency region.

The low frequency region of the bremsstrahlung spectrum is defined as the region in which the final momentum of the electron is approximately equal to its initial momentum. In this region, screening effects of the target atom are important. Also, the Coulomb effect ([16]) is important for certain electron energy regions, although this effect is not as large in the low frequency as in the high frequency region.

A basic distinction between the low and high freguency regions is the relative importance of electron spin effects. For relativistic electron energies, the spin terms of the bremsstrahlung matrix element are large in the high frequency region and become negligibly small in the low frequency region for $k \ll m_0c^2$ ([19]). Therefore, the polarization properties of the low frequency radiation are determined mostly by orbital rather than spin current effects.

The low frequency linear polarization tends to be *perpendicular* to the emission plane. This perpendicular polarization is a consequence of the transverse acceleration effect discussed in Section **1**˙1. Screening effects decrease the low frequency perpendicular polarization (see Section **2**˙1) by decreasing the average impact parameter with a corresponding decrease in the transverse effect. Because of the absence of spin-orbit interference effects ([3]), the low frequency polarization cannot be expected to exhibit any reversal as a function of the photon emission angle as in the high frequency region. The details of the low frequency polarization behavior must be considered for specific electron energies, photon angles, and target atomic numbers.

3˙1. *Non-relativistic electron energies.* – At non-relativistic electron energies, no accurate estimates or measurements of the low frequency polarization are available. The non-relativistic Sommerfeld calculations ([8]) are inadequate at low frequencies because of the neglect of screening effects. However, the Sommerfeld results show that the Coulomb effect ([16]) is important even near the limit of $k = 0$. For example, the peak polarization values predicted by the Sommerfeld-Kirkpatrick-Wiedmann results near the low frequency limit with 0.5 keV electrons are approximately 0.6 for $Z = 1$, and 0.5 for $Z = 10$. This polarization change near the low frequency limit, which is due to the Coulomb effect, is much smaller than the change near the high frequency limit where electrons get closer to the nucleus and where the polarization is approximately

([19]) See Eq. (6) in Ref. ([3]). Also, F. E. Low: *Phys. Rev.*, **110**, 974 (1958), shows that the bremsstrahlung cross section in the limit of $k = 0$ is given by the elastic scattering cross section times a factor which describes the X-ray emission associated with the scattering.

-1.0 for $Z=1$, and -0.6 for $Z=10$. It can be expected that if accurate screening corrections are made, the perpendicular polarization in the low frequency region will be considerably *smaller* than the values given above.

3·2. *Relativistic electron energies.* – As the initial electron kinetic energy increases above the electron rest mass energy, the maximum impact parameter increases ([20]) with a corresponding increase in transverse acceleration effects (see Section 1·1). The result of this change is that the low frequency perpendicular polarization increases slowly with the electron energy.

A general description of the low frequency perpendicular polarization is shown in Fig. 11, which gives the angular dependence of the polarization pre-

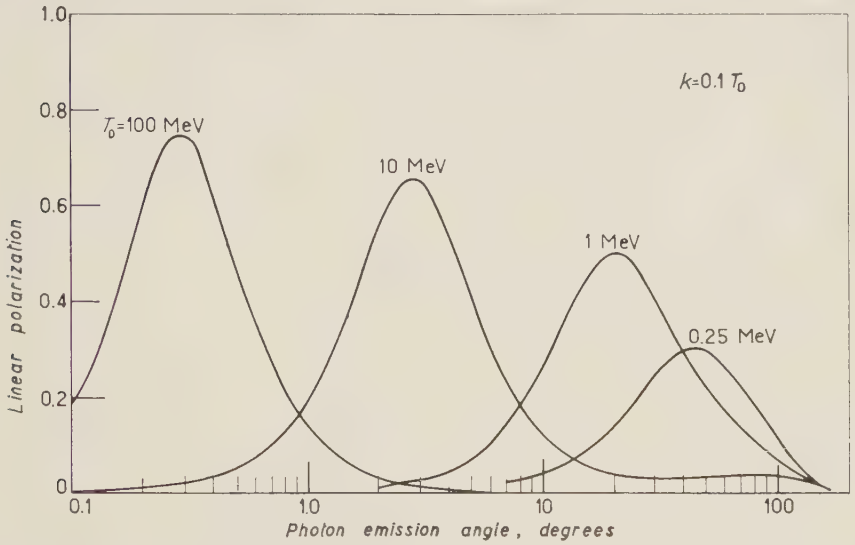

Fig. 11. – Angular dependence of the low frequency linear polarization predicted by the Gluckstern-Hull calculations ([10]) (without the screening correction) for photon energies, k, equal to 0.1 T_0, where the initial electron kinetic energy, T_0, is equal to 0.25, 1.0, 10, and 100 MeV.

dicted by the Gluckstern-Hull calculations ([10]) (without the screening correction) for photon energies, k, equal to $0.1T_0$, where the initial electron kinetic energy, T_0. is equal to 0.25, 1.0, 10, and 100 MeV. These results show a general increase of the peak polarization with electron energy, although if high Z screening corrections are included in the calculations, this increase becomes much smaller (see Section 4·1). The peak values for this low frequency polarization occur at an angle approximately equal to m_0c^2/E_0 (see Section 4·2).

([20]) H. W. Koch and J. W. Motz: *Rev. Mod. Phys.*, **31**, 920 (1959), (see Fig. 13).

For extreme-relativistic energies, accurate calculations of the low frequency polarization have beem made by OLSEN and MAXIMON [5]. These calculations include both Coulomb and screening corrections. However, the Olsen-Maximon results are valid only for a limited range of electron and photon energies and a limited range of photon emission angles. The photon energy, k, and the initial and final electron energies, E_0 and E, must satisfy the condition that E_0, E, and $k \gg m_0c^2$, while the photon emission angles must be confined to a region close to the peak angle where $p_0\theta_0 \sim 1$. The accuracy of the Olsen-Maximon predictions at angles far from the peak angle is uncertain.

3·3. *Experimental results for low frequency photons.* – The low frequency polarization measurements were made for photon energies equal to approximately $0.1\,T_0$, where the initial electron kinetic energy, T_0, is 500 and 1 000 keV. For each electron energy the angular dependence of the polarization was measured for both aluminum and gold targets. (Beryllium targets were not used

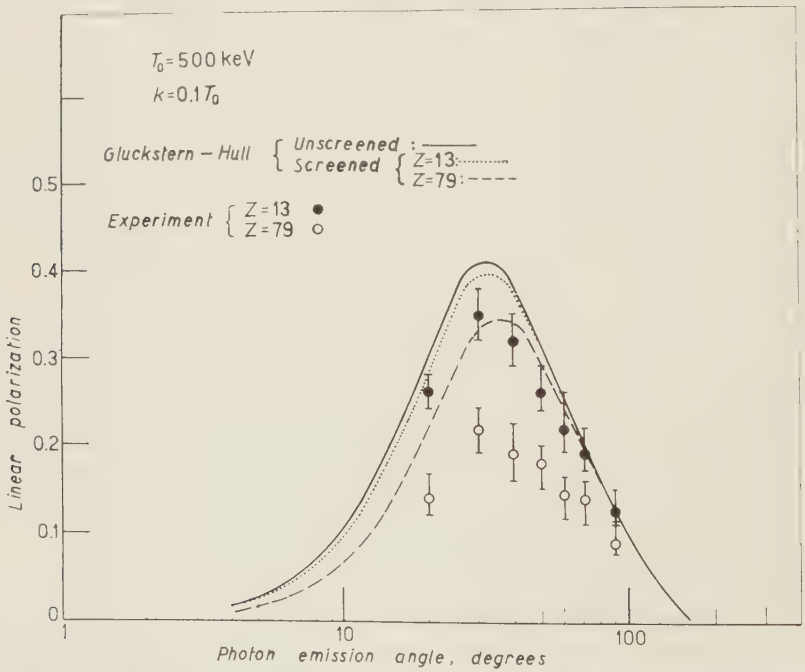

Fig. 12. Angular dependence of the bremsstrahlung linear polarization for an initial electron kinetic energy, T_0, equal to 500 keV. The Gluckstern-Hull predictions [10] for a photon energy, k, equal to 50 keV are given by the solid line (without the screening correction), the dotted line (with the screening correction for aluminum), and the dashed line (with the screening correction for gold). The experimental points with a 0.6 mg/cm² aluminum target (closed circles) and a 0.43 mg/cm² gold target (open circles) were obtained for a photon energy interval between approximately 45 and 55 keV.

in the low frequency region because of the contribution from electron-electron bremsstrahlung ([21]).) The experimental results are shown in Fig. 12 for $T_0 = 500$ keV and Fig. 13 for $T_0 = 1000$ keV. For these electron energies, the measurements are compared with the Gluckstern-Hull predictions with and without the screening correction ([10]).

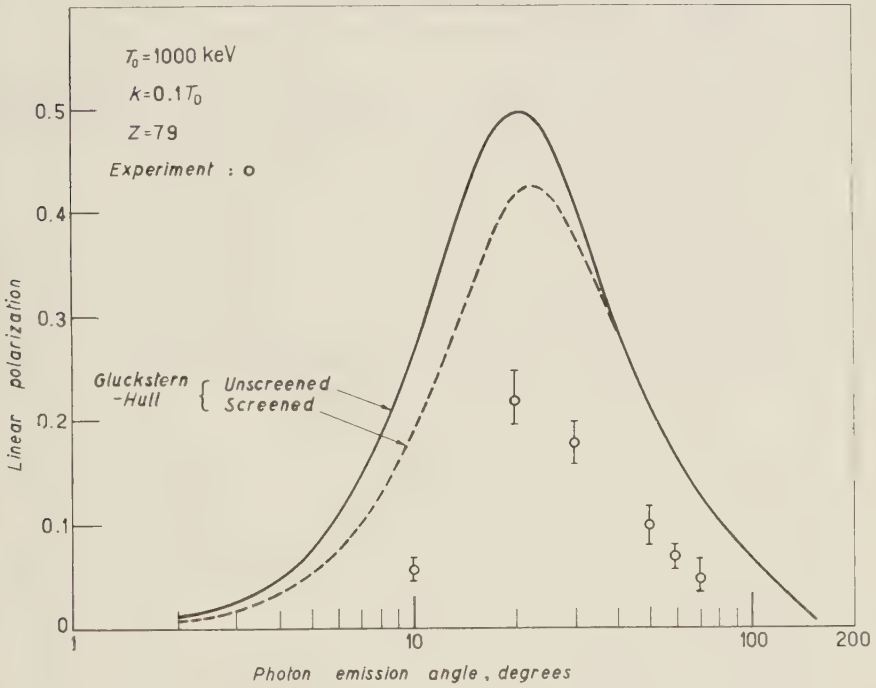

Fig. 13. – Angular dependence of the bremsstrahlung linear polarization for an initial electron kinetic energy, T_0, equal to 1000 keV. The Gluckstern-Hull predictions ([10]) for a photon energy, k, equal to 100 keV are given by the solid line (without the screening correction), and the dashed line (with the screening correction for gold). The experimental points for a 0.43 mg/cm^2 gold target (open circles) were obtained for a photon energy interval between approximately 95 and 105 keV.

The results show that the Gluckstern-Hull calculations with screening overestimate the experimental values for the polarization. The screening corrections are especially inadequate for the high Z (79) targets for which the disagreement at 1000 keV is as large as a factor of two, although part of this large discrepancy may arise because the calculations do not include the Coulomb corrections ([16]). However, the results for aluminum at 500 keV indi-

([21]) J. W. Motz: *Phys. Rev.*, **100**, 1560 (1955).

cate that for this region of electron energies, the Gluckstern-Hull predictions (with screening) for low frequencies and low atomic numbers have an accuracy of roughly 10 percent. Also, the results in Figs. 12 and 13 show that screening effects on the polarization are less important at the large angles where the momentum transfer to the nucleus is large.

4. – The peak linear polarization.

It is useful to condense the detailed information on the bremsstrahlung linear polarization in terms of the peak polarizations and the corresponding peak angles for given electron and photon energies. These peak values are obtained from data on the angular dependence of the polarization. For cases in the high frequency region where two peaks occur (see Fig. 3), the peak polarization refers only to the value at the smaller peak angle where the intensity is greater. The cases where the peak values are close to zero indicate that the angular distribution curves have no prominent peak at the small angles ($\theta_0 \sim m_0c^2/E_0$), and that larger polarization values occur at the large angles where the relative intensities are much smaller.

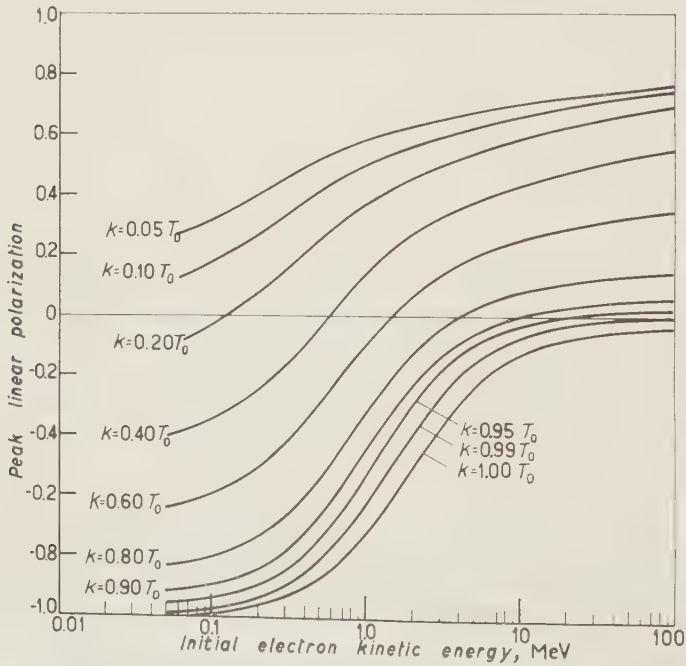

Fig. 14. – Dependence of the peak linear polarization predicted by the Gluckstern-Hull calculations [10] (without the screening correction) on the initial electron kinetic energy, T_0, for photon energies, k, equal to $0.05T_0$, $0.10T_0$, $0.20T_0$, $0.40T_0$, $0.60T_0$, $0.80T_0$, $0.90T_0$, $0.95T_0$, $0.99T_0$, and $1.0T_0$.

4·1. *Peak values.* – A general survey of the peak values for the polarization estimated from the Gluckstern-Hull theory ([10]) (without the screening correction) is given in Fig. 14. These results show the dependence of the peak polarization on the energies of both the initial electron and the photon. Because of the limitations of the Born approximation and the absence of screening corrections, these curves cannot be expected to give an accurate description of the polarization behavior. However, in a qualitative manner, the data show how the polarization tends to be parallel to the emission plane for high frequency photons and low energy electrons, and perpendicular to the emission plane for low frequency photons and high energy electrons.

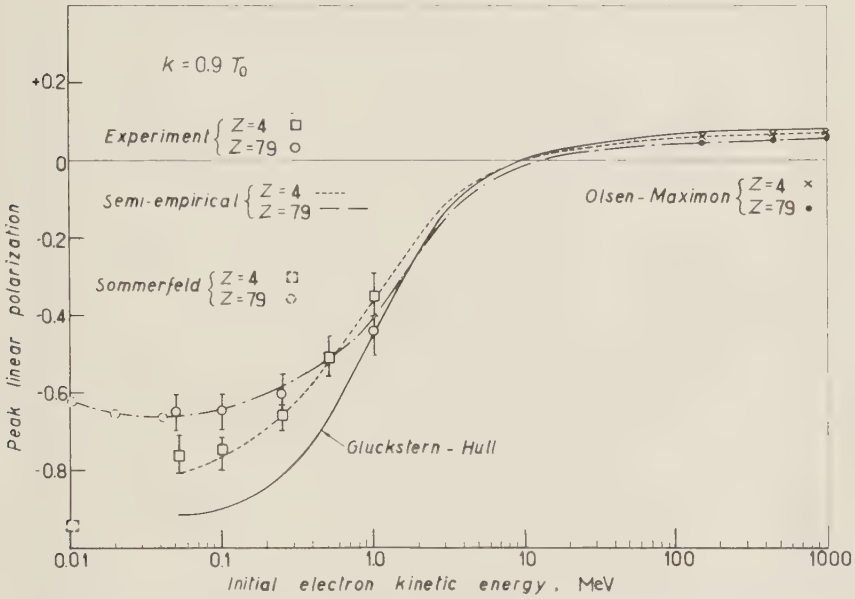

Fig. 15. - Dependence of the peak linear polarization on the initial electron kinetic energy, T_0, for photon energies, k, equal to 0.9 T_0. The solid line is predicted by the Gluckstern-Hull calculations ([10]) (without the screening correction). In the non-relativistic region, the Sommerfeld-Kirkpatrick-Wiedmann predictions ([9]) are shown by the dashed circles for gold and the dashed square for beryllium. In the extreme relativistic region, the Olsen-Maximon predictions ([5]) are shown by the closed circles for gold and the crosses for beryllium. The experimental values are shown by the open circles for gold and the squares for beryllium. The most accurate estimates of the polarization based on the combined data is given by the semi-empirical curves (dashed for beryllium and dot-dashed for gold).

The peak values for the high frequency polarization discussed in Sect. 2 are shown in Fig. 15. These data give the dependence of the peak polarization on the initial electron kinetic energy, T_0, in the range from 0.01 to 1000 MeV,

with the photon energy equal to $0.9T_0$. The solid line shows the predictions of GLUCKSTERN and HULL [10] (without the screening correction). Also, theoretical values for beryllium and gold are presented from the more accurate calculations of OLSEN and MAXIMON [5] in the extreme relativistic region (100 to 1000 MeV) and of SOMMERFELD, KIRKPATRICK, and WIEDMANN [9] in the non-relativistic region (0.01 to 0.04 MeV). The experimental values for beryllium and gold are given for electron energies of 0.05, 0.10, 0.25, 0.50, and 1.0 MeV. The results in the region of low electron energies show that the Gluckstern-Hull predictions overestimate the peak values. The most accurate estimates for the peak polarization with beryllium and gold targets are shown by the semi-empirical dashed and dot-dashed curves, which were plotted on

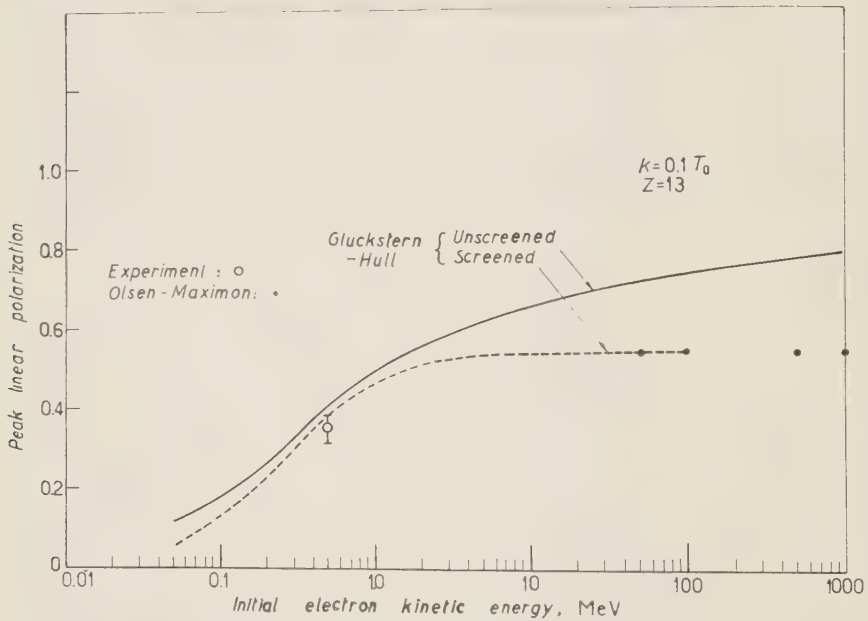

Fig. 16. – Dependence of the peak linear polarization on the initial electron kinetic energy, T_0, for photon energies, k, equal to $0.1T_0$ and for an aluminum target. The Gluckstern-Hull predictions [10] are shown by the solid line (without the screening correction) and by the dashed line (with the screening correction). The Olsen-Maximon predictions [5] are shown by the closed circles. The experimental results are shown by the open circles.

the basis of the combined experimental and theoretical data. These semi-empirical curves illustrate the Z-dependence of the peak polarization with the crossover feature (discussed in Section 2·3) at approximately 0.5 MeV. In the low energy region, it is interesting to observe that the peak polarization

for gold increases with electron energy up to a maximum value at about 0.05 MeV (see Section 2·2).

The peak values for the low frequency polarization discussed in Section 3·3 are shown in Figs. 16 and 17 for aluminum and gold respectively. These figures give the dependence of the peak polarization on the initial kinetic energy, T_0, in the range from 0.01 to 1000 MeV, with the photon energy equal to $0.1\,T_0$. The Gluckstern-Hull predictions with and without the screening corrections are compared with the experimental results for aluminum at 0.5 MeV (Fig. 16) and for gold at 0.5 and 1.0 MeV (Fig. 17). In the extreme-

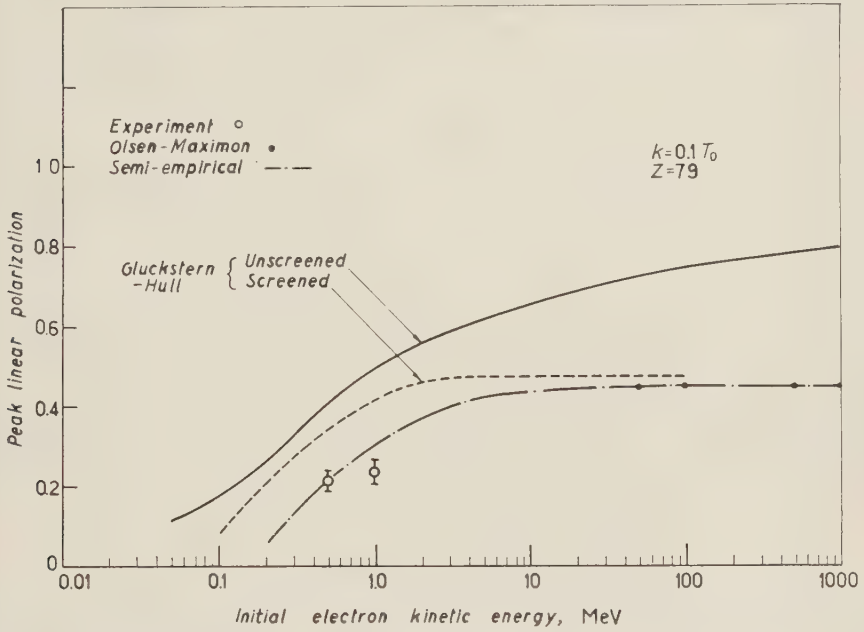

Fig. 17. – Dependence of the peak linear polarization on the initial electron kinetic energy, T_0, for photon energies, k, equal to $0.1\,T_0$ and for a gold target. The Gluckstern-Hull predictions ([10]) are shown by the solid line (without the screening correction) and by the dashed line (with the screening correction). The Olsen-Maximon predictions ([5]) are shown by the closed circles. The experimental results are shown by the open circles.

relativistic region from 50 to 1000 MeV, the Olsen-Maximon predictions of the peak polarization are shown. A comparison of the data shows that for low-Z targets, the predictions of the Gluckstern-Hull calculations with the screening correction agree reasonably well with the experimental results and with the Olsen-Maximon estimates. However, for high-Z targets, the Gluck-

stern-Hull calculations do not adequately take into account the screening or the Coulomb ([16]) effects with the result that the theoretical values are too large, especially at the lower electron energies. The most accurate estimates for the peak polarization with a gold target are given by the semi-empirical dot-dashed curve which was plotted from the experimental values and the Olsen-Maximon values. It is interesting to note that screening effects attenuate the rise in the polarization at the higher energies, so that above 2 MeV, the peak polarization is almost independent of the electron energy.

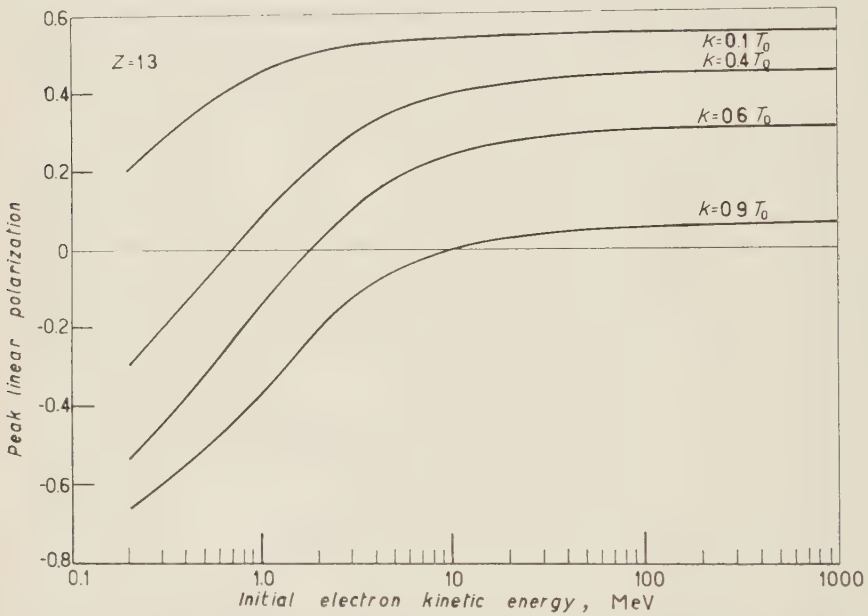

Fig. 18. · Dependence of the peak linear polarization with an aluminum target on the initial electron kinetic energy, T_0, for photon energies, k, equal to $0.1T_0$, $0.4T_0$, $0.6T_0$ and $0.9T_0$. These curves represent the best estimates of the peak polarization based on the combined experimental and theoretical data.

A summary of the most accurate estimates of the peak polarization is given by the semi-empirical curves in Fig. 18 for an aluminum target, and in Fig. 19 for a gold target. As shown in Figs. 15, 16, and 17, the data used to plot these curves consist of *a*) the Olsen-Maximon predictions ([5]) for the extreme-relativistic region, *b*) the present experimental values and previous measurements ([6]) for the intermediate energy region, and *c*) the Sommerfeld-Kirkpatrick-Wiedmann predictions ([9]) for the non-relativistic region. The accuracy of these curves is estimated to be approximately 10 percent in the low and intermediate energy region, and approximately 2 percent in the extreme-

relativistic region. The results indicate that under the best conditions it would be difficult to obtain a bremsstrahlung photon beam with a linear polarization

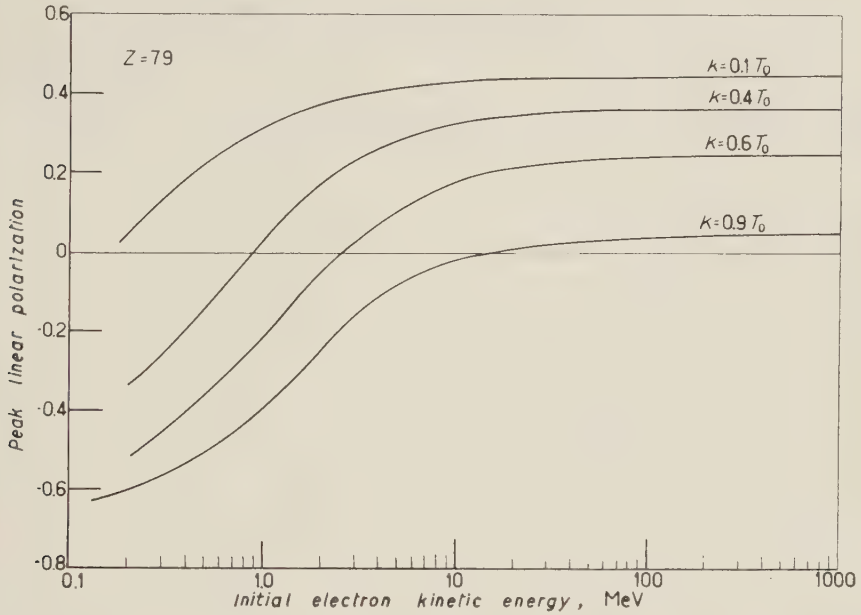

Fig. 19. – Dependence of the peak linear polarization with a gold target on the initial electron kinetic energy, T_0, for photon energies, k, equal to $0.1T_0$, $0.4T_0$, $0.6T_0$ and $0.9T_0$. These curves represent the best estimates of the peak polarization based on the combined experimental and theoretical data.

much greater than 50 percent (unless the photons were selected in coincidence with the recoil electrons).

4·2. *Peak angles.* – Because of the complicated expressions for the angular dependence of the polarization, it is convenient to have some general information on the angles corresponding to the peak values of the polarization discussed in Section 4·1. These peak angles depend on the electron and photon energies, as well as the atomic number of the target.

For non-relativistic electron energies where $\beta_0 \sim 0$, the Sommerfeld-Kirkpatrick-Wiedmann calculations [9] predict that the peak polarization occurs at 90 degrees. This peak angle is independent of both the photon energy and the atomic number of the target. Also at these low energies, the angular dependence of the polarization has a broad peak in which the polarization is not sensitive to small angular changes.

For extreme-relativistic electron energies (above 25 MeV), the Olsen- Maximon calculations ([5]) show that the angle for the peak polarization is approximately equal to m_0c^2/E_0. This relationship is reasonably accurate (see Section 1·2) for low-Z targets and for photon energies that are at least 5 MeV smaller than the high-energy limit. As the value of Z increases, the peak angle becomes larger than m_0c^2/E_0: for example, in this energy region the peak angle increases from m_0c^2/E_0 for beryllium ($Z = 4$) to approximately 1.13 m_0c^2/E_0 for gold ($Z = 79$). However, even though this high-Z shift for the peak angle

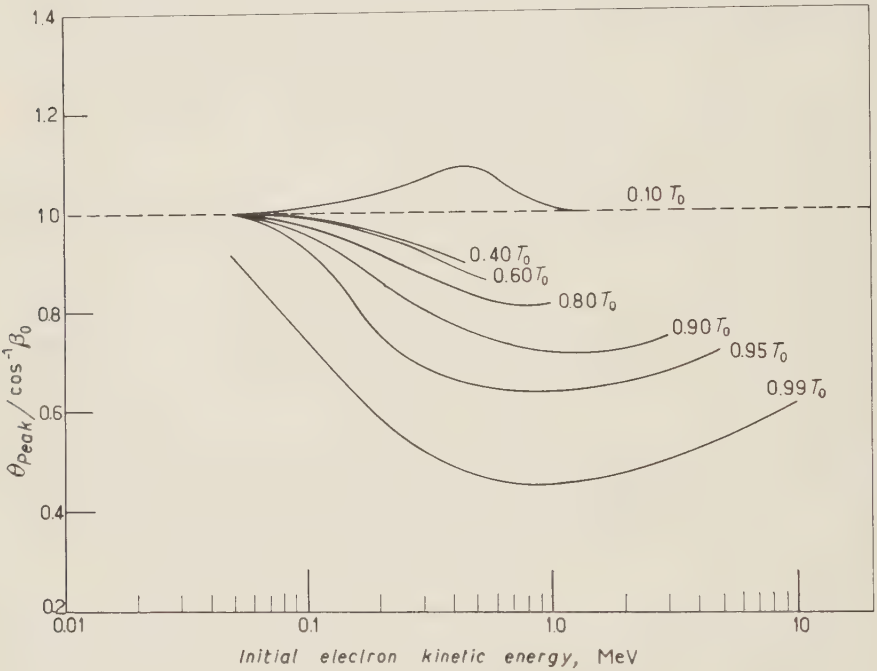

Fig. 20. – Dependence of the angle corresponding to the peak polarization on the initial electron kinetic energy, T_0, for photon energies, k, equal to 0.10 T_0, 0.40 T_0, 0.60 T_0, 0.80 T_0, 0.90 T_0, 0.95 T_0 and 0.99 T_0. The peak angle, θ_{peak}, is given in units of the Sommerfeld angle ([22]), $\cos^{-1}\beta_0$, where β_0 is the ratio of the initial electron velocity to the velocity of light. These curves are predicted by the Gluckstern-Hull calculations ([10]) (without the screening corrections).

represents an appreciable fractional increase in m_0c^2/E_0, the value of the polarization at an angle equal to m_0c^2/E_0 for high-Z targets is only about 2 percent smaller than the value at the peak angle. As the photon energies approach the high frequency limit, the estimates for the peak angle are uncertain, although the information at the lower electron energies (see Fig. 20) indicates that this

angle will be smaller than m_0c^2/E_0. In contrast to the non-relativistic region, the angular dependence of the polarization has a narrow peak which makes the polarization very sensitive to small angular changes. Quantitative details on this angular dependence are given by the Olsen-Maximon formulas (7.3) and (6.29) in reference ([5]).

KULENKAMPFF, SCHEER and ZEITLER ([22]) have suggested a general expression for the peak angle which covers the whole range of electron energies. This peak angle is given as $\cos^{-1}\beta_0$, where β_0 is the ratio of the initial electron velocity to the velocity of light. In agreement with the extreme cases discussed above, this peak angle becomes 90 degrees in the non-relativistic region and m_0c^2/E_0 in the extreme-relativistic region. For intermediate electron energies (of the order of the electron rest energy), the Gluckstern-Hull calculations ([10]) (without the screening correction), show that the peak polarization angle deviates from the quantity, $\cos^{-1}\beta_0$. The Gluckstern-Hull predictions are shown in Fig. 20 which gives the dependence of the peak angle on the initial electron kinetic energy. The peak angles are given for the energy regions where the polarization is larger than approximately 20 percent. The largest deviations from $\cos^{-1}\beta_0$ occur in the region near the high frequency limit, which is also the region where the Born approximation is least reliable. Except for this large uncertainty in the high frequency region, the theoretical peak angles in Fig. 20 do not show great differences with the experimental values in Figs. 6 through 10 for both low and high Z targets. Screening and Coulomb corrections generally make the peak angle for high Z targets larger than $\cos^{-1}\beta_0$ as indicated by Figs. 12 and 13 and by the Olsen-Maximon formulas (7.3) and (6.29) in reference ([5]).

* * *

We wish to give special thanks to Dr. U. FANO for many clarifying discussions on the bremsstrahlung process. Also, we are grateful to Dr. H. O. WYCKOFF for constructive suggestions during the course of this work, to Mr. GEORGE OFELT for assistance with some of the measurements, and to Dr. H. W. KOCH and Dr. M. DANOS for helpful discussions.

([22]) H. KULENKAMPFF, M. SCHEER and E. ZEITLER: *Zeits. Phys.*, **157**, 275 (1959). We are grateful to Dr. M. SCHEER for informing us of this work before its publication.

RIASSUNTO (*)

Nel presente lavoro si espone una descrizione quantitativa generale della polarizzazione lineare di bremsstrahlung sulla base dei dati sperimentali originali e dei calcoli teorici disponibili. I risultati danno la dipendenza della polarizzazione da: *a*) l'energia cinetica iniziale dell'elettrone, T_0, nel campo da 10^{-2} a 10^3 MeV; *b*) l'energia dei fotoni nel campo fra $0.1T_0$ e T_0; *c*) l'angolo di emissione dei fotoni nel campo fra 0° e 180°, e *d*) il numero atomico del bersaglio nel campo fra 4 e 79. I dati sperimentali sono stati ottenuti per una zona di energie dell'elettrone da 0.05 a 1.0 MeV con bersagli di berillio, alluminio ed oro. Le valutazioni teoriche della polarizzazione furono dedotte dai risultati di Sommerfeld-Kirkpatrick-Wiedmann per la regione non-relativistica di energia, dai risultati di Olsen-Maximon per la regione relativistica estrema, e dai risultati di Gluckstern-Hull (approssimazione di Born) per la regione intermedia. I risultati finali sono espressi in termini della polarizzazione di picco e il corrispondente angolo di picco come funzione delle energie dell'elettrone e del fotone, e le migliori valutazioni della polarizzazione sono espresse sulla base dei risultati sperimentali e teorici combinati.

(*) *Traduzione a cura della Redazione.*

IL NUOVO CIMENTO Vol. XV, N. 4 16 Febbraio 1959

Observation of Quantum Effects in an Electron Synchrotron (*).

M. Sands

California Istitute of Technology - Pasadena, Cal.

(ricevuto il 2 Novembre 1959)

Summary. — The rate of loss from synchronism of electrons in a synchrotron has been measured for various accelerating voltages and for electron energies from 800 to 1 200 MeV. The results agree with a computation of the loss expected from the quantum excitation of phase oscillations.

1. – Introduction.

When the electron synchrotron at the California Institute of Technology was first put into operation at energies near 1 GeV, in August 1956, the maximum energy which could be reached appeared to be limited by the maximum voltage available at the accelerating gap (120 kV), although this voltage was much larger that the computed radiation loss. It appeared that the limitation was due to the loss of electrons from synchronism owing to the excitations of phase oscillations by the quantum effects in the electron radiation. Measurements were made at that time which gave quantitative agreement with a theoretical analysis of the quantum effects [1]. The recent interest in quantum effects in electron accelerators—particularly with respect to the problems associated with storage rings—has prompted this report.

The CalTech synchrotron has some properties which make it possible to perform tests on the quantum effects under particularly simple conditions. First, the acceleration time is long (≈ 200 ms) compared with the damping

(*) This work was supported in part by the U. S. Atomic Energy Commission.

(1) These earlier results were included in a report on the C.I.T. synchrotron given at the West Coast Meeting of the A.P.S. in December 1956, *Bulletin*, **1**, 394 (1956).

time constant for radiation effects at high energies (≈ 10 ms). Second, the magnet excitation equipment can provide a « plateau », an interval of 20 ms during which the magnet current, and hence, the magnetic field strength, are held constant to within one part in 10^3. The magnet current increases linearly until the pleateu is reached. The plateau can be set to occur at magnetic fields which correspond to any electron energy up to the maximum obtainable. Third, the control of the program for the amplitude of the R.F. voltage on the accelerating cavity permits the selection of an arbitrary, constant amplitude at the cavity during the plateau, without influencing the program during the preceding acceleration interval.

We present below the theoretical expectation of the rate of loss from synchronism of electrons in a synchrotron with a stationary guide field and with a constant cavity voltage. We then give the results of some new measurements of the observed loss rates.

2. – Theory.

The equation which describes the phase oscillations in an electron synchrotron with a stationary guide field and a constant R.F. amplitude can be written,

$$\frac{\mathrm{d}^2\varphi}{\mathrm{d}t^2} + \varrho\,\frac{\mathrm{d}\varphi}{\mathrm{d}t} + \Omega_0^2\,(\sin\varphi - \sin\varphi_s) = g(t)\,, \tag{1}$$

where

$$\varrho = (4 - \alpha)\,\frac{P_{\gamma s}}{E_s}\,, \tag{2}$$

and

$$\Omega_0^2 = \frac{2\pi k \alpha e V}{\lambda t_s^2 E_s}\,. \tag{3}$$

Here, φ is the phase angle of the cavity voltage at the instant of passage of the electron, and φ_s is the equilibrium phase angle. The other parameters are:

- k: the harmonic number, the ratio of the cavity frequency to the electron rotation frequency.
- λ: the circumference factor, the ratio of the orbit length to 2π times the electron radius in the guide field.
- α: the momentum compaction; $\mathrm{d}r/r_s = \alpha\,\mathrm{d}p/p_s$.
- E_s: the energy of the synchronous electron.
- $P_{\gamma s}$: the average power radiated by a synchrotron electron.

eV: the energy gain of an electron which traverses the cavity at $\varphi = \pi/2$ ($\sin\varphi_s = P_{\gamma s}/eV$).

t_s: the period of circulation of the synchronous electron.

$g(t)$ is the driving function for the phase oscillations and has been discussed in an earlier paper ([2]).

Equation (1) describes the one dimensional motion of a model particle of unit mass in a potential of the form

$$U = \Omega_0^2(\cos\varphi + \varphi\sin\varphi_s)\,. \tag{4}$$

The model particle will oscillate about φ_s if its oscillation energy is less than the difference ΔU between the potential minimum at φ_s and the nearby maximum at $\varphi = \pi - \varphi_s$. The particles escape from the potential well if their oscillation energy exceeds the barrier height ΔU, which is given by

$$\Delta U = \Omega_0^2[2\cos\varphi_s - (\pi - 2\varphi_s)\sin\varphi_s]\,. \tag{5}$$

It has been shown ([2-5]) that phase oscillations in a synchrotron are excited by quantum emission and damped by the average radiation loss so that there is a « brownian motion » in phase with a mean square fluctuation σ_φ^2. This fluctuation corresponds to a mean « excitation energy » of the model particle, described above, of

$$U_{ex} = \sigma_\varphi^2\,\Omega_0^2\cos\varphi_s\,. \tag{6}$$

Excitation energies much larger than the mean value—which correspond to abnormal fluctuations in the radiation loss—give rise to amplitudes of phase oscillations sufficiently large that the model particle escapes over the potential barrier. The corresponding electron slips from synchronism.

The problem of the diffusion of thermally excited particles over a barrier near a harmonic well has been considered by KRAMERS ([6]) who finds that the relative loss rate of particles from the well is

$$-\frac{1}{N}\frac{\mathrm{d}N}{\mathrm{d}t} = \varrho\frac{\Delta U}{U_{ex}}\exp\left[\frac{\Delta U}{U_{ex}}\right], \tag{7}$$

where ϱ is the damping coefficient of eq. (1).

([2]) M. SANDS: *Phys. Rev.*, **97**, 470 (1955).

([3]) A. A. SOKOLOV, I. M. TERNOV and G. M. STRAČOVSKIJ: *Žurn. Èksp. Teor. Fiz.*, **31**, 439 (1956).

([4]) K. W. ROBINSON: *Phys. Rev.*, **111**, 373 (1958).

([5]) A. A. KOLOMENSKIJ and A. N. LEBEDEV: *Supp. Nuovo Cimento*, **7**, 43 (1958).

([6]) H. A. KRAMERS: *Physika*, **7**, 285 (1940).

R. F. CHRISTY has shown (7) that the method of Kramers is applicable to the problem of electron loss in a synchrotron, and that the approximations made in obtaining eq. (7) should probably introduce errors of less than 20%. ROBINSON has considered (8) the problem of the diffusion of electrons in the phase space of energy oscillations and arrived independently at the formula of eq. (7). No estimate was given of the errors introduced by the approximations made. MATVEEV (9) and MOROZ (10) have also considered the problem of loss from phase stability, but do not give expressions for the loss rate.

We define the time constant τ for electron loss as the inverse of the relative loss rate of eq. (7). Substituting the quantities of eqs. (4), (5) we obtain

$$\tau = \left[-\frac{1}{N}\frac{\mathrm{d}N}{\mathrm{d}t}\right]^{-1} = \theta \exp[\delta], \tag{8}$$

with

$$\theta = \frac{k\alpha t_s}{(4-\alpha)^2\lambda}\frac{E_1}{\Delta E_\gamma}\frac{1}{H(s)}, \tag{9}$$

and

$$\delta = \frac{(4-\alpha)\lambda}{k\alpha}\frac{E_s}{E_1}H(s). \tag{10}$$

We have written $\Delta E_\gamma = t_s P_{\gamma s}$ for the radiation loss in one revolution. E_1 is a universal constant with the dimensions of an energy:

$$E_1 = \frac{55\sqrt{3}}{64}\frac{hc}{e^2}mc^2 = 1.04\cdot 10^8 \text{ eV}. \tag{11}$$

The function $H(s)$ depends only on the « overvoltage »

$$s = eV/\Delta E_\varphi = [\sin\varphi_s]^{-1}.$$

$$H(s) = 2\operatorname{ctg}\varphi_s - \pi + 2\varphi_s = 2\sqrt{s^2-1} - \pi + 2\sin^{-1}\frac{1}{s}. \tag{12}$$

In the equations above we have used for σ_φ^2 the relation (*) given in Ref. (2) (there denoted by $\langle\psi^2\rangle_{AV}$).

(7) R. F. CHRISTY: *Synchrotron Beam Loss due to Quantum Fluctuations in the Radiation*, California Institute of Technology (1957), unpublished.

(8) K. W. ROBINSON: *Calculated Radiation Effects*, Cambridge Electron Accelerator Report CEA-69, Dec. 1958.

(9) A. N. MATVEEV: *Žurn. Èksp. Teor. Fiz.*, **33**, 1254 (1957).

(10) E. M. MOROZ: *Žurn. Èksp. Teor. Fiz.*, **33**, 1309 (1957).

(*) A. A. KOLOMENSKIJ and A. N. LEBEDEV (5) state that the result of Ref. (2) is in error by a factor of λ. The result of Ref. (2) agrees with that of ROBINSON (4) and I believe it to be correct.

The time constant for electron loss has been computed for the CalTech synchrotron for various energies and R.F. voltages, and is plotted in Fig. 1. The parameters used for the computations are

$$k = 4 \qquad t_s = 0.96 \cdot 10^{-7}\ \mathrm{s},$$

$$\lambda = 1.26 \qquad \Delta E_\gamma = 50\ \mathrm{keV}\,(E_s/1\ \mathrm{GeV})^4$$

$$\alpha = 2.5\ .$$

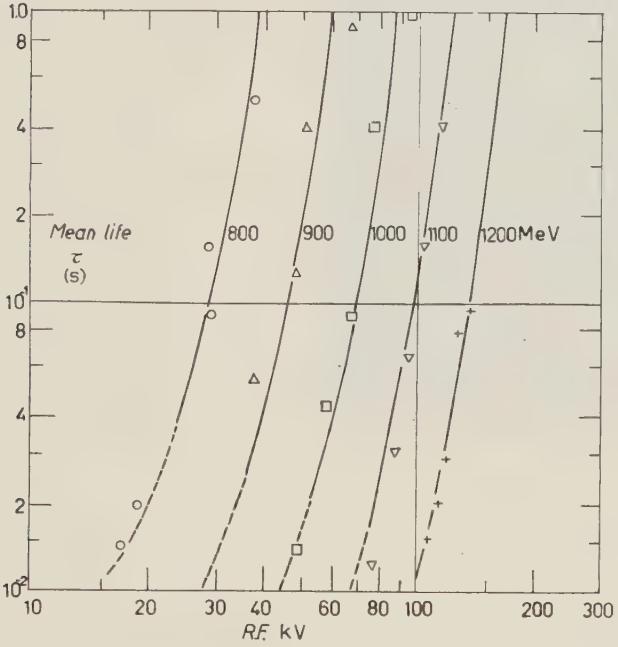

Fig. 1. – The mean life of the circulating electrons as a function of the amplitude of the R. F. voltage on the accelerating gap for various synchronous electron energies. The curves were computed from Eq. (8).

The broken line part of the curves correspond to loss time constants less than 5 times the damping constant $1/\varrho$. The theory should not be expected to apply for such high loss rates.

3. – Experiment.

Measurements were made of the time dependence of the number of electrons circulating in the synchrotron while holding constant the strength of the magnetic guide field and the amplitude of excitation of the R.F. cavity. Electrons

were accelerated to the plateau of the guide field by the normal R.F. program with which few electrons are lost. At the start of the 20 ms plateau of the guide field, the R.F. amplitude is reduced to a predetermined value and held at this value for the duration of the plateau. Oscilloscope signals proportional to the guide field strength at the orbit and to the R.F. amplitude are shown in the photograph of Fig. 2(*a*) for which the plateau has been set at 1000 MeV. The electron energy at the plateau is determined to 0.1% by a separate measurement of the magnetic field strength at the orbit.

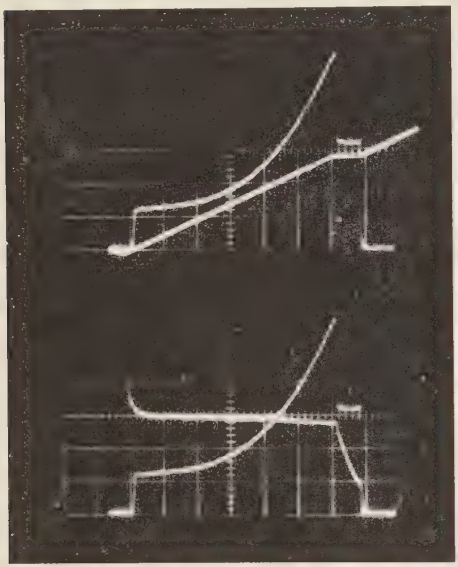

Fig. 2. – *a*) Oscillograms of magnetic field strength and R.F. voltage for the measurements at 1 GeV. *b*) Oscillograms of the R.F. voltage and the electron monitor.

The signal which indicates the R.F. amplitude is obtained from a diode rectifier driven by a loop in the R.F. cavity. The signal is proportional to the amplitude of excitation of the cavity for excitations encountered in these measurements and has been calibrated in terms of the cavity voltage ([11]).

The number of circulating electrons is determined by means of an induction electrode which encircles the electron trajectories. The current signal to the electrode is fed to an amplifier which is tuned (broadly) to the frequency of the accelerating cavity. The tuned amplifier operates a diode detector whose output is proportional to the number of electrons circulating in the synchtron—averaged over about 100 μs ([12]).

The rate of electron loss was measured by photographing an oscilloscope on which were displayed, simultaneously, the R.F. amplitude signal and the electron monitor signal. A typical photograph (for 1000 MeV) is shown in Fig. 2(*b*). From measurements on such photographs, the R.F. amplitude and the relative decrease in the number of circulating electrons during the 20 ms plateau interval were determined. From this latter number the loss time constant was computed.

([11]) Determined by R. M. Worlock and R. V. Langmuir, who were also responsible for the construction of the R. F. Cavity and drive system.

([12]) The author is indebted to H. Seidel and R. Hundley for assistance in the design and construction of this electron monitoring system.

The experimental results are shown by the indicated points in Fig. 1. The measurements were not extended to include loss time constants greater than one second, because electron losses of less than 5% could not be determined with significant accuracy.

For the experimental points of Fig. 1 the scale of R.F. voltage was adjusted to give the best fit with the theoretical curves. The scale of R.F. amplitude obtained in this way was 0.9 times that given by the calibration referred to above. Since the accuracy of that determination is estimated to be about 10%, the scale adjustment is probably justified.

It appears from Fig. 1 that over the region of energies and loss rates covered in this experiment the agreement with the theory is satisfactory.

It may be remarked that the sudden decrease of the R.F. voltage at the start of the plateau occurs in a time of a few hundred microseconds. It is, thus, not strictly true that the electron loss occurs under stationary conditions, particularly since the time to establish these conditions ($1/\varrho$) is comparable with the plateau duration. No attempt has been made to correct for such effects.

The experimental results given here were obtained in July 1959 after the installation of a new R.F. cavity and other equipment. The measurements reported earlier [1] were made (*) with a different electron monitor and at energies up to only 1000 MeV. For those measurements an adjustment of 15% percent in the R.F. calibration was required in order to obtain agreement with the theory.

(*) The earlier measurements were made in collaboration with A. B. Clegg.

RIASSUNTO

La perdita dalle fasi sincrone degli elettroni in un sincrotrone è stata misurata per varie tensioni sulla cavità acceleratrice e per energie degli elettroni da 800 a 1 200 MeV. I risultati sono confrontati con un calcolo della perdita prodotta per l'eccitazione di oscillazioni di fase nell'emissione di quanti nell'irraggiamento.

Note on the Target Exchange Corrections in Watson's Theory of the Optical Model Potential.

J. Sawicki

Department of Physics, University of California - Berkeley, Cal.

(ricevuto il 2 Novembre 1959)

Summary. — The generalization of Watson's theory of the optical model potential to the case of completely antisymmetrized wave functions of the $A+1$ particles system given by Rollnik is discussed. The lowest order corrections to the nuclear potential in the Takeda and Watson formulation being of the target exchange type are estimated for several energies of the scattering nucleon.

Takeda and Watson [1] have modified the original theory of the optical model potential given by Watson [2,3] by introducing the effects of the identity of the scattering particle and the target particles. However, their final expressions for the optical model potential involve only the two-body scattering t-operators antisymmetrized in the appropriate interacting pairs. If one leaves the cluster terms aside, one deals with the antisymmetrized impulse approximation of Riesenfeld and Watson [4]. In this way some terms of the «target exchange» type corresponding to the complete antisymmetrization of the system: projectile plus the target nucleus are left out. In fact, Takeda and Watson [1] have shown a very rough estimate of one of such target

[1] G. Takeda and K. M. Watson: *Phys. Rev.*, **97**, 1336 (1955).
[2] K. M. Watson: *Phys. Rev.*, **89**, 575 (1953).
[3] N. C. Francis and K. M. Watson: *Phys. Rev.*, **92**, 291 (1953).
[4] W. B. Riesenfeld and K. M. Watson: *Phys. Rev.*, **102**, 1157 (1956).

exchange terms on an example and they indicate that such terms could be important only in the low and medium energy range. The impulse approximation formula for the optical potential is a good asymptotic formula for high energy scattering. However, if one considers such refinements as, for example, the cluster terms corresponding to the multiple scattering corrections, one should be careful as the « target exchange » terms may be of the same order of magnitude.

In an earlier paper (5) the effects of the strong pair correlations in nuclear matter on the optical model potential were considered. Nuclear ground state wave functions of the Jastrow type were applied in the Takeda and Watson (1) formulation and the corrections to the Fermi gas model coming from the pair correlation functions were calculated as a function of energy.

The target exchange corrections discussed below are essentially closely related to the latter corrections as they do not occur in lowest order in the case of the completely uncorrelated (Fermi gas model, say) nuclear matter (*). It is the aim of this note to present some rough estimates of these correction terms upon the use of the Jastrow type wave functions of nuclear matter.

Coester and Kummel (7) and Rollnik (8) have given some formal derivations of the optical model potential in the case of the formally exact and completely antisymmetrized wave function of the total system: projectile plus the target nucleus. The criterion for the existence of this single particle potential is the existence of solutions of certain integral equations with proper boundary conditions and for realistic two-body nuclear forces. In the following we shall refer to Rollnik's formulation which is more closely related to the Watson theory.

Rollnik obtains the following system of integral operator equations determining the optical model potential V.

$$V = \sum_{\mu} \mathcal{V}_0^{\mu} \omega_{\mu} , \tag{1}$$

$$\omega_{\mu} = (E - E_{\mu} - K + i\eta)^{-1} \sum_{\nu} \mathcal{V}_{\mu}^{\nu} \omega_{\nu} , \qquad \omega_0 \equiv 1 \tag{2}$$

(5) J. Dabrowski and J. Sawicki: *Nucl. Phys.*, **13**, 621 (1959).

(*) In their distorted wave calculation of the inelastic scattering of protons from nuclei Levinson and Banerjee (6) have encountered analogous « target exchange » terms (compare their eq. (18)), but they propose to reject those terms as their nuclear wave functions are uncorrelated Slater determinants.

(6) C. A. Levinson and M. K. Banerjee: *Ann. of Phys.*, **2**, 471 (1957).

(7) F. Coester and H. Kummel: *Nucl. Phys.*, **9**, 225 (1958).

(8) H. Rollnik: *Zeits. f. Naturfor.*, **13** *a*, 59 (1958).

or

$$\omega_\mu = (E - E_\mu - K - \mathcal{V}_\mu^\mu + i\eta)^{-1} \sum_{\nu \neq \mu} \mathcal{V}_\mu^\nu \omega_\nu , \tag{2a}$$

where E_μ's are the energy eigenvalues of the target nucleus; K is the kinetic energy operator of the incoming nucleon: the operators $\mathcal{V}_\mu^\nu$ are defined by:

$$\mathcal{V}_{\mu' \boldsymbol{k}_0'}^{\mu \boldsymbol{k}_0} \equiv \langle X_{\mu' \boldsymbol{k}_0'} | \mathcal{V} | X^{\mu \boldsymbol{k}_0} \rangle , \tag{3}$$

where

$$\mathcal{V} X^{\mu \boldsymbol{k}_0} = \frac{1}{\sqrt{A+1}} \sum_P (-)^{\varepsilon_P} P \Big[\sum_{i=1}^{A} V_{0i} \varphi_{\boldsymbol{k}_0}(0) \psi_\mu(1, 2, \ldots A) \Big] , \tag{4}$$

and the «reciprocal» wave functions of the total system are defined by:

$$\langle X_{\mu' \boldsymbol{k}_0'} | X^{\mu \boldsymbol{k}_0} \rangle = \delta_{\mu\mu'} \delta(\boldsymbol{k}_0 - \boldsymbol{k}_0') , \tag{5}$$

while

$$X^{\mu \boldsymbol{k}_0} = \frac{1}{\sqrt{A+1}} \sum_P (-)^{\varepsilon_P} P [\varphi_{\boldsymbol{k}_0}(0) \psi_\mu(1, 2, \ldots A)] . \tag{5a}$$

Here $\boldsymbol{k}_0$ and $\boldsymbol{k}_0'$ are the initial and final momenta, respectively, of the scattering particle (0) described by the plane wave function $\varphi_{\boldsymbol{k}_0}(0)$; ψ_μ's are the target nuclear wave functions; ψ_0 corresponds to the ground state; $(-)^{\varepsilon_P} P$ is the antisymmetrization operator, and V_{0i} is the two-body interaction operator of the pair $(0, i)$. In the case of no antisymmetrization of the particle (0) with the target particles $\mathcal{V}_\mu^\nu$ would be replaced everywhere by $\mathcal{V}_{\mu\nu} = \langle \psi_\nu | \sum_{i=1}^{A} V_{0i} | \psi_\mu \rangle$. This difference between $\mathcal{V}_\mu^\nu$ and $\mathcal{V}_{\mu\nu}$ can be described by introducing the formal metric tensor $g_{\mu\nu}$ as:

$$\mathcal{V}_\mu^\nu = \sum_\varrho g_{\mu\varrho} \mathcal{V}^{\varrho\nu} = \sum_\varrho \mathcal{V}_{\mu\varrho} g^{\varrho\nu} . \tag{6}$$

We can write for the reciprocal matrix $g^{\mu\varrho}$:

$$\langle \boldsymbol{k}_0' | g^{\mu\nu} | \boldsymbol{k}_0 \rangle = \delta_{\mu\nu} \delta(\boldsymbol{k}_0 - \boldsymbol{k}_0') - \sum_{P \neq 1} \langle \varphi_{\boldsymbol{k}_0'}(0) \psi_\mu | P | \varphi_{\boldsymbol{k}_0}(0) \psi_\nu \rangle . \tag{7}$$

In order to get the feeling of the order of magnitude of the effects involved

we shall consider the leading term in Eq. (1) which corresponds to no «compound elastic» scattering or to first Born approximation only. This approximation provides no information on the possible contribution to the imaginary part of the optical potential and is useful only for the estimate of the correction to the real part. Now we write:

$$V \approx \mathcal{V}_0^0 = \mathcal{V}_{0\varrho} g^{\varrho 0} \tag{8}$$

or explicitly:

$$\langle \boldsymbol{k}_0' | V | \boldsymbol{k}_0 \rangle = \langle \boldsymbol{k}_0' | V_0 | \boldsymbol{k}_0 \rangle + \langle \boldsymbol{k}_0' | \Delta V | \boldsymbol{k}_0 \rangle \,. \tag{9}$$

The first matrix element is the usual expression for the single particle nuclear potential

$$(2\pi)^3 \langle \boldsymbol{k}_0' | V_0 | \boldsymbol{k}_0 \rangle = \tag{10}$$
$$= A \langle \varphi_{\boldsymbol{k}_0'}(0)\, \psi_0(1, 2, ..., A) | V_{01}(1 - P_{01}) | \varphi_{\boldsymbol{k}_0}(0)\, \psi_0(1, 2, ..., A) \rangle \,.$$

The operator $V_{01}(1 - P_{01})$ would be replaced by the t_{01}-matrix in the «antisymmetrized impulse approximation» of Riesenfeld and Watson ([4]). The second part of V is the correction term which we want to estimate in the following. This latter term can be put in the form:

$$(2\pi)^3 \langle \boldsymbol{k}_0' | \Delta V | \boldsymbol{k}_0 \rangle = \tag{11}$$
$$= - A(A-1) \langle \varphi_{\boldsymbol{k}_0'}(0)\, \psi_0(1, 2, ..., A) | V_{01} | \varphi_{\boldsymbol{k}_0}(2)\, \psi_0(1, 0, 3, ..., A) \rangle \,.$$

This term is of the type called by Takeda and Watson ([1]) the «target exchange terms». As in Eq. (10), here also V_{01} is the spin and isobaric spin averaged and weighted effective two-body potential. In the following we shall use one common symbolic notation V_{01} for the effective well depth in both the direct and the exchange terms of ΔV. However, if V_{01} contains explicit exchange operators we should distinguish between these respective (direct and exchange) well depth coefficients. It should be observed that for the computation of ΔV alone we could employ eq. (11) even if V_{01} contained a hard core part. Namely, the function $\psi_0(1, 0, 3, ..., A)$ contains a correlation function for the (1, 0) pair such that the product $V_{01}\psi_0(1, 0, 3, ..., A)$ is finite even within the hard core region (usually it is zero there). This is not the case with the expression of eq. (10) for V_0. In computing V_0 in the case of a V_{01} containing a hard core part the approximation of eq. (8) cannot be used, but rather we have to use the appropriate $T^{(\mu)}$-operators exactly; here $T^{(\mu)} = \mathcal{V}_0^\mu \omega_\mu$

and $V = \sum T^{(n)}$. We have not succeeded in finding a practical method for calculating these operators (*).

In the literature there are a number of numerical results published based on eq. (10), *i.e.*, for reasonably realistic nuclear potentials V_{01} without a hard core part. In the following we shall calculate the relative contributions of ΔV in form of the ratios $\langle \boldsymbol{k}_0' | \Delta V | \boldsymbol{k}_0 \rangle / \langle \boldsymbol{k}_0' | V_0 | \boldsymbol{k}_0 \rangle$ for the same V-potentials.

We shall now proceed to calculate ΔV of eq. (11) in momentum space. First we Fourier transform the nuclear ground state wave function as:

$$(12) \qquad \psi_0(1, 0, 3, \ldots A) = (2\pi)^{-3} \sum_{s_0'' t_0''} \sum_{s_1 t_1} \int \mathrm{d}\boldsymbol{k}_0'' \, \mathrm{d}\boldsymbol{k}_1 \exp[i\boldsymbol{k}_0'' \boldsymbol{r}_0 + i\boldsymbol{k}_1 \boldsymbol{r}_1] \eta_{s_0''} \eta_{s_1} \cdot \chi_{t_0''} \chi_{t_1} \Psi_0(\boldsymbol{k}_1 s_1 t_1; \boldsymbol{k}_0'' s_0'' t_0''; 3 \ldots A),$$

where $\eta_{s_i} \equiv \eta_{s_i}(\sigma_i)$ is the spin function of particle (i) with the spin magnetic number s_i; $\chi_{t_i} \equiv \chi_{t_i}(\tau_i)$ is the analogous i-spin function. Following the procedure similar to that of ref. ([5]), we can put eq. (11) in the form:

$$(13) \qquad (2\pi)^3 \langle \boldsymbol{k}_0' | \Delta V | \boldsymbol{k}_0 \rangle = -\frac{1}{4} (2\pi)^{-6} \int \mathrm{d}\boldsymbol{k}_1 \, \mathrm{d}\boldsymbol{k}_1' \, \mathrm{d}\boldsymbol{k}_0'' \left\langle \frac{\boldsymbol{k}_0' - \boldsymbol{k}_1'}{2} \middle| V_{01} \middle| \frac{\boldsymbol{k}_0'' - \boldsymbol{k}_1}{2} \right\rangle \cdot \delta(\boldsymbol{k}_0' + \boldsymbol{k}_1' - \boldsymbol{k}_0'' - \boldsymbol{k}_1) \int \mathrm{d}\boldsymbol{r}_a \, \mathrm{d}\boldsymbol{r}_a' \, \mathrm{d}\boldsymbol{r}_b \, \mathrm{d}\boldsymbol{r}_b' \exp[i\boldsymbol{k}_1' \boldsymbol{r}_a + i\boldsymbol{k}_0 \boldsymbol{r}_b - i\boldsymbol{k}_1 \boldsymbol{r}_a' - i\boldsymbol{k}_0'' \boldsymbol{r}_b'] \cdot \varrho(\boldsymbol{r}_a, \boldsymbol{r}_b; \boldsymbol{r}_a', \boldsymbol{r}_b'),$$

(*) If one computes the differential cross-section rather than the optical model potential one can calculate the part analogous to ΔV of eq. (11) by conveniently applying the impulse approximation with replacing V_{01} by the usual t-matrix. The $V_0 + \Delta V$ so obtained is not an approximation to a single particle potential describing the scattering by a single particle Schrödinger equation. The above-mentioned operator would follow from the equations of Takeda and Watson ([1]) in their notation in the following way:

$$\bar{\Omega} = \Lambda_0 \Omega(0) = \Omega(0) - \sum_{i=1}^{A} \Omega(i) = \Lambda_0 \left(1 + \frac{1}{a} V_0 |0\rangle\right) \approx \Lambda_0 \cdot 1 + \frac{1}{a(0)} V_0 \bar{\Omega} = \left(1 + \frac{1}{a} V_0\right) \Lambda_0 = \Omega_0 \Lambda_0,$$

where Λ_0 is the antisymmetrization operator,

$$a = E - H + i\eta; \qquad H = K + \sum_{i<j} V_{ij}; \qquad a(0) = a + V_0 = a + \sum_{j \neq 0}^{A} V_{0j}.$$

Consequently, the t-matrix is:

$$\bar{T}_0 = V_0 \bar{\Omega} \approx V_0 \Omega_0 \Lambda_0 = T_0 \Lambda_0 \approx \sum_{i \neq 0}^{A} t_{0i} \Lambda_0,$$

where the last step is the usual impulse approximation.

where the mixed two-particle density ϱ is defined as:

$$\varrho(\boldsymbol{r}_a, \boldsymbol{r}_b; \boldsymbol{r}'_a, \boldsymbol{r}'_b) = A(A-1)\int \mathrm{d}\sigma_1\,\mathrm{d}\tau_1\,\mathrm{d}\sigma_2\,\mathrm{d}\tau_2\,\mathrm{d}(3)\ldots\mathrm{d}(A)\cdot \Psi_0^*(\boldsymbol{r}_a\sigma_1\tau_1; \boldsymbol{r}_b\sigma_2\tau_2; 3\ldots A)\Psi_0(\boldsymbol{r}'_a\sigma_1\tau_1; \boldsymbol{r}'_b\sigma_2\tau_2; 3\ldots A)\,. \tag{14}$$

From eq. (13) we see that ΔV is A-independent. Similarly as in ref. [5], we shall use the usual Jastrow type of Ψ_0:

$$\begin{cases} \Psi_0 = \dfrac{1}{\sqrt{NA!}} \prod_{i>j}^{A} f(r_{ij}) \sum_P (-)^{\varepsilon_P} P \prod_{l=1}^{A} \varphi_{P_l}(l)\,, \\ \Phi_n(l) = \eta_{s_n}\chi_{t_n}\varphi_{\alpha_n}(\boldsymbol{r}_l)\,, \end{cases} \tag{15}$$

where the correlation function $f(r_{ij})$ has the property: $f \to 1$ for $r \to \infty$ and in the case of a repulsive core of the radius r_c it satisfies the condition $f = 0$ for $r \leqslant r_c$. We shall confine ourselves to the case of nuclear matter. It can be shown that in this case the lowest order term in the cluster development of ϱ is:

$$\varrho \approx \varrho_0^2[l(r_{aa'})l(r_{bb'}) - \tfrac{1}{4}l(r_{ab'})l(r_{a'b})]f(r_{ab})f(r_{a'b'})\,, \tag{16}$$

where $r_{ij} = |r_i - r_j|$, $\varrho_0 = 2k_F^3/3\pi^2$ is the usual density of the Fermi gas, $l(x) = 3j_1(k_F x)/k_F x$. We also write: $f(r_{ab})f(r_{a'b'}) = 1 + h(r_{ab}, r_{a'b'})$. If there are no dynamical correlations ($h = 0$) is it easy to ascertain that $\Delta V = 0$. We shall use the notation: $f(x) = 1 + \lambda(x)$; so $h(r_{ab}, r_{a'b'}) = \lambda(r_{ab}) + \lambda(r_{a'b'}) + \lambda(r_{ab})\lambda(r_{a'b'})$. Consequently, the approximate expression for ΔV can be written from eq. (13) as:

$$\langle \boldsymbol{k}'_0|\Delta V|\boldsymbol{k}_0\rangle = -\frac{1}{4}\varrho_0^2(2\pi)^{-6}\int \mathrm{d}\boldsymbol{k}_1\,\mathrm{d}\boldsymbol{k}'_1 \left\langle \frac{\boldsymbol{k}'_0 - \boldsymbol{k}'_1}{2}\middle| V_{01}\middle|\frac{\boldsymbol{k}'_0 + \boldsymbol{k}'_1}{2} - \boldsymbol{k}_1\right\rangle \cdot \int \mathrm{d}\boldsymbol{r}_a\,\mathrm{d}\boldsymbol{r}'_a\,\mathrm{d}\boldsymbol{r}_b\,\mathrm{d}\boldsymbol{r}'_b \exp[i\boldsymbol{k}'_1\boldsymbol{r}_a + i\boldsymbol{k}_0\boldsymbol{r}_b - i\boldsymbol{k}_1\boldsymbol{r}'_a - i(\boldsymbol{k}'_0 + \boldsymbol{k}'_1 - \boldsymbol{k}_1)\boldsymbol{r}'_b]\cdot (1 + h(r_{ab}, r_{a'b'}))[l(r_{aa'})l(r_{bb'}) - \tfrac{1}{4}l(r_{ab'})l(r_{a'b})]\ (*)\,. \tag{17}$$

(*) In the case where $\Psi(\boldsymbol{r}_1, \boldsymbol{r}_2)$ is the correlated pair function satisfying the Bethe-Goldstone equation corresponding to the levels $\boldsymbol{\varkappa}_1$, $\boldsymbol{\varkappa}_2$:

$$\Psi_{\boldsymbol{\varkappa}_1\boldsymbol{\varkappa}_2}(\boldsymbol{r}_1, \boldsymbol{r}_2) = \varphi_{\boldsymbol{\varkappa}_1}(\boldsymbol{r}_1)\varphi_{\boldsymbol{\varkappa}_2}(\boldsymbol{r}_2)(1 + \lambda_{\boldsymbol{\varkappa}_1\boldsymbol{\varkappa}_2}(\boldsymbol{r}_1, \boldsymbol{r}_2))\,,$$

it is useful to use the Fourier representation for the density ϱ. The corresponding expression for ΔV is then easily derived using eqs. (31)-(35) of ref. [5].

Eq. (17) can also be rewritten in the form:

$$(18)\qquad (2\pi)^3\langle \boldsymbol{k}_0'|\Delta V|\boldsymbol{k}_0\rangle = -\frac{4}{(2\pi)^6}\,\delta(\boldsymbol{k}_0-\boldsymbol{k}_0')\int \mathrm{d}\boldsymbol{k}_1\,\mathrm{d}\boldsymbol{k}_1'$$
$$\left\langle \frac{\boldsymbol{k}_0-\boldsymbol{k}_1'}{2}|V_{01}|\cdot\frac{\boldsymbol{k}_0+\boldsymbol{k}_1'}{2}-\boldsymbol{k}_1\right\rangle \int \mathrm{d}\boldsymbol{r}_{ab}\,\mathrm{d}\boldsymbol{r}_{a'b'}\int^{<k_F} \mathrm{d}\boldsymbol{\varkappa}\,[\exp[i(\boldsymbol{\varkappa}-\boldsymbol{k}_0)\boldsymbol{r}_{ab}\cdot$$
$$\cdot\exp[i(\boldsymbol{k}_0+\boldsymbol{k}_1'-\boldsymbol{k}_1-\boldsymbol{\varkappa})\boldsymbol{r}_{a'b'}]-\tfrac{1}{4}\exp[i(\boldsymbol{\varkappa}-\boldsymbol{k}_0)\boldsymbol{r}_{ab}]\exp[i(\boldsymbol{\varkappa}-\boldsymbol{k}_1)\boldsymbol{r}_{a'b'}]\cdot$$
$$\cdot(1+h(r_{ab},r_{a'b'}))\,.$$

Here we see explicitly that for the case of nuclear matter ΔV has only diagonal elements different from zero. However, for computational purposes it seems to be more useful to write ΔV with all the integrand expressed in configuration space as:

$$(19)\qquad (2\pi)^3\langle \boldsymbol{k}_0'|\Delta V|\boldsymbol{k}_0\rangle = -\frac{1}{4}\varrho_0^2\int \mathrm{d}\boldsymbol{r}_0\,\mathrm{d}\boldsymbol{r}_1\,\mathrm{d}\boldsymbol{r}_2\exp[-i\boldsymbol{k}_0'\boldsymbol{r}_0]\cdot$$
$$\cdot\left[l(r_{02})-\frac{1}{4}l(r_{12})l(r_{10})\right]\cdot V_{10}(r_{10})f(r_{10})f(r_{12})\exp[i\boldsymbol{k}_0\boldsymbol{r}_2]\,,$$

where $r_{ij}=|\boldsymbol{r}_i-\boldsymbol{r}_j|$. Let us introduce the new co-ordinates $(\boldsymbol{r}_0,\boldsymbol{r}_{10},\boldsymbol{r}_{20})$ and $(\boldsymbol{r}_{01},\boldsymbol{r}_{12},\boldsymbol{r}_2)$ in the two integrals of eq. (19), respectively. Upon performing one integration we can write:

$$(20)\qquad \langle \boldsymbol{k}_0'|\Delta V|\boldsymbol{k}_0\rangle = -\frac{1}{4}\varrho_0^2\,\delta(\boldsymbol{k}_0-\boldsymbol{k}_0')\left[\int \mathrm{d}\boldsymbol{x}\,l(x)\exp[i\boldsymbol{k}_0\boldsymbol{x}]\int \mathrm{d}\boldsymbol{y}\,V_{10}(y)\cdot\right.$$
$$\cdot f(y)f(|\boldsymbol{y}-\boldsymbol{x}|)-\frac{1}{4}\int \mathrm{d}\boldsymbol{x}'\,l(x')\exp[-i\boldsymbol{k}_0\boldsymbol{x}']\,V_{10}(x')f(x')\int \mathrm{d}\boldsymbol{y}'\,l(y')\cdot$$
$$\left.\cdot\exp[-i\boldsymbol{k}_0\boldsymbol{y}']f(y')\right] = \delta(\boldsymbol{k}_0-\boldsymbol{k}_0')\Delta V(k_0)\,.$$

If V_{01} does not contain a hard core part, we can replace the product $f(x)f(z)$ by $h(x,z)$. The correlation function $\lambda(x)$ is taken in the gaussian form: $\lambda(x)=-\exp[-\gamma x^2]$, $\gamma=1.25f^{-2}$ $(\lambda(x_c\approx 0.4f)\approx -1)$, given by AMADO [9]. Numerical results were obtained for two examples of V_{01}: *a*) the exponential form $V_{01}(x)=-(1.446/a^2)(\hbar^2/M)\exp[-x/a]$ discussed by BETHE [10] with the parameter $a=0.706f$, resulting from the effective range formula of BLATT and JACKSON [11]; *b*) the guassian form: $V_{01}(x)=\hat{O}A\exp[-\alpha^2x^2]$ used by VERLET [12] with the exchange dependence of the form:

$$(21)\qquad \hat{O}=-\tfrac{1}{4}[(1+P_\sigma)(1+P_x)+q(1-P_\sigma)(1+P_x)+$$
$$+p_3(1+P_\sigma)(1-P_x)+p_1(1-P_\sigma)(1-P_x)]\,,$$

---

[9] R. D. AMADO: *Phys. Rev.*, **111**, 821 (1958).
[10] H. A. BETHE: *Phys. Rev.*, **103**, 1353 (1956).
[11] J. M. BLATT and J. D. JACKSON: *Phys. Rev.*, **76**, 18 (1949).
[12] L. VERLET: *Nuovo Cimento*, **7**, 821 (1958).

where P_σ and P_x are the spin and space exchange operators, respectively, and $\Lambda = 72$ MeV, $\alpha = 0.86 f^{-1}$, $q = 0.65$; the two values of $\frac{1}{16}(p_1 + 9p_3) = \lambda'$ are used: -0.21 and -0.31; the direct terms are proportional to $\mathrm{Tr}\,\hat{O} = -3(1+q) - 16\lambda'$, and the exchange terms to $\mathrm{Tr}\,\hat{O}P_\sigma P_x = 3(1+q) - 16\lambda'$. The value of $k_F = 1.25 f^{-1}$ was used.

In the case *a*) of the exponential potential $\Delta V(k_0) \approx -0.1$ MeV for $k_0 = 2k_F$ (the laboratory energy of the incoming nucleon $E_0 \approx 80$ MeV), and $\approx +0.2$ MeV for $k_0 = 3k_F$ ($E_0 \approx 230$ MeV). For still higher values of k_0 ΔV decreases rapidly with increasing energy. In the case *b*) of the gaussian potential we obtain $\Delta V(k_0) \approx -0.27$ MeV for $k_0 = 2k_F$, and $+0.07$ MeV for $k_0 = 3k_F$ if the value $\lambda' = -0.21$ is used, and -0.08 MeV for $k_0 = 2k_F$, $+0.005$ MeV for $k_0 = 3k_F$ if $\lambda' = -0.31$. According to the results of VERLET [12] the latter value of λ' is more realistic.

We see from the numbers given above that ΔV changes sign and is small indicating that the target exchange terms are probably negligible at high energies. However, the particular smallness of ΔV in the case *b*) with $\lambda' = -0.31$ is due to the structure of the exchange operator $\hat{O}$ of eq. (21) and may overestimate this smallness. The magnitude ΔV drops off with increasing energy rather rapidly in all the cases in qualitative agreement with the suggestion of TAKEDA and WATSON [1]. Although all the approximations involved in eq. (20) are very rough, the general conclusion on the smallness of ΔV seems to hold for any reasonable V_{01}. If one compares the numbers of the seemingly more realistic case *b*) with $V_0(k_0)$ given by VERLET [12] computed for the same V_{01}, one finds $\Delta V/V_0 \approx +0.5\%$ at $k_0 = 2k_F$ and $\approx -0.1\%$ at $k = 3k_F$ for $\lambda' = -0.31$.

* * *

Several conversations with Dr. J. DABROWSKI on the problem of the « target exchange » terms are gratefully acknowledged. The author is indebted to Professor K. M. WATSON for his kind interest in this work.

RIASSUNTO (*)

Si discute la generalizzazione della teoria di Watson per il potenziale del modello ottico al caso delle funzioni d'onda completamente antisimmetrizzate dei sistemi ad $A+1$ particelle, esposta da Rollnik. Le correzioni dell'ordine minimo al potenziale nucleare nella formulazione di Takeda e Watson, che sono del tipo a scambio di bersaglio, vengono stimate per parecchie energie del nucleone soggetto a scattering.

(*) *Traduzione a cura della Redazione.*

On the Determination of the Magnetic Moment of the Λ^0.

N. Schmitz (*)

Max-Planck-Institut für Physik und Astrophysik - München

(ricevuto il 9 Novembre 1959)

Summary. — In the presence of a magnetic field, the polarization vector of the Λ's from the reaction $\pi^- + p \to \Lambda^0 + K^0$, precesses about the field direction and the angular distribution of the decay pions will be modified. The explicit expressions of the angular distributions for several cases have been worked out in this paper. Some numerical data are given as to the magnitude of the effect which depends on the field strength and the magnetic moment of the Λ^0. With the help of the theoretical formulas presented here, the magnitude and the sign of the Λ magnetic moment can be determined from the experimental distributions.

1. – Introduction.

It is known [1-3] that the Λ^0-hyperons from the reaction

$$\pi^- + p \to \Lambda^0 + K^0$$

are polarized perpendicularly to the production plane. The polarization $P(\theta)$ depends on the production angle θ between the momenta of the incoming pion

(*) Now at the University of California, Lawrence Radiation Laboratory, Berkeley, Cal.

(1) F. S. Crawford jr., M. Cresti, M. L. Good, K. Gottstein, E. M. Lyman, F. T. Solmitz, M. L. Stevenson and H. K. Ticho: *Phys. Rev.*, **108**, 1102 (1957); *Annual International Conference on High Energy Physics at CERN* (1958), Appendix to Session 5.

(2) F. Eisler, R. Plano, A. Prodell, N. Samios, M. Schwartz, J. Steinberger, P. Bassi, V. Borelli, G. Puppi, G. Tanaka, P. Waloschek, V. Zoboli, M. Conversi, P. Franzini, I. Mannelli, R. Santangelo, V. Silvestrini, D. A. Glaser, C. Graves and M. L. Perl: *Phys. Rev.*, **108**, 1353 (1958).

(3) F. S. Crawford jr., M. Cresti, M. L. Good, F. T. Solmitz and M. L. Stevenson: *Phys. Rev. Lett.*, **1**, 209 (1958); **2**, 11 (1959).

and the Λ^0. As parity is not conserved in the decay

$$\Lambda^0 \to \mathrm{p} + \pi^- \qquad (1)$$

the angular distribution of the decay pions in the rest system of the Λ^0 is given by [4]

$$W(\eta, \varphi)\,\mathrm{d}\eta\,\mathrm{d}\varphi = [1 + \alpha P(\theta)\eta]\,\mathrm{d}\eta\,\mathrm{d}\varphi\,, \qquad \eta = \cos\vartheta\,. \tag{1}$$

Here ϑ is the angle between the momentum $\boldsymbol{p}$ of the decay pion and the polarization vector, and φ the azimuth angle of $\boldsymbol{p}$ in the production plane. (In the rest system of the Λ^0 the distribution about the polarization is isotropic.)

If the Λ^0 is in an external magnetic field, during its lifetime, its magnetic moment and consequently the polarization vector precesses around the field direction. Therefore, at decay, the polarization generally is no longer perpendicular to the production plane and the angular distribution in the same system is described by a formula different from (1). It is the purpose of this paper to derive this formula which may be useful in determining the magnetic moment of Λ^0 from the measured angular distribution (*).

2. – Transformation of the magnetic field.

First of all we transform the magnetic field given in the laboratory system into the Λ^0 rest system. Let the laboratory system be given by the unit vectors $(\overline{\boldsymbol{n}}_1', \overline{\boldsymbol{n}}_2', \overline{\boldsymbol{n}}_3')$, where $\overline{\boldsymbol{n}}_2'$ is chosen perpendicular to the production plane along the polarization direction at production (primary direction); $\overline{\boldsymbol{n}}_1'$ and $\overline{\boldsymbol{n}}_3'$ lie in the production plane so that $\overline{\boldsymbol{n}}_1'$ points along the direction of the incoming pion. When in the experimental arrangement the magnetic field is perpendicular to the incoming pion beam, the components of the field in the system $(\overline{\boldsymbol{n}}_1', \overline{\boldsymbol{n}}_2', \overline{\boldsymbol{n}}_3')$ are

$$\begin{pmatrix} \bar{H}_1' \\ \bar{H}_2' \\ \bar{H}_3' \end{pmatrix} = H_0 \begin{pmatrix} 0 \\ \sin\gamma \\ \cos\gamma \end{pmatrix}.$$

(4) T. D. Lee, J. Steinberger, G. Feinberg, P. K. Kabir and C. N. Yang: *Phys. Rev.*, **106**, 1367 (1957).

(*) An experiment of this kind has been proposed by several authors (*e.g.* (5,6)).

(5) M. Goldhaber: *Phys. Rev.*, **101**, 1828 (1956).

(6) T. D. Lee and C. N. Yang: *Phys. Rev.*, **108**, 1645 (1957).

For the moment we keep the angle γ between the production plane and the magnetic field fixed; later on we have to integrate over all γ since the production planes are distributed isotropically about $\bar{n}_1'$.

We first transform the system $(\bar{n}_1', \bar{n}_2', \bar{n}_3')$ by a rotation D about $\bar{n}_2'$ into a system $(\bar{n}_1, \bar{n}_2, \bar{n}_3)$ in which $\bar{n}_1$ lies in the Λ^0 direction of flight. The transformation matrix D reads

$$D = \begin{pmatrix} \cos\theta & 0 & -\sin\theta \\ 0 & 1 & 0 \\ \sin\theta & 0 & \cos\theta \end{pmatrix}$$

with $D^{-1} = D^T$ as a consequence of the orthogonality of the transformation. For the component of the magnetic field in the system $(\bar{n}_1, \bar{n}_2, \bar{n}_3)$ we obtain the expressions

$$\begin{pmatrix} \bar{H}_1 \\ \bar{H}_2 \\ \bar{H}_3 \end{pmatrix} = D^{-1} \begin{pmatrix} \bar{H}_1' \\ \bar{H}_2' \\ \bar{H}_3' \end{pmatrix} = H_0 \begin{pmatrix} \sin\theta\cos\gamma \\ \sin\gamma \\ \cos\theta\cos\gamma \end{pmatrix}.$$

Now, the rest system moves into the direction of $\bar{n}_1$ with the velocity $V(\theta)$ of the Λ^0 ($c=1$). If we choose its axes (n_1, n_2, n_3) parallel to the axes of the system $(\bar{n}_1, \bar{n}_2, \bar{n}_3)$, the Special Lorentz Transformation leads to the following expressions for the magnetic field components in the system (n_1, n_2, n_3):

$$(2) \qquad \begin{cases} H_1 = \bar{H}_1 = H_0 \sin\theta\cos\gamma\,, \\ H_2 = \dfrac{\bar{H}_2}{\sqrt{1-V^2}} = \dfrac{H_0}{\sqrt{1-V^2}} \sin\gamma\,, \\ H_3 = \dfrac{\bar{H}_3}{\sqrt{1-V^2}} = \dfrac{H_0}{\sqrt{1-V_0}} \cos\theta\cos\gamma\,, \end{cases}$$

$$H' = |\boldsymbol{H}| = \frac{H_0}{\sqrt{1-V^2}} \sqrt{1 - V^2\sin^2\theta\cos^2\gamma}\,.$$

3. – Relation between the fixed and the precessing rest system.

The angular distributions without and with the magnetic field are to be measured in the fixed rest system (n_1, n_2, n_3) which we have introduced above. In this system the production plane is defined by the unit vectors n_1 and n_3; n_2 points along the primary direction of the polarization. Let n_2 be the polar

axis of the system so that the pion momentum $\boldsymbol{p}$ has the components

$$\begin{pmatrix} p_1 \\ p_2 \\ p_3 \end{pmatrix} = p \begin{pmatrix} \sqrt{1-\eta^2}\cos\varphi \\ \eta \\ \sqrt{1-\eta^2}\sin\varphi \end{pmatrix}. \tag{3}$$

In the absence of a magnetic field the polarization remains fixed and for the angular distribution formula (1) holds.

However, in the presence of a magnetic field $\boldsymbol{H}$, having the components (2) in the system $(\boldsymbol{n}_1, \boldsymbol{n}_2, \boldsymbol{n}_3)$, the polarization vector precesses around the field direction with the frequency

$$\omega = g_\Lambda \frac{eH}{2Mc}, \qquad (M \text{ is the nucleon mass}), \tag{4}$$

(g_Λ is the Landé factor of the Λ^0. The magnetic moment of the Λ^0, in units of the nuclear magneton, is $\mu_\Lambda = g_\Lambda s_\Lambda$, where $s_\Lambda = \frac{1}{2}$ [7] is the spin of the Λ^0). Therefore, it is useful to introduce a rest system $(\boldsymbol{n}_1^*(t), \boldsymbol{n}_2^*(t), \boldsymbol{n}_3^*(t))$ precessing about $\boldsymbol{H}$ with the same frequency ω, so that in this system the polarization vector is fixed and directed along $\boldsymbol{n}_2^*(t)$. The precessing system results from the fixed system $(\boldsymbol{n}_1, \boldsymbol{n}_2, \boldsymbol{n}_3)$ by a time dependent rotation $B(t)$ around $\boldsymbol{H}$; for $t = 0$ both systems coincide. The unit vectors of the two systems are related to each other by

$$(\boldsymbol{n}_1^*(t), \boldsymbol{n}_2^*(t), \boldsymbol{n}_3^*(t)) = (\boldsymbol{n}_1, \boldsymbol{n}_2, \boldsymbol{n}_3)B(t), \qquad \text{with } B(0) = 1. \tag{5}$$

To find the orthogonal matrix $B(t)$ we first transform the system $(\boldsymbol{n}_1, \boldsymbol{n}_2, \boldsymbol{n}_3)$ by a rotation into the system $(\boldsymbol{n}_1', \boldsymbol{n}_2', \boldsymbol{n}_3')$ in which the magnetic field points into the direction $\boldsymbol{n}_3'$. By this requirement and by the (arbitrary) postulation that $\boldsymbol{n}_2'$ has no component in the direction of $\boldsymbol{n}_3$, the transformation matrix T for the rotation is determined:

$$(\boldsymbol{n}_1', \boldsymbol{n}_2', \boldsymbol{n}_3') = (\boldsymbol{n}_1, \boldsymbol{n}_2, \boldsymbol{n}_3)T \tag{6}$$

with

$$T = \begin{pmatrix} \dfrac{H_1 H_3}{H\sqrt{H_1^2+H_2^2}} & -\dfrac{H_2}{\sqrt{H_1^2+H_2^2}} & \dfrac{H_1}{H} \\ \dfrac{H_2 H_3}{H\sqrt{H_1^2+H_2^2}} & \dfrac{H_1}{\sqrt{H_1^2+H_2^2}} & \dfrac{H_2}{H} \\ -\dfrac{\sqrt{H_1^2+H_2^2}}{H} & 0 & \dfrac{H_3}{H} \end{pmatrix}. \tag{7}$$

[7] F. S. Crawford jr., M. Cresti, M. L. Good, M. L. Stevenson and H. K. Ticho: *Phys. Rev. Lett.*, **2**, 114 (1959).

Now the system $(\boldsymbol{n}_1', \boldsymbol{n}_2', \boldsymbol{n}_3')$ precesses around the magnetic field, *i.e.*, around axis $\boldsymbol{n}_3'$, with the frequency ω; after the time t it has turned over into the the system $(\boldsymbol{n}_1^{*\prime}(t), \boldsymbol{n}_2^{*\prime}(t), \boldsymbol{n}_3^{*\prime}(t))$ which is given by

$$(\boldsymbol{n}_1^{*\prime}(t), \boldsymbol{n}_2^{*\prime}(t), \boldsymbol{n}_3^{*\prime}(t)) = (\boldsymbol{n}_1', \boldsymbol{n}_2', \boldsymbol{n}_3')A(t) \tag{8}$$

with

$$A(t) = \begin{pmatrix} \cos\omega t & -\sin\omega t & 0 \\ \sin\omega t & \cos\omega t & 0 \\ 0 & 0 & 1 \end{pmatrix}. \tag{9}$$

The precessing rest system $(\boldsymbol{n}_1^*(t), \boldsymbol{n}_2^*(t), \boldsymbol{n}_3^*(t))$ has the same geometrical position with respect to the system $(\boldsymbol{n}^{*\prime}_1(t), \boldsymbol{n}_2^{*\prime}(t), \boldsymbol{n}_3^{*\prime}(t))$ as the fixed rest system $(\boldsymbol{n}_1, \boldsymbol{n}_2\, \boldsymbol{n}_3)$ has with respect to the system $(\boldsymbol{n}_1', \boldsymbol{n}_2', \boldsymbol{n}_3')$. Therefore, we have in analogy to (6):

$$(\boldsymbol{n}_1^{*\prime}(t), \boldsymbol{n}_2^{*\prime}(t), \boldsymbol{n}_3^{*\prime}(t)) = (\boldsymbol{n}_1^*(t), \boldsymbol{n}_2^*(t), \boldsymbol{n}_3^*(t))\cdot T\,. \tag{10}$$

From (6), (8) and (10) follows

$$(\boldsymbol{n}_1^*(t), \boldsymbol{n}_2^*(t), \boldsymbol{n}_3^*(t)) = (\boldsymbol{n}_1, \boldsymbol{n}_2, \boldsymbol{n}_3)TA(t)T^{-1}\,,$$

that means (see (5))

$$B(t) = TA(t)T^{-1}\,, \tag{11}$$

where T and $A(t)$ are given by (7) and (9). Carrying out the matrix multiplication (11) we obtain

$$B(t) = \begin{pmatrix} b_{11} & b_{12} & b_{13} \\ b_{21} & b_{22} & b_{23} \\ b_{31} & b_{32} & b_{33} \end{pmatrix} = \tag{12}$$

$$= \begin{pmatrix} \frac{H_1^2}{H^2}(1-\cos\omega t)+\cos\omega t & \frac{H_1H_2}{H^2}(1-\cos\omega t)-\frac{H_3}{H}\sin\omega t & \frac{H_1H_3}{H^2}(1-\cos\omega t)+\frac{H_2}{H}\sin \\ \frac{H_1H_2}{H^2}(1-\cos\omega t)+\frac{H_3}{H}\sin\omega t & \frac{H_2^2}{H^2}(1-\cos\omega t)+\cos\omega t & \frac{H_2H_3}{H^2}(1-\cos\omega t)-\frac{H_1}{H}\sin \\ \frac{H_1H_3}{H^2}(1-\cos\omega t)-\frac{H_2}{H}\sin\omega t & \frac{H_2H_3}{H^2}(1-\cos\omega t)+\frac{H_1}{H}\sin\omega t & \frac{H_3^2}{H^2}(1-\cos\omega t)+\cos\omega \end{pmatrix}$$

The components of the pion momentum $\boldsymbol{p}$ in the precessing system

$(\boldsymbol{n}_1^*(t), \boldsymbol{n}_2^*(t), \boldsymbol{n}_3^*(t))$ are

$$\begin{pmatrix} p_1^*(t) \\ p_2^*(t) \\ p_3^*(t) \end{pmatrix} = p^* \begin{pmatrix} \sqrt{1-\eta^{*2}}\cos\varphi^* \\ \eta^* \\ \sqrt{1-\eta^{*2}}\sin\varphi^* \end{pmatrix}. \tag{13}$$

Then between (3) and (13) the relation

$$\begin{pmatrix} \sqrt{1-\eta^{*2}}\cos\varphi^* \\ \eta^* \\ \sqrt{1-\eta^{*2}}\sin\varphi^* \end{pmatrix} = B^{-1}(t) \begin{pmatrix} \sqrt{1-\eta^{2}}\cos\varphi \\ \eta \\ \sqrt{1-\eta^{2}}\sin\varphi \end{pmatrix}, \tag{14}$$

holds ($p^* = p = |\boldsymbol{p}|$). Thus we know η^* and φ^* as functions of η and φ.

4. – Angular distribution of the decay pions in the presence of a magnetic field.

An observer in the precessing rest system does not notice any influence of the magnetic field, since to him the polarization vector remains fixed along the direction $\boldsymbol{n}_2^*(t)$. Therefore, he observes in his system an angular distribution identical to (1), namely

$$W(\eta^*, \varphi^*)\,\mathrm{d}\eta^*\,\mathrm{d}\varphi^* = (1 + \alpha P(\theta)\eta^*)\,\mathrm{d}\eta^*\,\mathrm{d}\varphi^* . \tag{15}$$

From (15) we obtain by transformation (14) the angular distribution $\underset{\gamma,t}{W}(\eta, \varphi)\,\mathrm{d}\eta\,\mathrm{d}\varphi$ observed in the fixed rest system in the presence of the magnetic field (the magnetic field $\boldsymbol{H}$, *i.e.* γ, and the precession time t, *i.e.* the lifetime of the Λ^0, are still kept fixed):

$$\underset{\gamma,t}{W}(\eta, \varphi)\,\mathrm{d}\eta\,\mathrm{d}\varphi = W(\eta^*(\eta, \varphi), \varphi^*(\eta, \varphi))\,\frac{\partial(\eta^*, \varphi^*)}{\partial(\eta, \varphi)}\,\mathrm{d}\eta\,\mathrm{d}\varphi .$$

The Jacobian $\partial(\eta^*, \varphi^*)/\partial(\eta, \varphi)$ for the rotation $B(t)$ is equal to unity. Therefore, we obtain from (12), (14) and (15) ($B^{-1} = B^T$):

$$\underset{\gamma,t}{W}(\eta, \varphi)\,\mathrm{d}\eta\,\mathrm{d}\varphi = \tag{16}$$
$$= [1 + \alpha P(\theta)(b_{12}\sqrt{1-\eta^2}\cos\varphi + b_{22}\eta + b_{32}\sqrt{1-\eta^2}\sin\varphi)]\,\mathrm{d}\eta\,\mathrm{d}\varphi .$$

The coefficients b_{i2} result from (12) by inserting $\boldsymbol{H}$ from (2):

$$b_{12} = \sqrt{1 - V^2}\,\frac{\sin\theta\cos\gamma\sin\gamma}{1 - V^2\sin^2\theta\cos^2\gamma}\cdot(1 - \cos\omega t) - \frac{\cos\theta\cos\gamma}{\sqrt{1 - V^2\sin^2\theta\cos^2\gamma}}\sin\omega t,$$

$$b_{22} = \frac{\sin^2\gamma}{1 - V^2\sin^2\theta\cos^2\gamma}(1 - \cos\omega t) + \cos\omega t,$$

$$b_{32} = -\frac{\cos\theta\cos\gamma\sin\gamma}{1 - V^2\sin^2\theta\cos^2\gamma}(1 - \cos\omega t) + \sqrt{1 - V^2}\,\frac{\sin\theta\cos\gamma}{\sqrt{1 - V^2\sin^2\theta\cos^2\gamma}}\sin\omega t.$$

Now we multiply the distribution (16) by the probability

$$W(t)\,\mathrm{d}t = \lambda\exp[-\lambda t]\,\mathrm{d}t$$

for the lifetime t ($\lambda^{-1} = \tau_\Lambda$ is the mean lifetime of the Λ^0) and then integrate over all t (from 0 to ∞), over all φ (from 0 to 2π) and over all γ (from 0 to 2π). Thus we obtain the distribution $W(\eta)\,\mathrm{d}\eta$ for all Λ^0's at a certain production

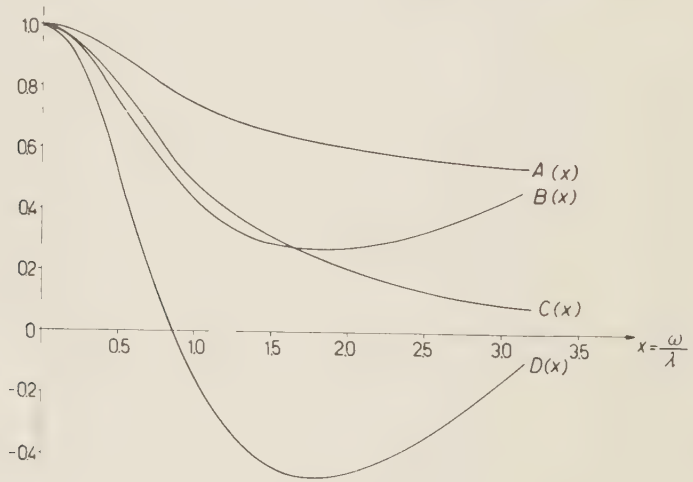

Fig. 1.

angle θ. (From formula (16) it can be seen that by the integration over φ the two terms with the coefficients b_{12} and b_{32} drop out). The integrations can be carried out very easily for the non-relativistic case ($V \approx 0$) where ω does not depend on γ (see (2) and (4)). The result is

$$W_{nr}(\eta)\,\mathrm{d}\eta = \left[1 + \frac{1}{2}\left(1 + \frac{1}{1 + x^2}\right)\alpha P(\theta)\,\eta\right]\mathrm{d}\eta. \tag{17}$$

where $x = \omega/\lambda$. So we find that the distribution in the presence of the magnetic field differs from that of the field free case by the factor

$$A(x) = \frac{1}{2}\left(1 + \frac{1}{1+x^2}\right), \qquad (A(x) \leqslant 1), \tag{18}$$

in the η-dependent terms. As $\alpha P(\theta)$ can be obtained from measurements without a magnetic field, a determination of $A(x)$ by the same kind of measurements, with a magnetic field, will yield the magnitude of g_Λ. In Table I the ratio $x = \omega/\lambda$ is listed for various values of the Landé factor g_Λ and of the magnetic field H_0 ($\tau_\Lambda = 2.6 \cdot 10^{-10}$ s, see *e.g.* [8]). In Fig. 1 $A(x)$ is plotted as a function of x. From the table and the figure it can be seen that even for very strong magnetic fields ($\sim 10^5$ gauss) $A(x)$ is not very different from unity. Therefore, one needs a rather large number of decays in order to observe the

TABLE I. – $x = \omega/\lambda$ *as a function of* g_Λ *and* H_0.

g_Λ \ H_0 (G)	$1 \cdot 10^5$	$2 \cdot 10^5$	$3 \cdot 10^5$	$4 \cdot 10^5$	$5 \cdot 10^5$
1	0.126	0.252	0.379	0.505	0.631
2	0.252	0.505	0.758	1.01	1.26
3	0.379	0.758	1.15	1.52	1.90
4	0.505	1.01	1.52	2.02	2.53
5	0.631	1.26	1.90	2.53	3.16

effect and even more to determine the magnetic moment. On the other hand, for large x values, the curve $A(x)$ becomes flat so that in this region even a small error in the measurement of $A(x)$ causes a large error in the Landé factor. $A(x)$ has its greatest steepness for $x = \sqrt{\frac{1}{3}}$.

By integrating from t_1 to t_2 one can easily derive the distribution $W(\eta)\,\mathrm{d}\eta$ for the case that one includes in the measurements only those Λ's which have lifetimes between t_1 and t_2. For instance, for the Λ's having lifetimes larger than the mean lifetime τ_Λ the non-relativistic distribution reads

$$W_{nr}(\eta)\,\mathrm{d}\eta = \left[1 + \frac{1}{2}\left\{1 + \frac{1}{1+x^2}\,(\cos x - x \sin x)\right\} \alpha P(\theta)\,\eta\right] \mathrm{d}\eta\,. \tag{19}$$

[8] *Annual International Conference on High Energy Physics at CERN* (1958), p. 270.

The factor

$$B(x) = \frac{1}{2}\left\{1 + \frac{1}{1+x^2}(\cos x - x \sin x)\right\} \tag{20}$$

is plotted in Fig. 1 as a function of x. It is seen that $B(x)$ differs from unity much more than $A(x)$. So the effect becomes greater as is expected because of the elimination of short lived Λ's which do not precess by an appreciable amount.

5. – Angular distributions for the magnetic field parallel to the incoming beam.

If the magnetic field is not perpendicular but parallel to the incoming pion beam the polarization vector is always perpendicular to the magnetic field. Therefore, the effect of the field upon the angular distribution is larger. For this situation we have instead of (2) the field components

$$\left\{\begin{aligned} H_1 &= H_0 \cos\theta\,, \\ H_2 &= 0\,, \\ H_3 &= -\frac{H_0}{\sqrt{1-V^2}}\sin\theta\,, \end{aligned}\right. \tag{21}$$

$$H = \frac{H_0}{\sqrt{1-V^2}}\sqrt{1 - V^2\cos^2\theta}\,,$$

in the fixed rest system. Inserting the components (21) instead of (2) into the above formulas we obtain in the same way the angular distributions in the presence of a parallel magnetic field. For instance, for the non-relativistic η-distribution of the pions from all Λ^0's at a certain production angle θ the formula

$$W_{nr}(\eta)\,\mathrm{d}\eta = \left[1 + \frac{1}{1+x^2}\,\alpha P(\theta)\eta\right]\mathrm{d}\eta \tag{22}$$

holds. In Fig. 1 the factor

$$C(x) = \frac{1}{1+x^2} \tag{23}$$

is plotted against x.

Again for the Λ's which have lifetimes larger than τ_Λ the non-relativistic distribution reads

$$W_{nr}(\eta)\,\mathrm{d}\eta = \left[1 + \frac{1}{1+x^2}(\cos x - x\sin x)\alpha P(\theta)\eta\right]\mathrm{d}\eta\,. \tag{24}$$

The factor

$$D(x) = \frac{1}{1+x^2}(\cos x - x \sin x) \tag{25}$$

is plotted in Fig. 1 against x.

Now let us consider the distribution $W(\varphi)\,\mathrm{d}\varphi$ about a vector normal to the production plane. For this we have to integrate the distribution (16) over η. For the case of the parallel magnetic field we obtain

$$W_{nr}(\varphi)\,\mathrm{d}\varphi = \left[1 + \frac{\pi}{4}\frac{x}{1+x^2}\,\alpha P(\theta)\sin(\varphi+\theta)\right]\mathrm{d}\varphi\,, \tag{26}$$

whereas for the perpendicular position $W_{nr}(\varphi)\,\mathrm{d}\varphi$ is isotropic as it is without a magnetic field. We want to point out that by measuring the distribution (26) one can determine x and thus also the sign of the magnetic moment, whereas from the distributions (17), (19), (22) and (24) one gets only its magnitude.

The number of events needed to keep the statistical errors sufficiently small depends on the experimental arrangement and the method applied for determining the factor in the η or φ dependent term (see *e.g.* [1-3]). One may readily estimate this number using the formulas, the table and the figure presented here.

* * *

I am very grateful to Dr. K. Gottstein for suggesting this problem, for his interest and for valuable discussions. I am also indebted to Dr. N. N. Biswas for his helpful interest in this paper.

Note added in proof:

It should be emphasized that the explicit formulas (17), (19), (21) and (24) are non-relativistic (in order to give an idea of the magnitude of the effect). For relativistic Λ's ω depends on γ, and V is not $\ll 1$. One has then to carry out the integrations of formula (16) numerically.

RIASSUNTO (*)

In presenza di un campo magnetico il vettore di polarizzazione dei Λ provenienti dalla reazione $\pi^+ + \mathrm{p} \to \Lambda^0 + \mathrm{K}^0$ assume un moto di precessione attorno alla direzione del campo che modifica la distribuzione angolare dei pioni di decadimento. In questo lavoro si ricavano le espressioni esplicite della distribuzione angolare per molti casi. Si danno anche alcuni valori numerici della grandezza dell'effetto che dipende dall'intensità del campo e dal momento magnetico del Λ^0. Con l'aiuto delle formule teoriche qui esposte, si può determinare la grandezza ed il segno del momento magnetico del Λ in base alle distribuzioni sperimentali.

(*) *Traduzione a cura della Redazione.*

IL NUOVO CIMENTO Vol. XV, N. 4 16 Febbraio 1960

A Generalization of the Foldy-Wouthuysen Transformation.

G. Morpurgo

Istituto di Fisica dell'Università - Firenze
Laboratori del C.N.R.N. - Frascati

(ricevuto il 6 Dicembre 1959)

Summary. — A method for constructing a unitary operator which transforms the Hamiltonian of a Dirac electron in the presence of an electric field into an even Hamiltonian is proposed and discussed. The transformation function and the transformed Hamiltonian are expressed through an operator G which satisfies an operator equation; when the electric field is absent (free particle) the Foldy-Wouthuysen transformation is re-derived; when the electric field is present and the equation for G is solved in series of m^{-1} the Pauli, Darwin, Foldy, Wouthuysen non relativistic Hamiltonian is re-obtained; but in addition a method of solution is now possible which converges rapidly and is *not* restricted to the non relativistic case; the expansion parameter in this method of solution is $(1/mc^2)(e\hbar/mc)E$ for an uniform electric field and $Ze^2/\hbar c$ for a Coulomb potential. Though the treatment in this paper considers in detail only the case of an electrostatic potential, the inclusion of any other term in the Hamiltonian is easy and, in particular, a magnetic field may be trivially included.

1. – Introduction.

In a well known paper [1] Foldy and Wouthuysen have shown how it is possible, for the case of a free particle, to obtain a representation of the Dirac Hamiltonian which does not contain odd matrices. Subsequently Case [2] has, among other things, shown that the F. W. transformation can be extended to the case in which a time independent magnetic field is present; in the sense

[1] L. Foldy and S. Wouthuysen: *Phys. Rev.*, **78**, 29 (1950).
[2] K. M. Case: *Phys. Rev.*, **95**, 1323 (1953).

hat, also in such case, an unitary transformation can be found which trans-
orms exactly the Dirac Hamiltonian into a Hamiltonian free from odd ma-
rices.

The fact that the Hamiltonian does not contain odd matrices implies that
wo component wave functions are sufficient for the description of a Dirac
article and in particular makes it possible to discuss the transition from the
elativistic to the non-relativistic case; this has been fully discussed by FOLDY
nd WOUTHUYSEN, who have shown, in addition, how some « paradoxes »
rising in the Dirac theory can be solved: for instance the fact that the velocity
f a free Dirac particle is always the velocity of light, or that, in the Dirac
heory, only the projection of the spin in the direction of the momentum is a
onstant of the motion for a free particle.

More recently ERIKSEN ([3]) has considered a more general problem: is it
ossible to find an unitary transformation leading to an even Hamiltonian
lso in cases more general than that of a free particle or of a particle in a
agnetic field? ERIKSEN has shown that this question may be answered in the
ffirmative; indeed he has been able to find an expression for the operator U
educing the transformation. While Eriksen's treatment is very appropriate
o discuss existence problems, it is not easy to find in general from the expres-
ion of U given by ERIKSEN the transformed Hamiltonian, in those cases where
he initial Hamiltonian contains both odd and even terms in addition to βmc^2.

The purpose of the present paper is to consider again the same problem
hat is to find in general an unitary transformation leading to an even Hamil-
onian) using a method different from that followed by ERIKSEN. We shall
ow that it is possible to give an expression for the transformed Hamiltonian,
terms of an operator G, which satisfies an operator equation; this operator
quation cannot, in general, be solved exactly, but approximation methods
an be invented to obtain solutions in many cases of interest. We shall confine
ere for simplicity, to an Hamiltonian containing only an electrostatic poten-
al; this case is already sufficiently general to illustrate the method; it is easy
o consider the presence in the Hamiltonian of other terms, and in particular
he addition of a magnetic field is trivial.

It should be remarked at this point that the problem of constructing an
nitary transformation leading to an even Hamiltonian in the presence of an
ectric and magnetic field has been already treated by FOLDY and WOUTHUYSEN
their original paper. The way followed by FOLDY and WOUTHUYSEN con-
sted in removing the odd parts of the Hamiltonian through a sequence of
nitary transformations, each of which eliminates the odd terms in the Hamil-
onian to one higher order in an expansion parameter which is chosen as m^{-1},
being the electron mass.

([3]) E. ERIKSEN: *Phys. Rev.*, **111**, 1011 (1958).

It will appear that in the particular case in which the solution of the operator equation mentioned above is constructed by successive approximations in m^{-1} the results of FOLDY and WOUTHUYSEN are reproduced; but in addition we shall suggest an other method of solution which does not depend on the expansion in m^{-1} and is not limited to the non-relativistic case.

2. – A group of transformations of the Dirac equation.

The problem described in the past section is to find an unitary operator U which eliminates the odd parts of the Dirac Hamiltonian H in the presence of an external time independent electric field described by a potential energy V. With the usual meaning of the simbols:

$$H = \gamma_5(\boldsymbol{\sigma}\cdot\boldsymbol{p}) + \beta m + V \,. \tag{1}$$

We want now to find an unitary U ($UU^+ = 1$) such that:

$$U^+ H U = h_1 + \beta h_2 \,, \tag{2}$$

where h_1 and h_2 are hermitian operators constructed through $\boldsymbol{x}$, $\boldsymbol{p}$ and $\boldsymbol{\sigma}$, but not containing odd matrices. From the unitarity of U the equation (2) may be rewritten:

$$HU = U(h_1 + \beta h_2) \,. \tag{3}$$

The most general operator U is now, as well known, a linear combination of the 16 independent Dirac matrices and may be written as:

$$U = A + B\beta + C\gamma_5 + iD\beta\gamma_5 \,, \tag{4}$$

where A, B, C, D are operators not containing β or γ_5 but depending on $\boldsymbol{x}$, $\boldsymbol{p}$ and $\boldsymbol{\sigma}$.

The equation (3) may be written explicitly, using (4) and (2):

$$(\gamma_5\boldsymbol{\sigma}\cdot\boldsymbol{p} + \beta m + V)(A + B\beta + C\gamma_5 + iD\beta\gamma_5) = \\ = (A + B\beta + C\gamma_5 + iD\beta\gamma_5)(h_1 + \beta h_2) \,. \tag{5}$$

For this equation to be satisfied it is necessary and sufficient that the operators which multiply respectively 1, β, γ_5, $\beta\gamma_5$ on the left and right hand

side of (5) are individually equal; we therefore obtain, setting $\boldsymbol{\sigma}\cdot\boldsymbol{p} - \Omega$:

$$VA + mB + \Omega C = Ah_1 + Bh_2 , \tag{6}$$

$$mA + VB - i\Omega D = Bh_1 + Ah_2 , \tag{7}$$

$$\Omega A + VC + imD = Ch_1 - iDh_2 , \tag{8}$$

$$-\Omega B + mC + iVD = -Ch_1 + iDh_2 . \tag{9}$$

We now sum and subtract the equations (6) and (7); and we do the same with the equations (8) and (9); we introduce also the following combinations of operators:

$$\begin{cases} X = A - B & Y = C + iD & R = V + m \\ \overline{X} = A + B & \overline{Y} = C - iD & R' = V - m \end{cases} \tag{10}$$

and

$$\begin{cases} x = h_1 - h_2 , \\ y = h_1 + h_2 . \end{cases} \tag{11}$$

We obtain in this way the two independent sets of operator equations:

$$\begin{cases} R\overline{X} + \Omega\overline{Y} = \overline{X}y \\ \Omega\overline{X} + R'\overline{Y} = \overline{Y}y \end{cases} \tag{12}$$

and

$$\begin{cases} R'X + \Omega Y = Xx , \\ \Omega X + RY = Yx . \end{cases} \tag{13}$$

In the two systems of equations (12) and (13), R, R', Ω are known operators and X, Y, x and $\overline{X}$, $\overline{Y}$, y are unknown operators. If x and y can be determined, h_1 and h_2 are then determined through (11). Similarly if X, Y, $\overline{X}$, $\overline{Y}$ are determined, the operators A, B, C, D are given by (10) and the expression of U is then known.

It must be remarked at this point that we have not yet considered the restrictions on X, Y, $\overline{X}$, $\overline{Y}$, arising from the unitarity condition. This will be done later (Section **3**); for the moment we concentrate on the equations (12) and (13), independently from the unitarity condition.

Consider the system (13); for the two equations to be compatible it is obviously necessary that:

$$X^{-1}(R'X + \Omega Y) = Y^{-1}(\Omega X + RY) \tag{14}$$

an equality which expresses that the operator x obtained from the first equation must be the same as that from the second. In obtaining the equation (14) we have assumed that the inverses both of X and of Y exist; in the following it will be stipulated that this is the case.

We now introduce the operator

$$G = XY^{-1} . \tag{15}$$

Multiplying both sides of the equation (14) by X from the left and by Y^{-1} from the right we obtain the following operator equation for G

$$G(\Omega G + R) = R'G + \Omega . \tag{16}$$

If a solution G of this equation can be found, x is then given by:

$$x = Y^{-1}(\Omega G + R)Y \tag{17}$$

and a relation between X and Y is established through:

$$X = GY . \tag{18}$$

In a completely similar way we have from the system (12):

$$\bar{G}(\Omega\bar{G} + R') = R\bar{G} + \Omega \tag{19}$$

and

$$y = \overline{Y}^{-1}(\Omega\bar{G} + R')\ \overline{Y} , \tag{20}$$

where now

$$\overline{X} = \bar{G}\overline{Y} . \tag{21}$$

Obviously the equations (17) and (20) show that x and y (and therefore h_1 and h_2) are not uniquely determined, even if the solutions G and $\bar{G}$ of the equations (16) and (19) were unique. This freedom in x, y, which is of course expected, will be discussed in Section **4**.

We end this section by rewriting the equations (16) and (19) in a more explicit form: using (10) we have:

$$G\Omega G + GV - VG + 2mG - \Omega = 0 \tag{22}$$

and

$$\bar{G}\Omega\bar{G} + \bar{G}V - V\bar{G} - 2m\bar{G} - \Omega = 0 . \tag{23}$$

The invariance of the above equations with respect to the substitution $V \to V +$ const. should be noted.

3. – The condition of unitarity.

We now determine the restrictions on A, B, C, D, or equivalently on X, Y, $\bar{X}$, $\bar{Y}$ implied by the unitarity condition. When the expression (4) for U is inserted in the equation $U^+U = 1$, four bilinear equations in A, B, C, D result; these four equations, when reexpressed using (10) in terms of X, Y, $\bar{X}$, $\bar{Y}$ are:

$$\bar{X}^+\bar{X} + \bar{Y}^+\bar{Y} = 1\,, \tag{24}$$

$$X^+X + Y^+Y = 1\,, \tag{25}$$

$$\bar{Y}^+X + \bar{X}^+Y = 0\,, \tag{26}$$

$$Y^+\bar{X} + X^+\bar{Y} = 0\,. \tag{27}$$

Recalling the equations (18) and (21) we obtain from the equation (26)

$$\bar{Y}^+\bar{G}^+Y + \bar{Y}^+GY = 0$$

that is

$$\bar{G}^+ = -G\,. \tag{28}$$

It follows that the operator $\bar{G}$ is determined from the operator G by the unitarity condition; it can be easily checked that the relation (28) is compatible with the equation (22) and (23) which have to be satisfied by G and $\bar{G}$. In fact the hermitian conjugate of the equation (23) is:

$$\bar{G}^+\Omega\bar{G}^+ + V\bar{G}^+ - \bar{G}^+V - 2m\bar{G}^+ - \Omega = 0 \tag{29}$$

which is just the equation satisfied by $-G$. In writing (29) use has been made of the hermiticity of Ω and V.

Coming back to the equations (24) to (27) we note that since the equation (27) is simply the hermitian conjugate of the equation (26) it is already satisfied by (28); we therefore have still to consider only the equations (24) and (25). They give respectively:

$$\bar{Y}^+\bar{G}^+\bar{G}\bar{Y} + \bar{Y}^+\bar{Y} = 1 \tag{30}$$

and

$$Y^+G^+GY + Y^+Y = 1 \tag{31}$$

which may be rewritten, using also the condition (28):

$$\overline{Y}\,\overline{Y}^{+} = (1 + \overline{G}^{+}\overline{G})^{-1} = (1 + G G^{+})^{-1}\,, \tag{32}$$

$$Y Y^{+} = (1 + G^{+} G)^{-1}\,. \tag{33}$$

The equations (32) and (33) are conditions on $\overline{Y}$ and Y. We notice that they may be in particular satisfied if we choose $\overline{Y}$ and Y to be hermitian operators, respectively equal to [4]:

$$\overline{Y} = -\,(1 + G G^{+})^{-\frac{1}{2}}\,, \tag{34}$$

$$Y = \quad (1 + G^{+} G)^{-\frac{1}{2}}\,. \tag{35}$$

To end this section we wish to check explicitly that the operators x and y defined by (17) and (20) are hermitian as they must be. Let us consider the expression (17) of x; using (33) we may write it as:

$$\begin{aligned} x &= Y^{+}(1 + G^{+}G)(\Omega G + R)\, Y = \\ &= Y^{+}(\Omega G + R + G^{+}G\Omega G + G^{+}G R)\, Y = \\ &= Y^{+}(\Omega G + R + G^{+}\Omega + G^{+}R'G)\, Y = x^{+}\,. \end{aligned} \tag{36}$$

A similar check can be made for y which can be written:

$$y = \overline{Y}^{+}(\Omega\overline{G} + R' + \overline{G}^{+}R\overline{G} + \overline{G}^{+}\Omega)\overline{Y} = y^{+}\,. \tag{37}$$

4. – The arbitrariness in x and y for a given G.

The results of the Sections **2** and **3** show that, if an operator G which obeys the equation (22) can be found, the operators x and y or equivalently h_1 and h_2 can be determined. In fact once a G has been found the equations (34) and (35) may be used to determine a particular choice of $\overline{Y}$ and Y; in addition $\overline{G}$ is simply equal to $-G^{+}$, so that all the operators which appear in the expressions (17) and (20) for x and y are available.

The question which we now ask is: having found an operator G which satisfies the equation (22) which is the arbitrariness in h_1 and h_2? It is easy to

---

[4] The choice of the – sign in eq. (34) has been made simply to re-obtain the same result of ref. [2] for U in the case of a free particle, but has no particular meaning; compare Sect. **4**.

answer this question simply by looking at the expressions which give x and y; it is convenient for this purpose to use the expressions (36) and (37). It is then apparent that for a given G the arbitrariness which remains in x is simply the arbitrariness in the choice of Y; the unitarity condition only fixes (compare the equation (33)) the product YY^+ but not separately Y and Y^+; if therefore Y is a particular operator satisfying the equation (33) (*e.g.* the operator (35)) the most general operator which still satisfies the equation (33) is:

$$Y' = YT , \tag{38}$$

where T is an arbitrary unitary operator; it follows from the equation (36) that x is correspondingly transformed into:

$$x' = T^+xT . \tag{39}$$

For a given G this is, therefore, the arbitrariness in x. A similar arbitrariness exists for y; in fact if $\overline{Y}$ is a particular solution of the equation (32) (*e.g.* the operator (34)) another solution is $\overline{Y}' = \overline{Y}S$, where S is again an unitary operator independent from T. From the equation (37) it then follows that:

$$y' = S^+yS . \tag{40}$$

The origin of the arbitrariness in x and y which we have just illustrated (we shall call it « normal ») is clear: at the beginning of the Section **2** we did ask to find an unitary operator U which transforms a given Hamiltonian into a Hamiltonian free from odd operators, that is of the form $h_1+\beta h_2$; but we have not put restrictions on the form of h_1 and h_2. This implies that, once a particular operator $h_1+\beta h_2$ has been found, the possibility remains of obtaining other even hamiltonians through unitary transformations produced by unitary operators of the form $L+\beta M$, where L and M are arbitrary operators constructed through $\boldsymbol{x}$, $\boldsymbol{p}$ and $\boldsymbol{\sigma}$. It is apparent that the normal arbitrariness illustrated above is just the arbitrariness which is present in such unitary trasnformations; it is easy to find the connection between the operators L and M and S and T previously introduced; we do not need however to write down the explicit formulas.

In addition to the normal arbitrariness in x and y there is another kind of arbitrariness; this stems from the fact that in general different solutions for the equation (22) for G can exist; it is not yet clear to us what is the extent and the meaning of this arbitrariness; some remarks concerning this point will be made in Section **9**.

5. – The operator equation for G.

We now discuss the equation (22) for G; we shall from now on use respectively mc^2 and $\hbar/mc$ as units for energy and length. In these units the equation for G is simply written:

$$G\Omega G + GV - VG + 2G - \Omega = 0\,, \tag{22'}$$

where now all the quantities which appear in the equation are dimensionless.

a) Free particle. As a first example we consider the case of a free particle ($V = 0$), simply to check that we obtain the same results as FOLDY and WOUTHUYSEN. The operator G for this case will be called G_0; we have:

$$G_0\Omega G_0 + 2G_0 - \Omega = 0\,. \tag{41}$$

Obviously G_0 is a function of the operator Ω only, so that Ω and G_0 commute and the solution of the equation (41) proceeds as if G_0 were a C number. We have two solutions:

$$G_0^{(1)} = \frac{-1+\sqrt{1+\Omega^2}}{\Omega} = \Omega\frac{\left(-1+\sqrt{1+p^2}\right)}{p^2} = \Omega\frac{1}{1+\sqrt{1+p^2}}\,, \tag{42}$$

$$G_0^{(2)} = \frac{\Omega\left(-1-\sqrt{1+p^2}\right)}{p^2} = -\frac{\Omega}{\sqrt{p^2+1}-1}\,, \tag{43}$$

where the properties $\Omega^2 = p_x^2 + p_y^2 + p_z^2 \equiv p^2$ and $\Omega^{-1} = \Omega p^{-2}$ have been used. Recalling the expressions (17) and (20) for x and y, noting that in this case Y^{-1} or $\overline{Y}^{-1}$ may be freely transferred to the right, using for x and y our system of units and taking the solution $G_0^{(1)}$ we get

$$x = \sqrt{1+p^2}\,,$$

$$y = -\sqrt{1+p^2}\,,$$

where the equation (28) has been used.

In the transformed hamiltonian one has accordingly:

$$h_1 = \tfrac{1}{2}(x+y) = 0\,, \qquad h_2 = \tfrac{1}{2}(y-x) = -\sqrt{1+p^2}\,,$$

in agreement with the result of FOLDY and WOUTHUYSEN.

Had we chosen the solution $G_0^{(2)}$ we would have obtained:

$$h_1 = 0\,, \qquad h_2 = +\sqrt{1+p^2}\,,$$

which differs from the previous result only for having exchanged the positive with the negative energy states.

It is also straightforward to deduce an expression for U, in this case; the general expression of U, in terms of G, will be given in Section **8** (formula (61)). Specializing this expression to the present case, using the solution $G^{(1)}$ and the formulas (34) and (35) of Section **3** we get:

$$U = G_0^{(1)} \frac{1}{\sqrt{1+G_0^{(1)2}}} + \beta\gamma_5 \frac{1}{\sqrt{1+G_0^{(1)2}}}\,. \tag{44}$$

Putting

$$\cos\frac{\varphi}{2} = G_0^{(1)} \frac{1}{\sqrt{1+G_0^{(1)2}}}\,,$$

and consequently $\operatorname{tg}\varphi = -\Omega$ the expression (44) may be rewritten:

$$U = \cos\frac{\varphi}{2} + \beta\gamma_5 \sin\frac{\varphi}{2} = \exp\left[\beta\gamma_5 \frac{\varphi}{2}\right],$$

in agreement with ref. ([2]).

b) It does not seem possible to find a formal solution of the equation (22′) in an arbitrary field. It is possible to find a solution in the particular case of an uniform electric field (compare the Section **9**); or it is possible to try to construct the solution by successive approximations in V (we recall that V is now adimensional, being equal to the potential energy, divided by mc^2). This will be done in the next Section.

6. – The perturbative solution of the operator equation for G.

The terms containing V in the equation (22′) are usually small with respect to the others; in fact the quantity V in (22′) appears usually multiplied by a very small coefficient whene verything is made adimensional. For instance in the case of an uniform electric field (putting $\tilde{\boldsymbol{r}} = (mc/\hbar)\boldsymbol{r}$)

$$V = -\frac{e}{mc^2}\boldsymbol{E}\cdot\boldsymbol{r} \equiv -\tilde{\boldsymbol{E}}\cdot\boldsymbol{r}\frac{mc}{\hbar} = -\tilde{\boldsymbol{E}}\cdot\tilde{\boldsymbol{r}}\,, \tag{45}$$

with $\tilde{E} = (e\hbar/mc)(1/mc^2)E$, a quantity which is exceedingly small ($< 10^{-12}$) even for the strongest macroscopic electric fields obtainable.

For the case of a Coulomb field:

$$V = \frac{Ze^2}{mc^2}\frac{mc}{\hbar}\frac{1}{\tilde{r}} = \frac{Ze^2}{\hbar c}\frac{1}{\tilde{r}}, \tag{46}$$

which is reasonably small for small Z.

It appears therefore reasonable to try to get the solution of the equation (22′) by perturbation theory, regarding V as small; this is what will be done in this Section.

We write:

$$G = G_0 + G_1 + G_2 + \dots, \tag{47}$$

where the lower index characterizes the order in V; and we proceed to determine the succeeding operators of the series by substituting the expansion (47) in the equation (22′) and equating to zero terms of any given order in V. In this way we obtain, of course, for G_0 the equation (41); for G_1 we have:

$$G_1 \Omega G_0 + G_0 \Omega G_1 + 2G_1 = VG_0 - G_0 V . \tag{48}$$

For G_2 we obtain:

$$G_2 \Omega G_0 + G_0 \Omega G_2 + 2G_2 = VG_1 - G_1 V - G_1 \Omega G_1 . \tag{49}$$

For the successive terms we have similar equations where in each case terms of any order are determined from the knowledge of terms of lower order.

We now choose for G_0 the solution $G_0^{(1)}$ given by (42) and we confine here to the determination of G_1. From (48), using a representation in which σ_z and $\boldsymbol{p}$ are diagonal we have:

$$\langle \boldsymbol{p}'\lambda' | G_1 | \boldsymbol{p}''\lambda'' \rangle = \sigma_{\lambda'\lambda''} \cdot \left\{ \frac{\langle \boldsymbol{p}' | V | \boldsymbol{p}'' \rangle \boldsymbol{p}''(\sqrt{1+p''^2}+1)^{-1} - \boldsymbol{p}'(\sqrt{1+p'^2}+1)^{-1}\langle \boldsymbol{p}' | V | \boldsymbol{p}'' \rangle}{\sqrt{1+p'^2}+\sqrt{1+p''^2}} \right\} . \tag{50}$$

It is possible to write G_1 as follows:

$$G_1 = \int_{-\infty}^{0} \mathrm{d}s \exp\left[s\sqrt{1+p^2}\right] \left[V, \frac{\boldsymbol{\sigma}\cdot\boldsymbol{p}}{1+\sqrt{1+p^2}} \right] \exp\left[s\sqrt{1+p^2}\right], \tag{51}$$

where the brackets in the integrand indicate the commutator.

It is important to recognize that, on account of the smallness of V pointed out at the beginning of this section, the term G_1 is sufficient for all practical purposes, at least in the case of macroscopic fields. Of course the convergence of the whole procedure has to be examined; some remarks on this point will be made in Section **9**.

It is also important to stress that the expansion discussed in this Section is *not* a non-relativistic approximation; it is simply an expansion in terms of a well defined parameter; in other words the formula (51), in particular, is completely general as far as the velocity of our electron is concerned.

We can now exhibit the connection between our procedure and the non-relativistic expansion in m^{-1} discussed by FOLDY and WOUTHUYSEN which we have mentioned in the introduction; this is very simple.

The non-relativistic limit of Pauli, Darwin, Foldy and Wouthuysen is simply obtained from our formulas by expanding G in series of m^{-1} and limiting ourselves to the terms of order m^{-2}.

We recall that our p stays for p/m and our V is V/m; it is then straightforward to show that to take into account all the terms up to the order m^{-2} it is sufficient to confine ourselves to G_0 and G_1; in other words G_2 is already of order m^{-4} and it does not contribute to terms of order m^{-2} in the expressions of h_1 and h_2.

To be more definite we note below the relevant terms in the expansion in m^{-1} of the various quantities which are necessary for the determination of h_1 and h_2 including terms of order m^{-2}. In order to exhibit the mass explicitely we shall write the formulas below in conventional units. We have:

$$G_0^{(1)} = -\frac{1}{2}\frac{\Omega}{m} + 0\left(\frac{1}{m^3}\right), \tag{52}$$

$$G_1 = \int_{-\infty}^{0} \exp[2s]\,\mathrm{d}s \left(\frac{V\Omega}{2m^2} - \frac{\Omega V}{2m^2}\right) + 0\left(\frac{1}{m^4}\right) = -\frac{i\hbar e}{4m^2}(\boldsymbol{\sigma}\cdot\boldsymbol{E}) + 0\left(\frac{1}{m^4}\right) \tag{53}$$

$$[e\boldsymbol{E} = -\operatorname{grad} V],$$

$$G_2 = 0\left(\frac{1}{m^4}\right). \tag{54}$$

The expressions (17) and (20) of x and y may now be written:

$$x = m\,V^{-1}\left(\frac{\boldsymbol{\sigma}\cdot\boldsymbol{p}}{m}[G_0^{(1)} + G_1] + \frac{V}{m} - 1\right)V, \tag{55}$$

$$y = m\,\bar{V}^{-1}\left(\frac{\boldsymbol{\sigma}\cdot\boldsymbol{p}}{m}[-G_0^{(1)} + G_1] + \frac{V}{m} - 1\right)\bar{V}, \tag{56}$$

where use has been made of the relation $\overline{G}^{+} = -G$ and of the antihermiticity of G_1. It appears from (55), (56) that $\overline{Y}^{-1}$, Y, Y^{-1} and $\overline{Y}$ have to be calculated including terms of order m^{-3}.

We simply give here the expression of Y:

$$(57) \qquad Y = \frac{1}{\sqrt{1+G^{+}G}} \cong \frac{1}{\sqrt{1+G_0^2+G_0G_1-G_1G_0}} = \\ = 1 - \frac{1}{8}\frac{p^2}{m^2} + \frac{1}{16}\frac{e\hbar^2}{m^3}\operatorname{div}\boldsymbol{E} + \frac{e\hbar}{8m^3}\boldsymbol{\sigma}\cdot(\boldsymbol{E}\wedge\boldsymbol{p}) .$$

To obtain Y^{-1} simply change the sign of all the ferms in Y except the first: $-\overline{Y}$ differs from Y for a change in sign in the terms of order m^{-3} and $-\overline{Y}^{-1}$ differs in the same way from Y^{-1}.

Though we have written down the Y's correct to the order m^{-3}, the terms of order m^{-3} disappear in the calculation of x and y because div $\boldsymbol{E}$ and $\boldsymbol{\sigma}\cdot(\boldsymbol{E}\wedge\boldsymbol{p})$ both commute with V. Hence we obtain:

$$x = m\left(1+\frac{p^2}{8m^2}\right)\left(\frac{p^2}{2m^2} - \frac{i\hbar e}{4m^3}(\boldsymbol{\sigma}\cdot\boldsymbol{p})(\boldsymbol{\sigma}\cdot\boldsymbol{E}) + \frac{V}{m} + 1\right)\left(1-\frac{p^2}{8m^2}\right),$$

$$y = m\left(1+\frac{p^2}{8m^2}\right)\left(-\frac{p^2}{2m^2} - \frac{i\hbar e}{4m^3}\frac{(\boldsymbol{\sigma}\cdot\boldsymbol{p})(\boldsymbol{\sigma}\cdot\boldsymbol{E})}{m^3} + \frac{V}{m} - 1\right)\left(1-\frac{p^2}{8m^2}\right).$$

We then get easily:

$$(58) \qquad \begin{cases} h_1 = -\dfrac{e\hbar^2}{8m^2}\operatorname{div}\boldsymbol{E} - \dfrac{e\hbar}{4m^2}\boldsymbol{\sigma}\cdot(\boldsymbol{E}\wedge\boldsymbol{p}) + V, \\ h_2 = -\dfrac{p^2}{2m} - m , \end{cases}$$

which is the same result of Foldy and Wouthuysen, for a pure electric field.

The results of this Section may be summarized as follows: we have made an expansion of G in terms of the adimensional quantity V/m, a quantity which is usually very small. In this expansion, of which (42) and (51) give the zero and first order terms, no non-relativistic approximation is made; when each term of the expansion is further expanded in series of m^{-1}, the non-relativistic Foldy-Wouthuysen expansion is reobtained.

7. – The evaluation of G_1 for an uniform electric field.

The sense in which our series expansion is a generalization of the Foldy-Wouthuysen one may be fully appreciated if the example of an uniform electric field is considered. In such case G_1 may be easily determined exactly and h_1, h_2, may therefore be given exactly to the first order in $\widetilde{E}$.

We have:

$$G_1 = -\frac{i}{2}\frac{(\tilde{\boldsymbol{E}}\cdot\boldsymbol{\sigma})\sqrt{1+p^2}(1+\sqrt{1+p^2}) - (\tilde{\boldsymbol{E}}\cdot\boldsymbol{p})(\boldsymbol{\sigma}\cdot\boldsymbol{p})}{(1+p^2)(1+\sqrt{1+p^2})^2}, \tag{59}$$

where V has been again written, like in (45), as:

$$V = -\tilde{\boldsymbol{E}}\cdot\tilde{\boldsymbol{r}}\,.$$

The calculation of h_1 and h_2 gives:

$$h_1 = V + \frac{m}{2}\frac{\boldsymbol{\sigma}\cdot\boldsymbol{p}\wedge\tilde{\boldsymbol{E}}}{\sqrt{1+p^2}(1+\sqrt{1+p^2})}, \tag{60_1}$$

$$h_2 = -m\sqrt{1+p^2}\,. \tag{60_2}$$

The formulas are correct to the first order in the expansion parameter $\tilde{E}$ and to all orders in m^{-1}; from the formulas (60), the non-relativistic limit for the present case is obtained simply neglecting p^2 with respect to the unity in the second term on the right hand side of (60_1).

8. – Comparison with the results of Eriksen [5].

These results of the past Sections show that, if a G exists, the transformed hamiltonian is even; therefore for the transformed hamiltonian $h_1+\beta h_2$, β is a constant of the motion. This implies that $U\beta U^+$ is a constant of the motion for the initial hamiltonian H. Since the eigenvalues of β and $U\beta U^+$ must be the same, that is ± 1, Eriksen has observed that it should be possible to identify $U\beta U^+$ with an operator commuting with H and having only the two eigenvalues ± 1; he has called this operator λ and has remarked that a possible explicit expression for λ may be: $H/(H^2)^{\frac{1}{2}}$.

Eriksen then proceeds to determine U in terms of λ from the equation $U\beta U^+ = \lambda$ to which he adds the further restriction $U\beta = \beta U^+$ which is seen to be compatible with the previous one. As we have said in the introduction Eriksen has found an expression for U in terms of λ; this expression is useful for discussing existence problems; our method is perhaps more appropriate to determine the transformed hamiltonian explicitly, as we did already mention in the introduction. Obviously however a relation exists between the two procedures; we shall briefly show below which is the connection.

[5] Our U^+ is Eriksen's U.

From our formulas it is easy to obtain an expression for U; it is

$$U = \tfrac{1}{2}[(G+\gamma_5)(1-\beta)Y + (-G^+ + \gamma_5)(1+\beta)\overline{Y}]\,. \tag{61}$$

The connection between our G and Eriksen's λ [6] can be established constructing $U\beta U^+$ and identifying this quantity with λ. Explicitly:

$$U\beta U^+ = \frac{1}{1+GG^+} - \frac{1}{1+G^+G} + \beta\left(1 - \frac{1}{1+GG^+} - \frac{1}{1+G^+G}\right) - \tag{62}$$

$$-\gamma_5\left(G^+\frac{1}{1+GG^+} + G\frac{1}{1+G^+G}\right) + \beta\gamma_5\left(G^+\frac{1}{1+GG^+} - G\frac{1}{1+G^+G}\right) = \lambda\,.$$

Equation (62) shows that Eriksen's λ can be expressed through our G; however Eriksen's condition $U\beta = \beta U^+$ does not correspond to our particular hermitian choice of Y and $\overline{Y}$, but corresponds instead to the choice: $GY = Y^+G^+$ $YG = G^+Y^+$, $Y = -\overline{Y}^+$; these equations and the equations (32), (33) can be satisfied with $Y = G^{-1}(GG^+/(1+GG^+))^{\frac{1}{2}}$.

It should be noticed that the equation (62) is important for establishing the existence of a G once the existence of a λ is established; in fact if we write λ as $\lambda_1+\beta\lambda_2+\gamma_5\lambda_3+\beta\gamma_5\lambda_4$ G can be explicitly expressed in terms of λ_1, λ_2, λ_3, λ_4, by:

$$G = (-\lambda_3 + \lambda_4)(1-\lambda_1-\lambda_2)^{-1}\,.$$

This observation implies that the result of ERIKSEN showing the existence of an U entails necessarily the existence of a G, solution of the equation (22′).

9. – Some final problems.

This Section contains a few comments on some questions which arise naturally from the previous treatment; they are: *a*) how many solutions of the operator equation (22′) for G do exist? *b*) Which is the relation between the class of transformed (even) hamiltonians obtained using a particular solution and the class obtained using another solution? *c*) Does the sum of the perturbative series of Section 6 in V/m give a solution of the equation for G and which is the connection between this perturbative expansion and the general solution?

We are not able, at present, to answer these quenstions: we confine to

---

(6) When speaking of a λ from now on we do not imply that this must be the same as Eriksen's particular choice.

illustrate them on the simple example of the uniform electric field where the operator equation for G reduces to a differential equation: we have already examined the case of the uniform field in the first perturbative approximation in Section **7**.

It is easy to see that, since for an uniform field

$$GV - VG = -i\boldsymbol{E}\cdot\mathrm{grad}_p G$$

the equation (22′) becomes a differential equation.

If we write:

$$G = \frac{\boldsymbol{\sigma}(\boldsymbol{\epsilon}\mathscr{A} - \boldsymbol{p})}{\mathscr{B} - 1},$$

where $\boldsymbol{\epsilon}$ is a unit vector in the direction of B and $\mathscr{A}$, $\mathscr{B}$ are some functions of p_x, p_y, p_z, it is easy to see that $\mathscr{A}$ and $\mathscr{B}$ satisfy a pair of coupled differential equations. If we further introduce the function Z of p_x, p_y, p_z through:

$$\mathscr{A} = \frac{p^2 + 1 - Z^2}{2(\boldsymbol{p}\cdot\boldsymbol{\epsilon} - Z)} \qquad \text{and} \qquad \mathscr{B} = Z - \frac{p^2 + 1 - Z^2}{2(\boldsymbol{p}\cdot\boldsymbol{\epsilon} - Z)},$$

where $p^2 = p_x^2 + p_y^2 + p_z^2$, the problem reduces to find a function Z which satisfies the following ordinary differential equation:

$$Z^2 - i\tilde{E}\frac{\mathrm{d}Z}{\mathrm{d}p_x} - p^2 - 1 + i\tilde{E} = 0\,. \tag{63}$$

Here the direction of $\boldsymbol{\epsilon}$ has been assumed to be that of the x axis. The equation (63) is a Riccati equation with complex coefficients. It is therefore clear not only that a solution exists, but also that a manifold of them exist depending on an arbitrary complex constant C.

The questions which have been raised at the beginning of this Section reduce therefore in the present case to: 1) which relation exists between the transformed hamiltonian corresponding to different choices of the above mentioned complex constant? 2) It is possible to find two solutions of the equation (63) corresponding to two values of C, which are analytical in E near $E = 0$ and may be constructed by the perturbative approach? Notice that also here, as in general, there are two different perturbative series, one starting with $Z_0 = \sqrt{p^2+1}$ the other with $Z_0 = -\sqrt{p^2+1}$.

Now, in the present case, it would be clearly possible, using known results in the theory of differential equations, to give a detailed answer to the above questions 1) and 2). Since, however, the example of the uniform field was discussed here only with the purpose of making more concrete the general questions introduced at the beginning of this section, we shall stop our ana-

lysis here, adding only two remarks: the first is that, both in general and in the particular case of the uniform field, the simplest answer to our questions would be that the perturbation solutions converge at least asymptotically and at least for a certain range of values of the expansion parameter to a solution of the equation for G, while all the other solutions have some kind of irregularity which makes them not usable for the construction of the transformed hamiltonian; that this is true has been, however, not proved. The second remark is that, in the case of the uniform field at least an asymptotic convergence of the perturbative series exists almost certainly as one may conjecture from general theorems (7) on non-linear differential equations belonging to a class very near to that of equation (63).

(7) W. WASOV: *Asymptotic properties of non-linear analytic differential equations. Proc. of the Varenna Course 1954 Sponsored by C.I.M.E.* I thank prof. CONTI of the department of Mathematics for having indicated this reference to me.

RIASSUNTO

Viene proposto e discusso un metodo di costruzione di un operatore unitario che trasforma l'Hamiltoniana di Dirac in presenza di un campo elettrico in un'Hamiltoniana priva di matrici dispari. La funzione di trasformazione e l'Hamiltoniana trasformata sono espresse mediante un operatore G che soddisfa un'equazione operatoriale; quando il campo elettrico è assente (particella libera) si ricava di nuovo la trasformazione di Foldy-Wouthuysen; quando il campo elettrico è presente e l'equazione per G è risolta in serie di m^{-1} si riottiene l'Hamiltoniana non relativistica di Pauli, Darwin, Foldy, Wouthuysen; ma in aggiunta un nuovo metodo di soluzione è possibile che converge rapidamente e non è limitato al caso non relativistico; il parametro di sviluppo in questo metodo è $(1/mc^2)(e\hbar/mc)E$ per un campo elettrico uniforme e $Ze^2/\hbar c$ per un potenziale coulombiano. Sebbene in questo lavoro si consideri soltanto il caso di un potenziale elettrostatico è facile includere un qualsiasi altro termine nell'Hamiltoniana ed in particolare l'introduzione di un campo magnetico non presenta alcuna difficoltà.

IL NUOVO CIMENTO Vol. XV, N. 4 16 Febbraio 1960

An Experimental Test of Parity Conservation in π^0-Meson Production by Neutrons.

D. G. Davis (*), R. C. Hanna (**), F. F. Heymann (*) and C. Whitehead (**)

CERN - Geneva

(ricevuto il 9 Dicembre 1959)

Summary. — A carbon target was bombarded with a beam of transversely polarized neutrons of energy up to 540 MeV. π^0-mesons ejected at right angles to the neutron beam were detected through their decay γ-rays in energy-sensitive Čerenkov counters. A fore-aft asymmetry in π^0 production relative to the polarization vector of the neutron beam was sought which would have been indicative of a parity violating term of the form $\boldsymbol{\sigma}_n \cdot \boldsymbol{k}_{\pi^0}$. A reversible longitudinal magnetic field was used to precess the neutron beam polarization vector to enable the asymmetries to be measured with minimal systematic errors. The experiment was sensitive to asymmetries of 1 in 10^3. Values of P, the parity violating polarization in the reaction, of -0.005 ± 0.020 to -0.079 ± 0.050 were found for π^0's of various energies.

1. – Introduction.

Lee and Yang [1] drew attention to experimentally verifiable consequences of the breakdown of parity conservation in weak interactions: many experiments since then have confirmed that parity is not conserved in these interactions [2]. In the field of strong interactions between nucleons at energies of a few MeV, several experiments [3] have shown that parity is conserved to a very high degree; the most sensitive experiment by Tanner [4] has

(*) Member of visiting team from University College London.

(**) Member of visiting team from AERE, Harwell.

[1] T. D. Lee and C. N. Yang: *Phys. Rev.*, **105**, 1671 (1957).

[2] C. S. Wu, E. Ambler, R. W. Hayward, D. D. Hoppes and R. P. Hudson: *Phys. Rev.*, **105**, 1413 (1957).

[3] R. E. Segel, J. V. Kane and D. H. Wilkinson: *Phil. Mag.*, **3**, 204 (1958).

[4] N. Tanner: *Phys. Rev.*, **107**, 1203 (1957).

established that f^2, the ratio of the strength of the parity violating to the parity conserving interaction, does not exceed 10^{-7}. It may be that for energies of a few MeV, parity conservation is not fundamental but follows from invariance under charge conjugation (C) and time reversal (T) and the Pauli-Lüders [5] PCT theorem. FEINBERG [6] has pointed out that charge conjugation invariance no longer holds when strange particles are produced in the interaction; in this case, parity conservation would not follow automatically from time reversal invariance. This reasoning suggested that experiments on parity conservation in strong interactions should be extended to energies where virtual strange particle production could play a part, even though in this energy range the accuracy with present techniques is substantially less than has been achieved at low energies.

So far, only two high energy experiments have been reported. ROBERTS *et al.* [7] have sought an asymmetry in the production of 40 MeV charged pions by a 209 MeV polarized proton beam arising from a term $\boldsymbol{\sigma}_p \cdot \boldsymbol{k}_\pi$ in the interaction; JONES *et al.* [8] have looked for a longitudinal polarization of the neutrons produced at 0° by 385-MeV unpolarized protons which could arise from a term $\boldsymbol{\sigma}_n \cdot \boldsymbol{k}_n$ in the production interaction. Both experiments gave negative results. The interaction studied in the present experiment was the production of π^0 mesons by polarized neutrons; a term of the form $\boldsymbol{\sigma}_n \cdot \boldsymbol{k}_{\pi^0}$ was sought in the intensity distribution of the emitted π^0's relative to the direction of the neutron beam polarization vector. This term, $\boldsymbol{\sigma}_n \cdot \boldsymbol{k}_{\pi^0}$, changes sign on reversal of space co-ordinates and its presence would be evidence of parity violation. If parity non-conservation arises through the virtual production of strange particles, an effect is most likely to be found for close encounters of high energy nucleons. A π^0 production angle of 90° was chosen to concentrate attention on s-wave interactions which predominate at this angle. To attain maximum sensitivity to parity violation, close attention was paid to minimizing systematic errors and high efficiency counters were used to obtain good statistical accuracy.

2. – Experimental method.

The presence of a $\boldsymbol{\sigma}_n \cdot \boldsymbol{k}_{\pi^0}$ term may be established by studying the effect on π^0 emission intensity of a change in $\boldsymbol{\sigma}_n$ or $\boldsymbol{k}_\pi$, *i.e.* by changing the polarization direction of the incident beam or by rotating the detector about the

(5) W. PAULI: *Niels Bohr and the Development of Physics* (London, 1955); G. LÜDERS: *Ann. of Phys.*, **2**, 1 (1957).

(6) G. FEINBERG: *Phys. Rev.*, **108**, 878 (1957).

(7) E. HEER, A. ROBERTS and J. TINLOT: *Phys. Rev.*, **111**, 645 (1958).

(8) D. P. JONES, P. G. MURPHY and P. L. O'NEILL: *Proc. Phys. Soc.*, **72**, 429 (1958).

effective centre of the production target. This centre is generally ill-defined and accordingly systematic errors easily arise. HILLMAN, STAFFORD and WHITEHEAD (9) have shown that σ_n may be changed without introducing systematic errors by passing a transversely polarized beam through a long solenoid in which the neutron spin direction precesses around the beam direction. The method is less well adapted to proton beams as focusing effects, absent for neutrons, may cause a displacement of the effective beam centre. There is thus an advantage with neutron beams which helps compensate for their generally lower intensity and less complete polarization relative to proton beams. Studying the emission of π^0 mesons rather than other reaction products has the advantage that a high efficiency wide-angle detector can be used which nevertheless gives good discrimination against other particles. To simplify the interpretation of results, π^0 production from hydrogen should have been studied; the available intensity from a liquid hydrogen target did not permit this and carbon was chosen instead.

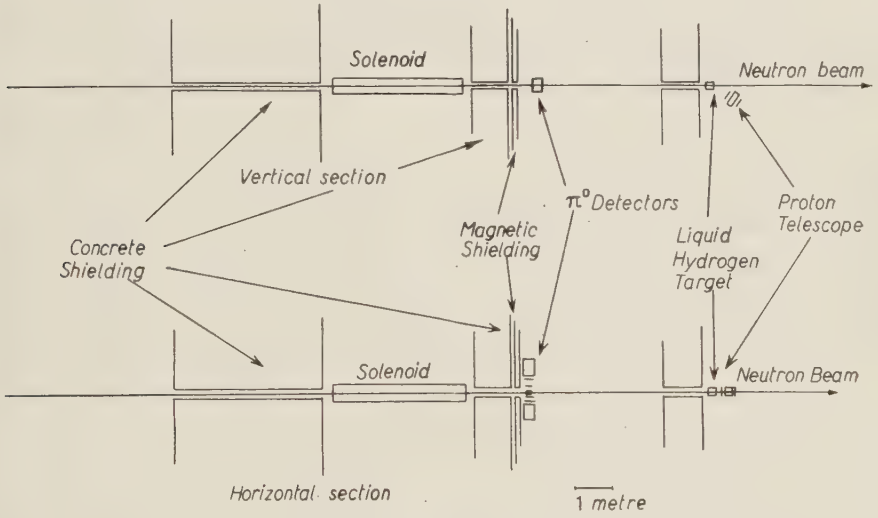

Fig. 1. – General layout.

The general layout of the apparatus is shown in Fig. 1 and the details of the detecting system in Fig. 2. The neutron beam was produced by bombarding either of two beryllium targets with a 540 MeV internal proton beam of the CERN synchro-cyclotron. Neutrons emitted at angles of either + or − 14° relative to the incident protons passed through 2.5 cm of lead to remove γ-ray contamination, and along a collimation channel 4.5 m long and of area

(9) P. HILLMAN, G. H. STAFFORD and C. WHITEHEAD: *Nuovo Cimento*, **4**, 67 (1956).

(1.6 × 1.6) cm. They then passed through a reversible longitudinal field of 4100 gauss provided by the 3.3 m long solenoid. After the solenoid, a clearing collimator (90 cm long, 3 × 3 cm) removed neutrons scattered from the walls

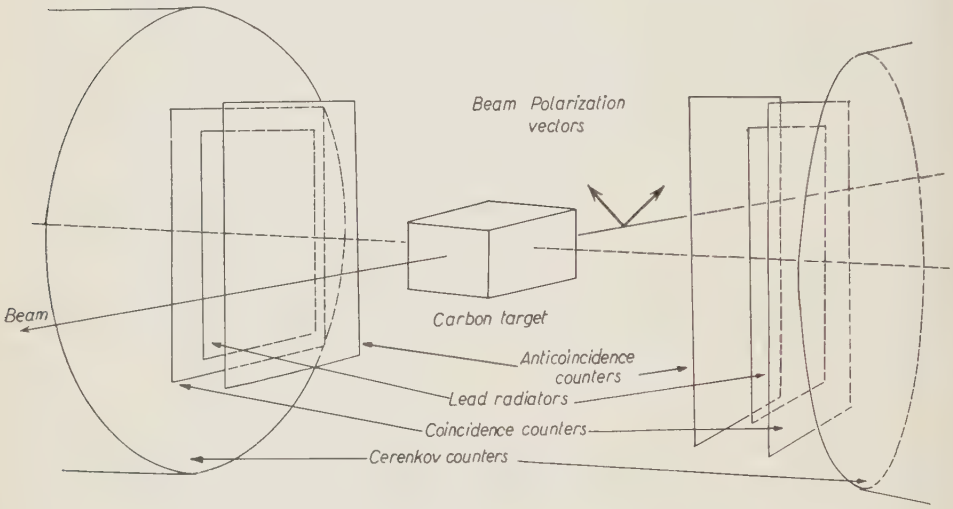

Fig. 2. – Detector system.

of the first collimator. Beyond the clearing collimator was the carbon target; this was 8.2 cm long. 4 cm wide and 2.3 cm high. Neutrons traversing the carbon target travelled a further 3 metres to reach a liquid hydrogen target. Protons recoiling at 20° in a downward direction from (np) elastic scattering were detected in a range telescope which included an anticoincidence water Čerenkov counter to reject π's or electrons produced in the hydrogen target. This detecting system was used to measure the beam polarization during the accumulation of data on parity non-conservation.

π^0 mesons were detected through their decay γ-rays in either of two detector systems set in a horizontal plane on either side of the carbon target. The first element of each system was an anticoincidence plastic scintillation counter which rejected events in which charged particles were emitted from the target. The second element was a 5 mm thick lead radiator, 8.2 cm × 10.8 cm —13 cm from the target centre—in which γ-rays materialized; the electron pairs passed through a second scintillator (12.5 cm × 10 cm) connected in fast coincidence with a lead glass Čerenkov detector (22 cm diameter, 20 cm long). A second output of the Čerenkov counter gave a pulse proportional to the total energy of the shower leaving the lead, a function of π^0 energy and the angle of emission of the decay γ-ray relative to the π^0 direction. To ensure the required stability, discussed later, the proportional outputs from the two

Čerenkov detectors were amplified in one common amplifier and passed through the same three discriminators to a sorting network. Here, pulses from the fast coincidence-anticoincidence events were used to determine which of the two Čerenkov counters gave a pulse exceeding a particular discriminator threshold; the sorted pulse was then recorded in one of six scaling units. Each Čerenkov counter with amplifier and discriminator was calibrated with the electron contamination of a beam of π^+ mesons of well-defined momentum. The mean π^+ energy was deduced from a range measurement, and the electron energy calculated from the meson momentum. The three discriminators were set to correspond to shower energies of 60, 90 and 150 MeV.

3. – Possible systematic errors.

In the design of the experiment the limit of accuracy on the measurement of asymmetry due to parity non-conservation in the π^0 production process was set at 0.001; errors other than those due to counting statistics had to be reduced well below this limit. Such errors arise from monitoring and electronic instability, and from parity conserving asymmetries in π^0 production (terms of the form $\boldsymbol{\sigma}_n \cdot \boldsymbol{k}_n \times \boldsymbol{k}_{\pi^0}$).

Let x represent the total number of mesons as produced in the carbon target, ε_1 and ε_2 the over-all efficiencies of the two detecting systems, P_1 the beam polarization and P_2 the parity non-conserving polarization in the π^0 production process. Subscripts R and N refer to data taken consecutively with the solenoid field in the two directions; for « N » neutron spin is taken to be directed to counters system 1, for « R » to counter system 2. During two successive runs, the numbers of counts recorded will be

$$C_{1N} = x_N \varepsilon_{1N}(1 + P_1 P_2)\,, \qquad C_{2N} = x_N \varepsilon_{2N}(1 - P_1 P_2)\,,$$

and

$$C_{1R} = x_R \varepsilon_{1R}(1 - P_1 P_2)\,, \qquad C_{2R} = x_R \varepsilon_{2R}(1 + P_1 P_2)\,.$$

Then

$$f = \frac{C_{1N}\, C_{2R}}{C_{1R} C_{2N}} = \left(\frac{\varepsilon_{1N}}{\varepsilon_{2N}}\right)\left(\frac{\varepsilon_{2R}}{\varepsilon_{1R}}\right) \cdot \left(\frac{1 + P_1 P_2}{1 - P_1 P_2}\right)^2 \sim \left(\frac{\varepsilon_{1N}}{\varepsilon_{2N}}\right)\left(\frac{\varepsilon_{2R}}{\varepsilon_{1R}}\right)(1 + 4 P_1 P_2)\,,$$

for $P_1 P_2$ small, or $(\varepsilon_{1N}/\varepsilon_{2N})(\varepsilon_{2R}/\varepsilon_{1R})(1 + 4 P_1 P_2 \sin q)$ in the case that the solenoid precesses the neutrons through an angle φ different from $\pm 90°$.

Thus with the two detecting systems, one each side of the target, P_2 can be determined without knowing x. In this way there is no need to have a π^0 monitor. This is a great advantage since it would be difficult to make a π^0 monitor independent of neutron polarization to the required accuracy.

Further, the efficiencies of the detectors (ε) are very sensitive to electronic drifts. Fluctuations in the quantity « f » beyond statistics only arise, however, if there are changes in the ratio of the efficiencies of the two detecting systems between « normal » and « reverse » runs. This ratio can be maintained much more constant than can the absolute efficiency of either detector if the same photomultiplier EHT supply, amplifier and discriminator units are used with the two detectors. As a further precaution, the solenoid field was reversed frequently during the measurement to cancel any residual drifts. An important source of error would arise if the stray solenoid field of a few tenths of a gauss at the detectors influenced the two detecting systems differently. There would then be a consis ent difference between $(\varepsilon_{1N}/\varepsilon_{2N})$ and $(\varepsilon_{1R}/\varepsilon_{2R})$, and f would differ from unity even for P_2 equal to zero. With good magnetic shielding and the best orientation of the photomultipliers relative to the field this asymmetry was shown to be $.000\,2 \pm .000\,2$ from measurements with radio-active sources. As a further precaution, two different neutron production targets were used in the cyclotron to produce neutrons at + and $-14°$ to the proton beam. The sign of P_1 is thereby reversed, changing the sign of any effect due to finite P_2 but leaving unchanged the spurious effect of stray field from the solenoid. The values of P_2 from the two targets were statistically indistinguishable, confirming the absence of any instrumental effect.

With parity conserved it is possible to have an asymmetry of π^0 production relative to the neutron spin direction of the form $\boldsymbol{\sigma}_n \cdot \boldsymbol{k}_n \times \boldsymbol{k}_{\pi^0}$. Since the values of the solenoid currents in the two directions are known to be accurately equal, the corresponding angles through which neutron spins are precessed are also equal and opposite. Suppose that, through misalignment, the normal to the line joining the centres of the two detector systems makes a small angle δ (radians) with the spin direction of unprecessed neutrons; then it can be shown that if there is a parity conserving polarization P_3 in π^0 production, such misalignment gives a spurious contribution to P_2, the parity non-conserving polarization, equal to $P_3\delta$. It was possible to make a crude measurement of P_3 by comparing the counting rates with precessed and unprecessed neutron beams and to show that values of δ up to 0.02 would not produce appreciable spurious polarization.

At the neutron producing target, the direction of neutron polarization is along the direction $\boldsymbol{k}_n \times \boldsymbol{k}_p$. Surveys of the magnet pole face, and measurements on current carrying wires in the pole gap, showed that the plane of symmetry of the proton orbits can be expected to be horizontal to within $2 \cdot 10^{-4}$ radians. The collimators axis, and hence $\boldsymbol{k}_n$, lay in a horizontal plane to within the same accuracy. In spite of the effect being geometrically enhanced by the small (14°) neutron production angle, the polarization vector of the neutrons could be calculated to be within $0.8 \cdot 10^{-3}$ radians of the vertical. The direction of polarization having been settled as accurately vertical, it

remained only to set horizontal the line joining the detector centres. With a system of telescope, mirror and prism table, it was easy to ensure that the centres of lead radiators, scintillation and Čerenkov counters lay on a horizontal line perpendicular to the neutron beam within a small fraction of a millimetre As the detectors were 26 cm apart, the value of δ could not have exceeded $2 \cdot 10^{-3}$ radians, well within the required accuracy. As a further check, subsidiary experiments were made with lead radiators of small vertical extent, placed near the top, bottom or centre of the area normally occupied by the full sized radiators; with these it was shown that the geometric centres coincided with the effective centres of the detectors within about 1 mm.

4. – Results and interpretation.

The results are given in Table I. From eighty runs, forty values of « f » were calculated. In the second row is tabulated the « measured asymmetry »

$$P_1 P_2 \sin\varphi = (\bar{f} - 1)/4$$

Table I.

γ-ray threshold energy	60 MeV	90 MeV	120 MeV
Measured asymmetries	-0.0003 ± 0.0010	$+0.0003 \pm 0.0013$	-0.0038 ± 0.0023
Observed errors	± 0.0009	± 0.0013	± 0.0022
Parity non-conserving polarization	-0.005 ± 0.020	$+0.005 \pm 0.028$	-0.079 ± 0.050

for each of the three discriminator bias settings (60, 90 and 150 MeV). The errors attached to the asymmetries are calculated from the total number of counts recorded. The errors in the third row are those calculated from the distributions of the forty measured values of f for each individual bias. The near identity of these two sets of errors indicates that effects of instability in counter sensitivity have been successfully eliminated. A χ-squared test indicates that the probabilities of obtaining a worse correspondence of the two sets of errors are 38%, 53% and 40% for the three γ-ray threshold energies. $P_1 \sin\varphi$ was calculated from the asymmetry in the counting rate of protons recoiling at 20° from the liquid hydrogen target into the range telescope described earlier. The neutrons which give detectable proton recoils have energies between 380 and 540 MeV and angles of precession between 49° and 39°.

The measurements of DZHELEPOV *et al.* [10] at 635 MeV, SIEGEL *et al.* [11] at 350 MeV, and CHAMBERLAIN *et al.* [12] at 315 MeV show a constant value of polarization in the n-p scattering process for forward recoiling protons over this wide range of incident neutron energies. Combining this data with the measured asymmetry of recoil proton production gives a value for the beam polarization P_1 of $(10.3 \pm 1.6)\%$. As the cross-section for the production of π^0's in carbon by protons (and presumably also by neutrons) rises by a factor of about six as the energy of the incident particle increases from 350 MeV to 550 MeV, (PROKOSHKIN [13]), and the neutron spectrum is peaked between 400 and 500 MeV (DZHELEPOV *et al* [11,15]), it is likely that these values of P_1 and precession angle are also appropriate for the energy band of neutrons responsible for the production of the observed π^0 mesons.

A series of corrections must be applied before a final value of P_2 is extracted from the asymmetry measurements. The discriminator circuits of the linear system were not capable of handling fast rising pulses; consequently long ($\sim 5\ \mu$s) resolving times were used in the sorting network. Consequently there were some 10% of random coincidences between fast coincidences in one detector, in which the linear Čerenkov pulse was to small to actuate a discriminator by itself, and larger linear pulses from the other Čerenkov detector. It was checked that there could be no significant dependence of this chance rate on solenoid field direction, so that its only effect was to dilute the measured value of P_2 by 10%; no spurious asymmetry could be introduced.

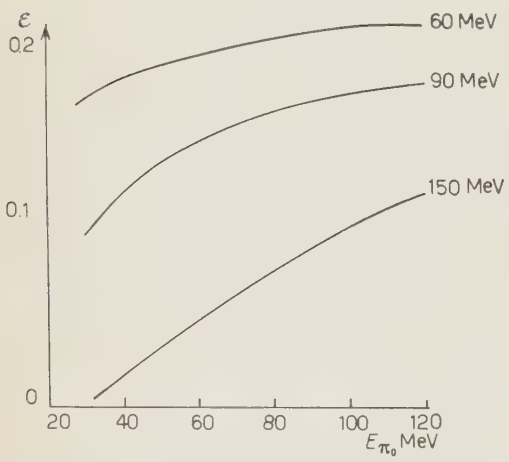

Fig. 3. – Detector efficiency *versus* π^0 energy at discriminator settings of 60, 90 and 150 MeV.

Further corrections arise from the finite target and detector sizes, and the mechanics of the

[10] V. P. DZHELEPOV, B. M. GOLOVIN, YU. V. KATYSCHEV, A. D. KONIN, S. V. MEDVED, V. S. NADEZHDIN and V. J. SATAROV: *Annual International Conference on High Energy Physics at CERN* (1958), p. 303.

[11] R. T. SIEGEL, A. J. HARTZLER and W. A. LOVE: *Phys. Rev.*, **101**, 838 (1956).

[12] O. CHAMBERLAIN, E. SEGRÈ, R. D. TRIPP, C. WIEGAND and T. YPSILANTIS: *Phys. Rev.*, **102**, 1659 (1956).

[13] IU. D. PROKOSHKIN: *CERN Symposium* (1956), p. 385.

[14] V. P. DZHELEPOV and Y. M. KAZARINOV: *Dokl. Akad. Nauk.*, **99**, 943 (1954).

[15] V. P. DZHELEPOV, B. M. GOLOVIN, IU. M. KAZARINOV and N. N. SEMENOV: *CERN Symposium* (1956), p. 115.

$\pi^0 \rightarrow 2\gamma$ decay process in which the spread in angle of the γ-rays relative to the π^0 is a function of the energies of π^0 meson and γ-ray. Detailed calculations of these effects were made with the «Mercury» digital computer at CERN. The main results are shown in Figs. 3 and 4. In Fig. 3 is plotted, as a function of π^0 energy, the absolute overall efficiency of the detector at the 60, 90 and 150 MeV bias settings for mono-energetic isotropic π^0's. Fig. 4 shows, again as a function of mono-energetic π^0 energy and for the same three discriminator settings, the mean value of the cosine of the angle χ between the neutron polarization direction and the emission direction of a π^0 whose decay γ-ray is detected. For the assumed 45° precession, the value of cos χ would be 0.707 for point source, point detector and γ emission exactly along the π^0 direction. A preliminary calculation showed that the finite geometry could be expected to give a reduction of cos χ to 0.66; the remainder of the reduction is due to the spread of γ emission about the π^0 direction. To apply accurately the results shown in Figs. 3 and 4 to the interpretation of this experiment requires that the π^0 spectrum be known, which it is not. π^+ mesons emitted at 90° from bombardment of carbon with protons of energy 660 MeV are found [16] to have a flat spectrum extending up to ~ 120 MeV; this is the energy limit expected for $p+p \rightarrow \pi^+ + d$ under these conditions. From considerations of charge independence the same energy spectrum may be expected in π^0 production by neutrons on carbon and the mean effective π^0 energy will be about 60 MeV. The corresponding values of cos χ have been used, together with the measured value of P_2, to calculate the corrected values of P_2 shown in the fourth row of Table I. A negative sign of P_2 implies preferential emission against the direction of neutron spin. The uncertainties in the factors relating asymmetry and P_2 and possible effects from systematic errors make no appreciable contribution to the uncertainty on P_2.

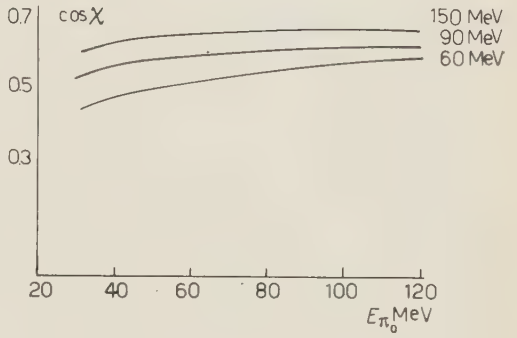

Fig. 4. – Cos χ *versus* π^0 energy at discriminator settings of 60, 90 and 150 MeV. (Cos χ is the mean value of the cosine of the angle between detected π^0-mesons and the neutron polarization vector).

[16] V. M. Sidorov: *CERN Symposium* (1956), p. 366.

5. – Discussion.

The results of Table I show no evidence for a finite parity non-conserving interaction, with the possible exception of the highest bias results where the chance of the departure being statistical rather than real is 10%. The only comparable result, that of ROBERTS, gave a value of P_2 of 0.016 ± 0.042 for production of 40 MeV π^+ mesons by protons of 209 MeV incident on carbon and aluminium. The experiment of JONES *et al.* on longitudinal polarization in neutron production by 360 MeV protons gives a value for P_2 in this case $(3.2 \pm 17) \cdot 10^{-4}$.

FUBINI and WALECKA [17] have considered the consequences of parity non-conservation in strange particle production in low energy π-nucleon interactions and have shown that the effects are likely to be small. In a companion paper [18], LURIÉ and POWER apply their results to the production of π^0 mesons by polarized neutrons. They find an upper bound to P_2 (corresponding to maximum parity violation in K-hyperon interactions) of $0.003 \to 0.01$, depending on the choice of phase shifts, for high energy mesons; these predicted values would be reduced for the meson energies involved in this experiment. Direct evidence that parity is conserved in strange particle production is available from the experiments of CRAWFORD *et al.* [19], LANDER *et al.* [20] and LEITNER *et al.* [21], where the longitudinal polarization of the product particle was found to be zero with a standard deviation of about 20%. To achieve comparable significance in π^0 production experiments would therefore require a determination of P_2 to better than 0.2 of the prediction of LURIÉ and POWER, *i.e.* $6 \cdot 10^{-4} \to 2 \cdot 10^{-3}$. This has not been achieved in the present work. In that the accuracy attained here has been limited entirely by statistics rather than systematic errors, a continuation of similar work with neutron beams of higher intensity, and especially higher polarization, could give results of interest for their own sake, and for the light they could throw on the strange particle processes where the accuracy of experiments is likely to be somewhat limited for a considerable time.

* * *

The authors wish to thank Professors BERNARDINI and LEDERMAN for suggesting the investigation and for many fruitful discussions. Čerenkov counters

(17) S. FUBINI and D. WALECKA: *Phys. Rev.*, **116**, 194 (1959).

(18) D. LURIÉ and E. A. POWER: *Nuovo Cimento*, **14**, 1145 (1959).

(19) F. S. CRAWFORD, M. CRESTI, M. L. GOOD, F. T. SOLMITZ and M. L. STEVENSON: *Phys. Rev. Lett.*, **1**, 209 (1958).

(20) R. L. LANDER, W. M. POWELL and H. S. WHITE: *Phys. Rev. Lett.*, **3**, 236 (1959).

(21) J. LEITNER, P. NORDIN, A. H. ROSENFELD, F. T. SOLMITZ and R. D. TRIPP: *Phys. Rev. Lett.*, **3**, 238 (1959).

were made available through the kindness of Drs. Fidecaro, Merrison and Zavattini and for the hydrogen target and help in taking readings we are indebted to Mr. G. Heymann. We also acknowledge the facilities and hospitality offered by CERN and in particular the services given by the operating crew of the synchrocyclotron.

RIASSUNTO (*)

Un bersaglio di carbonio è stato bombardato con un fascio di neutroni polarizzati trasversalmente aventi energie sino a 540 MeV. I mesoni π^0 emessi normalmente rispetto al fascio di neutroni furono rivelati a mezzo dei loro raggi γ di decadimento con contatori di Čerenkov sensibili all'energia. Si è ricercata una asimmetria antero-posteriore nella produzione di π^0 rispetto al vettore di polarizzazione del fascio di neutroni, che avrebbe indicato un termine di violazione della parità della forma $\boldsymbol{\sigma}_n \cdot \boldsymbol{k}_{\pi^0}$. Si è usato un campo magnetico longitudinale reversibile per ottenere la precessione della polarizzazione del fascio di neutroni alla scopo di misurare le asimmetrie con errori sistematici minimi. L'esperimento era capace di segnalare asimmetrie di $1 : 10^3$. Si sono trovati valori di P, polarizzazione che provoca la violazione della parità nella reazione, fra -0.005 ± 0.020 e -0.079 ± 0.050 per mesoni π^0 di varie energie.

(*) *Traduzione a cura della Redazione.*

Simple Models for Associated Production in Proton-Proton Collisions.

E. Ferrari

Istituto di Fisica dell'Università - Roma
Istituto Nazionale di Fisica Nucleare - Sezione di Roma

(ricevuto il 9 Dicembre 1959)

Summary. — The process $p+p \to \Lambda^0+K^++p$ is investigated by means of two simple models in which only the contribution of poles due to the exchange of an intermediate π^0-meson or K^+-meson respectively is taken into account. The total cross section is then calculated in terms of the total cross-sections for simpler processes. Numerical values are given for an energy of 3 GeV of the incident proton in the l.s.

The present experimental information about the process

$$p + p \to K^+ + \Lambda^0 + p \tag{1}$$

is still rather poor (1). Some values with large errors have been given by various authors, and are not in very good agreement between themselves: they give an order of magnitude of 0.1 mb for the total cross-section for a kinetic energy $T = 3$ GeV of the incident proton in the lab. system (2). In this note we will

(1) See P. Baumel, G. Harris, J. Orear and S. Taylor: *Phys. Rev.*, **108**, 1322. (1957); D. Berley and G. B. Collins: *Phys. Rev.*, **112**, 614 (1958); J. Hornbostel, E. O. Salant and G. T. Zorn: *Phys. Rev.*, **112**, 1311 (1958). These papers contain reference to earlier work.

(2) Berley and Collins' value is $\sigma_{tot} = (0.04 \pm 0.06)$ mb (including also Σ^0 and Σ^+ production); Baumel and coll. have measured the differential cross-section at a certain energy and angle of the final K^-, and derived the total cross-section by multiplying by statistical factors (assuming a constant interaction matrix element). They get $\sigma_{tot} = 0.21$ mb.

show that this order of magnitude can be obtained by two simplified models, which relate process (1) to simpler processes. The procedure of calculation is similar to that outlined in a preceding letter ([3]).

We assume in our simplified models that in the matrix element for process (1) only the contribution of poles associated to one intermediate boson is relevant. If we consider the pole due to an intermediate π^0-meson, we describe the whole process by a graph of this type

(2)

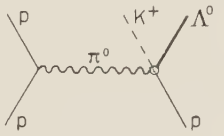

If we consider the pole due to an intermediate (pseudoscalar) K^+-meson, we describe the process by a graph of this type

(3)

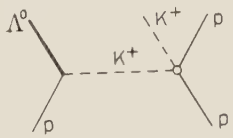

In both cases all other contributions will be neglected.

In order to calculate the matrix element associated to graphs of the type (2) or (3), we will need the physical amplitudes for the « partial » processes involving the particle exchanged. For physical values of the momenta in process (1), however, the intermediate particle is no longer on the mass shell, but we still assume that the matrix element is obtained also in this case by analytic continuation from its value when the intermediate particle is on the mass shell, *i.e.* from a non-physical region for process (1). This is the well-known conjecture first introduced by CHEW and LOW ([4]), who give a prescription for determining the residue of the pole in a graph of the type (2) or (3) from the physical amplitudes for the « partial » processes.

In this way process (1) is related to the following reactions:

a) in the case of graph (2) to

(4) $$\pi^0 + p \to K^+ + \Lambda^0$$

([3]) E. FERRARI: *Nuovo Cimento*, **13**, 1285 (1959).

([4]) G. F. CHEW and F. E. LOW: *Phys. Rev.*, **113**, 1640 (1959).

and then, by simple isotopic spin considerations, to

$$\pi^- + p \to K^0 + \Lambda^0 ; \tag{5}$$

b) in the case of graph (3) to

$$K^+ + p \to K^+ + p . \tag{6}$$

If we follow Chew's normalization and define [5]

$$d\sigma = \frac{2\pi}{kW} |\langle T \rangle|^2 \delta(p_1 + k_1 - p_2 - k_2 - q_2)\, \delta(p_2^2 + \Lambda^2)\, \delta(q_2^2 + m^2) \cdot \cdot \delta(k_2^2 + M^2)\, d^4p_2\, d^4k_2\, d^4q_2 , \tag{7}$$

the total cross-section will be obtained by inserting in (7) the contributions either of graph (2) or of graph (3), and by integrating over the momenta of the final particles. The models lend themselves to give much more information (*e.g.* differential cross-sections with respect to the energy of the final Λ^0 or proton, which can be obtained as differential cross-sections with respect to the variables $s^2 = (p_2 - k_1)^2$ or $\Lambda^2 = (k_2 - k_1)^2$). We think, however, that these calculations will be worth being worked out only when a larger amount of experimental information will enable us to check the reliability of the models presented.

We note that in both cases (2) and (3) two graphs give a contribution: they are obtained one from the other by exchanging the momenta of the initial protons ($p_1 \leftrightarrow k_1$). The square of the matrix element in (7) will therefore consist of three parts:

a) two « cross-section terms » which, upon complete integration, give exactly the same contribution σ_1 to the cross-section for process (1):

$$\sigma_1 = \frac{1}{8\pi} \left(\frac{G^2}{4\pi} \right) \frac{1}{(k) W^2} \int_{u_{\min}}^{u_{\max}} 2\varkappa u^2 \sigma_0(u) I(u)\, du , \tag{8}$$

where $\sigma_0(u)$ is the total cross-section for process (4) or (6) at total c.m.s. energy u, and $G^2/4\pi$ is the renormalized coupling constant of the vertex ($pp\pi^0$) or ($p\Lambda^0K^+$) respectively. K and $I(u)$ are kinematical factors (not de-

[5] We denote by p_1 and k_1 the 4-momenta of the incident and target protons, by k_2, p_2 and q_2 the 4-momenta of the final proton, Λ^0 and K^+ respectively. $W^2 = -(p_1 + k_1)^2 = 4M^2(1 + (T/2M))$ is the square of the total c.m.s. energy, and $k = ((W^2/4) - M^2)^{\frac{1}{2}}$ is the c.m.s. momentum of the initial protons. M = nucleon mass, $m = K^+$-mass, $\Lambda = \Lambda^0$-mass, μ = pion mass.

pending on the «secondary» interaction (4) or (6)) which will be explicited at the end of this paper;

b) one «interference term» which depends strongly on the phase-shifts of the «secondary» interaction (4) or (6). If more than one phase-shift is present, the calculation of this term becomes very complicated. In the case of only one phase-shift present, the calculation is much simplified and the contribution σ_{int} can be brought to a form very close to (8), namely

$$\sigma_{int} = -\frac{1}{8\pi}\left(\frac{G^2}{4\pi}\right)\frac{1}{(kW)^2}\int_{u_{min}}^{u_{max}} 2\pi u^2 \sigma_0(u) I_{int}(u)\,du\,. \tag{9}$$

The shape, the magnitude and the sign of the function $I_{int}(u)$, however, depend strongly on the type of phase-shift chosen. We have carried out the calculation assuming that only the *s*-wave phase-shift is relevant. This assumption is verified experimentally for process (6), since the K^--p elastic cross-section is isotropic up to high energies, with a value practically constant (on the average ~ 16 mb) (6). The assumption is not verified experimentally for process (5), since we know that at rather high energies the Λ^0 is emitted preferentially backwards in the c.m. system: the experimental data can be fitted in terms of *s* and *p* waves, with amplitudes of the same order of magnitude (7). However, if only one phase-shift has to be retained for an order of magnitude calculation, it is more reasonable to keep the *s* phase-shift when we are dealing with an interval of energies which includes the whole low-energy region (8). For $T = 3$ GeV ($w = 3.224\,M$) we get the following numerical results for the total cross-section for process (1):

	Contribution of term (8) (σ_1)	Complete contribution ($2\sigma_1 + \sigma_{int}$)
Model (2)	0.040 mb	0.052 mb
Model (3)	0.10 mb	0.115 mb

(6) O. R. Price, D. H. Stork and H. K. Ticho: *Phys. Rev. Lett.*, **1**, 212 (1958). See also the *Kiev Conf. Report on the Interaction of Strange Particles* by L. W. Alvarez.

(7) See the *Reports of the International Conference on High Energy Physics at CERN* (1958), p. 323.

(8) We have also carried out the calculation of σ_{int} for the case (2) if only p^3-waves are supposed to be present. It turns out that the contribution is small, so that practically $\sigma \sim 2\sigma_1$. We expect that in any case the magnitude of σ_{int} does not exceed that of σ_1.

The values of the cross-section for process (5) as a function of the energy have been taken from the 1958 CERN Conference data [9]. These values are affected by errors of the order 10%; this error affects our results too.

We see that both models give the correct order of magnitude for the cross-section considered. At present it is not possible to try an improvement of the model by considering graphs of the type (2) and (3) together, since the calculation of the interference terms between graphs with a different particle exchanged would require the relative signs of the phase-shifts of processes (4) and (6), as well as of the coupling constants of the vertices, which are not given by the experiment. It is hoped that a larger number of experimental data for process (1) as well as for processes (5) and (6) could give further support to the idea that one of the simple models proposed describes the experimental situation with a good approximation.

* * *

We are indebted to Prof. R. Gatto for his suggestions and for his interest in this work.

Notation and Formulae.

$$I(u) = -\log\frac{1+\alpha}{1-\alpha} - \frac{2A^2}{\Gamma}\frac{\alpha}{1-\alpha^2},$$

$$I_{\text{int}}(u) = \frac{1}{2u(E+M)}\left\{4kk' + \frac{1}{\Gamma}\left[2M(-w'W + m_0M)(2M + m_0 + u) + \right.\right.$$
$$\left.\left. + (W^2 - 2M^2)(2M - m_0 + u)m_0 + b^2(2\Gamma + b^2)\right]\log\frac{1+\alpha}{1-\alpha}\right\}.$$

For model (2):

$$u^2 = -(p_2 + q_2)^2; \qquad \varkappa = \frac{1}{2u}\left(u^4 - 2(M^2 + \mu^2)u^2 + (M^2 - \mu^2)^2\right)^{\frac{1}{2}};$$
$$u_{\min} = m + \Lambda; \qquad u_{\max} = W - M;$$

$$A^2 = \mu^2; \quad m_0 = M; \quad b^2 = (2M^2 - \mu^2); \quad E = (\varkappa^2 + M^2)^{\frac{1}{2}}; \quad w' = \frac{1}{2W}(W^2 + M^2 - u^2);$$

$$k' = (w'^2 - M^2)^{\frac{1}{2}}; \qquad \Gamma = w'W - 2M^2 + \mu^2; \qquad \alpha = \frac{2kk'}{\Gamma}.$$

[9] See the above-mentioned Report, p. 148.

For mode):

$$u^2 = -(k_2 + q_2)^2; \qquad \varkappa = \frac{1}{2u}\left(u^4 - 2(M^2 + m^2)u^2 + (M^2 - m^2)^2\right)^{\frac{1}{2}};$$

$$u_{\min} = m + M; \qquad u_{\max} = W - \Lambda;$$

$$A^2 = m^2 - (\Lambda - M)^2; \qquad m_0 = \Lambda; \qquad b^2 = (M^2 + \Lambda^2 - m^2);$$

$$E = (\varkappa^2 + M^2)^{\frac{1}{2}}; \qquad w' = \frac{1}{2W}(W^2 + \Lambda^2 - u^2);$$

$$k' = (w'^2 - \Lambda^2)^{\frac{1}{2}}; \qquad \Gamma = w'W - \Lambda^2 - M^2 + m^2; \qquad \alpha = \frac{2kk'}{\Gamma}.$$

Integration over u has has been performed graphycally.

RIASSUNTO

Il processo $p+p \to \Lambda^0 + K^+ + p$ è studiato per mezzo di due semplici modelli in cui si tiene conto soltanto del contributo dei poli associati allo scambio di un mesone π^0 o K^- rispettivamente. È calcolata quindi la sezione d'urto totale, che risulta legata alla sezione d'urto totale per processi più semplici. Si danno valori numerici per una energia di 3 GeV nel s.l. del protone incidente.

IL NUOVO CIMENTO Vol. XV, N. 4 16 Febbraio 1960

Some Rigorous Analytic Properties of Transition Amplitudes (*).

S. MANDELSTAM

Department of Physics, University of California - Berkeley, Cal.

(ricevuto il 21 Dicembre 1959)

Summary. — The causality and mass-spectral conditions are used to derive analytic properties of two-particle transition amplitudes as functions of energy and momentum transfer. While the complete double-dispersion representation cannot be proved from these postulates alone, it is shown that, within a certain domain in the space of two complex variables, the only singularities are the expected poles and cuts along the real axis. This domain surrounds the low-energy physical region. The proof is restricted to the scattering of the lightest particles in the theory. As long as no attempt is made to find the largest possible domain, the calculations are not very difficult. The domain of analyticity can then be extended by the unitarity condition. The magnitude of the extension is not very large, but the new domain differs from the old in including part of the region in which the two-dimensional spectral functions are non-zero. We only use the unitarity condition below the threshold for inelastic processes; if such processes could also be treated and the unitarity condition used at higher energies, it seems possible that the domain could be extended arbitrarily far. In the present results, the boundary of the domain of analyticity is sufficiently far from the low energy region to justify the analytic properties assumed in applications of the double-dispersion representation. Other results that can be proved are that partial-wave amplitudes are analytic functions of the energy in a certain region, that the determination of coupling constants by extrapolation in the angle is valid if the energy is not too high, and that ordinary dispersion relations are true over a slightly larger range of momentum transfer than had previously been established.

(*) This research was supported by the United States Air Force under Contract no. AF 49(638)-327 monitored by the AF Office of Scientific Research of the Air Research and Development Command.

1. – Introduction.

The purpose of this paper is to begin a study of the analytic properties of transition amplitudes that follow from the general principles of quantum field theory, such as local commutativity—or causality—and unitarity. At present there exist proofs for the analytic properties as a function of one variable while the other is held fixed. If the momentum transfer is kept constant, the analytic properties as a function of the energy are given by the usual dispersion relations, which have been proved as long as the momentum transfer is sufficiently small ([1-3]). LEHMANN has also proved that the scattering amplitude has analytic properties as a function of the momentum transfer when the energy is held fixed ([3]).

In order to make full use of the power provided by the analytic properties, however, it is necessary to treat the transition amplitude as a function of two complex variables, the square of the energy and the square of the momentum transfer, and to consider analyticity as a function of both variables. On the basis of consistency requirements and perturbation theory, the author has postulated a representation, the « double dispersion representation », which exhibits the analytic properties as a function of the two variables ([4]). Thus far, no non-perturbation proof has been given that the transition amplitude has these analytic properties. In fact, the analytic properties of transition amplitudes as a function of two variables have not been studied at all on a rigorous basis.

In principle, the requirements of local commutativity and mass spectra enable one to show that any Green's function of quantum field theory is, in momentum space, an analytic function of the squares of the momenta within a certain domain. This domain has been explicitly computed by KÄLLÉN and WIGHTMAN ([5]) for the three-point function without any mass-spectral conditions. If the corresponding region could be computed for the four-point function with spectral conditions, we would have the solution to our problem. Such a calculation appears at the moment to be extremely complicated and is not attempted here. If, however, we do not insist on finding the *complete* region in which analyticity can be proved from the general principles, the problem becomes much simpler. In the present paper we shall not make any

([1]) N. N. BOGOLIUBOV, B. V. MEDVEDEV and M. K. POLIVANOV: *Fort. d. Phys.*, **6**, 159 (1959). See N. N. BOGOLIUBOV and D. V. SHIRKOV: *Introduction to the Theory of Quantized Fields* (New York, 1959), chap. IX.

([2]) H. J. BREMERMANN, R. OEHME and J. G. TAYLOR: *Phys. Rev.*, **109**, 2178 (1958).

([3]) H. LEHMANN: *Nuovo Cimento*, **10**, 579 (1958).

([4]) S. MANDELSTAM: *Phys. Rev.* **115**, 1741 (1959).

([5]) G. KÄLLÉN and A. WIGHTMAN: *Mat. Fys. Skr. Dan. Vid. Selsk.*, **1**, no. 6 (1958).

new application of the causality conditions. Starting only from the knowledge that the transition amplitude satisfies dispersion relations and that it has the analytic properties derived by LEHMANN ([3]), we shall be able to establish that it is an analytic function of its two variables in a certain domain. We have here a further example of a phenomenon already used several times in this branch of physics ([1,2,5]) that analytic properties of a function of several complex variables can be derived solely from the knowledge that the function possesses certain other analytic properties. There is no reason to suppose that the domain of analyticity we reach by such a procedure is the complete domain which follows from causality, and we shall not even attempt to find the maximum domain which could theoretically be obtained by our method.

Our results will be restricted to the scattering of the lightest particles in the theory. A possible method of overcoming this limitation will be surveyed in the final section, but, at present, we cannot deal with other cases, as we have to know that the dispersion relations for at least two pairs of the three reactions are valid. The only practical process which can now be treated rigorously is therefore pion-pion scattering, but, with a view to later more general applications, we shall allow a three-particle vertex. We shall not assume that the particles are identical, though their masses will be assumed equal.

We thus obtain a domain in the space of the two complex variables which surrounds the low-energy physical region and within which the only singularities are the expected cuts and poles on the real axis. The area in which the two-dimensional spectral functions would be non-zero if the double dispersion relation were assumed to be true lies completely outside our domain and, at the moment, these functions do not play any part in describing the analytic properties.

Though we have by no means obtained the complete domain of analyticity which follows from the causality requirements, it is unlikely that it will be anything like as large as has been postulated. In order to extend the domain, therefore, we have to make use of the unitarity requirements, which, up till now, have not been employed in proving analytic properties. One of the greatest advantages of considering analyticity in two variables is that *the domain of analyticity can be extended by the unitarity equations in a particularly neat and simple way* ([6]). Though it had always been realized that the unitarity equations might be used in principle to prove analytic properties, it was thought that the infinite number of possible intermediate states would make them essen-

([6]) The consequence of the unitarity condition that, if the scattering amplitude is analytic in the momentum transfer in a certain region, its absorptive part is analytic in a larger region, was already known. However, all attempts to use it in connection with ordinary dispersion relations flounder on the rock that the Lehmann ellipses close down around the physical region at high energies.

tially unmanageable in a rigorous treatment. Fortunately the situation turns out to be much more favourable. By restricting oneself to a region where all but a certain number of processes do not enter the unitarity condition, one can obtain, rigorously, an extension of the domain of analyticity.

In this paper we shall apply the unitarity condition only below the threshold for all inelastic processes. Though the extension of the domain of analyticity thereby obtained is in fact very small, we feel that it is most significant that an extension can be made using the unitarity condition. The new domain of analyticity is sufficiently large to include some of the region in which the two-dimension spectral functions are non-zero, and it is found that these spectral functions must now be included in describing our analytic properties. The calculation of the two-dimensional spectral functions in this exact treatment is in fact very similar to what it was in the earlier perturbation treatment (7).

It should be emphasized that the only factor limiting the size of the domain of analyticity is the inapplicability (at present) of the unitarity condition above the threshold for the inelastic processes. This strongly suggests that, if we were also to examine the analytic properties of the transition amplitudes for inelastic processes and include them in our unitarity condition, we could enlarge the domain of analyticity still further, and that, by taking more and more processes into account, the domain could be extended arbitrarily far. There would of course be the singularities given by the double dispersion representation, and perhaps other singularities of a similar type in the complex plane. Unitarity thus appears to be a very powerful tool in establishing analytic properties, but we are not yet able to explore its possibilities when inelastic processes must be included.

In the application of the double dispersion representation to calculations in field theory (8), one has in practice to neglect contributions to the transition amplitude from singularities above a certain threshold, and no attempt has yet been made to include contributions from any inelastic processes. The argument given for neglecting the higher singularities is that they are fairly far away from the region of interest, and will therefore not give too large a contribution to the transition amplitude. Now the boundary of the domain of analyticity established by us is about as far from the low-energy physical region as are the singularities we neglect; this is not a coincidence, since it is precisely below these singularities that we can use the unitarity condition. According to the approximation scheme, we can therefore ignore any singularities which might occur on the boundary of the domain of analyticity. In neglecting the contributions of the inelastic processes, it is usually argued that

(7) S. MANDELSTAM: *Phys. Rev.* **115**, 1752 (1959).
(8) G. F. CHEW and S. MANDELSTAM: U.C.R.L. report 8728.

such contributions are small until we are well above threshold. With equal force we could argue that the unitarity condition in the elastic approximation is very nearly correct until well above threshold, so that, if we used it in the intermediate region to extend still further our domain of analyticity, we would not go far wrong. Thus the possible singularities on the boundary of our domain are still at a distance from the low-energy region comparable to that of the singularities we have to neglect. It can therefore be maintained that the calculations based on the double-dispersion representation are on a firm footing with regard to the assumed analytic properties. The present work, needless to say, has no bearing on the fundamental assumption of the approximations that distant singularities do not contribute very much to the scattering amplitude. We may also repeat at this point that, at the moment, our results only apply to the scattering of the lightest particles in the theory.

As a consequence of analytic properties established here, it can be shown that the transition amplitude for a fixed angular-momentum state is an analytic function of the square of the energy within a certain region, except for the usual cuts. The distance of the boundary of this region from the low-energy region is of the same order of magnitude as the distance of the threshold for inelastic processes. Another result is that it is possible to justify the determination of coupling constants by extrapolation to poles at imaginary angles, as suggested by CHEW [9], if there is a three-particle vertex associated with the lightest particles in the theory. The scattering amplitude is then an analytic function of the momentum transfer in a region which includes the pole as long as the centre-of-mass energy is less than $\sqrt{35}\mu$, where μ is the mass of the particle. Also, the range of values of the momentum transfer for which ordinary dispersion relations can be proved may be slightly extended. The previous upper limit on $-t$, t being the square of the momentum transfer, was $8\mu^2$; the limit is raised to $9\mu^2$ in the present paper. We can only obtain an increase after using the unitarity condition.

2. – Analytic properties of the transition amplitude.

2·1. *Kinematics and preliminary results.* – In this Section we shall discuss the analyticity properties of the transition amplitude which can be obtained rigorously from the causality and mass-spectral conditions without unitarity, leaving the proof to the next section. We use the same kinematic notation as in previous papers: the four-momenta of the incoming particles A and B are denoted by p_1 and p_2, and those of the outgoing particles C and D by

[9] G. F. CHEW: *Phys. Rev.*, **112**, 1380 (1958).

$-p_3$ and $-p_4$. We then define the three invariants (positive if time-like)

$$s = (p_1 + p_2)^2 , \tag{2.1a}$$

$$t = (p_1 + p_3)^2 , \tag{2.1b}$$

$$u = (p_1 + p_4)^2 . \tag{2.1c}$$

Only two of these variables are independent, since they are related by the equation

$$s + t + u = 4\mu^2 , \tag{2.2}$$

where μ is the mass of the particle, s is the square of the energy, and t and u the squares of the momentum transfer, for the reaction A+B→C+D (reaction I). We would also represent the reaction II (A+D→B+C) and III (A−C→B+D) by the same analytic function, in which cases u or t would be the energies. The square of the centre of mass momentum is given by the formula

$$q^2 = \tfrac{1}{4}s - \mu^2 \tag{2.3}$$

and the cosine z of the angle of scattering by the formula

$$z = (t/2q^2) + 1 . \tag{2.4}$$

We begin by recapitulating the analytic properties of the transition amplitude as a function of momentum transfer — or, equivalently, of the cosine of the angle. LEHMANN [3] has shown that the transition amplitude is an analytic function of z in an ellipse with foci ± 1 and semi-major axis z_0, where

$$z_0 = \left[1 + \frac{(m_1^2 - \mu^2)^2}{sq^2}\right]^{\frac{1}{2}} , \tag{2.5}$$

m_1 in this formula is the mass of the lightest state (except the one-particle state itself) whose quantum numbers are the same as those of the one-particle state. If we allow a three-particle vertex, m_1 will be equal to 2μ, so that (2.5) becomes

$$z_0 = \left[1 + \frac{9\mu^2}{sq^2}\right]^{\frac{1}{2}} . \tag{2.6}$$

LEHMANN also showed that the absorptive part of the scattering amplitude associated with the reaction I is an analytic function of z in a larger ellipse;

the foci are ± 1 as before, but the semi-major axis is now

$$2z_0^2 - 1 = 1 + \frac{2(m_1^2 - \mu^2)^2}{sq^2}, \tag{2.7}$$

or, if $m_1 = 2\mu$,

$$2z_0^2 - 1 = 1 + \frac{18\mu^2}{sq^2}. \tag{2.8}$$

Expressed in terms of the variable t instead of z, the domain of analyticity of the imaginary part is an ellipse with foci at the points 0 and $4q^2$, and semi-major axis given by

$$t_0 = 2q^2 + \frac{4(m_1^2 - \mu^2)^2}{s}, \tag{2.9}$$

or, if $m_1 = 2\mu$,

$$t_0 = 2q^2 + \frac{36\mu^4}{s}. \tag{2.10}$$

The absorptive part of the scattering amplitude associated with the other two reactions are analytic functions of the momentum transfer for these reactions within corresponding ellipses. We shall refer to these ellipses as the ellipses associated with the reactions I, II and III, and, if no reaction is mentioned, it will be implied that the ellipse associated with the reaction I is being referred to.

The small Lehmann ellipse never includes the poles, at t or $u = \mu^2$, and the branch points, at t or $u = 4\mu^2$, which we expect the scattering amplitude to have as a function of t. It touches the pole at the points $s = 6\mu^2$, $t = \mu^2$ and $s = 6\mu^2$, $u = \mu^2$. The large Lehmann ellipse correspondingly never includes the regions where the two-dimensional spectral functions of the double-dispersion relation are non-zero, but touches them at the points $s = 6\mu^2$, $t = 6\mu^2$ and $s = 6\mu^2$, $u = 6\mu^2$.

2·2. *Proposed domain of analyticity.* – We now proceed to study the analytic properties of the transition amplitude as a function of two variables, and we shall try to find a domain within which the only singularities are along the real axis. We shall only consider domains of the form

$$|f(s, t)| < a, \tag{2.11}$$

where $f(s, t)$ is an analytic function of s and t, an a is a positive real number. The boundary of the domain is given by the equation $|f(s, t)| = a$, which is

the equation of *analytic hypersurface*. The maximum domain of analyticity which could in principle be obtained from the requirements of local commutativity and the mass-spectral conditions is not bounded by an analytic hypersurface [10], so that it is a restriction to consider only regions of this form. However, as we have explained in the introduction, we are not attempting to find the maximum domain of analyticity.

Within the domain given by (2.11), the function will, of course, have cuts when either s, t or u is real and greater than $4\mu^2$, and the discontinuity across the cuts will be given by the absorptive parts A_1, A_2 and A_3. Now we will clearly be in a much better position to prove analyticity within the domain if we know beforehand that these discontinuities are analytic functions of the momentum transfer throughout the domain. We therefore impose on the region (2.11) the restriction that all points within this region for which s, u and t are real and greater than $4\mu^2$, lie respectively in the large Lehmann ellipses associated with the reactions I, II and III. We also impose the restriction, the reason for which will appear later, that for at least one real value, greater than $4\mu^2$, of s, t or u, the region must lie within the small Lehmann ellipse. These requirements certainly do not determine the function f, but they do restrict its form.

The function f could simply be taken to be st, but a choice which will turn out in Section 4 to be better is stu, so that (2.11) becomes

$$|stu| < a \,. \tag{2.12}$$

We shall concentrate entirely on domains of this form, and shall begin by investigating the region in the complex t-plane when s is real. We shall then be able to determine the maximum value a can have in order that this region lie entirely within the large Lehmann ellipse when s is greater than $4\mu^2$. Expressing u in terms of s and t by (2.2) and solving the equation

$$-stu = \alpha \,. \tag{2.13}$$

for t, we find that

$$t = -\frac{s-4\mu^2}{2} \pm \sqrt{\left\{\frac{(s-4\mu^2)^2}{4} - \frac{\alpha}{s}\right\}} \,. \tag{2.14}$$

Our region consists of the values of t obtained from (2.14) with $|\alpha| < a$. If s is greater than that root of the equation

$$s(s-4\mu^2)^2 - 4a = 0 \tag{2.15}$$

[10] G. Källén and J. S. Toll: unpublished.

which is real and greater than $4\mu^2$, the region breaks up into two parts, one surrounding the point $t=0$ and the other the point $u=0$ (or $t=s+4\mu^2$). There will thus be some real values of t between $-s+4\mu^2$ and 0, corresponding to points in the physical region, which are not included in (2.14). If s is less than the relevant root of (2.15), the two regions join into one, and all points in the physical region are included.

For either case, the maximum and minimum real values of t will be given by putting α in (2.14) equal to a and if, for a particular value of s, these points lie within the large Lehmann ellipse, it is not difficult to show that the whole region lies within the ellipse. The Lehmann ellipse whose semimajor axis is given by (2.10) intersects the real axis at the points $t=-36\mu^4/s$, $t=4q^2-36\mu^4/s$, corresponding to which $u=-4q^2-36\mu^4/s$, $u=36\mu^4/s$, and the condition on a is therefore that these points lie outside our region. It is thus necessary that

$$-s\cdot\frac{36\mu^4}{s}\left(-4q^2-\frac{36\mu^4}{s}\right)>a\,. \tag{2.16}$$

The minimum value of the left-hand side is $+288\mu^6$, when $s=6\mu^2$. We can therefore take a equal to this value, and the region (2.12) is

$$|stu|<288\mu^6\,. \tag{2.17}$$

As this expression is symmetric in s, t and u, the region will also lie within the large Lehmann ellipse when t or u is real and greater than $4\mu^2$. Further, if s is real and sufficiently large, the region will lie within the small Lehmann ellipse. All the requirements are therefore fulfilled, and we shall adopt (2.17) as the domain within which we shall attempt to prove analyticity.

We may remark at this point that, if s is real and positive but not too large, the region (2.17) will include the point $t=\mu^2$ and even $t=4\mu^2$. The scattering amplitude, considered as a function of momentum transfer, will have the poles and cuts at these points. We have already mentioned that the old region of analyticity, as given by the small Lehmann ellipse, did not include any singularities in the momentum transfer.

It has been emphasized that the region (2.17) is not the maximum region obtainable in principle from our hypotheses, and we have also seen in the course of the reasoning that it does not even include the whole physical region. However, since the excluded points in the physical region are at rather high energies, where the analytic properties can in any case not be applied, this should not be a serious drawback.

2·3. *Analytic representation of the amplitude.* – We next want to write down a representation for a function with the analytic properties we are proposing. There exists a general formula, the Bergmann-Weil formula, for representing

a function analytic in certain types of region bounded by analytic hypersurfaces. The formula is really nothing more than a repeated application of Cauchy's theorem, and it will be as easy to derive it for our particular case as to state it in general and then apply it. Suppose first that the transition amplitude were analytic in the region (2.17) except for a cut along the real s-axis only. If it were, in addition, an even function of the variable $2t+s-4\mu^2$, for fixed s, we could replace the variable t by α, equal to $-stu$. The evenness restriction is necessary in order that, when t is expressed in terms of α by (2.14), no square roots appear. We then have a function $\varphi(s, \alpha)$, analytic if $|\alpha|<a(=288\mu^2)$, except for a cut when s is real and greater than $4\mu^2$. If α is fixed and less in magnitude than a, we have the dispersion relation

$$\varphi(s, \alpha) = \frac{g^2}{s-\mu^2} + \frac{1}{\pi}\int_{4\mu^2}^{\infty} \mathrm{d}s' \, \frac{\varphi_1(s', \alpha)}{s'-s} . \tag{2.18}$$

There may, of course, be subtraction terms. The absorptive part φ_1 is an analytic function of α if $|\alpha|<a$, so that, by Cauchy's theorem it is given by the contour integral

$$\varphi_1(s', \alpha) = \frac{1}{2\pi i}\int_{|\alpha'|=a} \mathrm{d}\alpha' \, \frac{\varphi_1(s', \alpha')}{\alpha'-\alpha} . \tag{2.19}$$

Note that α', unlike all our other primed variables, is complex. Substituting (2.19) into (2.18), we obtain

$$\varphi(s, \alpha) = \frac{g^2}{s-\mu^2} + \frac{1}{2\pi^2 i}\int_{\substack{s'>4\mu^2 \\ |\alpha'|=a}} \mathrm{d}s' \, \mathrm{d}\alpha' \, \frac{\varphi_1(s', \alpha')}{(s'-s)(\alpha'-\alpha)} . \tag{2.20}$$

We can now transform back to our variables s and t, and, if $\varphi(s, \alpha) = \psi(s, t)$, we find that

$$\psi(s, t) = \frac{g^2}{s-\mu^2} + \frac{1}{2\pi^2 i}\int_{\substack{s'>4\mu^2 \\ |s't'u'|=a}} \mathrm{d}s' \, \mathrm{d}t' \, \frac{s'(s'+2t-4\mu^2)\psi_1(s', t')}{(s'-s)(s't'u'-stu)} , \tag{2.21}$$

where u' is given in terms of s' and t' by (2.2).

The transition amplitude $A(s, t)$ will not be an even function of $s+2t-4\mu^2$, but we can consider instead the even functions $A(s, t)+A(s, u)$ and $\{A(s, t)-A(s, u)\}/(s+2t-4\mu^2)$. On expressing each of them by means of (2.21) and recombining them to form $A(s, t)$, we arrive at the equation

$$A(s, t) = \frac{g^2}{s-\mu^2} + \frac{1}{2\pi^2 i}\int_{\substack{s'>4\mu^2 \\ |s't'u'|=a}} \mathrm{d}s' \, \mathrm{d}t' \, \frac{s'(t+t'-u-u')A_1(s', t')}{2(s'-s)(s't'u'-stu)} . \tag{2.22}$$

If, finally, we add corresonding terms for the singularities when t and u are real, we obtain the representation

$$A = \frac{g_1^2}{s-\mu^2} + \frac{g_2^2}{u-\mu^2} + \frac{g_3^2}{t-\mu^2} + \frac{1}{2\pi^2 i}\int_{\substack{s'>4\mu^2 \\ |s't'u'|=a}} ds'\,dt'\,\frac{s'(t+t'-u-u')A_1(s',t')}{2(s'-s)(s't'u'-stu)} +$$

$$+ \frac{1}{2\pi^2 i}\int_{\substack{u'>4\mu^2 \\ |s't'u'|=a}} du'\,dt'\,\frac{u'(t+t'-s-s')A_2(u',t')}{2(u'-u)(s't'u'-stu)} + \frac{1}{2\pi^2 i}\int_{\substack{t'>4\mu^2 \\ |s't'u'|=a}} ds'\,dt'\,\frac{t'(s+s'-u-u')A_3(s',t')}{2(t'-t)(s't'u'-stu)}\,. \tag{2.23}$$

Should there be subtraction terms, the denominators $s'-s$, $t'-t$ and $u'-u$ become modified in the usual way. The subtraction terms themselves will be of the form

$$\int_{|\alpha'|=a} d\alpha'\,\frac{g(\alpha')}{\alpha'-stu}\,, \tag{2.24}$$

multiplied by polynomials in s or t. There will be no subtractions associated with the integration over α', as this is an ordinary Cauchy integral over a finite range.

The validity of the representation (2.23) is thus a necessary condition for our analytic properties. That it is also a sufficient condition is obvious, as singularities can only occur when one of the denominators vanish. They will do so if s, t or u is real and greater than $4\mu^2$ or if $stu = a$. The espression (2.23) is therefore an analytic function of both variables in the region (2.17), except for the poles and cuts. Further, along the cuts, the expression is an analytic function of the momentum-transfer variable. This may be seen by performing—for example—the s'-integration in the first integral. None of the denominators remaining will vanish if s is real and greater than $4\mu^2$ and $|stu| < a$, and the integrands will be functions only of s and the variables of integration. The expression is therefore an analytic function of t.

The absorptive parts A_1, A_2 and A_3 in the representation (2.23) are required for complex values of the momentum transfer. As these values are always within the large Lehmann ellipse, the absorptive parts can be found by analytic continuation from the physical region, or by using the Legendre expansion. To calculate the subtraction terms (2.24) we have to know the transition amplitude A for a particular value of s (or t or u) and all values of t within the domain of analyticity. We choose a value of s for which the domain lies entirely within the small Lehmann ellipse—we have already imposed the requirement that such a value exist. The transition amplitude at this value of s can then be found by analytic continuation from the physical region, or by using the Legendre expansion.

It will be noticed that (2.23) contains no terms corresponding to the « double dispersion terms » of the double dispersion representation. This is not surprising, as the region in which the two-dimensional spectral functions would be non-zero lies entirely outside the domain (2.17). The region touches the boundary of the domain at the points $s=6\mu^2$, $t=6\mu^2$; $s=6\mu^2$, $u=6\mu^2$; and $t=6\mu^2$, $u=6\mu^2$. The double spectral functions only enter into the representation after applying the unitarity condition.

It is actually unnecessary to assume that the transition amplitude is analytic in the whole region (2.17) in order to derive the representation (2.23). The derivation just given really assumed only that it was analytic in some region of the form $|stu|<a_1$, where a_1 can be arbitrarily small. The dispersion relation (2.18) is then true if $|\alpha|<a_1$. The equation (2.19), on the other hand, is valid if the integration is taken over any contour $|\alpha|=a(<288\mu^6)$, as it only requires A_1 to be analytic function of the momentum transfer in the large Lehmann ellipse. We can then repeat the steps leading to (2.23), with the contour of integration $|s't'u'|=288\mu^6$. This representation is thus shown to be valid in the domain $|stu|<a_1$. Further, we have already seen that (2.23) is analytic in the momentum transfer in that part of the physical region for which $|stu|<288\mu^6$, and we know from Lehmann's results that the transition amplitude is an analytic function of the momentum transfer in the whole physical region. We can thus conclude from analytic continuation that (2.23) represents the transition amplitude in the entire physical region if $|stu|<288\mu^6$.

The proof can be carried out in the same way if there are subtraction terms. We know that the contour $|\alpha'|=288\mu^6$ in the integral (2.24) is contained in the small Lehmann ellipse, where the transition amplitude is certainly an analytic function of the momentum transfer. It is therefore permissible to perform out the integration over this contour.

The derivation of the representation (2.23) from the assumption that the transition amplitude is analytic in the domain $|stu|<a_1$ may be taken as a proof that, if it is analytic in this domain, it is analytic in the domain $|stu|<288\mu^6$. It remain to prove that the transition amplitude is analytic in some domain $|stu|<a_1$, which we proceed to do in the next section.

3. – Proof of the results of the last section.

We have now to prove that the transition amplitude is actually an analytic function of s and t in a region of the form (2.12), for some value of a. An understanding of this section is not required in the remainder of the paper, so that the reader who is willing to accept it or to defer reading it may pass on to Section **4**, in which the unitarity condition is used to derive further results.

It will be slightly more convenient to discuss regions of the form

$$|st| < b \tag{3.1}$$

than of the form (2.12). As long as $b < 9\mu^4$, this region will fulfil the conditions stated in the previous section. (The limitation at $9\mu^4$ comes from the requirement that, for some real value of s, the region must lie within the small Lehmann ellipse.) Once we have proved analyticity within a region of the form (3.1), we can prove it once in a region of the form (2.12). For, by symmetry, it follows that the transition amplitude is also analytic in regions of the form $|tu| < b$, $|su| < b$, and, if $|stu| < b^{\frac{3}{2}}$, at least one of the moduli $|st|$, $|tu|$ and $|su|$ is less than b.

If a function is analytic in the region (3.1), the Bergmann-Weil representation corresponding to (2.23) will be

$$B(s,t) \quad \frac{g_1^2}{s-\mu^2} + \frac{g_2^2}{u-\mu^2} + \frac{g_3^2}{t-\mu^2} + \frac{1}{2\pi^2 i}\int_{\substack{s'>4\mu^2\\ |s't'|=b}} \mathrm{d}s'\,\mathrm{d}t' \frac{s'A_1(s',t')}{(s'-s)(s't'-st)} + \tag{3.2}$$

$$+ \frac{1}{2\pi^2 i}\int_{\substack{t'>4\mu^2\\ |s't'|=b}} \mathrm{d}s'\,\mathrm{d}t' \frac{t'A_3(s',t')}{(t'-t)(s't'-st')} + \frac{1}{2\pi^2 i}\int_{\substack{u'>4\mu^2\\ |s't'|=b}} \mathrm{d}u'\,\mathrm{d}t' \frac{(t+t'-s-s')A_2(u',t')}{2(u'-u)(s't'-st)}.$$

We can always define a function $B(s,t)$ by (3.2), and it will have the analytic properties discussed above. Our aim is now to prove that, within those portions of the physical regions for the three reaction that fall within the region (3.1), $B(s,t)$ is equal to the transition amplitude $A(s,t)$. In writing down (3.2), we have again omitted subtraction terms, which will be of the form

$$\int_{|\alpha'|=a} \mathrm{d}\alpha' \frac{f(\alpha')}{\alpha'-st}, \tag{3.3}$$

multiplied by polynomials in s or t. They are obtained by requiring that

$$B(s_0,t) = A(s_0,t), \tag{3.4}$$

where s_0 is a real value of s for which the region (3.1) lies within the small Lehmann ellipse. If there is more than one subtraction term, we impose similar conditions on the derivatives of B.

Our method will be to prove that, when $t = 0$, the function B and all its derivatives with respect to t are equal to the transition amplitude A and its corresponding derivatives. We shall show this in the physical regions for the reaction I ($s > 4\mu^2$) or for the reaction II ($u > 4\mu^2$). As both A and B are

analytic functions of t, for fixed s ($s > 4\mu^2$) or u ($u > 4\mu^2$) in those portions of the physical regions for the reactions I and II which fall within the domain (3.1), we will then have proved that A and B are identical in these regions. If u is real and sufficiently large, the region (3.1) in the t-plane consists of two parts, one surrounding the point $t = 0$ and the other surrounding the point $s = 0$, and, at the moment, we can only equate A and B in the first part. By repeating the argument with the variables s and t interchanged, we can then show that A and B are also identical in the physical region for the reaction III and in the remaining part of the physical region for the reaction II.

3·1. *Proof neglecting polynomials.* – At $t = 0$, the transition amplitude A will satisfy the ordinary dispersion relations

$$A(s, t=0) = \frac{1}{\pi}\int \mathrm{d}s' \frac{A_1(s', t=0)}{s'-s} + \frac{1}{\pi}\int \mathrm{d}u' \frac{A_2(u', t=0)}{u'-u} . \tag{3.5}$$

As usual, we have omitted subtraction terms. The derivatives of A with respect to t will satisfy the dispersion relations

$$\frac{\partial^n}{\partial t^n} A(s, t=0) = \frac{1}{\pi}\int \mathrm{d}s' \frac{(\partial^n/\partial t^n) A_1(s', t=0)}{s'-s} + \frac{1}{\pi}\int \mathrm{d}u' \frac{(\partial^n/\partial t^n)|_s A_2(u', t=0)}{u'-u} . \tag{3.6}$$

The derivative in the first integrand certainly exists, as A_1 is an analytic function of t for fixed s, but the derivative in the second integrand may have to be interpreted as a distribution. Eq. (3.6) has been proved by SYMANZIK [11], and could also be proved by differentiating (3.5) with respect to t, on the assumption that the right-hand integral is convergent. We could also prove directly that $(\partial^n/\partial t^n)(A(s, t-0))$ satisfies (3.6) as it can be written as the Fourier transform of a function which vanishes in certain regions [12]. By doing so we can also see that the number of subtraction in (3.6) is the same as in (3.5).

If s is set equal to zero, we have the dispersion relations

$$A(s=0, t) = \frac{1}{\pi}\int \mathrm{d}t' \frac{A_3(s=0, t')}{t'-t} + \frac{1}{\pi}\int \mathrm{d}u' \frac{A_2\{u', t(u', s=0)\}}{u'-u} , \tag{3.7}$$

$$\frac{\partial^n}{\partial s^n} A(s=0, t) = \frac{1}{\pi}\int \mathrm{d}t' \frac{(\partial^n/\partial s^n) A_3(s=0, t')}{t'-t} + \frac{1}{\pi}\int \mathrm{d}u' \frac{(\partial^n/\partial s^n)|_t A_2\{u', t(u', s=0)\}}{u'-u} . \tag{3.8}$$

[11] K. SYMANZIK: *Phys. Rev.*, **105**, 743 (1957).

[12] We first prove this result for negative values of the squares of two of the momenta, and then continue analytically onto the mass shell in Bogoliubov's manner.

The expression $A_2\{u', t(u', s)\}$ indicates that t is to be expressed as a function of u' and s by (2.2). Note that A is originally only defined in the physical region for the three reactions, though it could be extended to other regions by (3.5) or (3.7). Around the point $s = 0$, $t = 0$, the functions A appearing in (3.5) and (3.6), and in (3.7) and (3.8), are the same function, the transition amplitude for the reaction II.

Now let us recapitulate that the function B is analytic in the region (3.1) except for cuts when s, t or u is real and greater than $4\mu^2$, and that the discontinuities across these cuts are respectively A_1, A_2, and A_3. This may be seen directly by examining the equation (3.2) which defines B. Indeed, B was specially constructed to have this property, as an equation of the form (2.18), but with α now equal to st instead of stu, and φ_1 equal to A_1, B occurs at an intermediate stage. If t is set equal to zero, the domain of analyticity (3.1) of B is the whole s-plane. The function $B(s, t = 0)$ is therefore analytic in s in the complex plane except for cuts along the real axis, and the discontinuities across these cuts are $A_1(s, t = 0)$ $(s \geqslant 4\mu^2)$ and $A_2(u, t = 0)$ $(u > 4\mu^2)$. It follows that B satisfies the dispersion relation (3.5), with the same spectral functions A_1 and A_2. Except for possible subtraction terms, $B(s, t = 0)$ will therefore be equal to $A(s, t = 0)$. We can show in a similar manner that $B(s = 0, t) = A(s = 0, t)$ except for possible subtractions.

The arguments regarding the derivatives proceed analogously. Since B is an analytic function in the region (3.1), with discontinuities across the cuts equal to A_1, A_2, and A_3, $(\partial^n/\partial t^n)(B(s, t))$ will be an analytic function with discontinuities equal to $(\partial^n/\partial t^n)(A_1(s, t))$, $(\partial^n/\partial t^n)|_s(A_2(u, t))$ and $(\partial^n/\partial t^n)(A_3(s, t))$ interpreted as distributions where necessary. If $t = 0$, $(\partial^n/\partial t^n)(B(s, t))$ will be an analytic function of s in the whole complex plane, apart from cuts along the real axis with discontinuities $(\partial^n/\partial t^n)(A_1(s, t = 0))$ and $(\partial^n/\partial t^n)(A_2(u, t = 0))$. It will accordingly satisfy the dispersion relation (3.6), with the same spectra functions, so that, except for a possible polynomial associated with subtraction terms, $(\partial^n/\partial t^n)(B(s, t=0))$ will be equal to $(\partial^n/\partial t^n)(A, (st=0))$. Likewise, $(\partial^n/\partial s^n)\cdot$ $\cdot(B(s = 0, t))$ will be equal to $(\partial^n/\partial s^n)(A(s = 0, t))$ except for a possible polynomial.

3·2. *Treatment of polynomials.* – The polynomials associated with the possible subtraction terms are not quite trivial, however. This is because differentiation of (3.2) with respect to s say, may increase the asymptotic behaviour of the function as s becomes infinite by one power of s. The number of subtraction terms may therefore increase by one at each differentiation. Let us suppose for definiteness that there is one subtraction in the formula for B, *i.e.* that B does not tend to infinity as s or t become infinite. There may then be $n+1$ subtractions in the formula for $(\partial^n/\partial t^n)(B(s, t = 0))$, so that $(\partial^n/\partial t^n)(B(s, t = 0))$ may differ from $(\partial^n/\partial t^n)(A(s, t = 0))$ by a polynomial of the

n-th degree. Before we can assert that $(\partial^n/\partial t^n)(B(s,\ t-0) - (\partial^n/\partial t^n)(A(s,\ t=0))$ we have to prove $n+1$ equalities between the two functions, or their derivatives with respect to s, at particular points. The same holds for $(\partial^n/\partial s^n)(B(s=0, t))$.

We start with the function $B(s,\ t=0)$, which we have to show to be equal to $A(s,\ t=0)$ at one value of s. As the subtraction term has been chosen to make (3.4) true, the two functions are in fact requal at s_0. We are therefore entitled to say that

$$B(s,\ t=0) = A(s,\ t=0)\ . \tag{3.9}$$

Next we prove that $B(s=0,\ t) = A(s=0,\ t)$. Again we have to verify this equality at one value of t, and eq. (3.9) shows that it is true at $t-0$. Hence

$$B(s=0,\ t) = A(s=0,\ t)\ . \tag{3.10}$$

To prove the equality $(\partial/\partial t)(B(s,\ t=0)) = (\partial/\partial t)(A(s, t=0))$, we have to verify it at two values of s. By differentiating (3.4) and (3.10) with respect to t, we see that it is true at $s=s_0$ and $s=0$, so that [13]

$$\frac{\partial}{\partial t} B(s,\ t=0) = \frac{\partial}{\partial t} A(s,\ t=0)\ . \tag{3.11}$$

To prove that $(\partial/\partial s)(B(s=0,\ t)) - (\partial/\partial s)(A(s=0,\ t))$, we differentiate (3.9) and (3.11) with respect to s, interchange the order of the s- and t-derivatives in the latter, and put s equal to zero. We thus have

$$\frac{\partial}{\partial s} B(s=0,\ t=0) = \frac{\partial}{\partial s} A(s=0,\ t=0)\ ,$$

$$\frac{\partial}{\partial t}\frac{\partial}{\partial s} B(s=0,\ t=0) = \frac{\partial}{\partial t}\frac{\partial}{\partial s} A(s=0,\ t=0)\ .$$

The two functions $(\partial/\partial s)(B(s=0,\ t))$ and $(\partial/\partial s)(A(s-0,\ t))$ and their first derivatives with respect to t are therefore equal at $t=0$. We may therefore assert that

$$\frac{\partial}{\partial s} B(s=0,\ t) = \frac{\partial}{\partial s} A(s=0,\ t)\ . \tag{3.12}$$

---

[13] Strictly speaking we cannot really say anything about $(\partial/\partial t)(B(s, t=0))$ from its value at the single point $s=0$ if the expression is a distribution rather than a function. However, it is not difficult to show that, in the neighborhood of the point $s=0$, $t=0$, the function $B(s, t) - A(s, t)$ and all of its partial derivatives are continuous functions of each of the variables s and t. The reasoning here and in the following argument is thus justified.

To prove that $(\partial^2/\partial t^2)(A(s, t=0)) = (\partial^2/\partial t^2)(B(s, t=0))$, we have to verify three conditions. This can be done by differentiating (3.4), (3.10) and (3.12) twice with respect to t, interchanging the order of the derivatives in the last expression, and setting t equal zero. Thus

$$\frac{\partial^2}{\partial t^2} B(s_0, t=0) = \frac{\partial^2}{\partial t^2} A(s_0, t=0) ,$$

$$\frac{\partial^2}{\partial t^2} B(s=0, t=0) = \frac{\partial^2}{\partial t^2} A(s=0, t=0) ,$$

$$\frac{\partial}{\partial s}\frac{\partial^2}{\partial t^2} B(s=0, t=0) = \frac{\partial}{\partial s}\frac{\partial^2}{\partial t^2} A(s=0, t=0) .$$

The two functions are therefore equal at $s = s_0$ and $s = 0$, and their first derivatives with respect to s are equal at $s = 0$, so that we may write

$$\frac{\partial^2}{\partial t^2} B(s, t=0) = \frac{\partial^2}{\partial t^2} A(s, t=0) . \tag{3.13}$$

It is now clear how the argument proceeds, and we always have just enough conditions to assert that

$$\frac{\partial^n}{\partial t^n} B(s, t=0) = \frac{\partial^n}{\partial t^n} A(s, t=0) , \tag{3.14}$$

$$\frac{\partial^n}{\partial s^n} B(s=0, t) = \frac{\partial^n}{\partial s^n} A(s=0, t) . \tag{3.15}$$

We may remark that, if we were to try to verify these equations directly, by differentiating (3.2) and comparing the result with (3.6) and (3.8), we should find that the two sides differ by polynomials whose coefficients are integrals involving the absorptive parts A_1, A_2 and A_3. As we have proved that the polynomials do not occur, these coefficients must be equal to zero. We thus have restrictions on the absorptive parts A_1, A_2 and A_3 which must hold in order that the ordinary dispersion relations, with t and s constant, be consistent with one another. Since we make no use of these restrictions, except implicitly in the derivation of (3.14) and (3.15), we shall not dwell further on this point.

As we have explained above, the equalities (3.9), (3.10), (3.14) and (3.15) are sufficient to show that, in those parts of the physical regions for the three reactions which are within the domain (3.1), the function $B(s, t)$ is equal to the scattering amplitude $A(s, t)$. B thus defines an analytic continuation of the scattering amplitude, as a function of s and t, in the region (3.1), which is the result we set out to prove.

4. – Use of the unitarity condition.

4·1. *Outline of the procedure.* – In this Section our aim is to use the unitarity condition to extend the region of analyticity (2.17). The manner of doing so is both in principle and in practice exceedingly simple. If the transition amplitude A is an analytic function of z, the cosine of the angle of scattering, for fixed s (real and greater than $4\mu^2$) in an ellipse with foci ± 1 and semi-major axis z_0, then the unitarity condition shows that the absorptive part A_1 is an analytic function of z in an ellipse with foci ± 1 and semi-major axis $2z_0^2 - 1$. This result assumes that A has no singularities as a function of z in the ellipse. However, if A has singularities within the ellipse along the real axis we can obtain similar results. Let z_1 be the minimum value of z for which these singularities exist; the absorptive part A_1 will then be analytic in an ellipse with foci ± 1 and semi-major axis $z_0 z_1 + \sqrt{(z_0^2 - 1)(z_1^2 - 1)}$. Within this ellipse, it may have cuts if $|z|$ is real and greater than $2z_1^2 - 1$ ([14]). At present we can prove these results only below the threshold for inelastic processes, where the unitarity condition takes its simple form.

The method of procedure is then, in outline, as follows: we know that A is analytic in the region (2.17), except for poles and cuts along the real axis. If s has a fixed real value which is not too large, we can inscribe an ellipse with foci ± 1. It then follows from unitarity that A_1 is analytic in a larger ellipse. If s is sufficiently small, this ellipse turns out to be larger than the original ellipse within which A_1 was analytic. We can therefore increase the value of a in (2.12) and still satisfy the condition of section 2, namely that, if s, t or u is real and greater than $4\mu^2$, the domain lies within the ellipse of analiticity of A_1. The scattering amplitude will be analytic in the new domain. Having increased the domain of analiticity of A we can increase the ellipse of analyticity of A_1 (in the t-plane) still further. We could proceed indefinitely in this way, alternately increasing the domain of analyticity of A and its absorptive parts, if it were not for the fact that the required results can now be established only below the threshold for inelastic processes.

4·2. *Consequences of the unitarity equation.* – Let us first prove our assertions about the unitarity condition. Below the threshold for inelastic processes

---

([14]) These results are reminiscent of those obtained by LEHMANN in passing from the small to the large ellipse and, in fact, the integral we have to perform has certain similarities to Lehmann's. However, our results are dependent on the unitarity condition and are only valid below the threshold for inelastic processes, whereas those of Lehmann do *not* involve unitarity and are valid at all energies.

in the reaction I, the unitarity equation is

$$A_1\{s, t(z)\} = (q/32\pi^2 w)\int \mathrm{d}^2\boldsymbol{n}_i A^*_{ie}\{s, t(z_{ie})\}A_{i0}\{s, t(z_{i0})\}\,. \tag{4.1}$$

A'_{ie} and A'_{i0} are the transition amplitudes between the initial and intermediate, and the intermediate and final states. If the particles are not identical but have equal masses, these transition amplitudes will not be equal to A, but they will have the same analytic properties. $\boldsymbol{n}_i$ is a vector representing the direction of the momenta of the particles in the intermediate state, z_{ie} the cosine of the angle between the incoming particles and $\boldsymbol{n}_i$, and z_{i0} the cosine of the angle between the outgoing particles and $\boldsymbol{n}_i$: q is the centre-of-mass momentum and w the centre-of-mass energy $\sqrt{s}$.

If A_{ie} and A_{i0} are analytic functions of z in an ellipse with foci ± 1 and semi-major axis z_0, except for cuts along the real axis when $|z| > z_1$, they may be expressed as dispersion integrals

$$A_{ie}\{s, t(z_{ie})\} = \frac{1}{\pi}\int \mathrm{d}z'_{ie}\,\frac{a_1(s, z'_{ie})}{z'_{ie} - z_{ie}} + \frac{1}{2\pi i}\int \mathrm{d}z'_{ie}\,\frac{a_2(s, z'_{ie})}{z'_{ie} - z_{ie}}\,, \tag{4.2a}$$

$$A_{i0}\{s, t(z_{i0})\} = \frac{1}{\pi}\int \mathrm{d}z'_{i0}\,\frac{b_1(s, z'_{i0})}{z'_{i0} - z_{i0}} + \frac{1}{2\pi i}\int \mathrm{d}z'_{i0}\,\frac{b_2(s, z'_{i0})}{z'_{i0} - z_{i0}}\,. \tag{4.2b}$$

The integration variables z_{ie} and z_{i0} in the first terms are real and greater in magnitude than z_1, while in the second terms they are on the ellipse. (4.2a) and (4.2b) can then be substituted into (4.1) and the integral over $\boldsymbol{n}_i$ can be performed. This has been done in references ([3]) and ([7]); the result (appropriately modified) is

$$\begin{aligned} A_1\{s, t(z)\} = \int \mathrm{d}z_{ie}\,\mathrm{d}z_{i0} G(z, z_{ie}, z_{i0})\{&a_1(s, z_{ie})b_1(s, z_{i0}) + \\ &+ (1/2i)a_1(s, z_{ie})b_2(s, z_{i0}) + (1/2i)a_2(s, z_{ie})b_1(s, z_{i0}) - \frac{1}{4}a_2(s, z_{ie})b_2(s, z_{i0})\}\,, \end{aligned} \tag{4.3}$$

where

$$G(z, z_{ie}, z_{i0}) = \frac{1}{16\pi^3 q^3 w\{k(z, z_{ie}, z_{i0})\}^{\frac{1}{2}}}\ln\frac{z - z_{ie}z_{i0} + \{k(z, z_{ie}, z_{i0})\}^{\frac{1}{2}}}{z - z_{ie}z_{i0} - \{k(z, z_{ie}, z_{i0})\}^{\frac{1}{2}}}\,, \tag{4.4a}$$

$$k(z, z_{ie}, z_{i0}) = z^2 + z_{ie}^2 + z_{i0}^2 - 1 - 2zz_{ie}z_{i0}\,. \tag{4.4b}$$

The primes on z_{ie} and z_{i0} have been dropped. The exact form of G is unimportant, and all we need observe is that it is analytic except when

$$z = z_{ie}z_{i0} + \sqrt{(z_{ie}^2 - 1)(z_{i0}^2 - 1)}\,. \tag{4.5}$$

If both z_{ie} and z_{i0} are real and positive, the positive sign is taken before the radical in (4.5). Otherwise, the sign is determined by analytic continuation in z_{ie} and z_{i0} from real positive values, without crossing the real axis between $+1$ and -1.

The singularities of A_1 as a function of z can now easily be found. In the first term of (4.3), both z_{ie} and z_{i0} will be real, and their minimum absolute value will be z_1. Thus, from (4.5), there may be singularities in A_1 when z is real and greater in magnitude than $2z_1^2 - 1$. In the second term of (4.3), z_{ie} will be real and greater than z_1, but z_{i0} will be on an ellipse with foci ± 1 and semi-major axis z_0. It will therefore have the form

$$z_{i0} = \cosh(\alpha + i\theta), \tag{4.6}$$

where

$$\alpha = \cosh^{-1} z_0 \tag{4.7}$$

and θ varies from 0 to 2π. From (4.5) and (4.6), the singularities of A_1 will occur when

$$z = z_{ie}\cosh(\alpha + i\theta) + \sqrt{(z_{ie}^2 - 1)\sinh^2(\alpha + i\theta)} = \cosh(\beta + i\theta), \tag{4.8}$$

where

$$\beta = \alpha + \cosh^{-1} z_{ie}.$$

The points given by (4.8) lie on an ellipse with foci ± 1 and semi-major axis

$$\cosh^{-1}\beta = z_0 z_{ie} + \sqrt{(z_0^2 - 1)(z_{ie}^2 - 1)}. \tag{4.9}$$

As the minimum value of z_{ie} is z_1, the singularities will all lie on or outside an ellipse with foci ± 1 and semi-major axis $z_0 z_1 + \sqrt{(z_0^2 - 1)(z_1^2 - 1)}$. The singularities associated with the third term of (4.3) will be similarly located. In the fourth term of (4.3), both z_{ie} and z_{i0} are given by (4.6), so that, by (4.5), the singularities in A_1 will be at the points

$$\begin{cases} z = \cosh(\alpha + i\theta_1)\cosh(\alpha + i\theta_2) + \sinh(\alpha + i\theta_1)\sinh(\alpha + i\theta_2) \\ \quad = \cosh(2\alpha + i\theta), \end{cases} \tag{4.10}$$

where $\theta = \theta_1 + \theta_2$. These points (4.10) on an ellipse with foci ± 1 and semi-

---

(15) S. MANDELSTAM: *Phys. Rev.*, **112**, 1344 (1956).

major axis

$$\cosh^{-1} 2\alpha = 2z_0^2 - 1 \,. \tag{4.11}$$

The statements made at the beginning of the section about the analyticity of A_1 as a function of z are thus proved.

It will be noticed that the first term of (4.3), which gives rise to the singularities of A_1 along the real z-axis, is exactly the same as in previous treatments ([7,15]). Within the ellipse with foci ± 1 and semi-major axis $z_0 z_1 + \sqrt{(z_0^2-1)(z_1^2-1)}$, therefore, the existence and calculation of the double spectral functions has been justified.

4·3. *Extension of the analyticity domain.* – We can now use these properties of the unitarity condition to extend the domain of analyticity (2.17) in the manner indicated above. As the unitarity condition is being used only below $s = 9\mu^2$, the threshold for inelastic processes, we still have to ensure that, if s is real and greater than $9\mu^2$, the new domain lies within the original large Lehmann ellipse. This will be true if (2.17) is changed to ([16])

$$|stu| < 324\mu^6 \,. \tag{4.12}$$

If $s = 9\mu^2$, t or $u = 4\mu^2$, the domain (4.12) touches the large Lehmann ellipse; at all real values of s greater than $9\mu^2$, it lies within the ellipse.

By using the unitarity condition with s between $4\mu^2$ and $9\mu^2$, we can show that the region (4.12) can be reached from (2.17) in one step. For any fixed real s ($> 4\mu^2$) it is easy to see that the ellipse with foci ± 1 in the z-plane lies within the region (2.17) if its minor axis does so. The end of the minor axis will be the point

$$t = (\tfrac{1}{2}s - \mu^2)\{1 + i\sqrt{(z_0^2-1)}\}, \tag{4.13}$$

$$\text{at which} \qquad u = (\tfrac{1}{2}s - \mu^2)\{1 - i\sqrt{(z_0^2-1)}\},$$

where z_0 is the semi-major axis of the ellipse in the z-plane. Inserting these values into (2.17), we find that if

$$z_0 \leqslant 6\sqrt{2}\mu^3/q^2\sqrt{s} \,, \tag{4.14}$$

the ellipse lies within the region of analyticity. Also, the minimum value of t or u for which there is a singularity along the real axis is μ^2, corresponding

([16]) If we had taken our original domain to be $|st| < b$ rather than $|stu| < a$, the value of b would have remained unchanged when the restrictions below $9\mu^2$ were removed. It is for this reason that we chose the second form in preference to the first.

to a value of z equal in absolute value to

$$z_1 = 1 + \mu^2/2q^2 \,. \tag{4.15}$$

The expression (4.14) and (4.15) are to be inserted into the formula $z_0 z_1 + \sqrt{(z_0^2 - 1)(z_1^2 - 1)}$ in order to obtain the major axis of the new ellipse within which A_1 is an analytic function of the momentum transfer. Bearing in mind that the minimum value of $|tu|$ on such an ellipse occurs when z is real, we can then show that, for a given s, all points with

$$|stu| < \{12\sqrt{2}\,\mu^3(\mu^2/q^2 + \mu^4/q^4)^{\frac{1}{2}} + (144\mu^6 - 2q^2 s)^{\frac{1}{2}}(1 + \mu^2/2q^2)^{\frac{1}{2}}\}^2$$

lie within the ellipse. If s is between $4\mu^2$ and $9\mu^2$, the right-hand side is always greater than $324\mu^6$. Any point in the domain (4.12) for which s is real and greater than $4\mu^2$, is thus in the region of analyticity of A_1 as a function of momentum transfer. As our whole problem is symmetric in s, t and u, similar results are true if t and u are real and greater than $4\mu^2$. The transition amplitude is thus analytic in the region (4.12), apart from the expected singularities.

It is not surprising that the value of a could only be increased by the very small amount from $288\mu^6$ to $324\mu^6$. The initial value of a was the minimum value of $|stu|$ on the large Lehmann ellipse, and this occurred at $s = 6\mu^2$. Our present value of a is the minimum value, with respect to t, of the same modulus at $s = 9\mu^2$, and it would not be expected to change very appreciably from its absolute minimum with this small change in s. On the other hand, once s increases a certain distance, the minimum value of $|stu|$ begins to rise rapidly, and it tends to infinity with s. The method of extending the domain of analiticity by using the unitarity condition has therefore great promise if inelastic processes can be taken into account and included. Only a finite number of processes need be included at one time. For the method to work it is of course necessary that the ellipse of analyticity of A_1 increases at each stage. This will not occur if we consider only domains of the form (2.12); if s is sufficiently large, we shall not be able to get beyond the original large Lehmann ellipse. However, we can proceed further by investigating other types of domains as well—for example, we might examine domains of the type $|(s+s_0)(t+t_0)(u+u_0)| < a$, with s_0, t_0 and u_0 real and positive. It seems likely that, by proceeding in this way, the domain can be extended arbitrarily far, though this has not actually been verified. The structure of the unitarity equation for inelastic processes may be such that some of the singularities of A_1 as a function of t lie in the complex plane. These singularities will not be more difficult to treat than the singularities along the real axis.

4·4. *Analytic representation.* – A representation similar to (2.23) can be written down to exhibit the analytic properties of the transition amplitude derived in this section. As the absorptive part A_1 now has singularities along the real axis within the region (4.12), there will be additional terms to correspond to these singularities. These terms are just the integrals over the two-dimensional spectral functions in the double dispersion representatoin, so that our new representation becomes

$$A = \frac{g_1^2}{s-\mu^2} + \frac{g_2^2}{u-\mu^2} + \frac{g_3^2}{t-\mu^2} + \frac{1}{\pi^2}\int ds'\,dt'\,\frac{A_{13}(s',t')}{(s'-s)(t'-t)} +$$

$$+ \frac{1}{\pi^2}\int dt'\,du'\,\frac{A_{23}(t',u')}{(t'-t)(u'-u)} + \frac{1}{\pi^2}\int ds'du'\,\frac{A_{12}(s',t')}{(s'-s)(u'-u)} +$$

$$- \frac{1}{2\pi^2 i}\int_{\substack{s'>4\mu^2\\ |s't'u'|=324\mu^6}} ds'\,dt'\,\frac{s'(t+t'-u-u')A_1(s',t')}{2(s'-s)(s't'u'-stu)} + \frac{1}{2\pi^2 i}\int_{\substack{u'>4\mu^2\\ |s't'u'|=324\mu^6}} du'\,dt'\,\frac{u'(t+t'-s-s')A_2(u',t')}{2(u'-u)(s't'u'-stu)} +$$

$$+ \frac{1}{2\pi^2 i}\int_{\substack{t'>4\mu^2\\ |s't'u'|=324\mu^6}} ds'\,dt'\,\frac{t'(s+s'-u-u')A_3(s',t')}{2(t'-t)(s't'u'-stu)}\,. \tag{4.16}$$

In the term involving A_{13}, the range of integration will be that portion of the real plane for which

$$s' > 4\mu^2\,, \qquad t' > 4\mu^2\,, \qquad s't' - 4\mu^2(s'+t') + 12\mu^4 > 0\,, \tag{4.17a}$$

$$-s't'u' < 324\mu^6\,. \tag{4.17b}$$

The range of integration of the next two terms will be given by similar formulae. The absorptive part A_1 in the following term could be replaced by

$$A_1'(s',t') = A_1(s',t') - \frac{1}{\pi}\int dt''\,\frac{A_{13}(s',t'')}{t''-t} - \frac{1}{\pi}\int du''\,\frac{A_{12}(s',u'')}{u''-u}\,, \tag{4.18}$$

where the range of integration is given by (4.17) for the first term, and corresponding formulae for the second term. The function A_1' is now analytic in the whole region $|s't'u| < 324\mu^6$, s' real, and can be obtained from its Legendre expansion. The other absorptive parts may be modified in the same way. We could also drop the restriction (4.17*b*) in the ranges of integration of the double dispersion terms *and* of the last two terms in (4.18).

In the previous calculations of the double spectral functions [7,15] we saw that they are given exactly by their fourth-order perturbation terms if the variables s' and t' are sufficiently small. We can now obtain this result rigorously, and, in fact, it is always true within the domain (4.12). To see this

we divide the first term of (4.2*a*) and (4.2*b*) into two parts, one from the δ-function contribution to a_1 and b_1 at $t = \mu^2$ and $u = \mu^2$, and the other from the continuum contributions beginning at $t = 4\mu^2$, $u = 4\mu^2$. On inserting them into the integral (4.3) for A_1, we find that the singularities from the terms with the continuum contributions to either a_1 or b_1 begin outside the region (4.17*b*). We are left with the term from the δ-function contributions to both a_1 and b_1, and this is precisely the fourth-order term. Within the region (4.12)) therefore, the double spectral functions are given by formulae (2.11) and (2.12, of reference [7]).

If s is real and between $4\mu^2$ and $9\mu^2$, we can make another application of the unitarity condition to show that A_1 is an analytic function of z in an ellipse with foci ± 1 and semi-major axis

$$\frac{9\mu^3}{q^2\sqrt{s}}\left(1+\frac{\mu^2}{2q^2}\right)+\left(\frac{81\mu^6}{q^4 s}-1\right)^{\frac{1}{2}}\left(\frac{\mu^2}{q^2}+\frac{\mu^4}{4q^4}\right)^{\frac{1}{2}}, \tag{4.19}$$

except for a cut on the real axis. This ellipse is sufficiently large to include part of the region in which other terms besides the fourth-order term contribute to the two-dimensional spectral function. The function cannot then be calculated exactly.

5. – Some miscellaneous analyticity properties.

5·1. *Fixed angular momentum states.* – One of the important applications of the double dispersion representation is to demonstrate that the transition amplitudes for fixed angular-momentum states satisfy dispersion relations. From the results of this paper we shall be able to show that, within a certain region, the partial-wave scattering amplitudes are analytic functions of s except for the expected singularities. By putting $t = 2q^2(-1+z)$, $u = 2q^2(-1-z)$ into (4.16), multiplying by $P_l(z)$ and integrating over z from -1 to 1, we obtain the partial wave amplitude. The expression will be analytic except where the denominators vanish. The singularities corresponding to the denominators $s - s'$, $t - t'$ and $u - u'$ have been examined in previous papers [8,17] and, for the equal-mass case, lie along the real axis. We therefore need examine only the denominators $s't'u' - stu$. They will vanish when

$$|4q^2 s(-1+z)(-1-z)| = 324\mu^6$$

or

$$|s(s-4\mu^2)^2| = \frac{1296\mu^6}{1-z^2}.$$

(17) S. W. MacDowell: *Phys. Rev.*, **116**, 774 (1959).

The partial waves will thus be analytic functions of s, except for the cuts along the real axis, as long as

$$|s(s-4\mu^2)^2|<1296\mu^6\,. \tag{5.1}$$

This region includes that portion of the real axis between $-8.4\mu^2$ and $13.7\mu^2$ As is shown in reference ([8]) and ([17]), there will be a cut along the real axis except between 0 and $4\mu^2$. On the left cut, the discontinuity can be calculated by crossing symmetry from the discontinuity on the right, and the partial-wave expansion for this calculation converges if $s>-8\mu^2$.

5·2. *Ordinary dispersion relations.* – The range of values of the momentum transfer for which ordinary dispersion relations are valid can be increased slightly. Previously, the range was $-8\mu^2>t>0$. The condition on t is that it must lie within the large Lehmann ellipse for all values of s greater than $4\mu^2$, and the value of s which gave the minimum value of t was $6\mu^2$. Now, however, the original large Lehmann ellipse gives the region of analyticity of A_1 as a function of t only if s is greater than $9\mu^2$, and, at this value of s, the minimum real value of t within the ellipse is $-9\mu^2$. For s less than $9\mu^2$, A_1 is analytic in an ellipse whose semi-major axis is given by (4.19), except for singularities along the real axis, and the value $t=-9\mu^2$ is always included. Dispersion relations are therefore valid if

$$-9\mu^2<t<0\,. \tag{5.2}$$

We saw in reference ([3]) that the singularities of A_1 along the real axis do not invalidate the dispersion relations, as the singularities in A_2 will always be equal and opposite to that in A_1. The present treatment is thus able to extend, rigorously, the validity of the dispersion relations into the region where these singularities occur.

5·3. *Extrapolation to poles.* – Another analytic property of the transition amplitude which has not been rigorously proved up till now is that, if it is extrapolated to unphysical angles at a fixed value of the energy, it will remain analytic until we reach the pole at $t=\mu^2$. Chew ([9]) has suggested exploiting this fact in determining coupling constants. We saw in Section 2 that our domain of analyticity includes the pole if s is sufficiently small. In order to find the maximum value of s for which this occurs, it is more advantageous to look at regions of the form

$$|tu|<c$$

than of the form (2.17). The maximum value of c which fulfils the conditions on A_2 and A_3 is $36\mu^4$, but, to fulfil the condition on A_1, it must be less than $32\mu^4$. In addition, to fulfil the condition that, for some real value of s greater than $4\mu^2$, the region must lie within the small Lehmann ellipse, b must be less than $9\mu^4$. We can get rid of the last limitation by considering domains of the form $|t(u+\varepsilon)|<c$ $(\varepsilon>0)$; the domain is then always within the small Lehmann ellipse if is sufficiently large. By letting ε tend to zero, we obtain the results that the transition amplitude is analytic if

$$|tu|<32\mu^4 .$$

The condition that the point $t=\mu^2$ be included is

$$s<35\mu^2 \tag{5.3}$$

and the procedure for extrapolation to poles can now be justified if (5.3) is true.

5'4. *Pion-pion amplitude.* – In this paper we have been treating the case where there is a three-particle vertex, as our results are best illustrated thereby. However, since the method is as yet applicable to the scattering of the lightest particles in the theory alone, the only actual process which can be treated is pion-pion scattering, where there is no three-particle vertex. We shall therefore present the results for the pion-pion scattering amplitude. The value of m_1 in eq. (2.5) is now 3μ instead of 2μ, and all our limits are accordingly increased. In order that the numbers do not become too large, we shall use the variable $s/4$, $t/4$, $u/4$. The domain of analyticity is

$$\left|\frac{s}{4}\frac{t}{4}\frac{u}{4}\right|<112\mu^6 . \tag{5.4}$$

This touces the large Lehmann ellipse at $s=16\mu^2$, $t=16\mu^2$, *i.e.*, at the threshold for inelastic processes. The domain therefore cannot be increased by using the unitarity condition in its simple form. The partial waves will be analytic in the region

$$\left|\frac{s}{4}\left(\frac{s}{4}-\mu^2\right)^2\right|<448\mu^6 , \tag{5.5}$$

except for cuts along the real axis. The portion of the real axis included by (5.5) is from $s/4=-7\mu^2$ to $s/4=8.3\mu^2$.

6. – Concluding remarks.

The method developed in Sections 2 and 3 enables us to show that, in the region of greatest physical interest, the amplitude for the scattering of the lightest particles in the theory is an analytic function of its two variables, apart from the expected singularities. We were unable to find the maximum domain of analyticity which followed from the causality and mass-spectrum requirements, or even the maximum domain that could be obtained from our present knowledge without going off the mass shell. The former question would probably be very difficult to answer at present; the latter might be easier and the result would be of great interest.

Nevertheless, it is felt that the most powerful method for extending the domain of analyticity is to use the unitarity condition rather than to make further use of the causality condition. We have seen that it is possible to make some progress without knowing anything about inelastic processes, and that this is adequate for calculations we wish to perform without taking such processes into account. If the unitarity equation including inelastic processes has the same properties as the simple equation we have been discussing, it should be possible to use it to extend the domain of analyticity arbitrarily far except for certain singularities which can be taken into account. It was found that the use of the simple unitarity condition in the present treatment followed fairly closely its use in the perturbation treatment, and such may well be the case if inelastic processes are included. There seems to be no reason why such processes cannot be incorporated into our scheme, but this has not been done as yet.

The most serious limitation on our results as presented here is that they apply only to the scattering of the lightest particles in the theory. We had to make use of forward and near-forward dispersion relations for at least two of the cases $s \approx 0$, $t \approx 0$, $u \approx 0$, and such relations have not been proved for the general mass case. We could relax slightly our requirement that there be no lighter particles in the theory since, if the mass of these lighter particles is more than $(\sqrt{2} - 1)$ of the mass of the particles being treated, the dispersion relations can still be proved ([2]) and our method will go through. Above this limit it will have to be substantially modified.

It could have been anticipated that we would not have been able to treat the general mass without going off the mass shell, since a similar situation occurred in perturbation theory ([7]). The earlier treatment therefore suggests once more the manner of overcoming the difficulty: first treat the Green's function with the squares of the external momenta of the havy particle fixed, not at its mass value, but at some sufficiently small value. Then continue analytically onto the mass shell. If we do this without using unitarity, we shall obtain exactly the same restriction on the mass-ratio as before—in fact,

this is how the limiting mass-ratio was originally derived. It is therefore necessary to apply unitarity before doing the analytic continuation. The procedure discussed in Section **4** does not appear to be adequate, but we can take advantage of the fact that the difficult region is always the energy range below the sum of the masses of the particles. In this region the unitarity condition is linear, and the equations can be solved by Omnès' method ([18]). We shall not be able to treat the pion-nucleon problem until multi-particles states can be included in the unitarity condition, but we may at least be able to decrease slightly the minimum mass-ratio by using the unitarity equation in its simple form. It is hoped to develop these ideas in a further paper.

We may therefore feel optimistic that the programme of using the general requirements of quantum field theory to find the analytic properties of the transition amplitudes, and employing these properties in the actual determination of the amplitudes, is in principle capable of solution. Whether the approximation scheme is adequate or convergent, and whether it can in practice be taken beyond its lowest approximation are questions which we do not wish to discuss here.

([18]) R. Omnès: *Nuovo Cimento*, **8**, 316 (1958).

RIASSUNTO (*)

Le condizioni di causalità e dello spettro di massa vengono usate per derivare le proprietà analitiche delle ampiezze di transizione come funzioni del trasferimento dell'energia e dell'impulso. Pur non potendosi determinare le rappresentazioni delle doppie dispersioni complete basandosi soltanto su questi postulati, si mostra che, entro un certo dominio nello spazio di due variabili complesse, le sole singolarità sono i poli previsti ed i tagli lungo l'asse reale. Questo dominio circonda la regione fisica di bassa energia. La dimostrazione è limitata allo scattering delle particelle più leggere nella teoria. Sinchè non si cerca di trovare il più grande dominio possibile, i calcoli non sono molto difficili. Si può poi estendere il dominio di analicitità con la condizione di unitarietà. La grandezza dell'estensione non è molto grande, ma il nuovo dominio differisce dal precedente in quanto comprende parte della regione in cui le funzioni spettrali bidimensionali sono non nulle. Noi usiamo la condizione di unitarietà solo sotto la soglia per i processi anelastici; se si potessero trattare anche questi processi e si potesse usare la condizione di unitarietà, sembrerebbe possibile estendere ad arbitrario il dominio. Nei presenti risultati i limiti del dominio di analiticità sono abbastanza lontani dalla zona di basse energie da giustificare le proprietà analitiche presupposte in applicazione della rappresentazione a doppia dispersione. Altri risultati dimostrabili sono che le ampiezze delle onde parziali sono funzioni analitiche dell'energia in una certa zona, che la determinazione delle costanti di accoppiamento mediante estrapolazione rispetto agli angoli è valida se l'energia non è troppo elevata, e che le ordinarie relazioni di dispersione sono vere per un campo di valori del trasferimento dell'impulso leggermente più ampio di quello fissato precedentemente.

(*) *Traduzione a cura della Redazione.*

Effect of Nuclear Magnetic Moment on the Bremsstrahlung of Electrons.

Sasabindu Sarkar

Department of Theoretical Physics
Indian Association for the Cultivation of Science - Jadavpur, Calcutta

(ricevuto il 22 Dicembre 1959)

Summary. — In this paper electron-nucleus bremsstrahlung is treated by representing the nucleus as a static model having charge and magnetic moment, the electromagnetic potentials of which have been given by Newton. The cross-section is first derived for the case of targets with definite direction of the magnetic moment of the nuclei and then it is averaged over all such possible directions.

1. – Introduction.

In the collision of high energy electrons with the nucleus, the electron suffers deflection in the Coulomb field of the nucleus and in consequence bremsstrahlung is produced. The nucleus has a magnetic moment which can also influence the motion of the electron. Taking into account the recoil of the proton under the combined interaction of the charge and the magnetic moment of the proton with the radiation field, Berg and Lindner [1] have calculated the high energy bremsstrahlung in electron-proton collisions. However their method can not be easily extended to nuclei other than protons because the representation of the magnetic moment operator offers difficulties for nuclei whose magnetic moments come from both orbital and spin motion of several nucleons.

In this paper we calculate the production of electron-nucleus bremsstrahlung by representing the nucleus as a static model having charge and magnetic

[1] R. A. Berg and C. N. Lindner: *Phys. Rev.*, **112**, 2072 (1958).

moment, the electromagnetic potentials of such a model has been given by NEWTON (2) who has investigated the double scattering of polarized and unpolarized electrons by polarized nuclei. For an electron with one GeV energy, the neglect of the recoil effect in our calculation seems to be justified when the mass of the target nucleus is much heavier than that of the proton. As shown by NEWTON (2), the ratio of the interactions due to the magnetic moment and Coulomb charge is of the order of magnitude as

$$\frac{|\boldsymbol{p}|\mu}{eZ} = \frac{1}{2}\frac{|\boldsymbol{p}|}{M_p c}\frac{\mu/\mu_{\mathcal{N}}}{Z},$$

where μ and Z are the magnetic moment and atomic number of the nucleus, $\mu_{\mathcal{N}}$ and M_p are respectively the nuclear magneton and proton mass and $\boldsymbol{p}$ is the momentum of the electron. It can be shown that the fractional increase in the differential cross-section for bremsstrahlung is of the order of magnitude of the square of the above mentioned ratio. To make the ratio appreciable it is desirable to choose the energy of the electron as of the order of rest energy of the proton *i.e.* of the order of one GeV and also to choose targets with small values of Z. The effect of magnetic moment interaction is more pronounced in the formula derived for the case of targets with lined up nuclear spins than in that obtained by averaging over all possible directions of magnetic moments of nuclei.

2. – Calculation.

The interaction Hamiltonian of the electron in the field of a point model nucleus having charge and magnetic moment is (cf. NEWTON (2)),

$$e^2 Z(\beta + \lambda\mu^{-1}\beta\boldsymbol{\alpha}\cdot\boldsymbol{\mu}\times\boldsymbol{\nabla})r^{-1},$$

where $\lambda = (1/2M_p c)(\mu/\mu_{\mathcal{N}})Z^{-1}$, β and $\boldsymbol{\alpha}$ are the usual Dirac matrices. The matrix element responsible for the transition of the electron in the case of bremsstrahlung is given by

$$M = 4\sqrt{\frac{2\pi^3}{k}}\frac{Ze^3}{q^2}\sum\left[\frac{(\varphi\alpha_l\varphi')(\varphi', (1+\lambda\mu^{-1}\boldsymbol{\alpha}\cdot\boldsymbol{\mu}\times\boldsymbol{\nabla})r^{-1}\varphi_0)}{E'-E_0} + \right.$$
$$\left. + \frac{(\varphi, (1+\lambda\mu^{-1}\boldsymbol{\alpha}\cdot\boldsymbol{\mu}\times\boldsymbol{\nabla})r^{-1}\varphi'')(\varphi'', \alpha_l\varphi_0)}{E''-E}\right],$$

(2) R. G. NEWTON: *Phys. Rev.*, **103**, 385 (1956).

where φ_0, φ, φ' and φ'' are respectively the initial, final and the two intermediate spinor states of the electron. E_0, E, E' and E'' and $\boldsymbol{p}_0$, $\boldsymbol{p}$, $\boldsymbol{p}'$ and $\boldsymbol{p}''$ are the corresponding energies and momenta respectively. Taking $\boldsymbol{k}$ to be the momentum of the photon we have the usual momenta relations

$$\boldsymbol{p}' = \boldsymbol{p} + \boldsymbol{k}\,, \qquad \boldsymbol{p}'' = \boldsymbol{p}_0 - \boldsymbol{k} \qquad \text{and let} \quad \boldsymbol{q} = \boldsymbol{p}_0 - \boldsymbol{p} - \boldsymbol{k}\,.$$

Here α_l is the component of $\boldsymbol{\alpha}$ in the direction of polarization of the emitted photon.

Following the notations and methods of GLUCKSTERN, HULL and BREIT [3] we introduce the matrices

$$\gamma'' = (\boldsymbol{\gamma}, \gamma^4)\,, \qquad \boldsymbol{\gamma} = -i\beta\boldsymbol{\alpha}\,, \qquad \gamma^4 = -\beta$$

and

$$p_\mu = (\boldsymbol{p}, iE)\,.$$

Then we can write the absolute square of the bracketted term of the matrix element in the form

$$\sum |\varphi, (A + B)\varphi_0|^2\,,$$

where

$$A = \gamma^l\gamma^4(\gamma p' + im)(\gamma^4 + \lambda\boldsymbol{\gamma}\cdot\boldsymbol{L})/\varepsilon'^2$$

$$B = (1 - \lambda\boldsymbol{\gamma}\cdot\boldsymbol{L}\gamma^4)(\gamma p'' + im)\gamma^4\gamma^l\gamma^4/\varepsilon''^2$$

$$\varepsilon'^2 = E'^2 - E_0^2 = -2(kE - \boldsymbol{k}\cdot\boldsymbol{p}) = -2k\Delta$$

$$\varepsilon''^2 = E''^2 - E^2 = \quad 2(kE_0 - \boldsymbol{k}\cdot\boldsymbol{p}_0) = \quad 2k\Delta_0$$

and

$$L = \boldsymbol{\mu}\times\boldsymbol{q}/\mu\,.$$

After summing over the spin directions of the initial and final states of the electron the expression for the differential cross-section is

$$\mathrm{d}\sigma = (Z^2e^6/8\pi^2)(p/p_0)(k\,\mathrm{d}k/q^4)\,\mathrm{Tr}\,\{(A^\dagger + B^\dagger)(H + E)(A + B)(H_0 + E_0)\}\,\mathrm{d}\Omega\,\mathrm{d}\Omega_k\,,$$

---

[3] R. L. GLUCKSTERN, M. H. HULL jr. and G. BREIT: *Phys. Rev.*, **90**, 1026 (1953).

where $d\Omega$ and $d\Omega_k$ are respectively the solid angles in which the electron is scattered and the photon is emitted.

After some calculation we can show that the trace of the term dependent on the magnetic moment is

$$
\begin{aligned}
-\left[\tfrac{1}{2}(1/M_p)(\mu/\mu_{q\tau})Z^{-1}\right]^2 \Big\{ & -2(\boldsymbol{\mu}\cdot\boldsymbol{q}\times\boldsymbol{e}_l)^2 + \\
& + (\mu^2 q^2 - (\boldsymbol{\mu}\cdot\boldsymbol{q})^2)\left(1 + \frac{1}{2}\frac{\varepsilon'^2}{\varepsilon''^2} + \frac{1}{2}\frac{\varepsilon''^2}{\varepsilon'^2} - \frac{2p_l^2 q^2}{\varepsilon'^4} - \frac{2p_{0l}^2 q^2}{\varepsilon''^4} - \frac{4q^2 p_l p_{0l}}{\varepsilon'^2\varepsilon''^2}\right) + \\
& + 8(\boldsymbol{\mu}\cdot\boldsymbol{q}\times\boldsymbol{e}_l)(\boldsymbol{\mu}\cdot\boldsymbol{q}\times\boldsymbol{p}_0)p_l/\varepsilon'^2 + 8(\boldsymbol{\mu}\cdot\boldsymbol{q}\times\boldsymbol{e}_l)(\boldsymbol{\mu}\cdot\boldsymbol{q}\times\boldsymbol{p})p_{0l}/\varepsilon''^2 + \\
& + 2(\boldsymbol{\mu}\cdot\boldsymbol{q}\times\boldsymbol{p}_0)^2(q^2/\varepsilon'^2\varepsilon''^2 - 4p_l^2/\varepsilon'^4) + 2(\boldsymbol{\mu}\cdot\boldsymbol{q}\times\boldsymbol{p})^2(q^2/\varepsilon'^2\varepsilon''^2 - 4p_{0l}^2/\varepsilon''^4) - \\
& - 4(\boldsymbol{\mu}\cdot\boldsymbol{q}\times\boldsymbol{p})(\boldsymbol{\mu}\cdot\boldsymbol{q}\times\boldsymbol{p}_0)\frac{q^2 + 4p_{0l}p_l}{\varepsilon'^2\varepsilon''^2}\Big\},
\end{aligned}
$$

where $\boldsymbol{e}_l$ is the unit vector in the direction of polarization of the photon. This expression shows the dependence of the cross-section on the direction of the polarized target and polarization of the emitted photon.

Now averaging over all equally possible directions of the magnetic moments of the targets the expression for the trace becomes

$$
\begin{aligned}
\frac{2}{k^2}\Big\{ & \frac{(4E_0^2 - q^2)p_l^2}{\Delta^2} + \frac{(4E^2 - q^2)p_{0l}^2}{\Delta_0^2} - \frac{2(4EE_0 - q^2)p_l p_{0l}}{\Delta\Delta_0} - k^2\left(\frac{1}{\Delta_0} + \frac{1}{\Delta} - 2 - \frac{q^2}{\Delta\Delta_0}\right)\Big\} + \\
& + \frac{1}{3}\frac{q^2}{M_p^2}\Big[\frac{1}{2}(\mu/\mu_{q\tau})Z^{-1}\Big]^2\frac{1}{k^2}\Big\{\frac{p_{0l}p_l(-q^2 + 4m^2 - 4E_0E)}{\Delta\Delta_0} + p_l^2\frac{q^2 + 4p_0^2}{2\Delta^2} + \\
& + p_{0l}^2\frac{q^2 + 4p^2}{2\Delta_0^2} + \frac{1}{2}k^2\left(\frac{\Delta_0}{\Delta} + \frac{\Delta}{\Delta_0} + 2 + \frac{q^2}{\Delta\Delta_0}\right)\Big\}.
\end{aligned}
$$

For the nuclear target we choose ^{7}Li the magnetic moment of which is $(3.255\,86 \pm 11)$ nuclear magnetons; further to simplify calculation we consider the special case when $\boldsymbol{p}_0 \parallel \boldsymbol{k}$, $\boldsymbol{p} \perp \boldsymbol{k}$, $E_0 = 1$ GeV and $k = 1$ MeV. The ratio of the differential cross-section with the effect of charge and the magnetic moment to that with charge alone is 1.1167, *i.e.* there is about 12% increase in the differential cross-section. From the above formula it is evident that the effect of magnetic moment is appreciable for large values of $\boldsymbol{q}$, *i.e.*, large angles of scattering. For a target having extended charge and magnetic moment distribution both the interaction terms of the scattering matrix element should be multiplied by the appropriate form factors.

* * *

The author is greatly indebted to Prof. D. BASU for his constant help and guidance throughout the progress of the work.

RIASSUNTO (*)

In questo articolo si discute la bremsstrahlung elettrone-nucleo rappresentando il nucleo come un modello statico avente carica e momento magnetico, i cui potenziali elettromagnetici sono stati dati da Newton. Prima viene dedotta la sezione trasversale per il caso di bersagli con definite direzioni del momento magnetico dei nuclei e poi ne vien fatta la media su tutte le direzioni possibili.

(*) *Traduzione a cura della Redazione.*

LETTERE ALLA REDAZIONE

La responsabilità scientifica degli scritti inseriti in questa rubrica è completamente lasciata dalla Direzione del periodico ai singoli autori)

On the Relativistic K-Shell Photoeffect.

M. Gavrila

Department of Physics, Parhon University - Bucharest

(ricevuto il 26 Ottobre 1959)

1. – The study of the high energy photoeffect has been resumed lately both from the experimental [1] and theoretical [2] points of view. In the case of the K shell the present author has obtained, extending Sauter's results, the form of the relativistic cross sections, correct to first order in αZ [3]. To this end the Born approximation method has been used for describing the final state of the electron, the integration of the involved matrix element being carried out in momentum space. Concomitantly Banerjee [4] has considered the same problem using the Sommerfeld-Maue approximation for the final state of the electron [5]. However, in this way only the extreme relativistic expression of the αZ corrective terms to the cross sections can be found. Further, the problem of the forward emission of photoelectrons has been considered in a work by Sauter and Wüster [6]. The polarization dependence of the cross-sections has also been investigated [4,7]. Finally, the study of the high energy limit of the total cross sections has been completed [4,8]. The aim of this note is to discuss some of the connections existing between the previously quoted works and the present author's one (G).

---

[1] S. Hultberg *et al.*: *Ark. f. Fys.*, **9**, 245 (1955); **13**, 117 (1958); **14**, 565 (1959); *Nucl. Phys.*, **4**, 120 (1957); **10**, 118 (1959); E. P. Grigoryev and A. V. Zolotavin: *Žurn. Èksp. Teor. Fiz.*, **36**, 393 (1959); W. Titus: *Phys. Rev.*, **115**, 351 (1959).

[2] New theoretical results have been obtained also for the L shell, that is: the relativistic differential and total cross sections for low Z (M. Gavrila: to be published); the extreme relativistic total cross sections, exact in Z (R. H. Pratt: to be published).

[3] M. Gavrila: *Phys. Rev.*, **113**, 514 (1959), hereafter referred to as (G).

[4] H. Banerjee: *Nuovo Cimento*, **10**, 863 (1958), hereafter referred to as (B); **11**, 220 (1959).

[5] The same method has been used previously in an unpublished work by F. G. Nagasaka (*Ph. D. Thesis*, University of Notre Dame, 1955) with similar results.

[6] F. Sauter and H. Wüster: *Zeits. f. Phys.*, **141**, 83 (1955).

[7] K. Mc Voy: *Phys. Rev.*, **108**, 365 (1958); U. Fano, K. Mc Voy and J. Albers: to be published.

[8] M. Gavrila: *Nuovo Cimento*, **9**, 327 (1958). R. H. Pratt: *Ph. D. Thesis*, University of Chicago (1959) (to be published); this contains an extensive comparison of various results obtained for the high energy limit.

2. – Sommerfeld and Maue used the approximate form they had discovered for the final state spinor of the electron, only for establishing Sauter's formula. Banerjee has remarked that the same calculation, somewhat modified, can be extended for obtaining the *extreme relativistic* contribution to the cross sections of the αZ corrective terms; an explicit evaluation can be worked out only to first order in αZ. To obtain the *complete energy dependence* to first order in αZ, as in (G), a higher order approximation should be used for the final state spinor; however, this has not yet been determined explicitly in the frame of the Sommerfeld-Maue method.

The differential cross section of the relativistic K shell photoeffect, correct to first order in αZ, may be put into the form of Eq. (G.92),

$$(1) \qquad \mathrm{d}\sigma_K = 4\alpha^6 Z^5 \lambda_0^2 \frac{\beta^3(1-\beta^2)^3}{(1-\sqrt{1-\beta^2})^5}\left[\mathscr{F}\left(1-\frac{\pi\alpha Z}{\beta}\right)+\pi\alpha Z\mathscr{G}\right]\mathrm{d}\omega,$$

where $\lambda_0 = \hbar/mc$. By setting here $\pi\alpha Z = 0$, the Sauter formula is obtained. From Banerjee's result Eq. (B. 31), the extreme relativistic form of $\mathscr{G}$ is found to be

$$(2) \qquad \mathscr{G}_B = -\frac{1}{2\sqrt{2}}\frac{\sin^2(\theta/2)}{\Theta^{\frac{7}{2}}}\varepsilon^2 .$$

The notations used here are similar to those of (B):

$$\varepsilon = \frac{1}{\sqrt{1-\beta^2}}, \qquad \Theta = 1-\beta\cos\theta , \qquad a = \alpha Z .$$

Following the calculations of (B) it may be easily seen that the term (2) results from the combination in the matrix element of the $(\alpha Z)^2$ corrective terms to the ground state spinor with the final state wave function.

Nevertheless, the term (2) can not be traced anywhere in the complete expression derived for $\mathscr{G}$ in Eq. (G. 94). This is due to the fact that the formula of $\mathscr{G}$ given there is valid whatever the magnitude of β, whereas $\mathscr{G}_B$ of (2) has been deduced on the assumption that $\beta \to 1$ ($\varepsilon \to \infty$). It will be shown in the following that if one neglects only terms of order $(\alpha Z)^2$ but does not introduce the assumption that $\beta \to 1$, Banerejee's calculations lead to an identical result for $\mathscr{G}_B$ with the one of the calculations of (G).

When working on these lines only the last equations of (B) have to be modified. Upon recalculating I_0 of Eq. (B.29) one now finds

$$(3) \qquad I_0 = C' J_0 \frac{a(1-ia)}{\varepsilon-1}\left[\frac{1}{\varepsilon\Theta}-\varepsilon+\frac{\pi a}{4\sqrt{2}}\left(\frac{\varepsilon-1}{\varepsilon}\right)^{\frac{1}{2}}\frac{1}{\Theta^{\frac{1}{2}}}\right].$$

Further, the calculation of the quantities occuring in Eq. (B. 30) must be performed taking into account the modified expression of the corrective term of (3) and neglecting only order $(\alpha Z)^2$. One finds finally, instead of the corrective term (proportional to a) of $|H_{12}|^2$, given by Eq. (B. 31), the expression

$$T = \frac{\pi a}{4\sqrt{2}}\left(\frac{\varepsilon-1}{\varepsilon}\right)^{\frac{1}{2}}\left\{\frac{1}{\Theta^{\frac{7}{2}}}\left[\frac{\varepsilon-1}{\varepsilon^2}+\frac{2(\varepsilon^2-1)}{\varepsilon^2}\sin^2\theta\cos^2\varphi\right]-\frac{2(\varepsilon-1)}{\Theta^{\frac{5}{2}}}+\frac{\varepsilon-1}{\Theta^{\frac{3}{2}}}\right\}.$$

Using the equality

$$\sin^2\theta = \frac{1}{1-\varepsilon^2}\,(1 - 2\varepsilon^2\Theta + \varepsilon^2\Theta^2)\,,$$

T becomes

$$T = \frac{\pi a}{4\sqrt{2}}\left(\frac{\varepsilon-1}{\varepsilon}\right)^{\frac{1}{2}}\cdot\frac{\varepsilon^2-1}{\varepsilon^2}\left[-(\varepsilon-1)\frac{\sin^2\theta}{\Theta^{\frac{7}{2}}} + \frac{2\sin^2\theta\cos^2\varphi}{\Theta^{\frac{7}{2}}}\right]. \tag{4}$$

Returning to the notations adopted in (1), one gets

$$\mathcal{G}'_B = \frac{1}{2\pi a\beta^2\sqrt{1-\beta^2}}\,T = \tag{5}$$

$$= \frac{\left(1-\sqrt{1-\beta^2}\right)^{\frac{1}{2}}}{8\sqrt{2}}\left[-\frac{1-\sqrt{1-\beta^2}}{1-\beta^2}\,\frac{\sin^2\theta}{\Theta^{\frac{7}{2}}} + \frac{2}{\sqrt{1-\beta^2}}\,\frac{\sin^2\theta\cos^2\varphi}{\Theta^{\frac{7}{2}}}\right].$$

Hence, formula (5) represents the contribution (exact in β) to $\mathcal{G}$ of (1), of the $(\alpha Z)^2$ corrective terms to the ground state spinor.

If one adopts the Born approximation method, as done in (G), it is to be expected that the term $\mathcal{G}'_B$ of (5) should come from the contribution to the matrix element of the spinor $u_{12}(\boldsymbol{p})$ of Eq. (G. 10). Tracing this contribution throughout the calculation of (G), one may easily ascertain that it appears succesively in Eqs. (G. 17), (G. 31), (G. 61), (G. 74), (G. 75). The part of Ξ, given by Eq. (G. 91), which pertains to Γ_1 and Θ_1 of Eqs. (G. 74) and (G. 75), is (with the notations used there)

$$\frac{1}{16m^2\varkappa(\boldsymbol{k}-\boldsymbol{\varkappa})^6\,|\boldsymbol{k}-\boldsymbol{\varkappa}|}\left[4m^2\varkappa(\boldsymbol{k}\boldsymbol{s})^2 - 2mk^2\varkappa^2\sin^2\theta\right]. \tag{6}$$

It may be checked that this gives a contribution to $\mathcal{G}$ which is identical with the expression given by formula (5), as was to be expected.

In the extreme relativistic limit one finds from equation (5)

$$\mathcal{G}'_B \xrightarrow[\varepsilon\to\infty]{} -\frac{1}{8\sqrt{2}}\,\frac{\sin^2\theta}{\Theta^{\frac{7}{2}}}\,\varepsilon^2\,. \tag{7}$$

Clearly the preceding expression has large magnitude only for small angles θ. A more attentive inspection of the general formula of $\mathcal{G}$ given by Eq. (G. 94) shows that, for $\beta\to 1$ and small angles θ, its dominant term is indeed given by (7); this confirms the remark of Banerjee regarding the possibility of extending the Sommerfeld-Maue calculation. Also, if $\theta^2 \ll 1$, $\mathcal{G}'_B$ of (7) coincides with the form given by Banerjee in (2). Nevertheless, the substitution of expression (2) for (7) is not advisable, because one loses the fact that $\mathcal{G}'_B$ vanishes not only for $\theta = 0$, but also for $\theta = \pi$. As regards the calculation of the total cross section, where only the small angle region contributes, the use of formula (7) or (2) is equivalent. One gets thus the already known contribution of $(-4\pi a/15)$ to the high energy limit of the cross section [5,8].

3. – The $\mathscr{F}$ term of (1), which corresponds to Sauter's approximation, is proportional to $\sin^2\theta$ [9]; hence, in this approximation no photoelectrons are emitted in forward or backward directions $\theta = 0, \pi$. In order to find out the contribution of the corrective term $\mathscr{G}(\theta, \varphi)$ of Eq. (G. 94), one can write

$$\mathscr{G}(0, \varphi) = A\cos^2\varphi + B; \qquad \mathscr{G}(\pi, \varphi) = A'\cos^2\varphi + B', \tag{8}$$

where at a fist glance A, B, A', B' seem to be complicated functions of β. However upon collecting terms and using the identity

$$(1-\sqrt{1-\beta^2})^{\frac{1}{2}} = \frac{1}{\sqrt{2}}(\sqrt{1+\beta}-\sqrt{1-\beta}),$$

one finds in the end the unexpected result

$$A = B = A' = B' = 0; \qquad \mathscr{G}(0, \varphi) = \mathscr{G}(\pi, \varphi) = 0. \tag{9}$$

Thus, also to first order in αZ no photoelectrons are emitted for $\theta = 0, \pi$ [10].

This result is at variance with one of the conclusions of the work of SAUTER and WÜSTER [6]. Indeed, one finds there, by using Sauter's original working method, that to first order in αZ the differential cross section is nonvanisihing for $\theta = 0$ [11]. The explanation of this discrepancy is the following. When he initially derived his formula, Sauter made two kinds of approximation [12]: (*a*) replaced square roots like $j = \sqrt{l^2 - \alpha^2 Z^2}$, occuring in the continuum and initial state spinors, by l; (*b*) retained only the lowest order non-vanishing terms of an expansion in $\alpha Z/\beta$. Now, contrary to what may be expected, approximation (*a*) does not lead to an error of order $(\alpha Z)^2$ for the cross sections but to one of order αZ; indeed, as may be seen from (G), for obtaining the form of the cross sections correct to *first* order in αZ one must use spinors correct to *second* order in αZ. In order to calculate the differential cross section for $\theta = 0$ to first order in αZ, SAUTER and WÜSTER considered the first order corrections to (*b*), but no correction to (*a*). Their result is thus not consistent in αZ and represents no contradiction to (9).

---

[9] See for example (G), Eq. (G.93).
[10] This is contrary to what has been incorrectly stated in (G), after Eq. (G.94).
[11] For $Z = 82$, $h\nu = 1.33$ MeV one finds that $I(0)/I_{\max} = 0.21$.
[12] See F. SAUTER: *Ann. d. Phys.*, **11**, 454 (1931); also reference [6].

IL NUOVO CIMENTO Vol. XV, N. 4 16 Febbraio 1960

Solar Flare Connected with an Increase of Intensity of Cosmic Rays.

L. Křivský

Astronomical Institute of the Czechoslovak Academy of Sciences - Ondřejov

J. Hladký and P. Mokrý

Physical Institute of the Czechoslovak Academy of Sciences - Prague

P. Chaloupka

Laboratory of Physics of the Slovak Academy of Sciences - Bratislava

T. Kowalski

Institute for Geophysics of the Polish Academy of Sciences - Warsaw

(ricevuto il 14 Dicembre 1959)

The following phenomena were observed on the 6th October 1959: from 14.09 till 14.45 GMT a chromospheric flare of medium importance 1+ was recorded at the Astronomical Observatory Ondřejov near Prague. Its position was 30.5° N, 63° E. The flare was accompanied by an active filament of the « surge » type. It had the form of a loop with very rapid changes. An increase of solar radio emission at $\lambda = 56$ and 130 cm was detected during the course of this process. A usual increase of atmospheric noise at 27 kHz in the course of the flare (disturbance of D ionospheric zone by extraordinary X radiation) and a striking decrease of noise level from 15.20 till 15.50 GMT probably caused by the disturbance of D zone by cosmic rays was recorded.

An increase of cosmic ray intensity was recorded at the cosmic ray observatories Lomnický Štít (2 634 m) and Prague-Karlov (228 m) which are equipped with standard neutron monitors and cubical telescopes. It lasted about 25 min about $(50 \div 70)$ min after the maximum of brightness of the flare and of the maximum development of the « surge ». The neutron monitors recorded an increase of $(2.5 \pm 0{,}7)\%$ at Lomnický Štít and of $(2.8 \pm 1.6)\%$ at Prague; the intensity of the hard component increased by $(3.3 \pm 0.6)\%$ at Lomnický Štít and by $(0.72 \pm 0.45)\%$ at Prague. This increase begun nearly simultaneously at all detectors and seems to be far above the statistical fluctuations at least at the mountain observatory. Because of the rather small

importance of the solar flare the observed increase of cosmic ray intensity in the diffuse impact zone is unexpectedly large. It seems to be therefore important to prove the effect at cosmic ray observatories which lie in the region of maximum impact of particles where a much larger increase of intensity is to be expected.

We are inclined to suppose a correlation of the observed increase with rapid changes of the magnetic field during the development of the solar flare and filament.

Direttore responsabile: G. POLVANI

Tipografia Compositori - Bologna

Questo Fascicolo è stato licenziato dai torchi il 29-II-1960